



UNIL | Université de Lausanne

Unicentre

CH-1015 Lausanne

<http://serval.unil.ch>

Year : 2019

Interplay between lipid metabolism and gut immunology during experimental model of Multiple sclerosis

Duc Donovan

Duc Donovan, 2019, Interplay between lipid metabolism and gut immunology during experimental model of Multiple sclerosis

Originally published at : Thesis, University of Lausanne

Posted at the University of Lausanne Open Archive <http://serval.unil.ch>

Document URN : urn:nbn:ch:serval-BIB_0656FFE5EC708

Droits d'auteur

L'Université de Lausanne attire expressément l'attention des utilisateurs sur le fait que tous les documents publiés dans l'Archive SERVAL sont protégés par le droit d'auteur, conformément à la loi fédérale sur le droit d'auteur et les droits voisins (LDA). A ce titre, il est indispensable d'obtenir le consentement préalable de l'auteur et/ou de l'éditeur avant toute utilisation d'une oeuvre ou d'une partie d'une oeuvre ne relevant pas d'une utilisation à des fins personnelles au sens de la LDA (art. 19, al. 1 lettre a). A défaut, tout contrevenant s'expose aux sanctions prévues par cette loi. Nous déclinons toute responsabilité en la matière.

Copyright

The University of Lausanne expressly draws the attention of users to the fact that all documents published in the SERVAL Archive are protected by copyright in accordance with federal law on copyright and similar rights (LDA). Accordingly it is indispensable to obtain prior consent from the author and/or publisher before any use of a work or part of a work for purposes other than personal use within the meaning of LDA (art. 19, para. 1 letter a). Failure to do so will expose offenders to the sanctions laid down by this law. We accept no liability in this respect.



UNIL | Université de Lausanne

Faculté de biologie
et de médecine

Département des Neurosciences Cliniques

**Interplay between lipid metabolism and gut immunology
during experimental model of Multiple sclerosis**

Thèse de doctorat ès sciences de la vie (PhD)

présentée à la

Faculté de biologie et de médecine
de l'Université de Lausanne

par

Donovan DUC

Master en Biologie Médicale de l'Université de Lausanne, Suisse

Jury

Prof. Petr Broz, Président
Prof. Caroline Pot, Directrice de thèse
Prof. Fabio Martinon, Expert
Dr. Michel Maillard, Expert
Prof. Andrew Chan, Expert

Lausanne
(2019)

Imprimatur

Vu le rapport présenté par le jury d'examen, composé de

Président·e	Monsieur	Prof.	Petr	Broz
Directeur·trice de thèse	Madame	Prof.	Caroline	Pot
Expert·e·s	Monsieur	Prof.	Fabio	Martinon
	Monsieur	Dr	Michel	Maillard
	Monsieur	Prof.	Andrew	Chan

le Conseil de Faculté autorise l'impression de la thèse de

Monsieur Donovan Duc

Master ès Sciences en biologie médicale, Université de Lausanne

intitulée

Interplay between lipid metabolism and gut immunology during experimental model of Multiple sclerosis

Lausanne, le 11 octobre 2019

pour le Doyen
de la Faculté de biologie et de médecine



Prof. Petr Broz

ACKNOWLEDGEMENTS

This page is dedicated to all the people that have contributed to the achievement of my PhD.

A huge and warm *thank you* goes first to my thesis director, Prof. Caroline Pot. I'm deeply grateful to Caroline for giving me the chance to work on these interesting projects and for the priceless support during my PhD thesis. I really appreciated her great advice, her incredible availability to answer questions and to review the abstracts, papers, the thesis and finally her extreme kindness.

Beside my thesis director, I would like to thank Prof. Andrew Chan, Dr. Michel Maillard, Prof. Fabio Martinon and Prof. Petr Broz for having accepted to join my thesis committee and for the review of my work.

I'm deeply thankful to all the member of my lab for creating an amazing working environment. Thank you Solenne, Yannick, Florian and Benjamin for their essential help in these projects and for all the nice moments we shared and the memorable laughs we had together. These thoughts go also for all the former members of the lab: Aurélie, Valentina, Lucie, Rachelle and Oaklyne.

A special thanks to all the team of Prof. Renaud Du Pasquier, for their great help and their collaboration. They all provide great inputs on our projects and precious feedbacks during our *NeuroImmuno* meetings.

I would like to also thank all the present and the former members of the Division of Immunology and Allergy. We received a huge help from them when we established the lab in Lausanne and they continuously provided support when we needed. Thank you also for their feedbacks and the scientific discussions about our projects during the labmeetings.

Special acknowledgments to all the people from our national and international collaborations without whom we could not have realized such a work: Jeremiah Bernier-Latmani and Prof. Tatiana Petrova; Dominique Velin and his team; Prof. Jacques Schrenzel, Vladimir Lazarevic and his team; Alejandra Gomez Cadena from the group Jandus; Gael Boivin from the group Vozenin; and the team of Prof. Giulio Muccioli.

Finally, a warm thanks goes to all my close friends and my family for their continuous support and their strong encouragements along this PhD journey.

ABSTRACT (ENGLISH)

Multiple sclerosis (MS) and its animal model, the experimental autoimmune encephalomyelitis (EAE), are characterized by inflammatory cell infiltrates and demyelination in the central nervous system (CNS) leading to neurological damages. Despite the unknown etiology, combination of both genetic and environmental factors is thought to trigger the disease. While obesity has been recently identified as a risk factor for MS, the role of cholesterol metabolism, intestinal immune responses and gut microbiota remains still unclear. In the present report composed of three projects, we aimed to understand the relation between the gut environment and the cholesterol-derivates oxysterols during the development of CNS autoimmunity. In our first project, we demonstrated that gut immunology and microbiota are involved in the development of EAE disease and affects the pathogenic T cells immunology responsible for the disease. We found that myelin-specific Th17 cells infiltrate the large intestine before neurological symptom development in two murine MS models, the active and adoptive-transfer EAE. Specifically targeting Th17 intestinal homing by blocking integrin pathway impairs T cell migration to the large intestine and further dampened EAE severity in Th17 adoptive-transfer model. Moreover, myelin-specific Th17 cells proliferate in the colon and affected gut microbiota composition pointing towards a contribution of the gut-brain axis in CNS autoimmunity development. This has resulted in a manuscript published in the journal *Cell Reports*.

The second project investigated how oxysterols can modulate gut environment during the development of CNS autoimmunity and the development of gut-specific colitis. In a previous study, we found that mice lacking oxysterols developed milder EAE disease associated with delayed of Th17 migration to the CNS. We found here that infiltration of Th17 cells was delayed in the intestine during the development of EAE disease in mice deficient for a certain oxysterol pathway. Using enteric infectious model, we further reported an impaired innate immune response resulting in a delayed bacterial clearance in mice deficient for oxysterols. New evidence about the role of oxysterols in the gut immunology suggest interesting directions of future research such as the mechanism of the local source of oxysterols.

In the third project, we assessed the effect of hypercholesterolemia on oxysterols and their contribution in EAE disease development. We found that perturbation of circulating lipids level induces modulation of oxysterol-related gene expression without affecting significantly the development of EAE disease. We provided also new evidence that lowering circulating cholesterol does not impact the development of CNS autoimmunity in EAE.

This report provides evidence that the gut immunology is important in EAE development and MS. Furthermore, our studies support the immunomodulatory role of oxysterols during EAE and colitis disease and identify oxysterols as potential therapeutic targets to treat inflammatory and autoimmune disease.

RESUME (FRENCH)

La sclérose en plaques (SEP) et son modèle animal, l'encéphalite auto-immune expérimentale (EAE), sont caractérisées par des infiltrats de cellules inflammatoires et par la démyélinisation du système nerveux central (SNC) donnant lieu à des atteintes neurologiques. Malgré une étiologie inconnue, la combinaison à la fois de facteurs génétiques et de facteurs environnementaux participent au déclenchement de la maladie. Bien que l'obésité ait récemment été identifiée comme un facteur de risque pour la SEP, le rôle du métabolisme du cholestérol, des réponses immunitaires intestinales et du microbiote intestinal reste encore incertain. Dans le présent rapport composé de trois projets, nous cherchons à comprendre la relation entre l'environnement intestinal et les oxystérols, dérivés du cholestérol, lors du développement de l'auto-immunité du SNC.

Dans notre premier projet, nous avons démontré que l'immunologie intestinale et le microbiote sont impliqués dans le développement de la maladie EAE et affectent l'immunologie des cellules T pathogènes responsable de la maladie. Nous avons constaté que les cellules Th17 spécifiques de la myéline s'infiltrèrent dans le colon avant le développement des symptômes neurologiques dans deux modèles de SEP murine, l'EAE active et le EAE par transfert adoptif. Le fait de cibler spécifiquement la localisation intestinale des Th17 en bloquant la voie des intégrines perturbe la migration des lymphocytes T vers le colon et atténue la gravité de la maladie dans le modèle de transfert adoptif. De plus, les cellules Th17 spécifiques de la myéline prolifèrent dans le colon et ont une incidence sur la composition du microbiote intestinal, ce qui semble indiquer une contribution de l'axe intestin-cerveau dans le développement de l'auto-immunité du SNC. Ce travail fait l'objet d'une publication dans la revue *Cell Reports*.

Le deuxième projet a étudié comment les oxystérols modulent l'environnement intestinal lors du développement de l'auto-immunité du SNC et du développement d'une colite infectieuse. En effet dans une précédente étude, nous avons découvert que les souris déficientes pour certains oxystérols développent une maladie moins sévère associée à des retards de migrations de cellule Th17 dans le SNC. Nous avons constaté que l'infiltration de cellules Th17 était aussi retardée dans l'intestin lors du développement de la maladie à l'EAE chez les souris déficientes pour certains oxystérols. En utilisant un modèle infectieux spécifique de l'intestin, nous avons observé une réponse immunitaire innée altérée associée avec une élimination du pathogène retardée chez les souris déficientes en oxystérols. Avec notre étude, de nouvelles évidences suggèrent des orientations intéressantes pour des recherches futures telles que le mécanisme de la source locale d'oxystérols.

Dans le troisième projet, nous avons évalué l'effet de l'hypercholestérolémie sur les oxystérols et leur contribution au développement de la maladie EAE. Nous avons trouvé que la perturbation du taux de lipides en circulation induit une modulation de l'expression de gènes liés aux oxystérols, sans affecter significativement le développement de la maladie EAE. Nous avons aussi fourni de nouvelles preuves montrant que la perturbation du cholestérol circulant n'a pas d'impact sur le développement de l'auto-immunité du SNC.

Ce rapport fournit des arguments confortant le rôle de l'immunologie intestinale dans le développement de l'EAE. De plus, nos études confirment le rôle immunomodulateur des oxystérols au cours de l'EAE et de la colite et identifient les oxystérols comme cibles thérapeutiques potentielles pour le traitement des maladies inflammatoires et auto-immunes.

LIST OF ABBREVIATIONS

AID	Activation induced cytidine deaminase
BBB	Blood-brain barrier
BMDC	Bone marrow-derived dendritic cell
BMI	Body mass index
CFA	Complete Freund adjuvant
CH25H	Cholesterol 25-hydroxylase
CIS	Clinically isolated syndrome
cLP	Colonic lamina propria
CNS	Central nervous system
CP	Colonic patch
CSF	Cerebrospinal fluid
DC	Dendritic cell
DMT	Disease-modifying therapies
dLN	Dermal inguinal lymph node
EAE	Experimental autoimmune encephalomyelitis
EBI2	Epstein-Barr virus-induced G-protein coupled receptor 2
EBV	Epstein-Barr virus
FCS	Fetal calf serum
GALT	Gut-associated lymphoid tissue
HDL	High density lipoprotein
HFD	High fat diet
HLA	Human leukocyte antigens
IEL	Intraepithelial lymphocyte
IBD	Inflammatory bowel disease
IFL	Isolated lymphoid follicle
IgA	Immunoglobulin A
IL-1 β	Interleukin-1 β
IL-6	Interleukin-6
IL-10	Interleukin-10
IL-23	Interleukin-23
IL-27	Interleukin-27
ILC	Innate lymphoid cell
iNOS	Inducible nitric oxide synthase
LDL	Low density lipoprotein
LN	Lymph node
LP	Lamina propria
LTi	Lymphoid tissue inducer
LXR	Liver X receptor
MadCAM-1	Mucosal vascular addressin cell adhesion molecule 1
MBP	Myelin basic protein
MHC	Major histocompatibility complex
mLN	Mesenteric lymph node
MOG	Myelin oligodendrocyte glycoprotein
MOI	Multiplicity of infection
MRI	Magnetic resonance imaging

MS	Multiple sclerosis
OHC	Hydroxycholesterol
PBS	Phosphate-buffered saline
PP	Peyer's patch
PPMS	Primary progressive multiple sclerosis
ROR	Retinoic acid-related orphan receptors
ROS	Reactive oxygen species
RRMS	Relapsing remitting multiple sclerosis
SFB	Segmented-filamentous bacteria
siLP	Small intestine lamina propria
SILT	Solitary intestinal lymphoid tissue
SNP	Single nucleotide polymorphism
SPMS	Secondary progressive multiple sclerosis
SREBP	Sterol regulatory element-binding proteins
tChol	Total cholesterol
TCR	T-cell receptor
TG	Triglyceride
Th17	T helper 17
TNF α	Tumor necrosis factor α
Treg	Regulatory T
UC	Ulcerative colitis
VCAM-1	Vascular cell adhesion molecule 1
WT	Wild-type

TABLE OF CONTENTS

ACKNOWLEDGEMENTS	II
ABSTRACT (ENGLISH)	III
RESUME (FRENCH)	IV
LIST OF ABBREVIATIONS	V
TABLE OF CONTENTS	VII
LIST OF FIGURES	XI
LIST OF TABLES	XIII
1 INTRODUCTION	1
1.1 Multiple sclerosis.....	1
1.1.1 Introduction.....	1
1.1.2 Epidemiology.....	2
1.1.3 Treatments.....	3
1.1.4 Pathogenesis.....	3
1.1.4.1 Autoreactive T cell establishment.....	3
1.1.4.2 Migration to CNS via BBB.....	5
1.1.4.3 Inflammation against myelin and demyelination of axons.....	5
1.1.5 Etiology.....	6
1.1.5.1 Genetic factors.....	6
1.1.5.2 Environmental factors.....	7
1.1.5.2.1 Smoking.....	7
1.1.5.2.2 Epstein-Barr virus (EBV).....	7
1.1.5.2.3 Sunlight exposure and vitamin D.....	8
1.1.5.2.4 Gut environment and diet.....	9
1.1.5.2.5 Obesity, lipids and cholesterol metabolism.....	17
1.2 Oxysterols.....	18
1.2.1 Introduction.....	18
1.2.2 Immune active oxysterols and their ligands.....	19
1.2.2.1 Liver X receptor (LXR).....	19
1.2.2.2 Retinoic acid receptor-related orphan receptor (ROR).....	20
1.2.2.3 Epstein-Barr virus-induced G-protein coupled receptor 2 (Ebi2).....	20
1.2.3 Oxysterols in CNS autoimmunity.....	21

2 AIMS	24
3 PROJECT I: Impact of the gut environment during experimental models of multiple sclerosis	26
3.1 Materials and Methods.....	26
3.1.1 Animals.....	26
3.1.2 EAE induction and clinical evaluation.....	26
3.1.3 Antibody treatment.....	27
3.1.4 Antibiotic treatment.....	27
3.1.5 Isolation of immune cells.....	27
3.1.6 Flow cytometric analysis.....	27
3.1.7 Tetramer staining.....	28
3.1.8 RNA isolation and quantitative PCR analysis.....	28
3.1.9 Whole-mount immunostaining.....	28
3.1.10 Microbiome analysis.....	29
3.1.11 Statistical analysis.....	29
3.1.12 Key Resources Table.....	30
3.2 Results.....	32
3.2.1 Antigen-specific MOG Th17 cells infiltrate the colonic lamina propria during active EAE.....	32
3.2.2 Encephalitogenic TCR ^{MOG} 2D2 Th17 cells preferentially infiltrate the large intestine.....	34
3.2.3 Encephalitogenic TCR ^{MOG} 2D2 Th17 cells are in close contact with colonic blood vessels and egress via lymphatic vessels.....	37
3.2.4 Blocking integrin $\alpha 4\beta 7$ /MAdCAM-1 interactions inhibits TCR ^{MOG} 2D2 Th17 entry to the large intestine and significantly attenuates EAE.....	40
3.2.5 Colonic TCR ^{MOG} 2D2 Th17 cell express CNS-Integrin and their intestinal infiltrate resolves upon CNS invasion.....	44
3.2.6 Encephalitogenic TCR ^{MOG} 2D2 Th17 cells proliferate in the large intestine.....	48
3.2.7 Encephalitogenic TCR ^{MOG} 2D2 Th17 cells induce an intestinal dysbiosis and antibiotics treatments decrease encephalitogenic properties of Th17 cells.....	50
3.3 Discussion.....	55
4 PROJECT II: Role of oxysterols on gut immunology during EAE and pathogen-induced colitis	59
4.1 Materials and Methods.....	59
4.1.1 EAE induction and clinical evaluation.....	59
4.1.2 Isolation of immune cells.....	59

4.1.3 Flow cytometric analysis.....	59
4.1.4 Quantification of oxysterols.....	59
4.1.5 Whole-mount immunostaining.....	59
4.1.6 Microbiome analysis.....	59
4.1.7 RNA isolation and quantitative PCR analysis.....	60
4.1.8 <i>Citrobacter rodentium</i> infection.....	60
4.1.9 Generation, culture, and stimulation of BMDCs.....	60
4.1.10 Statistical analysis.....	60
4.2 Results.....	61
4.2.1 Increase Ch25h expression in intestine during EAE.....	61
4.2.2 Modulation of oxysterol level in the gut during EAE.....	61
4.2.3 Reduced intestinal infiltration of Th17 cells in Ch25h ^{-/-} mice during EAE	63
4.2.4 EAE induces morphological changes in the small intestine that are less pronounced in Ch25h ^{-/-} mice	66
4.2.5 EAE induces gut microbiota changes that are not impacted by Ch25h deletion.....	66
4.2.6 Delayed clearance of <i>C. rodentium</i> in Ch25h ^{-/-} mice.....	67
4.2.7 Ch25h ^{-/-} mice show abnormal innate immune response to <i>C. rodentium</i>	69
4.2.8 Ch25h ^{-/-} BMDCs have an impaired IL-23 response to bacterial challenge.....	70
4.2.9 Ch25h ^{-/-} mice have decreased level of CD4 ⁺ type 3 innate lymphoid cells.....	72
4.3 Discussion.....	73

5 PROJECT III: Role of oxysterols during hypercholesterolemia and the contribution in EAE disease..... 77

5.1 Materials and Methods.....	77
5.1.1 Animals and diet.....	77
5.1.2 EAE induction and clinical evaluation.....	77
5.1.3 Antibody treatment.....	77
5.1.4 Flow cytometric analysis.....	77
5.1.5 Quantification of lipid profile.....	77
5.1.6 RNA isolation and quantitative PCR analysis.....	77
5.1.7 Isolation of CNS immune cells.....	77
5.1.8 Antigen-specific proliferative and cytokine responses.....	78
5.1.9 Statistical analysis.....	78
5.2 Results.....	78

5.2.1 Intestinal Ch25h expression increases during hypercholesterolemia.....	78
5.2.2 Ch25h deficiency has no major role on lipid profile in transgenic model of hypercholesterolemia.....	79
5.2.3 Ch25h ^{-/-} mice conserve their delayed EAE disease phenotype in hypercholesterolemic conditions.....	80
5.2.4 Effect of hypercholesterolemia during EAE on male and female mice.....	82
5.2.5 anti-PCSK9 decrease circulating cholesterol without alleviating EAE symptoms.....	83
5.2.6 anti-PCSK9 treatment does not show altered systemic immune responses....	85
5.3 Discussion.....	85
6 GENERAL CONCLUSIONS.....	87
7 REFERENCES.....	89
8 APPENDICES.....	107
8.1 Appendix A - Curriculum vitae.....	107
8.2 Related articles published in scientific peer-reviewed journals.....	109
8.2.1 Appendix B - Disrupting myelin-specific Th17 cell gut homing confers protection in an adoptive transfer experimental autoimmune encephalomyelitis.....	109
8.2.2 Appendix C - Oxysterols and autoimmunity.....	135

LIST OF FIGURES

Figure 1. Different forms of MS.....	page 1
Figure 2. Global prevalence of multiple sclerosis in 2013.....	page 2
Figure 3. Immune system dysregulation outside the CNS.....	page 4
Figure 4. Intestinal mucosal immune system.....	page 11
Figure 5. Gut microbiota affects extra-intestinal autoimmune diseases.....	page 12
Figure 6. Immunoactive oxysterols and their pathways of activation.....	page 21
Figure 7. Schematic drawing illustrating the interplay between lipid metabolism, gut environment and central nervous system inflammation.....	page 25
Figure 8. MOG-specific Th17 cells infiltrate the large intestine during active EAE.....	page 33
Figure 9. Encephalitogenic TCR ^{MOG} 2D2 Th17 cells infiltrate preferentially the large intestine and are located in the colonic lamina propria during EAE.....	page 35
Figure 10. TCR ^{MOG} 2D2 Th17 cells enter the colon in an antigen-independent manner but at higher levels than TCR ^{MOG} 2D2 Th1 cells.....	page 36
Figure 11. Encephalitogenic TCR ^{MOG} 2D2 Th17 cells are located in close contact to blood and lymphatic vessels.....	page 38
Figure 12. Encephalitogenic TCR ^{MOG} 2D2 Th17 cells migrated through the mesenteric lymph nodes but not the dermal inguinal lymph nodes.....	page 39
Figure 13. Blocking integrin $\alpha 4\beta 7$ reduces migration of encephalitogenic TCR ^{MOG} 2D2 cells to the colon and delays the progression of EAE disease.....	page 41
Figure 14. Continuously blocking of $\alpha 4\beta 7$ -integrin alleviates adoptive-transfer EAE but not active EAE.....	page 43
Figure 15. Encephalitogenic TCR ^{MOG} 2D2 Th17 cells infiltrate the large intestine and express CNS-specific integrin before reaching the CNS.....	page 45
Figure 16. Encephalitogenic TCR ^{MOG} 2D2 Th17 cells maintain their pathogenic phenotype throughout EAE disease.....	page 47
Figure 17. Encephalitogenic TCR ^{MOG} 2D2 Th17 cells proliferate in the colon.....	page 49
Figure 18. Encephalitogenic TCR ^{MOG} 2D2 Th17 cells impact gut microbiota composition...	page 51
Figure 19. Antibiotic treatment does not influence TCR ^{MOG} 2D2 Th17 infiltration in the colon.....	page 53
Figure 20. Disrupting myelin-specific Th17 cell gut homing confers protection in an adoptive transfer experimental autoimmune encephalomyelitis.....	page 58
Figure 21. Increase Ch25h expression in the gut during EAE disease.....	page 61
Figure 22. Oxysterol levels in the small intestine and the colon during the development of CNS autoimmunity.....	page 62
Figure 23. Reduced Th17 proportion in the small and large intestine during EAE disease.....	page 64
Figure 24. EAE disease affects intestinal morphology.....	page 66
Figure 25. Ch25h deletion have no major impact on gut microbiota during EAE.....	page 67
Figure 26. Delayed clearance of <i>C. rodentium</i> in Ch25h ^{-/-} mice.....	page 68

Figure 27. Ch25h^{-/-} mice have an abnormal innate immune response during infection..... page 69

Figure 28. Ch25h^{-/-} BMDCs have an ineffective IL-23 response to bacterial challenge..... page 71

Figure 29. Ch25h^{-/-} mice have decreased level of CD4⁺ ILC3 cells in the colonic lamina propria.....page 72

Figure 30. Ch25h expression increases in the gut during hypercholesterolemia..... page 79

Figure 31. Ch25h deficiency has no major role on baseline lipid profile in transgenic model of hypercholesterolemia under normal diet page 80

Figure 32. Effect of hypercholesterolemia and oxysterols during EAE disease..... page 81

Figure 33. Hypercholesterolemia do not exacerbate EAE disease in male nor in female mice..... page 82

Figure 34. anti-PCSK9 decrease circulating cholesterol without alleviating EAE symptoms.....page 84

Figure 35. anti-PCSK9 treatment do not show altered systemic immune responses..... page 85

LIST OF TABLES

Table 1. Established and possible lifestyle and environmental risk factors for MS.....	page 9
Table 2. Role of the gut microbiome during EAE.....	page 13
Table 3. Impact of diet intervention during EAE.....	page 15
Table 4. Dietary studies on MS patients.....	page 16
Table 5. Blocking integrin $\alpha 4\beta 7$ attenuates disease course in adoptive transfer EAE.....	page 42
Table 6. Changes in the relative abundance of bacterial taxa in fecal mouse microbiota observed after injection of TCR ^{MOG} 2D2 Th17 cells.....	page 54
Table 7. Ch25h ^{-/-} mice depicted delayed EAE disease independently of hypercholesterolemia	page 82

1. INTRODUCTION

1.1 Multiple sclerosis

1.1.1 Introduction

Multiple sclerosis (MS) is chronic disease affecting the central nervous system (CNS) including the brain, spinal cord and optic nerves. It is a common neurologic and autoimmune disorder leading to demyelination and axonal damages. As the disease can target multiple sites of the CNS, the clinical symptoms are various. Fatigue is one of the most frequently reported symptoms of MS [1]. In addition, coordination and balance problems, altered sensation as well as visual troubles are symptoms often observed in patients. MS was first described by the French neurologists Jean-Martin Charcot and Alfred Vulpian in 1868 [2]. There are currently three types of MS defined: relapsing remitting (RRMS), secondary progressive (SPMS) and primary progressive multiple sclerosis (PPMS) [3] (Fig. 1). If a patient has symptoms of MS that do not fulfill entirely the diagnostic criteria (Mc-Donald criteria 2017), a clinically isolated syndrome (CIS) can be diagnosed. CIS is recognized as the first clinical episode of neurological symptoms characteristic of inflammatory and demyelination, mainly optic nerves, brainstem or spinal cord. Including up to 85% of total MS patients, RRMS is the most frequent MS disease course. This form is characterized by recurrent attacks in which symptoms appear (relapse) and resolve (remitting) completely or partially after time (Fig. 1A) [4]. SPMS starts by a relapse-remitting course, which is followed by a gradual worsening of neurological functions with or without acute relapses during the progressive course (Fig. 1B) [3]. 80% of untreated patients with RRMS convert to SPMS. However, disease-modifying therapies (DMT) have been associated with a lower risk of conversion to SPMS [5]. PPMS is characterized by a gradual exacerbation of neurological functions from the onset of the symptoms without relapsing-remitting episodes (Fig. 1C).

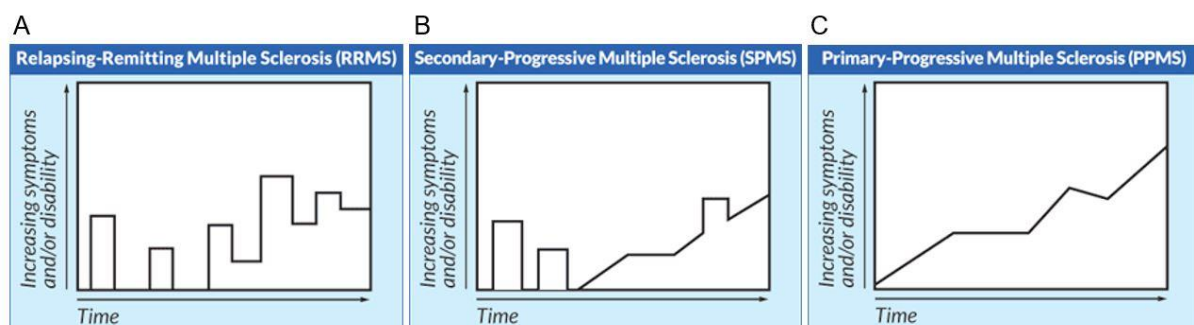


Figure 1. Different forms of MS.

Representation of typical RRMS (A), SPMS (B), and PPMS (C) disease course over time. Adapted from: <https://mymsaa.org/ms-information/overview/types/>

1.1.2 Epidemiology

MS is the most common cause of non-traumatic disease of the CNS among young adults. Most MS patients are diagnosed between 20 to 50 years old although the disease can also occur in children and older adults. The disease affects more than 2 million of people worldwide and constantly increase [6]. The prevalence of the disease differs in term of geographical area (Fig. 2). In Switzerland, the last epidemiological study was done in 1986 and reported a minimal prevalence rate of 110 MS cases per 100,000 inhabitants. Switzerland is part of countries with the highest prevalence of MS, including USA, Canada, Spain, Great-Britain, Italy Germany and Nordic countries [7].

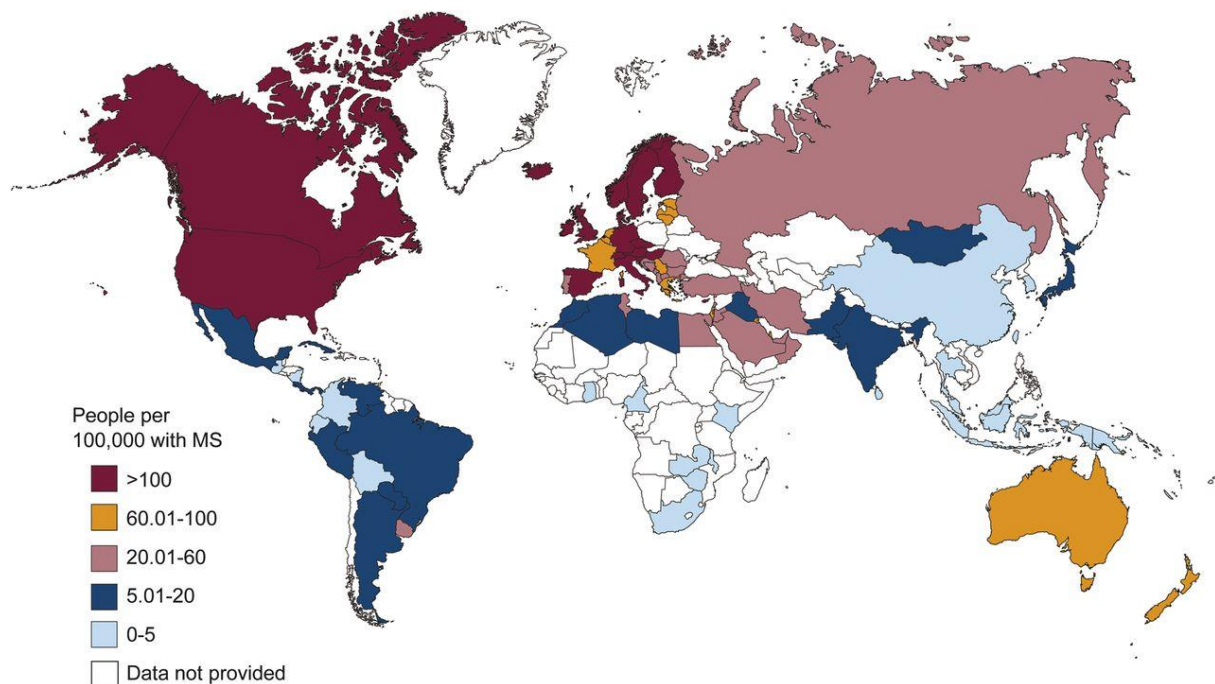


Figure 2. Global prevalence of multiple sclerosis in 2013.

Schematic representation of the individuals affected by MS per 100'000 individuals.

Taken from © www.atlasofms.org, MSIF 2013, [8].

Like for other autoimmune disease, male/female disparity has been reported. Indeed, MS disease is more frequently (two to three time more) observed in women than in men [9] [10], suggesting a potential role of hormonal factors in the development of MS. Another example supporting this theory is the fact that women have less relapses during their pregnancy [11]. Finally, individuals are more likely to develop MS if they already have other autoimmune disorders. It has been previously reported that patients type 1 diabetes have an increased risk to be affected by MS [12]. In the same line, studies have reported that patients with inflammatory bowel disease (IBD) have a higher risk to develop demyelinating disease and MS [13] [14].

1.1.3 Treatments

The exact cause of MS remains still unknown and there is currently no cure for the disease. Existing treatments focus on the symptoms and prevention of a new inflammatory relapse that can be either clinical or radiological. Treatments for MS can be divided in two categories. The first one is called symptomatic-therapies and focus on symptoms resulting from neurological dysfunction that can be used also in other type of disease [15]. Acute relapses of MS are caused by inflammation of CNS and most of them will resolve without treatment. Corticosteroids are often used to lower and relieve inflammation. These treatments aim to accelerate recovery from relapse but do not show benefit in long-term recovery [16]. The other category of treatments is called disease-modifying therapies (DMT) that are focusing on MS-specific inflammatory features in order to prevent relapses and possibly progression of the disease. This category includes immunomodulatory/immunosuppressive drugs (i.e. interferon beta, glatiramer acetate, fingolimod, teriflunomide, dimethylfumarate, natalizumab and ocrelizumab) [15]. They all act on the immune system to suppress at different levels inflammation and therefore MS disease activity. Recently other drugs called immune reconstitution therapies have been developed. They are given in short treatment course and lead to the reduction of immune cells in the body and reconstruction of immune cell reservoir. With this type of new treatments, including alemtuzumab and cladribine, immune system is reset in the direction of a non-self-aggressive or self-reactive immune system [17].

1.1.4 Pathogenesis

1.1.4.1 Autoreactive T cell establishment

During decades, the pathogenesis of MS has been much debated. MS is a complex disease with several forms including different clinical outcomes and potentially diverse pathological phenotypes associated. However, with progress in immunology and the benefits of immunomodulator treatments, it is now well accepted that inflammatory immune-mediated processes responsible for the disease could raise from autoimmune mechanisms involving autoreactive T lymphocytes (CD4⁺ or CD8⁺) that have aberrant responses against CNS self-antigens [18] [19]. For the moment, no specific autoantibody has been found in order to directly prove that MS is an autoimmune disease. However, previous studies have strongly supported the hypothesis of immune-mediated involvement for MS development. For example, T cells reactive for myelin basic protein (MBP), a protein component of the myelin sheet, have been described in MS plaques [20] [21]. Specific type of CD4⁺ T helper cells called T helper 17 (Th17) cells have been associated with active MS lesions [22] [23] [24]. Moreover, this theory is also consistent with the experimental models used to induce and study MS in animal model. Indeed, the induction of the so-called experimental autoimmune encephalomyelitis (EAE) is

done by the administration of myelin peptide and adjuvant in the periphery. It induces the development of reactive CD4+ T cells against myelin followed by their migration through blood-brain barrier (BBB) and the attack to the myelin sheath in the CNS. In MS, the precise reasons why autoreactive lymphocytes are created against CNS self-antigens remain still unknown. However, several mechanisms could potentially explain where this issue comes (Fig. 3). In the self/non-self discrimination, T cells must have a broad range of reactivity for foreign antigens and in parallel no reactivity to self-antigens (as known as tolerance). Mechanisms to assure tolerance involved deletion of autoreactive T lymphocytes during their maturation (central tolerance) and suppression of autoreactive T lymphocytes in the periphery that have escaped the selection (peripheral tolerance) [25]. The central tolerance occurring in the thymus eliminates most autoreactive T lymphocytes but not the totality and some of them are released in the periphery. In healthy individuals, peripheral tolerance can control these harmful cells through regulatory T (Treg) cells. Defects occurring in the peripheral tolerance such as Treg cells dysfunction or resistance from the effector B and T cells to the suppressive mechanisms can lead to autoimmunity, including MS disease [25]. In addition, autoreactive adaptive cells can be activated in the periphery by molecular mimicry. This mechanism involved the presentation of foreign antigens to T cell that share similar part of a self-protein. Typically, at mucosal surface, innate immune cells integrate bacteria or virus antigens and present their MHC-peptide complex to T cells triggering T cell activation and potential risk of autoimmune reaction if this antigen shares same structure as a self-antigen [26] [27] [28] [29].

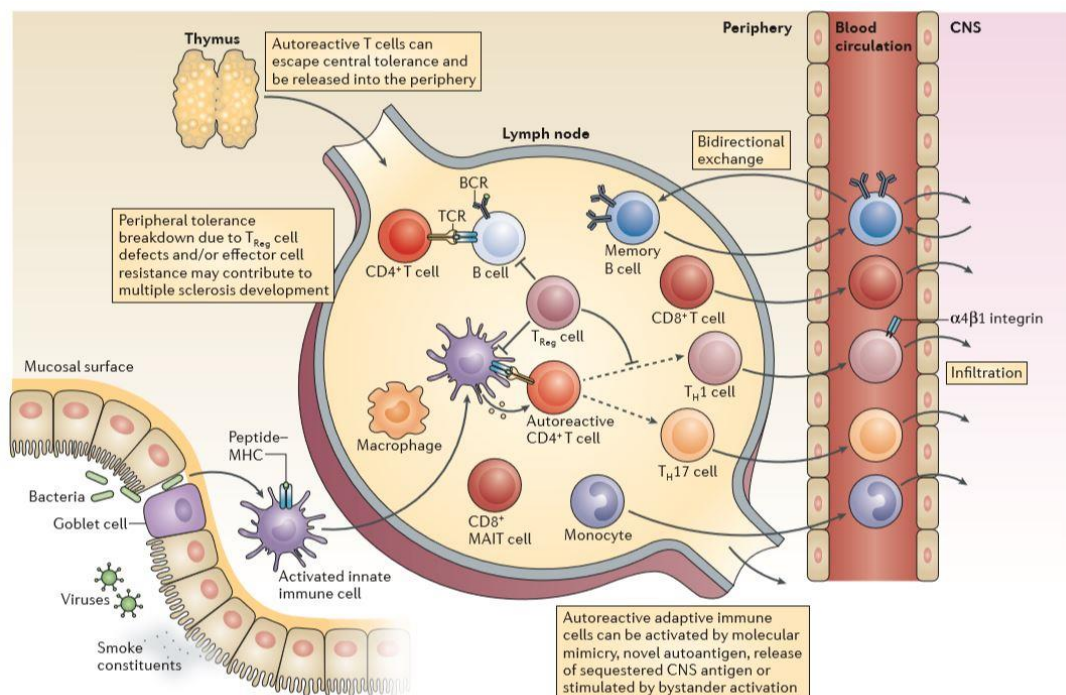


Figure 3. Immune system dysregulation outside the CNS. Schematic representation of how autoreactive T cells can escape the central and peripheral tolerance. Taken from [26].

1.1.4.2 Migration to CNS via BBB

After their activation in the periphery, autoreactive immune cells can migrate to the CNS through the BBB. The BBB is physical barrier composed of endothelial cells interconnect by tight junction that limit the trafficking from the blood to the CNS. Under physiological conditions, endothelial cells express molecular signals such as chemokines or interleukins that prevent the entry of leukocyte. Perturbation of BBB occurs during pathological conditions associated with a pro-inflammatory environment. The BBB is not anymore permeable and pathogenic immune cell can invade the CNS [30]. In MS disease, alteration of BBB is observed and associated with an increase permeability during the formation of new lesions [31]. Studies using magnetic resonance imaging (MRI) suggest that these alterations occur before the myelin damage and clinical manifestation of the disease in MS patients [32]. Interestingly, similar observations have been described in the EAE model [33] [34]. In relation with immune cell trafficking, the development of drug, such as natalizumab, is another example of BBB involvement in MS pathogenesis. At the blood endothelium surface, a series of cell adhesion molecules allow the binding with other cells and participate to leukocyte extravasation. Among them, vascular cell adhesion molecule 1 (VCAM-1) expressed on some type of endothelium (i.e. BBB) act as a ligand for $\alpha 4$ integrin present on lymphocytes, allowing strong adhesion and transmigration of lymphocytes across BBB [35]. In this context, natalizumab is the first $\alpha 4$ integrin antibody developed for the treatment of MS. The drug is a monoclonal antibody acting as $\alpha 4$ integrin antagonist and prevent the transmigration of lymphocytes through BBB. This drug was developed using EAE model and give another example that experimental model is relevant for evaluation of immune cell migration in the context of MS [36] [26].

1.1.4.3 Inflammation against myelin and demyelination of axons

Once autoreactive lymphocytes reach the CNS, they encounter their cognate myelin antigens. They secrete pro-inflammatory cytokines and chemokines leading to inflammatory environment and activation of glial cells including microglia and astrocytes. Microglia can have both damaging and protective functions in the context of neuropathology. Indeed, pro-inflammatory microglia can release inflammatory cytokines leading to tissue damage. On the other hand, anti-inflammatory subsets are able to decrease inflammation and help for tissue repairs processes [37] [38]. Beside activation of microglial cells, other type of cells are involved in the inflammatory plaque formation. As previously mentioned, T cells are present within the plaque to recruit and activate other immune cells. CD4⁺ T cells seems to be important in the initial phase of MS pathogenesis while CD8⁺ T cells are the predominant cells population present within plaques during relapses and potentially during chronic phase of the disease [39] [40]. CD8⁺ T, also known as cytotoxic T cells, can directly interact with

oligodendrocytes and kill them using perforin-based or Fas-based cytotoxicity [41]. Treg, that was previously presented as major cell type for peripheral tolerance, is also involved in CNS to dampen the inflammation. However in MS disease, studies have reported that Treg derived from peripheral blood of patients have a loss of functional suppression [42] and could explain partially the reduced amount of naïve Treg in MS patients compared to healthy controls [43] [44]. B cells and plasma cells are other type of immune cell important for pathogenesis of MS even if their mechanism in this pathology are currently under investigation. Studies have shown that B cells are present in MS plaques and oligoclonal immunoglobulin bands in the cerebrospinal fluid (CSF) are found in MS patients [45] [46]. In addition, B cell-depleting therapies have provided strong evidence for the involvement of B cells in MS disease [47] [48]. However, the proportion of plasma cells and antibodies level remain unchanged after B-cell depletion therapies, suggesting that B cell have other antibody-independent implications in MS such as antigen presentation, T cell activation or cytokine production [49] [50]. One recent example is the study, published by *Roja et al*, showing that some type of plasma cells, derived from the gut and not affected by B-depletion drug, can produced anti-inflammatory cytokine (interleukin-10) and improve the disease evolution in experimental EAE model [51]. In addition, B cells are known to become activated through T cells and this interaction is a major interrogation during MS development. One recent publication has demonstrated that this interaction lead to activation and autoproliiferation previously reported as important mechanism during MS pathogenesis [52] [53]. Altogether, these findings demonstrate how MS immunopathogenesis involves a multitude of cell types and how complex are their interactions that at the end lead to the destruction of myelin sheet of the axons indispensable for the proper signaling function of neurons.

1.1.5 Etiology

1.1.5.1 Genetic factors

The exact cause of MS is still unknown and appears to be multifactorial including both genetic and environmental factors [4]. MS disease is not an inherited disease, but it exists genetic predispositions inherited that increase the risk. The first genetic risk factor discovered for MS was HLA-DR2 (HLA-DRB1*15) which is a haplotype of human leukocyte antigens (HLA) encoded in the major histocompatibility complex (MHC) [54] [55]. Indeed, *HLA-DRB1*1501* and *DRB1*1503* are alleles susceptible to the onset of MS [56]. Genome-wide association studies have identified over 110 single nucleotide polymorphisms (SNPs) associated with MS susceptibility [57] [58]. These SNPs are part of genes mainly associated to immune system regulators (such as interleukin-2 receptor, interleukin-7 receptor and vitamin D metabolism [59] [60]). Finally, twin studies have reported that the concordance does not exceed 30% in

monozygotic twins, indicating that environmental factors contribute importantly in the development of MS [61].

1.1.5.2 Environmental factors

1.1.5.2.1 Smoking

Smoking has been described as environmental factor associated with development of MS [62]. Smoking is also described as an important risk factor for other autoimmune disease such as rheumatoid arthritis and systemic lupus [63] [64]. The dose of smoking is important as the more individual smokes, the higher is the risk of MS, showing a dose-response relationship [62]. Passive tobacco smoke exposure has also been reported to increase the risk of MS through lung irritation. However, the study was only done once and should be repeated to confirm these findings [65], as shown in Table 1. Lung irritation can also occur during exposure with air pollutant and organic solvent and could promote neuroinflammation and autoimmune disease [66] [67]. Smoking cause oxidative stress and pro-inflammatory responses in the lung that could lead to activation of potential autoantigenic cells present in the organs. Using experimental model, one study has demonstrated that the lung environment can contribute to the activation and the migration of encephalitogenic autoreactive immune cells [68]. Another possibility is that lung inflammation can lead to higher permeability of lung epithelium that increase the contact between immune cells and pathogens increasing the probability of molecular mimicry phenomenon described previously [69]. Interestingly, oral tobacco has a dose-dependent association with a decrease risk of MS [62]. The protective effect may be attributed to nicotine that can bind to alpha-7 subunit acetylcholine receptor of immune cells and reduce its activity important for regulation of immune function [70]. This study strengthen that lung inflammation drives the risk factor related to smoking, despite the potential protective effect of nicotine [71].

1.1.5.2.2 Epstein-Barr virus (EBV)

Several infectious agents including virus and bacteria have been proposed to contribute in MS disease. Among them, Epstein-Barr virus (EBV) have been intensively studied over the past years and number of research papers indicate that EBV seropositivity is strongly associated with onset of MS even if its causal role is still debated [72]. Studies have reported that 100% of adult MS patients are EBV seropositive in contrast to 96% of adult healthy controls. In children with MS, the proportion of seropositivity were also significantly higher when compared to aged-match healthy controls [73] [74]. EBV is a γ -herpes virus that infect B lymphocytes and establishes a latent infection. The infection is asymptomatic for most people but in some case, it can lead to an infectious mononucleosis in young adults [75]. Several hypotheses have been proposed to explain the role of EBV infection in the development of MS [76]. The first theory

was molecular mimicry. Indeed, past studies have demonstrated the presence of T cells specific for MBP, that also react with an antigen coming from EBV (EBVNA1) [77] [78]. One group found that CD4⁺ T cells from CSF of MS patients can recognize autologous EBV-transformed B cells. More recently, they demonstrated that a high proportion of these cells are able to cross-recognize EBV and MBP protein [79]. Besides from molecular mimicry, recent studies revealed other possible mechanisms such as transformation of B cell. As previously mentioned, B cells are part of the MS pathogenesis and autoreactive B-cells are normally controlled by central and peripheral tolerance. EBV gene products could change B cells physiology and create B cells that are resistant to peripheral B cell tolerance [80]. Regarding experiment models, EBV cannot be used in EAE model as the virus does not infect mice. However, using another animal model called Japanese monkey encephalomyelitis, in which nonhuman primates develop a spontaneous MS-like disease, Axthelm *et al.*, have isolated a new simian gamma-herpesvirus that was cultured from acute white matter lesions, belonging to the same family as EBV [81]. There is a clear association between EBV and MS but whether EBV is active on the pathogenesis of the disease or only a bystander effect remains to be further investigated [82].

1.1.5.2.3 Sunlight exposure and vitamin D

As previously shown in Figure 2, epidemiological studies have reported that MS incidence and prevalence have different geographical distributions. Indeed, several studies including one recent meta-analysis have reported a significant latitude-dependent variation in MS prevalence, even after adjustment for HLA-DRB1 allele frequencies that is enriched in certain regions [83] [84]. It supports a role for environmental factors that change with latitude. Seasonal sunlight exposure, which impacts ultraviolet radiation and furthermore vitamin D level, have been identified as the most potent factors to explain this association [6]. Indeed, high latitude regions have less ultraviolet radiation exposure [82]. As ultraviolet radiations are responsible for the synthesis of active vitamin D form, it is often difficult to separate these two factors [72]. Ultraviolet radiations and vitamin D level are both associated with a decreased risk of MS [85]. A protective effect of vitamin D has been supported by reduced risk of MS associated with sun exposure and use of diet vitamin D supplementation [86] [87]. Ongoing research suggests that vitamin D level in the serum impacts the risk of MS and can change disease activity in MS patients [88]. High circulating level of vitamin D is associated with reduced risk of MS [89]. On the contrary, low level of vitamin D correlates with an increased risk. Sources of vitamin D are low in food. Most of our vitamin D comes from cholesterol and is converted inside our body using sunlight. Cholesterol is converted to 7-dehydrocholesterol which is the vitamin D₃ precursor. In the skin, this precursor is further converted into cholecalciferol (vitamin D₃) by UVB irradiation. In the liver, vitamin D₃ is hydroxylated in 25-hydroxyvitamin

D3 and further metabolized in the kidney into 1,25-dihydroxyvitamin D3 which is the active form of vitamin D. Functionally, vitamin D is well known as a calcium homeostasis modulator. However, vitamin D have also several roles on immune system that could be associated with MS pathogenesis. For example, it has been shown that vitamin D receptor is expressed in several immune cells including dendritic cell and macrophage, B cells and T cells [90] [91] [92]. Studies have also suggested that 1,25-dihydroxyvitamin D can modulate CD4⁺ T cells and induces anti-inflammatory proprieties via dendritic cells [93]. 1,25-dihydroxyvitamin D have been described to reduce proliferation in B cells, differentiation of plasma cells and production of immunoglobulins [92]. Using EAE model, 1,25-dihydroxyvitamin D have been reported to reduce autoreactive T cells and the disease score activity [94] [95]. Contrary to expectations, mice deficient for vitamin D receptor significantly lower the EAE disease development [96] [97]. Even with the recent extensive literature on vitamin D, its association with MS need to be further investigated.

Factor	OR	HLA gene interaction	Combined OR (nongenetic factor + HLA allele)	Effect during adolescence	Immune system implied	Level of evidence
Smoking	~1.6	Yes	14	No	Yes	+++
EBV infection (seropositivity)	~3.6	Yes	~15	Yes	Yes	+++
Vitamin D level <50 nM	~1.4	No	NA	Probably	Yes	+++
Adolescent obesity (BMI >27 at age 20 years)	~2	Yes	~15	Yes	Yes	+++
CMV infection (seropositivity)	0.7	No	NA	Unknown	Yes	++
Night work	~1.7	No	NA	Yes	Yes	++
Low sun exposure	~2	No	NA	Probably	Yes	++
Infectious mononucleosis	~2	Yes	7	Yes	Yes	++
Passive smoking	~1.3	Yes	6	No	Yes	+
Organic solvent exposure	~1.5	Unknown	Unknown	Unknown	Unknown	+
Oral tobacco/nicotine	0.5	No	NA	Unknown	Yes	+
Alcohol	~0.6	No	NA	Unknown	Yes	+
Coffee	~0.7	No	NA	Unknown	Yes	+

Level of evidence for a role of a particular lifestyle or environmental factors in MS is not easy to define. Large prospective studies are, with few exceptions, rare in MS. CMV, cytomegalovirus; EBV, Epstein-Barr virus; HLA, human leukocyte antigen; MS, multiple sclerosis; NA, not applicable; OR, odds ratio; +++, high level of evidence: drawn from large prospective studies or if a case-control observation is supported by Mendelian randomization studies; ++, Case-control observations, if replicated and/or supported by independent methods; +, Non-replicated observations (included to enable further observations).

Table 1. Established and possible lifestyle and environmental risk factors for MS.
Taken from Olsson et al., 2017 [71].

1.1.5.2.4 Gut environment and diet

In the past decades, growing evidence have highlighted that the gut environment can influence processes occurring in CNS lead to the concept of “*gut-brain axis*”. In addition, gut environment has been suggested to play important roles at systemic level and particularly during autoimmune disease. Therefore, the scientific community has started to study the importance of the gut environment during MS disease. Among digestion and uptake of nutrients that are

essential for the body, the gastrointestinal tract is in close contact with many antigens from food and microbes and its immune system must maintain homeostasis [98]. Indeed, the gut environment includes also gut microbiota which is a complex community of bacteria that live inside the intestine. To maintain this homeostasis, the gastrointestinal tract can count on the largest immune reservoir in the body: the gut-associated lymphoid tissue (GALT) [99] [100] [101]. Structurally, GALTs include Peyer's patches (PPs), solitary intestinal lymphoid tissues (SILT), and mesenteric lymph nodes (mLNs) (Fig. 4) [102] [103]. In addition, diffusely distributed lymphoid and plasma cells located in the lamina propria (LP) of the gut and intraepithelial lymphocytes (IELs) are part of the GALTs.

PPs are one of the sites responsible for induction of immune response in the intestine. They are lymphoid aggregates found under the mucosal epithelial cell layer of the small intestine [104]. In the large intestine, colonic patches (CPs) represent the equivalent of PPs [105]. These lymphoid aggregates are composed of large B cell follicles with intervening smaller T-cell areas [98].

MLNs are another compartment involved in the induction phase. MLNs are the largest lymph nodes in the body in which the lymphatic fluid from the intestinal lamina propria is screened. The main role of mLNs is to initiate immune responses or tolerance against antigens present in the lymph, either in free form or carried by dendritic cells (DCs) [98] [106].

SILTs are organized lymphoid structures including isolated lymphoid follicle (IFL) and cryptopatches. Contrary to other secondary lymphoid organs, development of SILTs starts during the first days after birth with accumulation of lymphoid tissue inducer (LTi) cells that form clusters called cryptopatches. Cryptopatches recruit B cells and further develop into more complex structure called IFLs. Mature IFLs share similar appearances to PPs and CPs but contain only one large B cell follicle, while PPs and CPs contain several [107].

Lamina propria (LP) is the connective tissue situated under the epithelial cell layer. Most of intestinal immune cells are located in this space including mainly CD4⁺ T cells, CD8⁺ T cells, plasma cells producing IgA and the recently described innate lymphoid cells (ILCs) [98] [108]. In the LP, these cells exert their effector response in order to prevent entry and systemic spread of pathogens.

IELs are specialized lymphocytes located inside the mucosal layer, between the adjacent epithelial cells. These lymphocytes have an important role in immune defense against pathogens as they have access directly to gut antigens [109]. With their close contact with epithelial cells, they are also important in maintaining gut mucosal homeostasis [110].

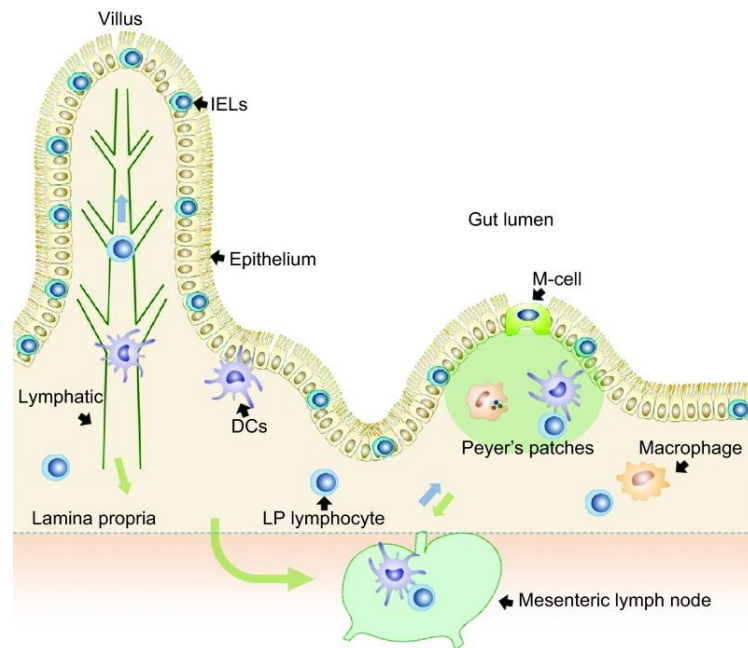


Figure 4. Intestinal mucosal immune system.

Schematic representation of the GALTs and the structural gut organization. Taken from Wu *et al.*, 2014 [111].

As previously mentioned, the major function of GALTs is to fight against harmful pathogen invasion and to maintain tolerance for commensal bacteria. To do so, DCs present under the epithelial cell layer can sample antigens present in the lumen using cellular extensions between epithelial layer into lumen [112]. In addition, special epithelial cell subsets called M cells can endocytosis and facilitate the uptake of antigens to DCs in the PPs [113]. DCs move to T cell areas or B cell follicles where they can activate naïve lymphocytes. In PPs and CPs, signals from DCs and T cells can further influence the development of immunoglobulin A (IgA) secreting B cells [114]. IgA is one of the first line of immune protection in mucosal surface as it has the capability to cross the epithelial cells and be secreted into the lumen [115]. Active lymphocytes can migrate through mLNs, the thoracic duct and then the blood circulation in order to reach the intestinal LP, where they will contribute to the effector phase [101] [104]. Gut microbiota is composed of a complex ecosystem, including both commensal and pathogenic strain of microbes. The colonization of our gut is estimated at 10^{13} bacteria comprising in more that thousands bacterial species [116]. Indeed, in one recent publication, authors have listed a total of 2172 species isolated in humans that can be classified into 12 different phyla. Most of them (93.5%) belong to four bacterial phyla: Firmicutes, Proteobacteria, Actinobacteria, and Bacteroidetes [117]. As described above, gut immune system is in close contact with microbes and their metabolites. The gut immune system is well known to shape the gut microbial community. On the other hand, microbiota can influence the host immune system. One interesting example in our context is the capacity of specific commensal bacteria

to induce Th17 cells, a subset of T cells enriched in the gut and important for host defense and autoimmunity [118]. It has been shown that germ-free mice have absence of Th17 cells in the intestine [119]. However, when the mice are recolonized with commensal microbiota, the level of Th17 cells reach the physiological level. By analyzing microbiota of mice divergent for Th17 cell level in the gut, Ivanov *et al.* found that a specific species called segmented-filamentous bacteria (SFB) are inducer of Th17 cells in the gut [120].

As previously introduced, recent evidence suggested that the gut environment has the capacity to affect the development of non-intestinal autoimmune disease including CNS autoimmunity, rheumatoid arthritis and type 1 diabetes (Fig. 5).

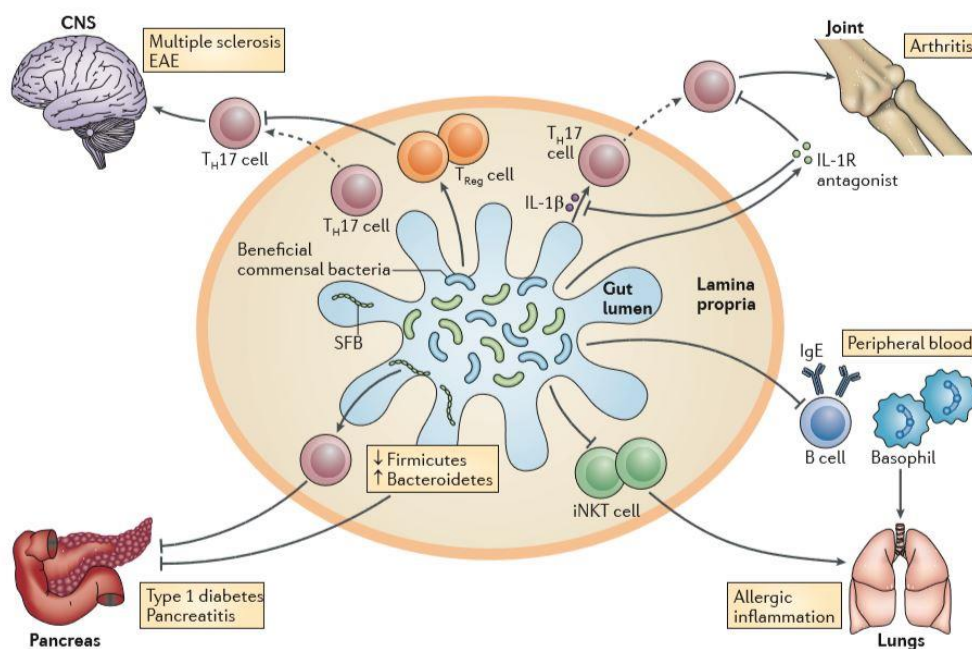


Figure 5. Gut microbiota affects extra-intestinal autoimmune diseases.

Schematic representation of the impact of gut environment in other peripheral tissues.

Taken from Kamada *et al.*, 2013 [118].

Regarding MS, several recent studies have reported a significant change in microbiota composition of MS patients compared to healthy controls [121] [122] [123]. Moreover, in one study, changes in the bacterial community (also known as dysbiosis) have been associated with variations in the expression of genes involved in immune response [121]. Focusing on the gut immune system, one interesting study has reported a high frequency of intestinal Th17 cells in MS patients compared to healthy individuals [124]. Moreover, this result correlated with microbiota alterations in MS patients and disease activity. As introduced previously, Th17 cells are suggested to be a major actor in the development of MS and activation of these cells occurs mainly in the gut. In addition, autoreactive lymphocytes that target myelin peptide enhances their pathogenicity when they acquire a Th17 phenotype in the

gut, suggesting a great role of gut-primed Th17 cells in CNS autoimmunity [125] [126]. However how precisely these processes occur in the gut remain to be further investigated. Interventional treatments on MS patients using bacteria are currently developed [127]. For example, effect of probiotics, defined as beneficial microorganisms, has been assessed in MS patients. Despite the small size of the cohort, Tankou *et al.* have report that supplementation of probiotic cocktail composed of 8 different strains (4 *Lactobacillus*, 3 *Bifidobacterium* and 1 *Streptococcus*) has the capability to reverse the dysbiosis observed in MS patients that were associated with increase anti-inflammatory response in peripheral monocytes and DCs [128]. As interventional studies using bacteria are still difficult to performed in human, a lot of knowledge in the field are coming from experimental models resumed in a recent review (Table 2).

Reference	Animal model	Intervention	Clinical score	Immune response
Berer et al. (47)	SJL anti-MOG ₃₂₋₁₀₆ TCR ^{tg}	Germfree housing	Protected	Reduced T _{H17} , impaired B-cell recruitment to brain-draining lymph nodes Reduced anti-MOG B cell response
Lee et al. (48)	C57Bl/6 MOG ₃₅₋₅₅	Germfree housing	Decreased	Reduced T _{H1} and T _{H17} , increased T _{reg} Reduced DC capacity to induce T _{H1} and T _{H17} responses
Yokote et al. (49)	C57Bl/6 MOG ₃₅₋₅₅	Broad spectrum antibiotics	Decreased	Decreased pro-inflammatory cytokines, decreased T _{H17}
Ochoa-Repáraz et al. (50)	SJL PLP ₁₃₉₋₁₅₁ ; C57Bl/6 MOG ₃₅₋₅₅	Broad spectrum antibiotics	Decreased	Reduced pro-inflammatory cytokines, increased T _{reg} Increased CD11c ^{hi} CD103 ⁺ cells
Ochoa-Repáraz et al. (51)	C57Bl/6 MOG ₃₅₋₅₅	Broad spectrum antibiotics	Decreased	Increased IL-10 producing CD5 ⁺ B-cells Shift from T _{H1} and T _{H17} toward T _{H2} response
Ochoa-Repáraz et al. (52)	SJL PLP ₁₃₉₋₁₅₁	Oral administration of <i>Bacteroides fragilis</i>	Decreased	Increased T _{reg} , reduced T _{H17}
Ochoa-Repáraz et al. (52)	SJL PLP ₁₃₉₋₁₅₁	Oral administration of PSA ^{-/-} <i>B. fragilis</i>	Normal	Normal
Ezendam et al. (53)	Lewis rats MBP	Oral administration of <i>Bifidobacterium animalis</i>	Decreased duration	Not investigated
Lavasani et al. (54)	C57Bl/6 MOG ₃₅₋₅₅	Oral administration of three <i>Lactobacilli</i> strains	Decreased	Reduced T _{H1} and T _{H17} , increased T _{reg} , IL-10 dependent
Takata et al. (55)	C57Bl/6 MOG ₃₅₋₅₅ ; SJL PLP ₁₃₉₋₁₅₁	Oral treatment with heat-killed <i>Pedococcus acidilactici</i>	Decreased	Reduced T _{H1} and T _{H17} , increased T _{reg}
Maassen and Claassen (56)	Lewis rats MBP; SJL PLP ₁₃₉₋₁₅₁	Oral treatment with commercially available probiotic drinks containing <i>Lactobacillus casei</i>	Decreased in Lewis rats, no effect in SJL model	Not investigated
Kwon et al. (57)	C57Bl/6 MOG ₃₅₋₅₅	Oral administration of <i>Bifidobacterium bifidum</i> , <i>Streptococcus thermophilus</i> and three <i>Lactobacillus</i> strains	Decreased	Reduced T _{H1} and T _{H17} response, increased T _{reg}
Rezende et al. (58)	C57Bl/6 MOG ₃₅₋₅₅	Oral administration of recombinant HSP65-producing <i>Lactococcus lactis</i> ^{ts}	Decreased	Decreased IL-17, increased IL-10, dependent on increased CD4 ⁺ LAP ⁺ T _{reg}
Wang et al.; Ochoa-Repáraz et al. (59–61)	SJL PLP ₁₃₉₋₁₅₁ ; C57Bl/6 MOG ₃₅₋₅₅	Oral treatment with <i>B. fragilis</i> -produced PSA	Decreased	Reduced T _{H1} and T _{H17} , increased T _{reg} and CD103 ⁺ DC, increased CD39 ⁺ T _{reg}
Kadowaki et al. (62)	2D2 anti-MOG TCR ^{tg} ; C57Bl/6 MOG ₃₅₋₅₅	Adoptive transfer of CD4 ⁺ induced IEL	Decreased	Reduced T _{H17} CD4 ⁺ induced IEL are dependent on gut microbiota and diet
Maassen et al. (63)	Lewis rats, MBP ₇₂₋₈₅	Oral administration of live/intranasal administration of soluble cell extracts from myelin proteins producing <i>L. casei</i>	Decreased, extracts from guinea pig MBP producing bacteria increased	Not investigated

Germfree housing, antibiotics, probiotics, and bacterial products affect the EAE clinical score.

DC, dendritic cells; EAE, experimental autoimmune encephalomyelitis; IEL, intraepithelial lymphocytes; MBP, myelin basic protein; MOG, myelin oligodendrocyte glycoprotein; PLP, proteolipid protein; PSA, polysaccharide A.

Table 2. Role of the gut microbiome during EAE.

Taken from Van den Hoogen *et al.*, 2017 [129].

Germ-free mice and broad-spectrum antibiotic treated mice depict reduced symptoms of EAE disease (Table 2). In the majority of the studies, protective effect of microbiota depletion was associated with reduced pro-inflammatory immune profile. Probiotic or metabolites produced from probiotics have been also intensively tested on EAE murine models and show protective effect on the disease with induction of Treg. By contrast, recolonized germ-free mice with SFB increase the proportion of pro-inflammatory Th17 cells in the gut but also in the CNS, resulting in a more severe EAE disease [118] [130]. Among these recent studies using EAE models, two have particularly demonstrated how microbiota can impact CNS autoimmunity. In the first one, the team of Prof Mazmanian and Prof Baranzini has transferred fecal microbiota from MS patients and healthy controls in germ-free mice. They have further induced CNS autoimmunity using active immunized EAE model and observed that mice having received microbiota from MS patients have increased symptoms and reduced proportion of interleukin-10 (IL-10) secreting Tregs [131]. In the second study, the group of Prof Wekerle and Prof Krishnamoorthy has observed similar results but using more powerful protocols. Indeed, they take advantage of a cohort composed by monozygotic twins discordant for MS to transferred germ-free mice with their fecal microbiota. The mice model used was a spontaneous model of EAE in which transgenic mice develop spontaneously the EAE disease without any intervention/immunization. After the colonization, MS twin-derived microbiota induced a higher incidence of EAE disease associated with reduced anti-inflammatory IL-10 secreting T cells compared to healthy twin-derived microbiota [132].

Regarding structural integrity of the gut mucosal barrier, gut dysbiosis is known to promote intestinal permeability [133]. Interestingly, it has been reported that MS patients have an increased intestinal permeability [134]. Using EAE model, a previous study has described an increased intestinal permeability during EAE development associated with increase pro-inflammatory Th1 and Th17 cells infiltrates in the gut [135]. However, the relative contribution of these infiltrates to neuroinflammation is still largely unknown.

Another major actor closely related to the gut environment is food. Food is known to change the gut microbial composition. It can also influence gut immune system by the dysbiosis or by itself with the micronutrients that can directly bind immune cells. One example is the salt that have been suggested to influence autoimmunity in experimental models. In several publications, sodium chloride has been reported to increase EAE disease associated with a higher Th17 responses [136] [137] [138] [139]. In MS patients, results based from observational studies found different conclusions. Using food frequency questionnaire, no association between dietary sodium intake and risk of MS or relapses were founded [140] [141]. Moreover, one study using urine sample from MS patients reported no association between urine sodium levels and clinical and MRI outcomes [142]. No clinical trial has been

performed to assess the benefit of sodium intake reduction in MS patients. However, one clinical trial is currently planned to study the effects of high versus low salt diet on the immune response in MS patients and healthy individuals (ClinicalTrials.gov - NCT02282878). Other examples on how diet/food are able to change the development of CNS autoimmunity in experimental models have been extensively reviewed by Van den Hoogen *et al.* and are summarized in Table 3.

Reference	Animal model	Intervention	Clinical score	Immune response
Haghikia <i>et al.</i> (64)	C57Bl/6 MOG ₃₅₋₆₅	Oral administration of propionic acid (short-chain fatty acid) and lauric acid (long-chain fatty acid)	Decreased	Increased T _{reg} , reduced T _{H17} on PA treatment Increased T _{H1} and T _{H17} , decreased <i>Prevotellaceae</i> and <i>Bacteroidetes</i> on lauric acid treatment
Lemire and Archer (65)	SJL spinal cord homogenate	Intraperitoneal vitamin D administration	Decreased	Reduced antibodies against MBP
Cantorna <i>et al.</i> (66)	B10.PL MBP ₇₉₋₈₇	Dietary vitamin D supplementation	Decreased	Not investigated
Spach <i>et al.</i> (67)	C57Bl/6 MOG ₃₅₋₆₅	Dietary vitamin D supplementation	Decreased	Reduced inflammatory cells, IFN γ in the spinal cord, IL-10 dependent
Piccio <i>et al.</i> (68)	SJL PLP ₁₃₀₋₁₅₁ ; C57Bl/6 MOG ₃₅₋₆₅	40% caloric restriction	Decreased	Increased plasma levels of corticosterone, adiponectin, reduced plasma levels of IL-6 and leptin
Esquifino <i>et al.</i> (69)	Lewis rats spinal cord homogenate	33 and 66% caloric restriction	66% caloric restriction protected from EAE signs	Reduced splenic CD8 ⁺ T cells and B cells, reduced lymphoid and thymic CD4 ⁺ T cells and B cells and IFN γ production
Kafami <i>et al.</i> (70)	C57Bl/6 MOG ₃₅₋₆₅	Intermittent feeding	Decreased	Not investigated
Harbige <i>et al.</i> (71)	SJL MOG ₃₂₋₁₀₀	Oral γ -linolenic acid treatment	Decreased	Increased TGF- β , prostaglandin E ₂ production by spleen mononuclear cells
Harbige <i>et al.</i> (72)	Lewis rats, guinea pig spinal cord homogenate	Oral γ -linolenic acid treatment	Decreased	Not investigated
Kong <i>et al.</i> (73)	C57Bl/6 MOG ₃₅₋₆₅	DHA-rich diet	Decreased	Reduced T _{H1} and T _{H17} cell differentiation, reduced amounts of T _{H1} , T _{H17} found in the spleen and spinal cord of mice on a DHA-rich diet. <i>In vitro</i> , DHA reduced the expression of costimulatory molecules on DC and reduced their production of pro-inflammatory cytokines
Unoda <i>et al.</i> (74)	C57Bl/6 MOG ₃₅₋₆₅	EPA supplementation	Decreased	Increased expression of PPAR α , β , and γ on CD4 ⁺ T cells in the spinal cord, reduced IFN γ and IL-17 cytokine production. CD4 ⁺ T cells from the spleen of EPA-treated mice expressed increased mRNA levels of Foxp3, but also of IL-17 and ROR γ t
Salvati <i>et al.</i> (75)	Dark agouti rats, guinea pig spinal cord homogenate	EPA supplementation	Delayed time before EAE symptoms appeared	Increased myelination of axons in the spinal cord
Kim <i>et al.</i> (76)	C57Bl/6 MOG ₃₅₋₆₅	Ketogenic diet	Decreased	Reduced T _{H1} , T _{H17} , and pro-inflammatory cytokines
Choi <i>et al.</i> (77)	C57Bl/6 MOG ₃₅₋₆₅	Cycles of fasting Ketogenic diet	Decreased	Fasting increased T _{reg} , corticosterone, reduced CD11 ⁺ DC, T _{H1} , T _{H17} , pro-inflammatory cytokines Ketogenic diet: not investigated
Jörg <i>et al.</i> (78)	C57Bl/6 MOG ₃₅₋₆₅	High-salt diet	Increased	Increased T _{H17}
Kremtsov <i>et al.</i> (79)	C57Bl/6 MOG ₃₅₋₆₅ , SJL PLP ₁₃₀₋₁₅₁	High-salt diet	Increased in C57Bl/6 mice, in SJL only increased in females	No difference in T _{reg} , T _{H1} , and T _{H17} cells
Wu <i>et al.</i> (80)	C57Bl/6 MOG ₃₅₋₆₅	High-salt diet	Increased	Increased T _{H17} in CNS and mesenteric lymph nodes, SGK-1 signaling dependent
Kleinewietfeld <i>et al.</i> (81)	C57Bl/6 MOG ₃₅₋₆₅	High-salt diet	Increased	Increased inflammatory cell infiltration into the CNS, increased T _{H17}
Veldhoen <i>et al.</i> (82)	C57Bl/6 MOG ₃₅₋₆₅	FICZ administration	Increased	Increased IL-17- and IL-22-producing CD4 ⁺ T cells in the spinal cords
Quintana <i>et al.</i> (83)	C57Bl/6 MOG ₃₅₋₆₅	FICZ, ITE, TCDD administration	FICZ increased, ITE and TCDD reduced	FICZ: increased IL-17 ⁺ CD4 ⁺ and IFN γ ⁺ CD4 ⁺ T cells in the spleen TCDD: increased Foxp3 ⁺ T _{reg}
Rothhammer <i>et al.</i> (84)	C57Bl/6 MOG ₃₅₋₆₅	Tryptophan-deficient diet, supplementation with tryptophan metabolites and tryptophanase	Increased, supplementation reduced EAE scores	IFN-1 signaling induces AHR expression in astrocytes, supplementation does not reduce EAE scores in astrocyte-specific AHR knockout mice

Dietary interventions affect the microbiota and EAE clinical scores.

AHR, aryl hydrocarbon receptor; CNS, central nervous system; DC, dendritic cells; DHA, docosahexaenoic acid; EAE, experimental autoimmune encephalomyelitis; EPA, eicosapentaenoic acid; FICZ, 6-formylindolo[3-2b]carbazole; ITE, 2-(1'H-indole-3'carbonyl)-thiazole-4-carboxylic acid methyl ester; MBP, myelin basic protein; MOG, myelin oligodendrocyte glycoprotein; PLP, proteolipid protein; SGK-1, serum/glucocorticoid kinase 1; TCDD, 2,3,7,8-tetrachlorodibenzo-p-dioxin.

Table 3. Impact of diet intervention during EAE.
Taken from Van den Hoogen *et al.*, 2017 [129].

However, currently, few of the corrective diet proposed have led to radical changes in MS patients as observed in the Table 4.

TABLE 4 | Dietary studies in MS patients.

Reference	Number of subjects, type of MS	Diet-groups	Main findings
Bates et al. (126)	292 RRMS	Ω-3 EPA and DHA vs oleic acid supplementation. Both groups also had vitamin E and antioxidant supplementation	No difference in relapse rate or EDSS
Weinstock-Guttman et al. (127)	27 RRMS	Low-fat diet (<15% calories) with Ω-3 EPA and DHA supplements vs low fat (<30% calories) with oleic acid supplements. Both groups received vitamin E, multivitamin, and calcium supplementation	No difference in relapse rate or EDSS between groups. Relapse rates, reduced compared to 1 year before the start of this study. EPA/DHA group had increased physical and mental parameters. Reduced fatigue score in the oleic acid group
Torkildsen et al. (128)	99 RRMS	Ω-3 EPA and DHA vs corn oil supplementation	No difference in relapse rate, EDSS, quality of life, and fatigue scores
Bates et al. (129)	134 SPMS	Ω-6 Linoleic acid and γ-linolenic acid vs linoleic acid vs oleic acid supplementation	No difference in relapse rate or EDSS
Bates et al. (130)	104 PPMS	Ω-6 Linoleic acid and γ-linolenic acid vs linoleic acid vs oleic acid supplementation	No difference in relapse rate or EDSS. High-dose linoleic acid group had less severe relapses
Harbige and Sharief (131)	28 RRMS	Ω-6 Linoleic acid supplementation vs placebo	Reduced relapse rate, improved EDSS
Jafarirad et al. (132)	35 RRMS	Vitamin A (retinyl palmitate) or placebo supplementation	Reduced T cell proliferation when incubated with MOG
Wingerchuk et al. (133)	15 RRMS	Vitamin D supplementation, uncontrolled	Reduced EDSS compared to baseline
Mahon et al. (134)	39 MS patients, subtype not specified	Vitamin D3 supplementation vs placebo. Both groups received calcium supplementation	Increased TGF-β concentration in serum of vitamin D3 supplemented group. No differences in TNFα, IFNγ, and IL-13 concentrations
Goldberg et al. (135)	10 MS patients, subtype not specified	Vitamin D3, calcium, and magnesium supplementation, uncontrolled	Fewer relapses than expected
Choi et al. (77)	48 RRMS	Cycles of fasting vs ketogenic diet vs control	Fasting and diet group had improved health related quality of life, reduced disability scores. Fasting and ketogenic diet were well tolerated
Haghikia et al. (136)	Not specified in abstract	Propionic acid treatment in patients and HC	No side effects of PA. 25–30% increase of T _{reg} and reduced T _{H17} cells in both groups
Farez et al. (137)	70 RRMS, replicated by a separate group of 52 patients		High salt excretion is associated with increased disease activity
Hadgkiss et al. (138)	2,087 MS patients, subtype not specified		A general healthy diet, based on fruit, vegetable, fat, meat and dairy consumption was associated with better clinical scores
Rezapour-Firouzi et al. (139)	65 RRMS	Three groups: 1. hemp seed/evening primrose oil; 2. olive oil; and 3. cosupplemented oil vs baseline measurements. Subjects were advised to have a general healthy diet	Reduced relapse rates, EDSS in groups 1 and 3 compared to baseline
Nordvik et al. (140)	16 RRMS	General health lifestyle and A, B, D, E, Ω-3 fatty acid supplementation	Reduced EDSS compared to baseline

Dietary studies in MS patients have been extensively reviewed by Schmitz et al. (141).

AHR, aryl hydrocarbon receptor; CNS, central nervous system; DC, dendritic cells; DHA, docosahexaenoic acid; EDSS, expanded disability status scale; EAE, experimental autoimmune encephalomyelitis; EPA, eicosapentaenoic acid; MOG, myelin oligodendrocyte glycoprotein; MS, multiple sclerosis; SGK-1, serum/glucocorticoid kinase 1.

Table 4. Dietary studies on MS patients.

Taken from Van den Hoogen *et al.*, 2017 [129].

For the few studies showing immunomodulatory effects on MS patients or impact on clinical outcomes, they will require large-scale clinical trials to prove their efficacy [143]. Nevertheless, continued prospective studies and clinical trial are important to further understand how diet can impact CNS autoimmunity.

1.1.5.2.5 Obesity, lipids and cholesterol metabolism

As demonstrated in the previous chapter, diet have direct impact on the gut environment and the CNS autoimmunity. In addition, diet have important indirect effects on the metabolism impacting body weight, fat storage, lipids homeostasis perturbation (dyslipidemia) and other factors that can affect MS development [143]. Obesity have been described as a risk factors for MS. Indeed, several studies have observed that higher is the body mass index (BMI) during the childhood [144] [145] or adolescence [146] [147], the higher is the risk to develop MS. Metabolic changes associated with obesity such as perturbation of lipid-related variables including triglycerides (TG), total cholesterol (tChol), high density lipoprotein cholesterol (HDL), low density lipoprotein cholesterol (LDL), have also been associated with poor outcome of MS [148] [149] [150] [151] [152]. However, the underlying mechanisms remain unclear. Obesity and diet rich in fat promote low-grade inflammation and increase pro-inflammatory cytokines production (i.e. interleukin 6 (IL-6) that can drive the generation of Th17 cells [153]). Therefore this Th17 sublineage bias could favor autoimmunity in obese individuals. Some studies using diet-induced obese mice have reported a worsening of clinical symptoms during EAE disease compared to control mice [153] [154]. Among the studies mentioned above, several reports have found high tChol level associated with worsening disability in MS patients [151] [155]. Nevertheless, still few studies have studied the impact of lipid-variable perturbations and especially tChol before or during development of the disease. Lowering cholesterol drugs such as statins have shown beneficial effects on EAE disease but the mechanisms are still debated and seems to be independent of their cholesterol-lowering effects [151] [156] [157].

Moreover, high fat diet (HFD) inducing a dyslipidemia has been shown to exacerbate neuroinflammation in EAE model using male [158] and female [154] mice. However, a recent publication showed that a transgenic mouse model for hypercholesterolemia called low-density lipoprotein (LDL) receptor knock-out (LDLr^{-/-}) mice display an attenuated EAE disease in female but not in male [159]. Finally, Berghoff and colleagues have shown that cholesterol supplementation does not affect EAE development [160]. Interestingly, expression profiles of cholesterol metabolism-related genes are found altered in the CNS during development of EAE [161]. Moreover, certain cholesterol metabolites have been reported to be modulated by HFD and during obesity [162]. With these recent findings, it suggests that perturbation of cholesterol metabolism may influence the progression of EAE and MS disease.

1.2 Oxysterols

1.2.1 Introduction

Cholesterol is a lipid part of sterol family, which is implicated in several biochemical processes of the body. Cholesterol is an essential component of the mammalian cells accounting for up to 50% of all membrane lipids [163]. As cholesterol has a rigid hydrophobic structure that confers stability of the plasma membrane and hamper the movement of other molecules, modifying the proportion of the cholesterol in the cell membrane influence membrane fluidity [164]. Cholesterol can interact with integral membrane proteins and modulate their functions. Cholesterol is also precursor of important molecules such as vitamin D, the bile acids, steroid hormones and oxysterols. Oxysterols are downstream metabolites of cholesterol oxidation. Research on oxysterols started in the early 1940's with studies on cholesterol autoxidation leading to the generation of oxysterols. Oxysterols really started to get interests in the late 1970 when Kandutsch and colleagues observed that some oxygen derivatives of cholesterol were capable to downregulate the synthesis of cholesterol [165]. The following years, people observed that these molecules were responsible for plenty of other biological processes. Oxysterols can be separated in two categories called primary and secondary oxysterols. The primary oxysterols, synthesized directly from the cholesterol, are composed of side-chain oxysterols and ring-modified oxysterols. Side-chain oxysterol family include 24S-, 25- and 27-hydroxycholesterol (-OHC) and ring-modified oxysterols include 7 α - and 7 β -hydroxycholesterol and 7-ketocholesterol [166]. The secondary oxysterols, including 7 α ,25-dihydroxycholesterol and 7 α ,27-dihydroxycholesterol are generated from primary oxysterols 25-OHC and 27-OHC respectively [166]. Oxysterols can be synthesized via enzymatic and non-enzymatic reactions. Specific hydroxylases are responsible for enzymatic oxidation while reactive oxygen species (ROS) oxidation is mainly responsible for non-enzymatic generation of oxysterols [167]. Oxysterols are well described as strong mediator of cholesterol metabolism. Oxysterols modulate the level of cholesterol intracellularly through transcriptional regulators like liver X receptor (LXR) and the sterol regulatory element binding protein (SREBP) [168]. LXR mediates the expression of ABC transporter intervening in cholesterol transport and efflux [169]. SREBP also regulates the cholesterol metabolism in the cell by inducing of the synthesis (through HMG-CoA synthase/reductase) or the uptake of cholesterol (through expression of LDL receptor) [168]. In addition to the modulation of cholesterol level, oxysterols are part of the bile acid and steroid hormones production acting as intermediates in their synthesis. More interestingly, research from the last decades have highlighted that oxysterols are active metabolites directly involved in immunology including trafficking of immune cells, anti-viral action, cytokines secretion and inflammasome modulation [170] .

1.2.2 Immune active oxysterols and their ligands

1.2.2.1 Liver X receptor (LXR)

Many different oxysterols have been discovered. They are all sharing close structural similarities, but they have various different targets and actions (Fig. 6). One of the most target sharing by oxysterols is LXR receptors. The side-chain oxysterol family such as 25- and 27-OHC are well characterized as LXR ligands. LXRs are part of the nuclear receptors' family of transcription factors. LXR α (NR1H3) and LXR β (NR1H2) are the two isoforms that have been identified [171]. Despite the close homology between the two isoforms (almost 80% identity of their amino acid sequences are the same), they are not sharing the same function and the same pattern of expression. LXR α is expressed mostly in metabolically active tissues like liver, gut and adipose tissue. LXR β is ubiquitously expressed (nusa.org). At physiological stage, LXR are important to control metabolic processes including cholesterol homeostasis. LXRs have also been characterized as important immunological modulator. LXRs are able to suppress inflammatory response through trans-repression [172]. Indeed, sumoylation of active LXR form can dampened the activity of nuclear factor kb and activator protein 1, that control proinflammatory genes expression [167] [173] [174]. In innate immunity, LXR pathways have been described to participate in clearance of bacteria during infection in macrophages. Indeed, induction of LXR α but not LXR β expression occurs during intracellular bacterial infection [175]. Using another model of intracellular bacterial infection, Matalonga *et al.* have discovered that LXR activation pathway impaired cytoskeletal changes associated with the infection [176]. Regarding adaptive immune system, LXRs have been described to decrease proliferation of both T and B cells [177]. LXR β is expressed in macrophages, T and B cells. On the other hand, LXR α is highly expressed in peritoneal-derived and bone-marrow derived macrophages but not in T cells or B cells. Mice lacking LXR β show lymphoid hyperplasia and have improved responses to antigenic challenge [177]. These results were found only in LXR $\beta^{-/-}$ but not in LXR $\alpha^{-/-}$. In addition, another group found that LXR activation inhibit interleukin-2- and interleukin-7-induced human T cell proliferation [178]. Regarding subtypes of T cells, LXRs are involved in the polarization of Th17 cells [179]. Indeed, Th17 induction is improved in LXR $^{-/-}$ mice and the LXR deficiency promotes Th17 polarization *in vitro* [179]. Finally, we recently demonstrated that LXRs can also act on regulatory T cells. In our study, we found that 25-OHC, through LXR pathway, acts as a negative regulator of IL-10 secretion of IL-27-induced Treg [180].

1.2.2.2 Retinoic acid receptor-related orphan receptor (ROR)

Like LXRs, RORs are member of the nuclear receptor family of transcription factor binding oxysterols. They are composed of three different forms; ROR α (NR1F1), ROR β (NR1F2), and ROR γ (NR1F3). RORs recognize and bind as monomer to specific ROR response elements on DNA [181]. After their activation, RORs recruit co-activator and activate gene transcription [182]. Several oxysterols (i.e. 25-OHC, 27-OHC, 7 α -OHC) can bind ROR α and ROR γ , however no study reported oxysterols as ligand of ROR β . ROR α is expressed in several tissues and participate in circadian rhythms, glucose and lipid metabolism, and during the development. ROR γ is also expressed in multiple organs and is an important transcription factor for immune system. ROR γ has also variant including ROR γ 1 and ROR γ 2 (also known as ROR γ T) isoforms [183]. ROR γ T was intensively described as essential transcription factor in Th17 cell development and therefore important for autoimmune conditions [184] [185]. Indeed, it has been reported that mice lacking ROR γ T, have a defected Th17 cell development and show attenuated autoimmune disease [184].

1.2.2.3 Epstein-Barr virus-induced G-protein coupled receptor 2 (Ebi2)

G-protein coupled receptor 183 also known as Epstein-Barr virus-induced G-protein coupled receptor 2 (Ebi2) is a membrane receptor from the GPCR family, that was first discovered in Burkitt's lymphoma cells after EBV infection [186]. Ebi2 was first observed in B cells but further studies have demonstrated that it was expressed in other type of cells such as T lymphocytes, monocytes, dendritic cells, astrocytes and innate lymphoid cells. Among the different signaling pathways of GPCR, Ebi2 receptor is defined as chemotactic receptor and participate in the migratory capability of cells. The most potent endogenous ligand of the receptor is the oxysterol 7 α ,25-OHC produced from oxidation of 25-OHC by Cyp7b1 enzyme. 25-OHC is oxidized from cholesterol by the enzyme cholesterol 25-hydroxylase (Ch25h) (Figure 6). Even if Ch25h is not directly the enzyme active in the production of 7 α ,25-OHC, Ch25h enzyme is on the same oxysterol pathway and is a critical player required for the generation of 7 α ,25-OHC. Indeed, mice deficient for Ebi2 show often similar phenotype observed in Ch25h-deficient (Ch25h^{-/-}) mice [187].

Functionally, cells expressing Ebi2 are able to move through oxysterol gradient dependent manner acting like chemokine processes. The migratory function of this receptor impacts several important immune processes. For example, Ebi2 is involved in the T-dependent antibody response in the germinal centers. Indeed, studies have demonstrated that mice lacking Ebi2 have an abnormal positioning of B cells in the follicular regions of secondary lymphoid organs. Indeed, lymphoid stromal cells create an oxysterol gradient that guide B cell movement during humoral responses [188]. A recent study demonstrated that Ebi2 drives

CD4⁺ T cells peripheralization in lymph node [189]. Mice lacking Ebi2 receptor have CD4⁺ T cell location issue and have delayed immune responses such as antigen recognition or proliferation.

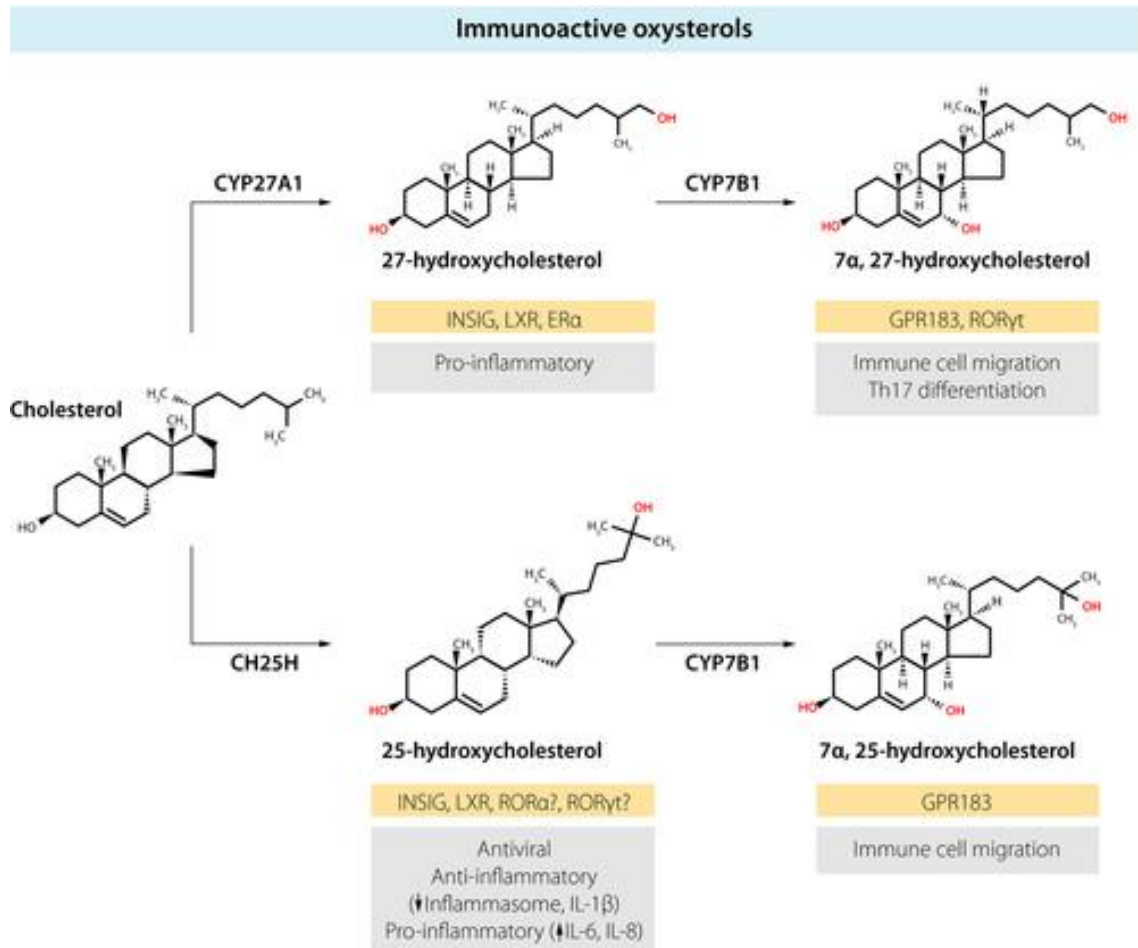


Figure 6. Immunoactive oxysterols and their pathways of activation.

Most studied immunologically active oxysterols are 27-OHC, 7α,27-OHC, 25-OHC and 7α,25-OHC. They are synthesis from cholesterol via specific enzyme including Ch25h, Cyp27a1 and Cyp7b1. These oxysterols act as ligand for several receptors (orange boxes) and have major role in immunology (grey boxes). Taken from Willinger *et al.*, 2019 [190].

1.2.3 Oxysterols in CNS autoimmunity

As growing evidence support potential roles on immune regulation by oxysterols, scientific community has started to study these cholesterol metabolites in autoimmune conditions. In CNS autoimmunity, previous reports have found oxysterol level perturbations in MS patients and experimental murine model [191] [192] [193]. Genetic analysis of patients has revealed an association between genetic variants of Ch25h and PPMS patients, supporting a role of Ch25h

in autoimmune diseases [194]. Our laboratory previously reported that Ch25h^{-/-} mice attenuated EAE disease course by limiting the trafficking of pathogenic Th17 lymphocytes to the CNS [195]. Indeed, we observed an accumulation of Th17 lymphocytes in the peripheral lymph nodes in the absence of oxysterols during EAE thus pointing towards a possible defect in T lymphocytes exit from the lymph nodes. Interestingly, this is reminiscent of the fingolimod mechanism of action, a drug that prevents MS inflammatory activity by trapping subset of T cell in the lymph nodes [196]. However, the accumulation of Th17 cells was only transient and we suggest that Th17 cells may be trapped in additional tissues such as the GALTs, that are important reservoirs of Th17 cells as previously explained. Moreover, Ch25h^{-/-} mice display an altered IgA production at the mucosal surface and could suggest an impact on maintenance of gut homeostasis and affecting microbiota composition. Indeed, 25-OHC has been reported to inhibit IgA production by repressing activation induced cytidine deaminase (AID) [197]. Interestingly, AID^{-/-} mice display dysbiosis [198].

On the same oxysterol metabolism pathway, Ebi2, for which 7 α ,25-OHC is the most potent agonist, has also exhibited important role in CNS autoimmunity. Our laboratory previously characterized Ebi2 biology in MS patient lymphocytes and observed that Ebi2 is functionally expressed on memory CD4⁺ T cells and is enhanced under natalizumab treatment [199]. In another study, Ebi2 expression have been found highly expressed in the inflamed white matter of MS patients [200]. Using experimental model, the same authors reported that Ch25h and Cyp7b1 expression as well as 7 α ,25-OHC level were increased in CNS during EAE development. Ebi2 was predominantly expressed in Th17 cell subset compared to Th1 or CD8⁺ T cells and its expression was maintained by pro-inflammatory cytokines (i.e. interleukin-23 (IL-23) and interleukin-1 beta (IL-1 β)). In addition, they studied the capacity of Ebi2^{-/-} Th17 cells to induce CNS autoimmunity using an adoptive transfer model of EAE. They found that mice transferred with encephalitogenic Ebi2^{-/-} Th17 cells have a delayed disease development compared to mice transferred with wild-type controls [200]. Interestingly, Ebi2-oxysterol interaction has also been recently study in IBDs. It has been reported that level of some oxysterols are perturbed in IBD patients [201]. Moreover, Ebi2, Ch25h and Cyp7b1 are found highly expressed in inflamed colon of ulcerative colitis (UC) patients [202]. Similar results have been observed using experimental model of colitis [201]. Moreover, two publications have described that a certain subset of ILCs are expressing high level of Ebi2 receptor in the gut [203] [204]. In both studies, the authors have found that ILC type 3 (ILC3), important cell type for innate defense mechanisms in the gut, highly express Ebi2 receptor and migrate towards oxysterols. Using Ebi2^{-/-} mice, Emgard *et al.* observed that Ebi2 expression in ILC3s promote their migration in the colonic lymphoid tissues (IFL and CP) and are necessary for the formation of these structures [203]. By analyzing expression profile of different cell population, stromal cells were defined as the source for 7 α ,25-OHC and provide a local signal for the development

of lymphoid structure in the colon. In an experimental colitis model, the authors showed that *Ebi2*^{-/-} mice have a significant lower inflammatory infiltrate and development a milder colitis compared to wild-type controls. Moreover, Chu *et al.* demonstrated that *Ebi2* expressed on ILC3 is required for the establishment of immune response against bacterial infection [204]. Altogether, these new discoveries point out important implications of oxysterols on the gut equilibrium. By the recent establishment of gut-brain interactions, we suggest that altered gut immune response may contribute to the EAE phenotype observed in *Ch25h*^{-/-} mice, pointing toward a major role of the interplay between oxysterols and gut environment during CNS autoimmunity development.

2. AIMS

My PhD thesis involved three interconnected projects that aimed to understand the relation between the oxysterols and the gut environment in the context of CNS autoimmunity.

The first project aimed to understand the role of the GALT in the modulation of pathogenic cells during EAE disease. As highlighted previously, recent studies have shown a potential relation between the gut and the development of EAE disease. Although it has been reported that infiltration of T cells occurs in the gut in MS patients and experimental model, how GALT impacts adaptive immune cells is not fully understood. Furthermore, the precise location, the timing of cell infiltration and the mechanisms of T cell regulations during EAE remain unknown. Therefore, the comprehension of these interactions is crucial to understand the role of the GALTs during MS disease and could give new opportunity of therapeutic intervention. Furthermore, the accomplishment of this project gave us the expertise and crucial information for the second and third projects.

The second project investigated how oxysterols can modulated EAE disease development by affecting the GALT immunity. In addition, we wanted to further understand what are the precise roles of oxysterols in the gut during gut-specific inflammation. As previously mentioned, EAE disease is attenuated in Ch25h^{-/-} mice compared to wild-type mice secondary to impaired Th17 cell trafficking to the CNS. A transient accumulation of Th17 cells was detected in the peripheral draining lymph nodes suggesting that Th17 cells may be trapped in additional tissues. We first investigated if the Ch25h pathway could be involved in shaping the gut immune response during EAE. In parallel to our investigations on the neuroinflammation using experimental model of MS, we explored the intestinal immune response in Ch25h^{-/-} using a model that induce gut specific inflammation. We studied the role of oxysterols in shaping gut immunity using the colitis model induced by the intestinal pathogen *Citrobacter rodentium*. This pathogen-induced inflammation model enabled us to assess the impact of lipid metabolism in the response to a well-known intestinal pathogen. This model is useful to study mucosal immune response in the gut as the eradication of the bacteria is dependent on coordinate innate and adaptive mucosal responses and includes large panel of immune processes [205]. We expected to highlight potential new roles of oxysterols in the mucosal immune response infectious-mediated inflammation. These knowledge will help us to understand how gut environment is perturbed by oxysterol deficiency and what impact it could have during CNS autoimmunity.

Finally, the third project aimed to understand the role of hypercholesterolemia on oxysterols and their contribution in promotion of CNS autoimmunity. As discussed, we suggested that perturbation of cholesterol metabolism may influence the progression of EAE. To answer this

hypothesis, we proposed to induce hypercholesterolemia in Ch25h^{-/-} and WT mice by HFD or with backcrossing mice with LDLr^{-/-} mice. We expected hypercholesterolemia to drive the expression of Ch25h thus the production of oxysterol 25-OHC that would exacerbate the EAE phenotype in WT but not in Ch25h^{-/-} mice.

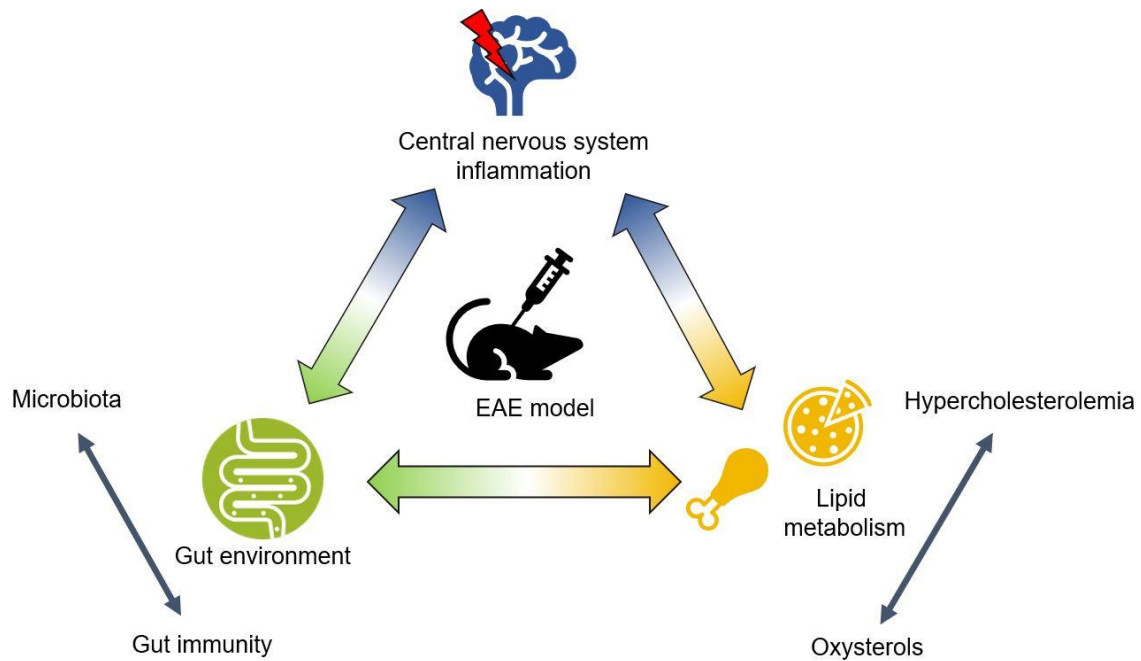


Figure 7: Schematic drawing illustrating the interplay between lipid metabolism, gut environment and central nervous system inflammation. We hypothesized that modulations of lipid metabolism, including oxysterols and hypercholesterolemia, contribute to the development of inflammation of the central nervous system by modulating the gut immunity and the microbiota using the experimental autoimmune encephalomyelitis.

3. PROJECT I: Impact of the gut environment during experimental models of multiple sclerosis

3.1 Materials & Methods

3.1.1 Animals

C57BL/6J mice were purchased from Charles River or bred in the animal facility. C57BL/6-Tg(Tcra2D2,Tcrb2D2)1Kuch/J (TCR^{MOG} 2D2) and C57BL/6-Tg(TcraTcrb)425Cbn/Crl (OT-II) transgenic mice were purchased from Charles River. All mice were maintained under specific-pathogen free conditions at Lausanne University Hospital. All experiments were performed in accordance with guidelines from the Cantonal Veterinary Service of state Vaud.

3.1.2 EAE induction and clinical evaluation

For induction of classical active EAE, mice were immunized with 100 µg myelin oligodendrocyte glycoprotein (MOG) peptide 35-55 (MOG₃₅₋₅₅) or PBS emulsified in complete Freund's adjuvant supplemented with 5 mg/ml *Mycobacterium tuberculosis* H37Ra. A total of 200 µl emulsion was subcutaneously injected into four sites on the flanks of mice. At days 0 and 2 after initial peptide injections, animals received additional intravenous injection of 100 ng pertussis toxin. For induction of EAE by adoptive transfer, naïve CD4⁺ T cells from 2D2 mice were polarized *in vitro* in Th17 or Th1 cells as previously described [206]. Differentiation status was checked on day 5 and after 2 days of restimulation with anti-mouse CD3/CD28 antibodies (2 µg/ml), 8 × 10⁶ CD4⁺ T cells were injected intraperitoneal (i.p.) into wild-type (WT) C57BL/6J recipient mice. Mice were scored daily for clinical symptoms. The classical EAE symptoms were assessed according to the following score: score 0 – no disease; score 0.5 – reduced tail tonus; score 1 - limp tail; score 1.5 – impaired righting reflex; score 2 – limp tail, hind limb weakness; score 2.5 – at least one hind limb paralyzed; score 3 – both hind limbs paralyzed; score 3.5 –complete paralysis of hind limbs; score 4 – paralysis until hip; score 5 – moribund or dead. The atypical EAE symptoms were assessed according to the following score: score 0 – no disease; score 1 – head turned slightly (ataxia, no tail paralysis); score 2 – head turned more pronounced; score 3 – inability to walk on a straight line; score 4 – laying on side; score 4.5 – rolling continuously unless supported; score 5 – moribund or dead. Combined score compiling typical and atypical scoring has also been applied and considers the highest score from the typical or atypical clinical signs [207]. Mice were euthanized if they reached a score > 3.

3.1.3 Antibody treatment

For homing experiment, mice were injected i.p. with 400 µg of anti-mouse α4β7 (DATK 32) or isotype control antibodies (IgG2a isotype control, 2A3) one day before TCR^{MOG} 2D2 Th17 cell injection and every three days post-injection until the development of disease or as indicated.

3.1.4 Antibiotic treatment

Mice were treated with 2.5 mg/ml enrofloxacin in drinking water for 2 weeks, followed by 0.8 mg/ml of amoxicillin and 0.114 mg/ml clavulanic acid in drinking water for 2 further weeks [208] prior to TCR^{MOG} 2D2 Th17 cell injection. Treatment with amoxicillin and clavulanic acid was then continued throughout the experiment.

3.1.5 Isolation of immune cells

Mice were perfused through cardiac ventricle with Phosphate-buffered saline (PBS) 1×. Whole colon, 15 cm-long pieces of terminal ileum and whole lung were excised and washed in PBS 1×. Gut was opened longitudinally. Washed gut and lung pieces were cut into 2 cm pieces and incubated for 20 min at 37°C in HBSS containing 10 mM EDTA under gentle agitation (80 rpm). Tissues were washed by vortexing with PBS 1×. Organ pieces were then incubated 2 times at 37°C for 20 min in a dissociation mix composed of 5 ml HBSS, Liberase TL (1 Wünsch unit/mL) and DNase I recombinant (1 U/mL) and 2% fetal calf serum (FCS). The remaining tissue pieces were mechanically disaggregated on a 70 µm cell strainer using a syringe plunger. For the preparation of CNS mononuclear cells, brain and spinal cord were cut into pieces and digested 45 min at 37°C with collagenase D (2.5mg/ml) and DNase I (1mg/ml) followed by 70%/37% Percoll gradient centrifugation. For the preparation of lymph nodes, organs were removed and single cell suspensions were prepared by disaggregation of the tissues through a 70 µm cell strainer. The cellular suspensions were washed and filtered through 40 µm cell strainer and resuspended in culture medium for further analysis.

3.1.6 Flow cytometric analysis

Single-cell suspensions in PBS 1× were stained with fixable viability dye eFluorTM 660. For cell surface stainings, cells were preincubated with anti-CD16/32 for 10 min to block Fc receptors and stained in FACS buffer (PBS containing 1% BSA) with directly labeled monoclonal antibodies for 30 min. For intracellular cytokine staining, cells were activated for 4 h with 50 ng/ml PMA, 1 µg/ml ionomycin in the presence of 10 mg/ml brefeldin A. After surface staining, cells were fixed and permeabilized using Foxp3/transcription factor staining buffer set and stained intracellularly with directly labeled monoclonal antibodies for 30 min. Data were acquired on a LSR II cytometer and all data were analyzed using FlowJo software.

Fluorochrome-conjugated antibodies were purchased from several commercial sources indicated below and listed in the Key Resources Table. Antibodies against CD45 (30-F11), $\alpha 4\beta 7$ (DATK32), CD45.1 (A20) were from Biolegend; CD3 (145-2C11), CD4 (GK1.5), IL-17 (ebio17B7), IFN- γ (XMG1.2), T-bet (eBio4B10), Foxp3 (clone FJK-16s), TCRV α 3.2 (RR3-16), CD29 (β 1) (HMb1-1), CD45.2 (104), Ki67 (SolA15) were from eBiosciences; ROR γ T (Q31-378) was from BD Biosciences and CD49d (α 4) (PS/2) was from Biorad.

3.1.7 Tetramer staining

Cellular suspensions from colon and CNS were prepared as previously described from immunized and non-immunized mice at the peak of the disease. Cells were stimulated 4h with 10 μ g/ml of MOG₃₅₋₅₅ peptide in the presence of hIL-2 (50 U/mL). I-A^b MOG₃₅₋₅₅ tetramer-positive CD4⁺ T cells were detected by flow cytometry after surface staining with corresponding directly labeled I-A^b MOG₃₅₋₅₅ tetramer.

3.1.8 RNA isolation and quantitative PCR analysis

RNA was extracted from tissue samples using RNeasy Mini Kit following the manufacturer's instructions. cDNA was produced from equivalent amounts of RNA with the Superscript II RT (Invitrogen) and the PCR products were amplified with the PowerUp SYBR Green Master Mix. Samples were detected on the StepOne Real-Time PCR System. β -actin was used to normalize samples and the comparative CT method was used to quantify relative mRNA expression. Expression of specific gene transcripts was measured by using the following primer pairs: IL-6, 5'-CCCCAATTTCCAATGCTCTCC-3' and 5'-CGCACTAGGTTTGCCGAGTA-3'; IL-1 β , 5'-TGCCACCTTTTGACAGTG ATG-3' and 5'-TGATACTGCCTGCCTGAAGC-3'; TNF- α , 5'-AAGCTCCTCAGCGAGGACAG-3' and 5'-TGGTTGGCTGCTTGCTTTTC-3'; MAdCAM-1, 5'-ACAGAGCCAGACCTCACCTA-3', and 5'-TGATGTTGAGCCCAGTGGAG-3'; VCAM-1, 5'-CTGGGAAGCTGGAACGAAGT-3' and 5'-GCCAAACACTTGACCGTGAC-3', β -actin, 5'-AAGTGTGACGTTGACATCCGTAAA-3' and 5'-CAGCTCAGTAACAGTCCGCCTAGA-3'.

3.1.9 Whole-mount immunostaining

Whole-mount immunostaining was performed as previously described [209]. Briefly, mice were perfused with 4% paraformaldehyde and intestines were fixed in picric acid fixation buffer. Colon immunostaining was performed with DAPI (1:4000) and the following primary and secondary antibodies: CD3 ϵ (145-2C11, 1:1000), VEGFR2 (1:100), LYVE1 (1:500), Ki67 (1:200), V α 3.2-APC (1:100), goat anti-Armenian hamster DyLight 488 (1:500) and donkey anti-goat AlexaFluor 555 (1:500). After immunostaining the colon was cut into ~0.5 mm thick strips

which were cleared and mounted in RIMS Buffer [210] on a microscope slide fitted with 0.1 mm spacers (Molecular Probes). Image acquisition was performed on a Zeiss LSM 880 confocal microscope and image analysis and 3D reconstruction was performed with Imaris (Bitplane) and Fiji.

3.1.10 Microbiome analysis

Two weeks prior the experiment, mice were randomized in cages of two mice. A fecal pellet (9–50 mg) was mixed with 550 μ L GT buffer (RBS Bioscience) and homogenized in a Nucleospin Bead Tube (Machery-Nagel, Düren, Germany) for 20 min at maximum speed on a Vortex-Genie 2 with a horizontal tube holder (Scientific Industries). After addition of 1 μ L of 50 mg/mL RNaseA, samples were incubated at room temperature for 5 min and centrifuged for 2 min at 11,000 \times g. DNA was extracted from 400 μ L of the supernatant using the MagCore Genomic DNA Tissue kit on a MagCore HF16 instrument and eluted in 100 μ L of 10 mM Tris-HCl pH 8. Two negative extraction controls were processed in parallel with fecal pellets by omitting addition of biological material in the GT buffer. Purified DNA was stored at -20°C . The V3–4 region of the bacterial 16S rRNA genes was amplified using 2 ng of extracted DNA (or 5 μ L of the eluate from negative extraction control) as described before [211], except 30 PCR cycles were used. The amplicon barcoding/purification and MiSeq (2×300) sequencing were performed at LGC Genomics (Berlin, Germany) as previously described [212]. After removal of adapter remnants and primer sequences from demultiplexed fastq files using proprietary LGC Genomics software, sequencing data were submitted to European Nucleotide Archive (ENA) database under study number PRJEB 29544. Clustering of quality filtered merged reads into OTUs and taxonomic assignments of representative OTUs using mothur [213] and EzBioCloud database [214] were performed following a pipeline described previously [211], with modified commande options in PEAR [215] (-m 450 -t 250) and USEARCH [216] (-usearch_global -wordlength 30). Principal Coordinates Analysis (PCoA) of Bray–Curtis similarity, based on the square-root transformed relative abundance of OTUs was performed in PRIMER (Primer-E Ltd., Plymouth, UK). Shannon diversity index ($H' = -\sum (p_i \times \ln p_i)$) was calculated in PRIMER from the relative abundance of OTUs (p_i).

3.1.11 Statistical analysis

Data analyses and graphs were performed using GraphPad Prism 7.0 software. P values < 0.05 were considered significant. Results are displayed as mean and SEM or mean and SD, as described in the figure legends. Differences in microbiota between before and after adoptive transfer EAE were assessed using PERmutational Multivariate Analysis Of Variance

(PERMANOVA) (PRIMER) with 9,999 permutations. Wilcoxon signed-rank test was used for statistical comparisons of individual taxa, with a confidence level set at 95% ($P < 0.05$).

3.1.12 Key Resources Table

REAGENT or RESOURCE	SOURCE	IDENTIFIER
Antibodies		
BV510 anti-CD45 (clone 30-F11)	BioLegend	Cat#: 103138 RRID: AB_2563061
PE anti-LPAM-1 (integrin $\alpha 4\beta 7$) (clone DATK32)	BioLegend	Cat#: 120606 RRID: AB_493267
APC-eFluor 780 anti-CD3e (clone 145-2C11)	eBiosciences	Cat#: 47-0031-82 RRID: AB_11149861
Alexa Fluor 700 anti-CD4 (clone GK1.5)	eBiosciences	Cat#: 56-0041-82 RRID: AB_493999
PE anti-IL-17A (clone eBio17B7)	eBiosciences	Cat#: 12-7177-81 RRID: AB_763582
Alexa Fluor 488 anti-IFN γ (clone XMG1.2)	eBiosciences	Cat#: 53-7311-82 RRID: AB_469932
PE anti-T-bet (clone eBio4B10)	eBiosciences	Cat#: 12-5825-82 RRID: AB_925761
APC anti-TCR V α 3.2 (clone RR3-16)	eBiosciences	Cat#: 17-5799-82 RRID: AB_10854272
eFluor 450 anti-CD29 (clone HMb1-1)	eBiosciences	Cat#: 48-0291-82 RRID: AB_11218304
PECy7 anti-Foxp3 (clone FJK-16s)	eBiosciences	Cat#: 25-5773-82 RRID: AB_891552
BV421 anti-ROR γ T (clone Q31-378)	BD Biosciences	Cat#: 562894 RRID: AB_2687545
AF488 anti-CD49d (clone PS/2)	BioRad	Cat#: MCA1230A488 RRID: AB_566805
AF647 anti-CD45.1 (clone A20)	BioLegend	Cat#: 110720 RRID: AB_492864
PE anti-CD45.2 (clone 104)	eBiosciences	Cat#: 12-0454-82 RRID: AB_465678
FITC Ki67 (clone SolA15)	eBiosciences	Cat# 11-5698-82 RRID: AB_11151330
anti-CD3e (clone 145-2C11)	BioLegend	Cat#: 100302 RRID: AB_312667
anti-VEGFR2	R&D Systems	Cat#: AF644 RRID: AB_355500
anti-Lyve-1	Reliatech	Cat# 103-PA50 RRID: AB_2783787
anti-Ki67	Abcam	Cat# ab15580 RRID: AB_443209
DyLight 488 anti-hamster IgG (clone Poly4055)	BioLegend	Cat#: 405503 RRID: AB_1575117
AF555 anti-goat IgG	Life Technologies	Cat#: A-21432 RRID: AB_2535853
anti-CD16/CD32 (clone 93)	Invitrogen	Cat#: 16-0161-85 RRID: AB_468899
anti-CD3e (clone 145-2C11)	BioXcell	Cat#: BE0001-1 RRID: AB_1107634
anti-CD28 (clone 37.51)	BioXcell	Cat#: BE0015-1 RRID: AB_1107624
anti-LPAM-1 (integrin $\alpha 4\beta 7$) (clone DATK32)	BioXcell	Cat#: BE0034 RRID: AB_1107713

anti-trinitrophenol IgG2a isotype control (clone 2A3)	BioXcell	Cat#: BE0089 RRID: AB_1107769
PE I-A ^b MOG ₃₅₋₅₅ Tetramer	MBL	Cat#: TS-M704-1
Chemicals, Peptides, and Recombinant Proteins		
MOG ₃₅₋₅₅ peptide	Anawa	Cat#: 000-001-M41
Adjuvant, Complete H37 Ra	BD Difco	Cat#: 231131
M. tuberculosis H37 Ra, desiccated	BD Difco	Cat#: 231141
Pertussis toxin	Sigma Aldrich	Cat#: P2980
Liberase TL	Roche	Cat#: 5401020001
DNase I recombinant	Roche	Cat#: 4716728001
DNase I	Roche	Cat#: 10104159001
RNaseA	Roche	Cat#: R4875
Collagenase D	Roche	Cat#: 11088866001
Percoll	GE Healthcare	Cat#: 17089101
PMA (Phorbol 12-myristate 13-acetate)	Sigma Aldrich	Cat#: P8139
Ionomycin	Sigma Aldrich	Cat#: I9657
Brefeldin A	Sigma Aldrich	Cat#: B7651
Fixable Viability Dye eFluor 660	eBioscience	Cat#: 65-0864-14
DAPI	Sigma-Aldrich	Cat#: D9542
Critical Commercial Assays		
Foxp3 / Transcription Factor Staining Buffer Set	eBioscience	Cat#: 00-5523-00
RNeasy Mini Kit	Qiagen	Cat#: 74104
Superscript II RT	Invitrogen	Cat#: 18064014
PowerUp SYBR Green Master Mix	Applied Biosystems	Cat#: A25742
MagCore Genomic DNA Tissue Kit	RBC Bioscience	Cat#: MGT-01
Experimental Models: Organisms/Strains		
Mouse: C57BL/6-Tg(Tcra2D2,Tcrb2D2)1Kuch/J	The Jackson Laboratory	Stock#: 006912
Mouse: C57BL/6-Tg(TcraTcrb)425Cbn/Crl	The Jackson Laboratory	Stock#: 004194
Mouse: C57BL/6J	The Jackson Laboratory	Stock#: 000664
Oligonucleotides		
IL-6-F: CCCCAATTTCCAATGCTCTCC	This paper	N/A
IL-6-R: CGCACTAGGTTTGCCGAGTA	This paper	N/A
IL-1 β -F: TGCCACCTTTTGACAGTG ATG	This paper	N/A
IL-1 β -R: TGATACTGCCTGCCTGAA GC	This paper	N/A
TNF α -F: AAGCTCCTCAGCGAGGACAG	This paper	N/A
TNF α -R: TGGTTGGCTGCTTGCTTTTC	This paper	N/A
MAdCAM-1-F: ACAGAGCCAGACCTCACCTA	This paper	N/A
MAdCAM-1-R: TGATGTTGAGCCCAGTGGAG	This paper	N/A
VCAM-1-F: CTGGGAAGCTGGAACGAAGT	This paper	N/A
VCAM-1-R: GCCAAACACTTGACCGTGAC	This paper	N/A
β -actin-F: AAGTGTGACGTTGACATCCGTA	This paper	N/A
β -actin-R: CAGCTCAGTAACAGTCCGCCTAGA	This paper	N/A
Software and Algorithms		
FlowJo software version 10.5.3	Tree Star	N/A
GraphPad Prism version 7.0	GraphPad software	N/A
Imaris	Bitplane	N/A
Fiji	ImageJ	N/A
Other		
StepOne Real-Time PCR System	Applied Biosystems	N/A

BD LSR II	BD Biosciences	N/A
Zeiss LSM 880	Carl Zeiss	N/A
MagCore HF16	RBC Bioscience	N/A

3.2 Results

3.2.1 Antigen-specific MOG Th17 cells infiltrate the colonic lamina propria during active EAE

We first evaluated if immune dysregulation was observed in the colon during EAE actively induced by subcutaneous immunization of myelin oligodendrocyte glycoprotein amino acids 35-55 (MOG₃₅₋₅₅). To evaluate the relative contribution of a CNS antigen-specific response versus the sole contribution of the complete Freund adjuvant (CFA), we immunized wild-type mice either with the antigen MOG₃₅₋₅₅ or PBS emulsified with CFA. Pertussis toxin was injected at day 0 and 2 in both groups. Only mice immunized with antigen MOG₃₅₋₅₅ developed neurological symptoms (Fig. 8A). Colonic transcript levels of innate immune cytokines, more specifically IL-6, IL-1 β and TNF- α , are known to play a critical role during the pathogenesis of inflammatory bowel disease (IBD) and experimental colitis [217]. We thus assessed by quantitative real-time PCR (RT-PCR) analysis the cytokine expression levels when the MOG-immunized mice displayed neurological symptoms. We observed that IL-6 and IL-1 β but not TNF- α were induced in an antigen-specific manner in the colon (Fig. 8B). As both IL-6 and IL-1 β promote Th17 cell differentiation [218], we further investigated by flow cytometry if Th17 lymphocytes infiltrated the large intestine during EAE. The MOG-immunized group significantly surpassed the PBS group in up-regulation of IL-17-producing CD4⁺ T cells (Fig. 8C, 8D) but not in IFN- γ -producing CD4⁺ T cells in the colon (Fig. 8E, 8F). Those results suggest that Th17 subsets specifically respond to the CNS-antigen. We completed the analysis with the use of MOG₃₅₋₅₅/IAb tetramers and tracked CD4⁺ T cells based on their myelin antigen specificity in the colon and the CNS. Notably, MOG-specific T cells are increased in the colon at the peak of EAE disease compared to non-immunized control animals, reaching approximately levels observed in the CNS, where about 3% of CD4⁺ T cells stained positive for MOG-tetramer in accordance with previous publication [219] (Fig. 8G). Collectively, these data indicate that MOG-specific Th17 cells are observed in the large intestine and suggest an activation of CD4⁺ T lymphocytes in the colon during active EAE.

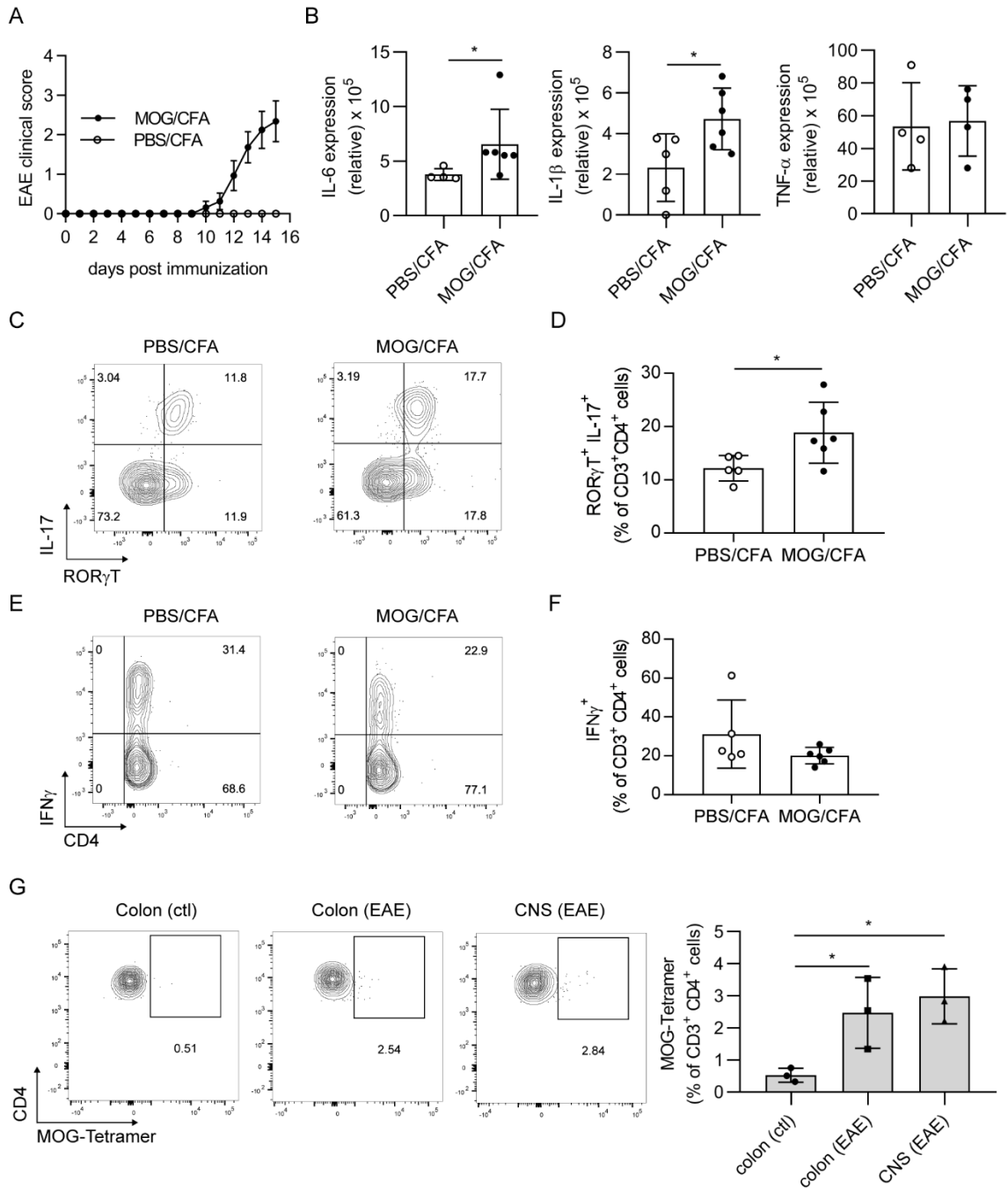


Figure 8. MOG-specific Th17 cells infiltrate the large intestine during active EAE. (A) Wild-type mice were immunized either with MOG₃₅₋₅₅ or PBS in CFA. The course of EAE in these mice is shown as clinical score (mean ± SEM; *n* = 8). (B) Relative mRNA expression of IL-6, IL-1β and TNF-α in colonic tissue as measured by real-time PCR in mice immunized with PBS/CFA or MOG/CFA when mice displayed neurological symptoms (mean ± SD; *n* = 4-6). Data are shown from one of two independent experiments with similar results. (C-F) Flow cytometric analysis of colonic lamina propria-infiltrating CD4⁺ T cells in PBS/CFA versus MOG/CFA group. Frequency of RORγT⁺/IL-17⁺ CD4⁺ T cells (C, D) and IFNγ⁺ CD4⁺ T cells (E, F) (mean ± SD; *n* = 5-6). (G) Cellular suspensions from colon and CNS were prepared from non-immunized (ctl) and immunized mice at the peak of the disease (EAE). After short-term culture of cells in the presence of MOG₃₅₋₅₅ peptide, FACS analysis of the total proportion (%) of MOG-specific CD4⁺ T cells were visualized by MOG₃₅₋₅₅/IAb tetramer staining (mean ± SD; *n* = 3). *, *P*

< 0.05; P values were determined by Mann-Whitney test (B (IL-6)), unpaired Student's *t* test (B (IL-1 β , TNF- α), D, F) and one-way ANOVA with Dunnett's post hoc test (G).

3.2.2 Encephalitogenic TCR^{MOG} 2D2 Th17 cells preferentially infiltrate the large intestine

To specifically study the relevance of the encephalitogenic Th17 cell infiltration in the large intestine during EAE, we performed adoptive transfer of CD4⁺ Th17 cells expressing a TCR specific for MOG (TCR^{MOG} 2D2). This model has the advantage to override the priming phase of T cells and to enable to focus solely on encephalitogenic potential of TCR^{MOG} 2D2 Th17 cell subsets. Briefly, CD4⁺ T cells from the spleen and lymph nodes (LN) of naive 2D2 mice, were differentiated *in vitro* into Th17 cells (Fig. 9A) and further transferred in C57BL/6J recipient mice as previously described [206] [207]. Following TCR^{MOG} 2D2 Th17 cell transfer, C57BL/6J recipient mice developed both typical and atypical EAE signs characterized by an ascending paralysis and an unbalanced gait with severe axial instability respectively [207]. However, when highly activated TCR^{MOG} 2D2 Th17 cell subsets are injected, neurological symptoms do not appear before 10 days after injection (Fig. 9B), suggesting that TCR^{MOG} 2D2 Th17 cell are activated in peripheral organs to acquire a phenotype enabling them to reach the CNS. We thus evaluated by flow cytometry analysis if TCR^{MOG} 2D2 Th17 cells (as defined by V α 3.2 expression) were detected in the small and large intestine before neurological symptoms appear. We detected a significant percentage of CD4⁺ T cells expressing V α 3.2 in the gut. In addition, the percentage of CD4⁺ T cells expressing TCR V α 3.2 was significantly higher in the colon (36.5% \pm 2.0) compared to the small intestine (10.4% \pm 2.9) (Fig. 9C, 9D) suggesting a predominant infiltration of the large intestine. In line with previous reports using the Lewis rat model of EAE [68] [220] [221], TCR^{MOG} 2D2 Th17 cells were present in the lungs (Fig. 9C). We further characterized the anatomical location of TCR^{MOG} 2D2 cells within the colon using whole-mount immunostaining. In agreement with flow cytometry analysis, high numbers of TCR^{MOG} 2D2 Th17 cells were found in the colonic lamina propria before EAE disease onset and were not observed in control non-injected WT animals (Fig. 9E).

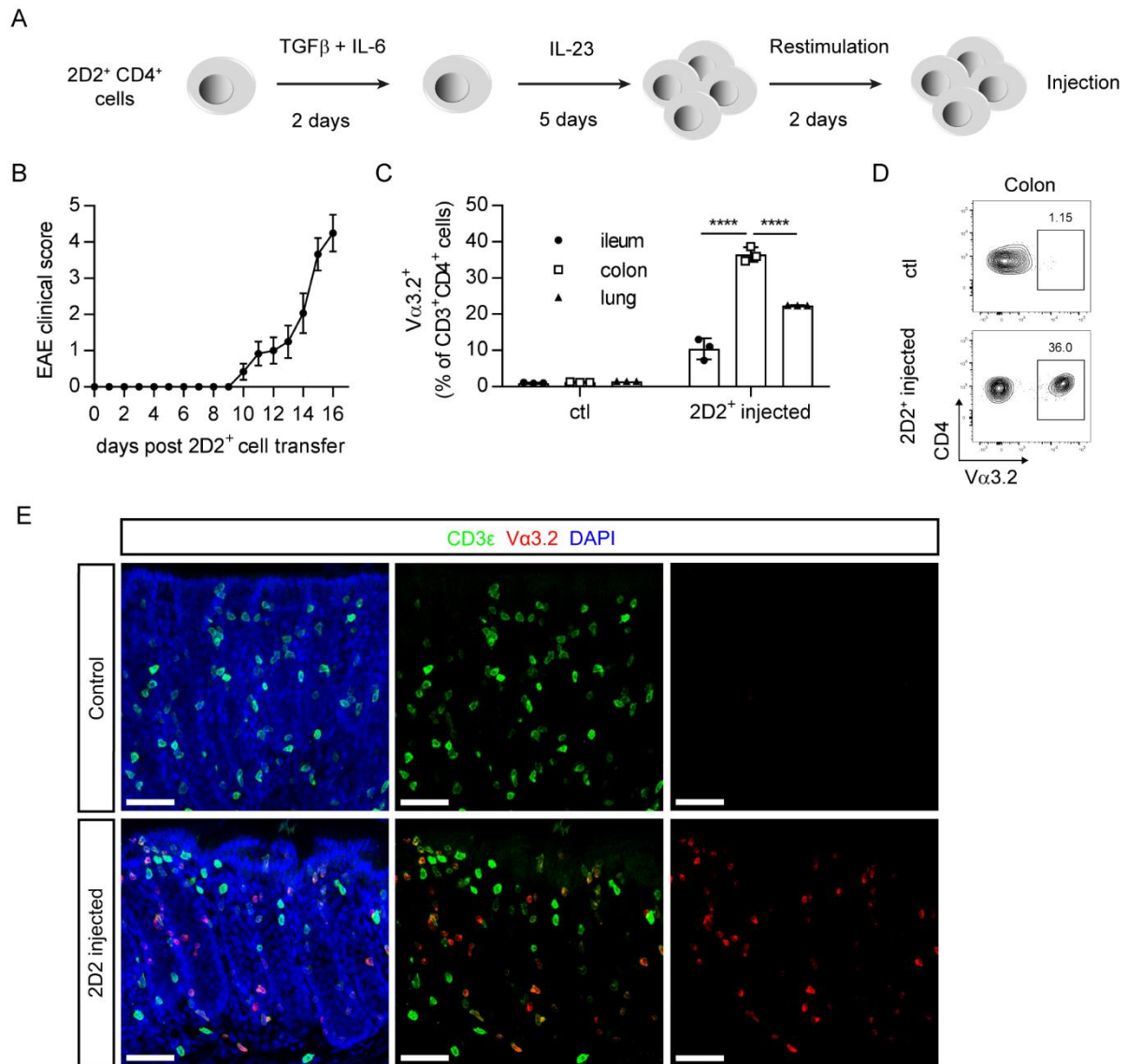


Figure 9. Encephalitogenic TCR^{MOG} 2D2 Th17 cells infiltrate preferentially the large intestine and are located in the colonic lamina propria during EAE. (A) CD4⁺ T cells from 2D2 mice were activated *in vitro* under Th17 polarizing conditions in the presence of TGFβ, IL-6 and IL-23. After 2 days of restimulation with anti-mouse CD3/CD28 antibodies, TCR^{MOG} 2D2 Th17 cells were injected into wild-type recipient mice. (B) Clinical scores of EAE in mice adoptively transferred with TCR^{MOG} 2D2 Th17 cells. The course of EAE in these mice is shown as clinical score (mean ± SEM; *n* = 12). (C) Flow cytometric analysis of the total proportion (%) of 2D2-TCR (Vα3.2⁺) expression in CD3⁺/CD4⁺ T cells at day 8 post injection among the lamina propria of ileum, colon and lung in non-injected control mice and mice injected with TCR^{MOG} 2D2 Th17 cells (mean ± SD; *n* = 3). Data are representative of two experiments. (D) Representative flow cytometry analysis of 2D2-TCR (Vα3.2⁺) expression in CD3⁺/CD4⁺ T cells obtained from the colonic lamina propria of non-injected control mice versus mice injected with TCR^{MOG} 2D2 Th17 cells 8 days after injection. (E) Colon whole-mount immunostaining for endogenous (green, CD3ε) and injected TCR^{MOG} 2D2 (red, Va3.2) T cells from control and TCR^{MOG} 2D2 T cell injected mice; blue, DAPI. Scale bar, 50μm. [Jeremiah Bernier-Latmani performed the whole-mount immunostaining and took the picture].

We then asked if Th17 cell colonic infiltration was MOG specific. To address this question, we took advantage of OT-II transgenic mice that display a TCR specific for the ovalbumin 323-339 peptide. CD4⁺ T cells, obtained from both OT-II and 2D2 mice on the CD45.2 background, were polarized into Th17 cells and transferred into CD45.1 recipient mice. Colonic tissue was examined by flow cytometry for the percentage of CD45.2⁺ on total CD45⁺ cells. 2D2 and OT-II cells migrated similarly to the colon suggesting that Th17 cell migration to the colon is not MOG specific (Fig. 10A). We further asked if different subset of encephalitogenic T cell subsets similarly migrate to the colon. We thus generated Th17 and Th1 cells from MOG-specific TCR 2D2 transgenic T cells *in vitro* as previously described [206] and transferred them into naive syngeneic wild-type C57Bl6/J recipients. The percentages of TCR^{MOG} 2D2 T cells were assessed by flow cytometry from the colon of recipient mice. Significantly higher percentage of TCR^{MOG} 2D2 T cells were detected in the colon when cells were differentiated into Th17 versus Th1 cells (Fig. 10B). Those results suggest that Th17 cells migrate to the colon during EAE independently of their antigen-specificity but at higher levels than Th1 cells.

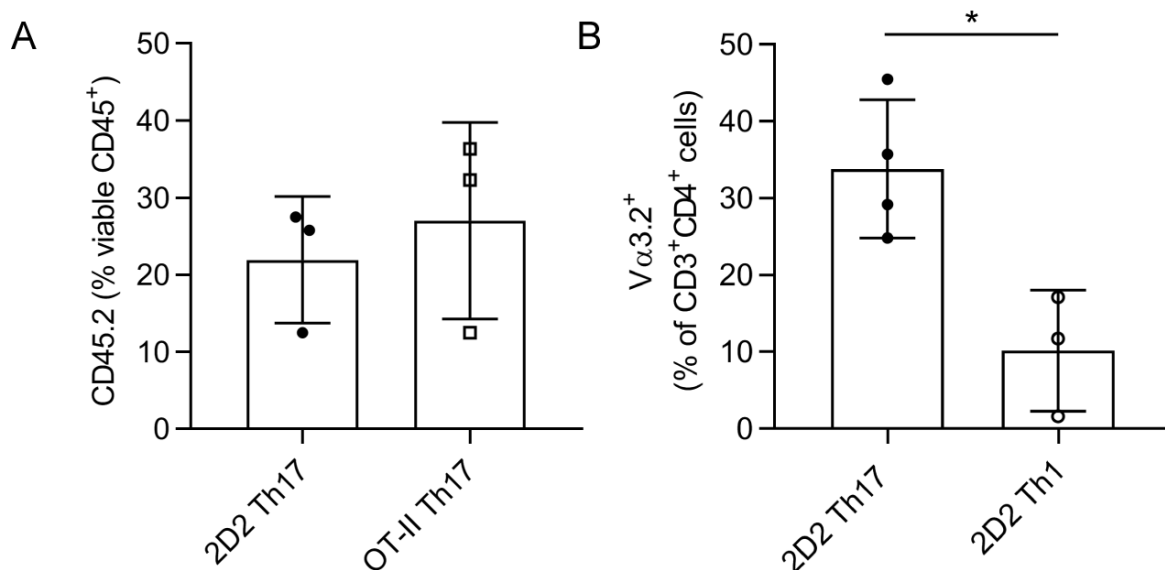


Figure 10: TCR^{MOG} 2D2 Th17 cells enter the colon in an antigen-independent manner but at higher levels than TCR^{MOG} 2D2 Th1 cells. (A) Flow cytometric analysis of the total proportion (%) of CD45.2⁺ cells (donor 2D2 or OT-II) obtained from the colon of CD45.1 recipient mice 15 days after T cell transfer (mean ± SD; n = 3). **(B)** Flow cytometric analysis of Vα3.2⁺ frequency in CD3⁺/CD4⁺ T cells at day 4 post injection in the colon of mice injected with TCR^{MOG} 2D2 Th17 cells or TCR^{MOG} 2D2 Th1 cells (mean ± SD; n = 3-4). *, P < 0.05; P values were determined by unpaired Student's *t* test (A, B).

3.2.3 Encephalitogenic TCR^{MOG} 2D2 Th17 cells are in close contact with colonic blood vessels and egress via lymphatic vessels

Using 3D image reconstruction we assessed the location of TCR^{MOG} 2D2 Th17 cells within the colonic lamina propria. While TCR^{MOG} 2D2 Th17 cells were found throughout the colonic lamina propria, we observed that many cells were closely associated with colon blood capillaries. Quantification of TCR^{MOG} 2D2 Th17 cells either in immediate vicinity (on) or not (off) with colon blood capillaries showed that more than 60% of the TCR^{MOG} 2D2 Th17 were contacting these vessels (Fig. 11A). We further observed that a fraction of TCR^{MOG} 2D2 Th17 cells showed an elongated morphology, suggesting a migratory phenotype (Fig. 11A). Furthermore, TCR^{MOG} 2D2 Th17 cells were detected closely associated with, and in the lumen of, dilated vessels below colonic crypts, identified as lymphatic capillaries by LYVE-1 staining (Fig. 11B-D). As intestinal lymphatic capillaries drain into mesenteric lymph nodes (mLN) [222], we assessed the percentage of TCR^{MOG} 2D2 by FACS analysis in the gut-draining mLN versus the dermal inguinal lymph nodes (dLN) of the same recipient mice 4 and 8 days after TCR^{MOG} 2D2 transfer and in PBS-injected recipient mice (Fig. 12). Around 1% CD4⁺ T cells were V α 3.2⁺ in the dLN (1.03% \pm 0.1) and mLN (1.0% \pm 0.1) of PBS-injected recipient mice, compatible with low levels of endogenous V α 3.2⁺ expression in lymphoid organs of C57Bl6/J mice [223]. We observed a significant 18-fold (18.7% \pm 4.5, 4 days) and 13-fold (13.3% \pm 1.9, 8 days) increase in CD4⁺ T cells harboring the V α 3.2⁺ marker in the mLN after TCR^{MOG} 2D2 Th17 cell transfer (Fig. 12). At the same time, there was only a minor tendency towards increase in V α 3.2⁺ T cells in the dLN of the same mice (2.6 % \pm 0.2, 4 days) and (2.9 % \pm 0.5, 8 days) after T cell transfer compared to the control dLN (1.03% \pm 0.1) (Fig. 12). Altogether, these data show that TCR^{MOG} 2D2 Th17 cells infiltrate the colonic lamina propria, migrate out of the colon via lymphatic vessels and likely re-enter blood circulation downstream of mLNs.

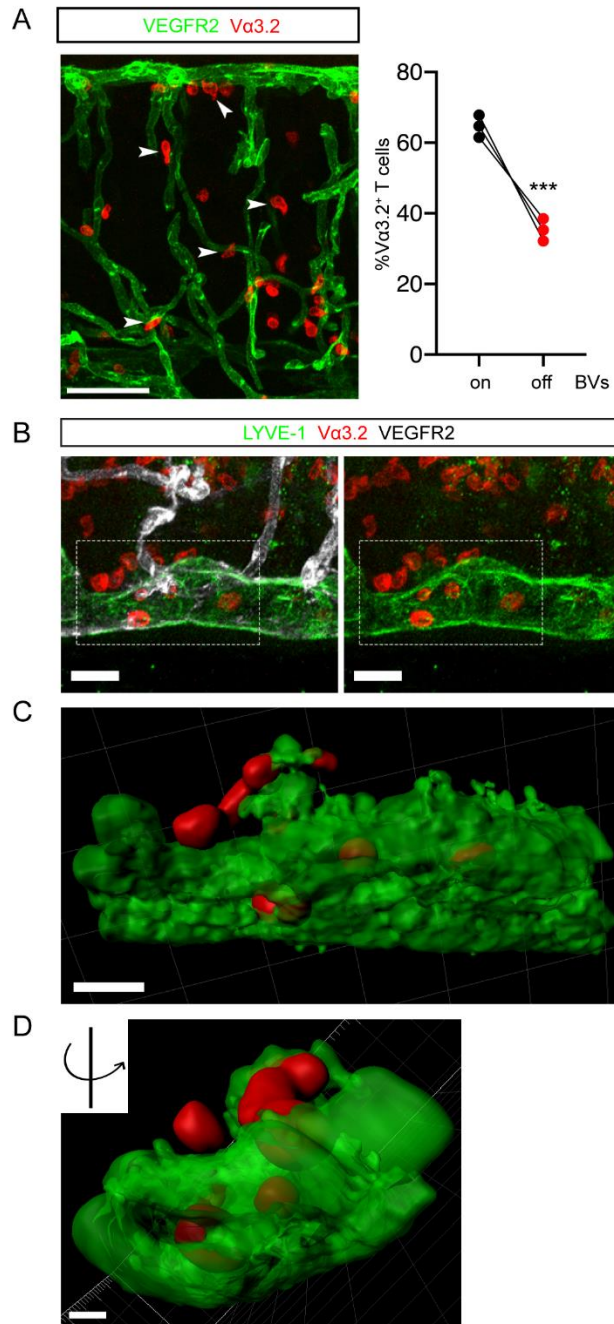


Figure 11. Encephalitogenic TCR^{MOG} 2D2 Th17 cells are located in close contact to blood and lymphatic vessels. (A) Injected TCR^{MOG} 2D2 T cells (red, Vα3.2) are located in the colonic lamina propria near blood vessels (green, VEGFR2). Arrowheads indicate TCR^{MOG} 2D2 T cells with an elongated morphology. Scale bar, 50μm. Percentage of TCR^{MOG} 2D2 T cells in direct contact (on) or not (off) with colon blood capillaries, *n*=3. **(B)** Whole-mount immunostaining of Vα3.2⁺ T cells (red) entering submucosal VEGFR2⁺ (white), LYVE1⁺ (green) lymphatic capillaries 4 days after T cell injection. **(C)** 3D reconstruction of Vα3.2⁺ T cells (red) entering lymphatic capillaries (green). **(D)** Same image as C, turned 90° on the Y-axis to show T cells in the lymphatic capillary lumen. Scale bars: A, 50μm; B, 20μm; C, 10μm. ***, *P* < 0.001; *P* values were determined by unpaired Student's *t*-test. [Jeremiah Bernier-Latmani performed the whole-mount immunostaining, took the picture and performed 3D reconstruction].

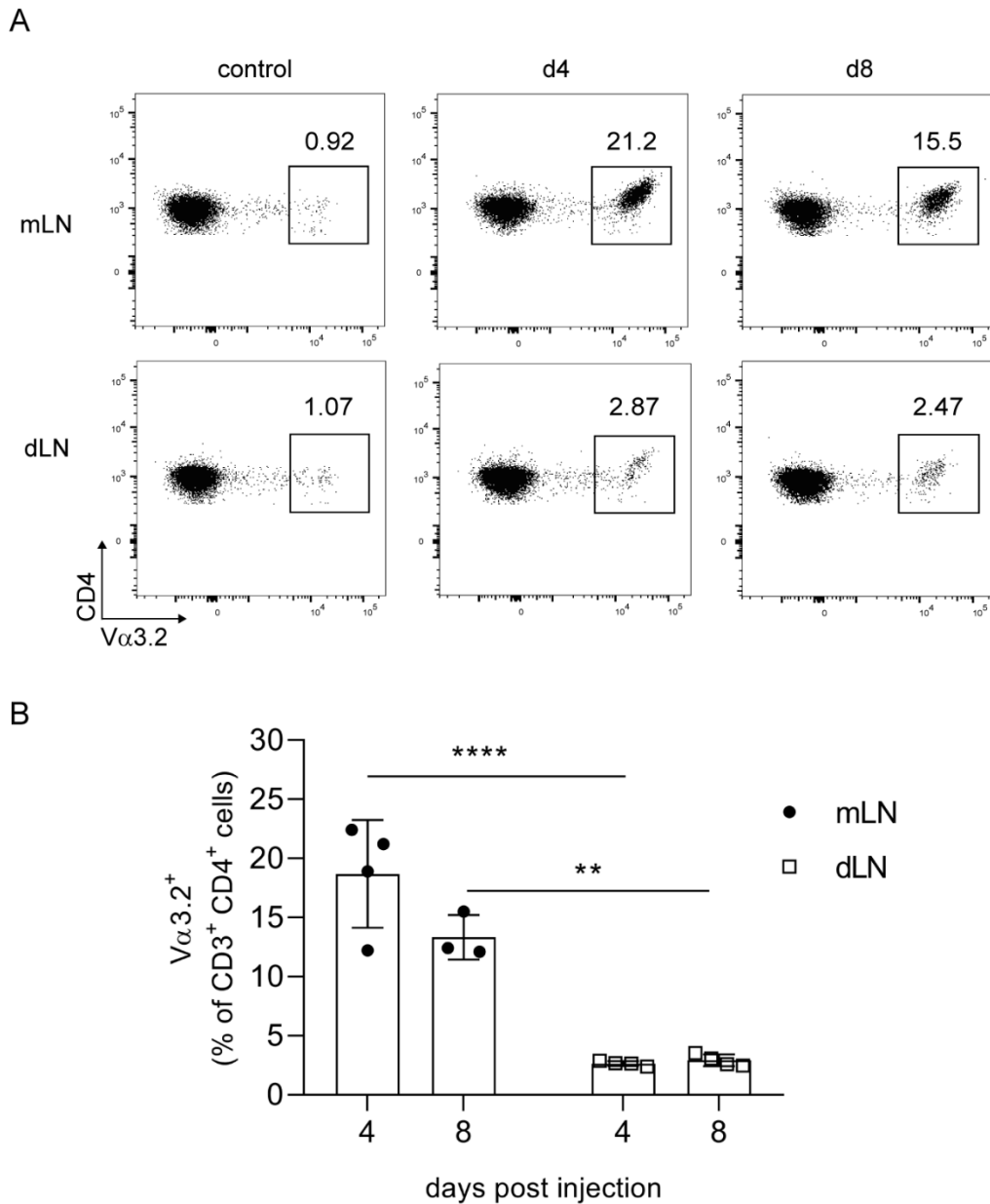


Figure 12. Encephalitogenic TCR^{MOG} 2D2 Th17 cells migrated through the mesenteric lymph nodes but not the dermal inguinal lymph nodes. (A) Representative flow cytometry analysis of 2D2-TCR (V α 3.2⁺) expression in CD3⁺/CD4⁺T cells from mesenteric lymph nodes (mLN) and dermal inguinal lymph nodes (dLN) isolated from PBS-injected (control) mice and from mice injected with TCR^{MOG} 2D2 Th17 cells at 4 days (d4) and 8 days (d8) post injection. **(B)** Flow cytometry analysis of the total proportion (%) of 2D2-TCR (V α 3.2⁺) expression in CD3⁺/CD4⁺ T cells of mLN and dLN at the indicated time points after TCR^{MOG} 2D2 Th17 cells transfer (mean \pm SD; $n = 3-4$). *, $P < 0.05$; **, $P < 0.01$; ***, $P < 0.001$, ****, $P < 0.0001$; P values were determined by two-way ANOVA with Tukey's post hoc test (B).

3.2.4 Blocking integrin $\alpha 4\beta 7$ /MAdCAM-1 interactions inhibits TCR^{MOG} 2D2 Th17 entry to the large intestine and significantly attenuates EAE

To explore whether colonic TCR^{MOG} 2D2 migration contributes to neuroinflammation, we asked if blocking TCR^{MOG} 2D2 entry to the gut influences EAE development. Autoimmune T cells receive signals to acquire a functional phenotype that allow them to invade their target tissues [224] [225]. Intestinal-targeting of T cells requires expression of the ligand $\alpha 4\beta 7$ integrin on immune cells and expression of its receptor mucosal vascular addressin cell adhesion molecule 1 (MAdCAM-1) on intestinal venules [226]. In our model, MAdCAM-1 was expressed in the colon at significant higher level compared to the CNS both at steady state and 4 days after adoptive transfer (Fig. 13A). As we detected large amount of TCR^{MOG} 2D2 Th17 in the large intestine, we evaluated whether these cells expressed the integrin $\alpha 4\beta 7$. Half ($50.2\% \pm 2.8$) of the colonic TCR^{MOG} 2D2 cells expressed $\alpha 4\beta 7$ four days after adoptive transfer while $\alpha 4\beta 7$ expression was significantly reduced ($14.5\% \pm 3.1$) at day 8, before neurological signs appear (Fig. 13B). Those results suggest that $\alpha 4\beta 7$ expression is involved in TCR^{MOG} 2D2 Th17 cell migration to the gut. In mouse models of T cell-mediated colitis, administration of $\alpha 4\beta 7$ antibodies reduces inflammation and the severity of colitis. Similarly, Vedolizumab, a humanized specific $\alpha 4\beta 7$ inhibitor, has proven effective in ulcerative colitis and Crohn's disease [227] [228] [229]. As we observed an important TCR^{MOG} 2D2 Th17 cell infiltration in the large intestine, we further tested whether selective blocking of $\alpha 4\beta 7$ could also influence EAE disease course. $\alpha 4\beta 7$ -blocking antibodies (DATK 32) were administered one day before adoptive transfer followed by injections every three days until the development of EAE disease. We observed during EAE a significant reduction of TCR^{MOG} 2D2 Th17 cell infiltration in the colon, but not in the ileum nor in the lung 4 days after T cell transfer in mice treated with anti- $\alpha 4\beta 7$ compared with the isotype control group (Fig. 13C, 13D). Moreover, $\alpha 4\beta 7$ blockade was efficient in dampening EAE neurological disease course (Fig. 13E and Table 5). In addition, a significantly reduced number of TCR^{MOG} 2D2 Th17 infiltrating the CNS was recorded 10 days after T cell adoptive transfer in mice treated with anti- $\alpha 4\beta 7$ compared with the isotype control group (Fig. 13F).

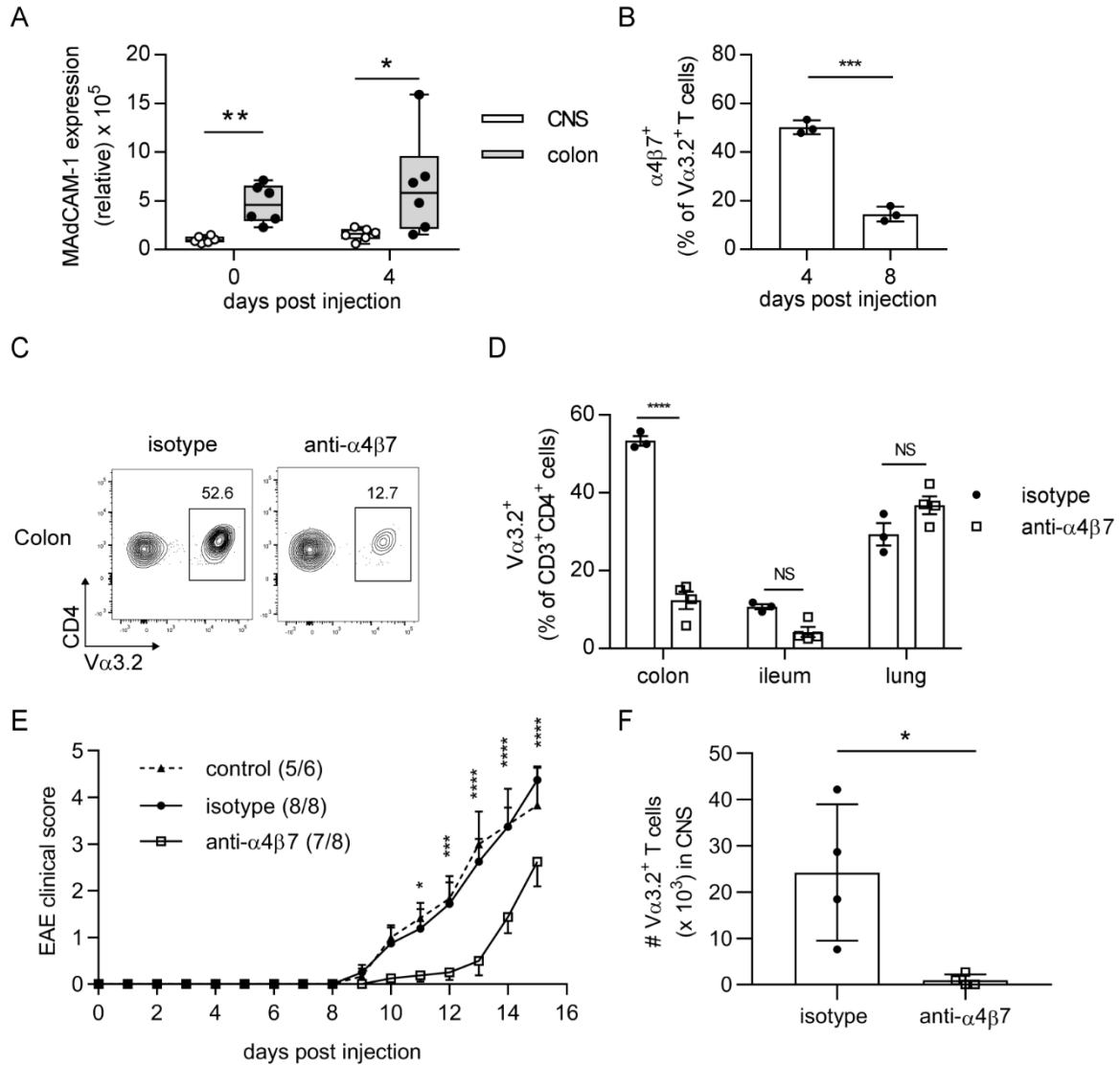


Figure 13. Blocking integrin $\alpha 4\beta 7$ reduces migration of encephalitogenic TCR^{MOG} 2D2 cells to the colon and delays the progression of EAE disease. (A) Relative mRNA expression of MAAdCAM-1 in CNS and colonic tissue as measured by real-time PCR in non-injected mice (day 0) and four day after TCR^{MOG} 2D2 Th17 cells injection. Box-and-whisker graphs show median, min., and max. values and 25th and 75th percentiles ($n = 6$). **(B)** Flow cytometry analysis of the total proportion (%) of the integrin $\alpha 4\beta 7$ expression in colonic 2D2-TCR ($V\alpha 3.2^+$) $CD4^+$ T cells at the indicated time points after TCR^{MOG} 2D2 Th17 cells injection (mean \pm SD; $n = 3$). Data are representative of two experiments. **(C, D)** Flow cytometry analysis of 2D2-TCR ($V\alpha 3.2^+$) proportion in $CD4^+$ T cells obtained from the colon, ileum and lung in isotype control versus anti- $\alpha 4\beta 7$ treated group at day 4 after TCR^{MOG} 2D2 Th17 cells transfer (mean \pm SEM; $n = 3-4$). Data are representative of two experiments. **(E)** Clinical scores of EAE in adoptively transferred mice treated with PBS 1X, isotype control or anti- $\alpha 4\beta 7$ antibodies. The course of EAE in these mice is shown as clinical score (mean \pm SEM; $n = 6-8$; P values are shown for comparison between anti- $\alpha 4\beta 7$ versus isotype groups). **(F)** Absolute numbers of TCR^{MOG} 2D2 Th17 cells infiltrating the CNS 10 days after adoptive transfer in mice treated with isotype control or anti- $\alpha 4\beta 7$ antibodies (mean \pm SD; $n = 4$). Data are representative of two experiments. *, $P < 0.05$; **, $P < 0.01$; ***, $P < 0.001$; ****, $P < 0.0001$; NS, not significant; P values were determined by unpaired Student's t test (A, B), two-way ANOVA with Sidak's post hoc test (D) and Tukey's post hoc test (E).

Group	Disease incidence	Maximum score	Day of onset	AUC
control	83.3% (5/6)	3.83 ± 2.04	9.8 ± 0.45	12.75 ± 2.36
isotype	100% (8/8)	4.38 ± 0.74	10.5 ± 1.31	12.22 ± 1.97
anti- α 4 β 7	87.5% (7/8)	2.63 ± 1.51 ^(p=0.06)	12.71 ± 1.89 ^(p=0.08)	3.81 ± 1.28 ^{****}

AUC, area under the curve

Table 5. Blocking integrin α 4 β 7 attenuates disease course in adoptive transfer EAE. EAE in mice treated with PBS, isotype control or anti- α 4 β 7 antibodies. EAE disease incidence (%), maximum scores (mean ± SD; $n = 6-8$), day of disease onset (mean ± SD; $n = 5-8$), area under the curve (AUC) (mean ± SD; $n = 6-8$). *, $P < 0.05$; **, $P < 0.01$; ***, $P < 0.001$; ****, $P < 0.0001$; P values were shown for comparison between anti- α 4 β 7 versus isotype groups and were determined by one-way ANOVA with Tukey's post hoc test (AUC, maximum score) and by Kruskal-Wallis test with Dunn's post hoc test (day of disease onset).

Similar results were obtained when we extended the anti- α 4 β 7 treatment until the end of the EAE disease (Fig. 14A) suggesting that the contribution of colonic Th17 cell on EAE takes place early during EAE. Furthermore, anti- α 4 β 7 antibody treatment was not able to delay active EAE development (Fig. 14B). In active EAE, Th1 cells play a predominant role compared to Th17 cells [206]. This is in accordance with our observation that Th17-polarized 2D2 cells are more prone to reach the colon compared to Th1-polarized 2D2 cells (Fig. 10B). Those results suggest a contribution of Th17 migration to the colon during EAE.

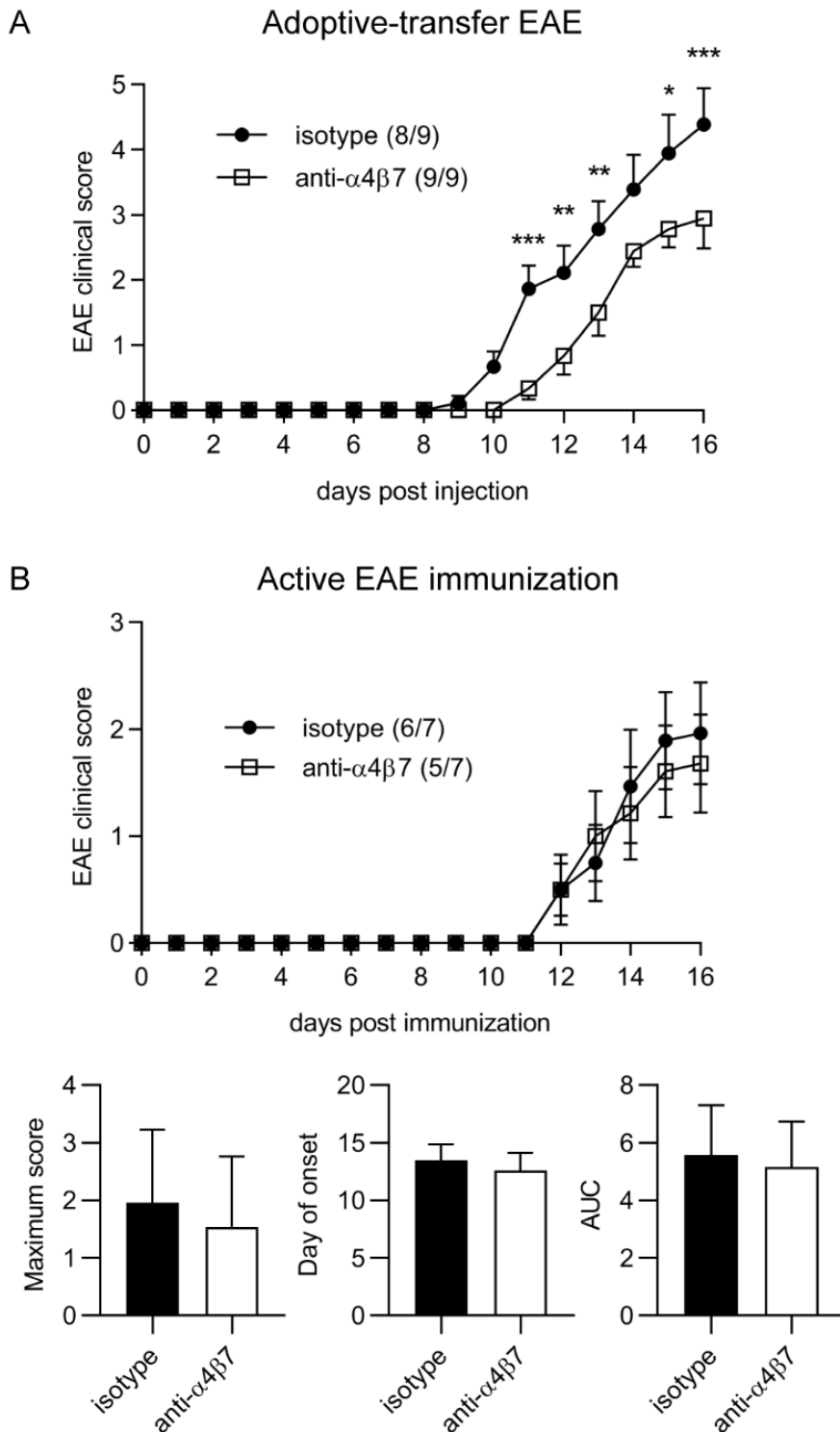


Figure 14. Continuously blocking of α 4 β 7-integrin alleviates adoptive-transfer EAE but not active EAE. (A) Clinical scores of Th17 adoptive-transfer EAE mice treated with anti- α 4 β 7 antibodies or isotype control every 3 days until the end of the experiment (mean \pm SEM; $n = 9$ per group). **(B)** EAE was induced in wild-type mice by immunization with MOG₃₅₋₅₅ in Complete Freund Adjuvant (CFA). Mice were injected with either anti- α 4 β 7 antibodies or an isotype control every 3 days. The course of EAE is shown as clinical score (mean \pm SEM; $n = 7$ per group). Maximum scores (mean \pm SD; $n = 7$), day of disease onset (mean \pm SD; $n = 5-6$), area under the curve (AUC) (mean \pm SD; $n = 7$). *, $P < 0.05$; **, $P < 0.01$; ***, $P < 0.001$, ****, $P < 0.0001$; P values were determined by two-way ANOVA with Sidak's post hoc test (A).

3.2.5 Colonic TCR^{MOG} 2D2 Th17 cell express CNS-Integrin and their intestinal infiltrate resolves upon CNS invasion

As we observed TCR^{MOG} 2D2 Th17 infiltration of the large intestine before neurological clinical signs, we wondered whether this infiltration persisted throughout the disease course. The frequency of TCR^{MOG} 2D2 Th17 was thus evaluated at different time points after T cell transfer by flow cytometry analysis simultaneously in the colon and the CNS samples. TCR^{MOG} 2D2 Th17 cells infiltrate the colonic lamina propria as early as 4 days after transfer, while no cells were detected in the CNS simultaneously (Fig. 15A). Eight days post-transfer, the frequency of colonic TCR^{MOG} 2D2 Th17 cells decreased by more than two-fold compared to day 4 while we found a concomitant significant increase in the percentage of 2D2 cells in the CNS from 0% at day 4 to 32.7% ± 6.4 at day 8 and then 67.5% ± 10.7 at the peak of the disease (Fig. 15A). Taken together, the data presented above demonstrate that CNS-specific Th17 cells are able to migrate and to infiltrate the large intestine during the preclinical phase of transfer EAE prior reaching the CNS. To assess if TCR^{MOG} 2D2 Th17 detected in the gut display encephalitogenic properties, we evaluated the level of α4β1 integrin (CNS-specific integrin) 4 days after T cell transfer and showed that α4β1 integrin was expressed at similar levels than α4β7 integrin known to be gut-specific (Fig. 15B). However, the α4β1 integrin ligand VCAM-1 was expressed solely in the CNS but not in the colon (Fig. 15C). In addition, α4β1 integrin expression decreases on TCR^{MOG} 2D2 Th17 cells of the colon over time while the expression remained high in the CNS when the TCR^{MOG} 2D2 reached the CNS (Fig. 15D). Those results strengthen our hypothesis that TCR^{MOG} 2D2 Th17 depict encephalitogenic properties while present in the colon.

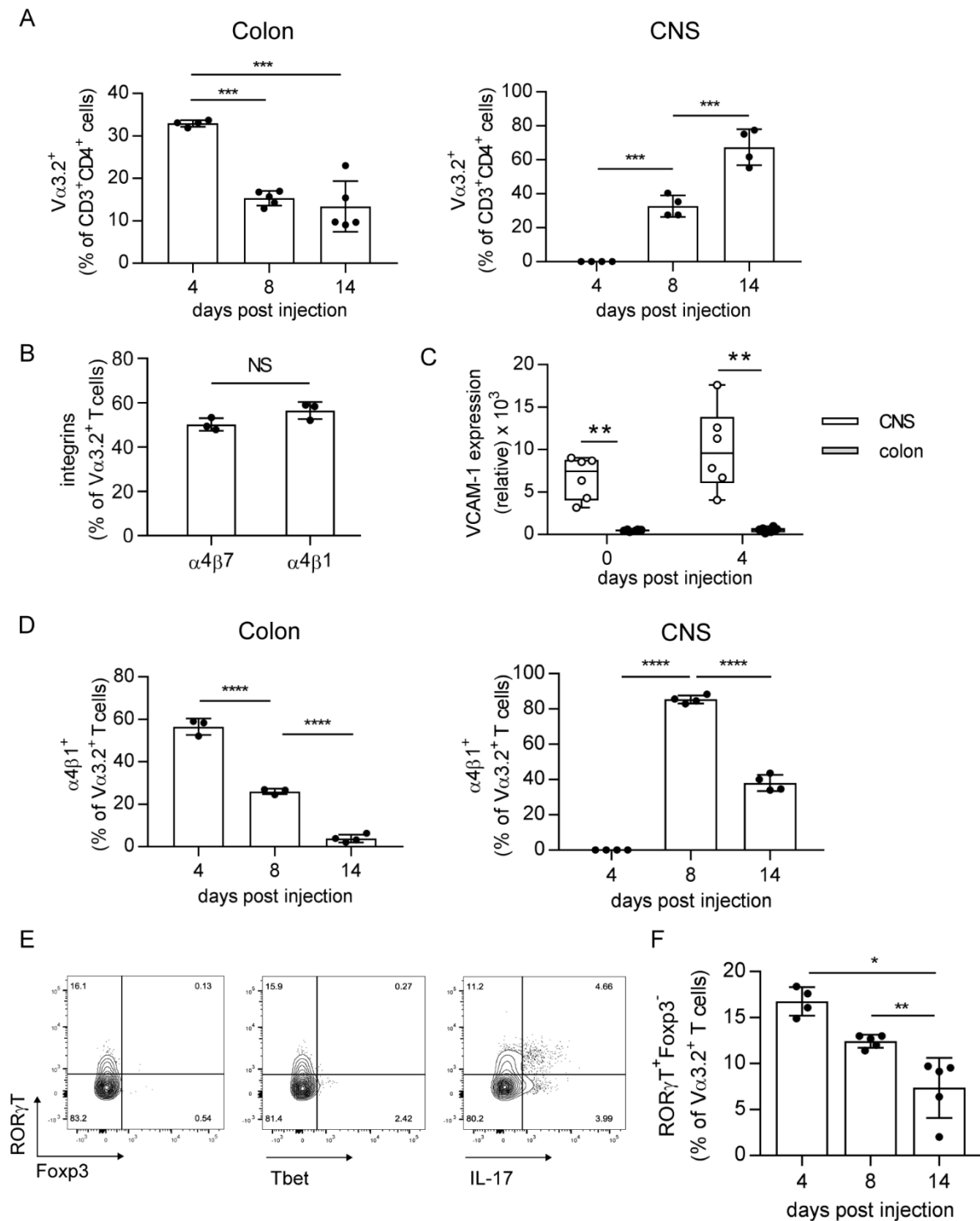


Figure 15. Encephalitogenic TCR^{MOG} 2D2 Th17 cells infiltrate the large intestine and express CNS-specific integrin before reaching the CNS. (A) Flow cytometry analysis of the total proportion (%) of 2D2-TCR ($V\alpha 3.2^+$) expression in $CD3^+/CD4^+$ T cells of colonic lamina propria and CNS at the indicated time points after TCR^{MOG} 2D2 Th17 cells transfer (mean \pm SD; $n = 4-5$). Data are representative of two experiments. **(B)** Flow cytometry analysis of the total proportion (%) of the integrin $\alpha 4\beta 7$ and $\alpha 4\beta 1$ expression in colonic 2D2-TCR ($V\alpha 3.2^+$) $CD4^+$ T cells four days after TCR^{MOG} 2D2 Th17 cells injection (mean \pm SD; $n = 3$). Data are representative of two experiments. **(C)** Relative mRNA

expression of VCAM-1 in CNS and colonic tissue as measured by real-time PCR in non-injected mice (day 0) and four days after TCR^{MOG} 2D2 Th17 cells injection. Box-and-whisker graphs show median, min., and max. values and 25th and 75th percentiles ($n = 6$). **(D)** Flow cytometry analysis of the total proportion (%) of the integrin $\alpha 4\beta 1$ expression of 2D2-TCR ($V\alpha 3.2^+$) $CD4^+$ T cells in the colon and the CNS at the indicated time points after TCR^{MOG} 2D2 Th17 cells injection (mean \pm SD; $n = 3$). Data are representative of two experiments. **(E)** Representative flow cytometry analysis of ROR γ T⁺/Foxp3⁻, ROR γ T⁺/Tbet⁻, ROR γ T⁺/IL-17⁺ expression in 2D2-TCR ($V\alpha 3.2^+$) $CD4^+$ T cells obtained from the colonic lamina propria of EAE mice at day 4 after TCR^{MOG} 2D2 Th17 cells transfer. **(F)** Time course of transferred TCR^{MOG} 2D2 analyzed by flow cytometry for ROR γ T⁺/Foxp3⁻ intracellular expression and shown as a percentage of the $V\alpha 3.2^+$ T cells population (mean \pm SD; $n = 4-5$). Data are representative of two experiments. *, $P < 0.05$; **, $P < 0.01$; ***, $P < 0.001$, ****, $P < 0.0001$; NS, not significant; P values were determined by one-way ANOVA with Tukey's post hoc test (A, D, F) and unpaired Student's *t* test (B, C).

Different Th17 cell subsets have been described in the colon, in particular the homeostatic Th17 cells co-expressing both Foxp3 and ROR γ T [230] and the pathogenic Th17 cells that do not express Foxp3. Thus, we evaluated the phenotypic profile of the TCR^{MOG} 2D2 Th17 cells detected in the colonic lamina propria. Four days after injection, colonic lamina propria $V\alpha 3.2^+$ $CD4^+$ T cells were analyzed by flow cytometry for ROR γ T, Foxp3, T-bet, and IL-17A expression. TCR^{MOG} 2D2 Th17 cells maintained ROR γ T expression, while neither T-bet nor Foxp3 expression was detected (Fig. 15E). We further conducted our analysis at different time points after T cell transfer and observed a reduction of the total frequencies of ROR γ T⁺ 2D2⁺ cell (Fig. 15F). However, the residual colonic 2D2⁺ $CD4^+$ T cells kept their capacity to secrete the pro-inflammatory IL-17 cytokine in colonic lamina propria at all time points examined (Fig. 16A, 16B). In addition, Foxp3 and ROR γ T co-expressing Th17 cells and Foxp3⁺ ROR γ T⁻ regulatory T cells, were both restricted to $V\alpha 3.2^-$ $CD4^+$ T cells (2D2⁻) and their frequencies were not impacted by time (Fig. 16C). We thus demonstrated that TCR^{MOG} 2D2 Th17 cells were predominantly detected in the large intestine before reaching the CNS and that these cells maintained their pro-inflammatory phenotype after *in vivo* transfer.

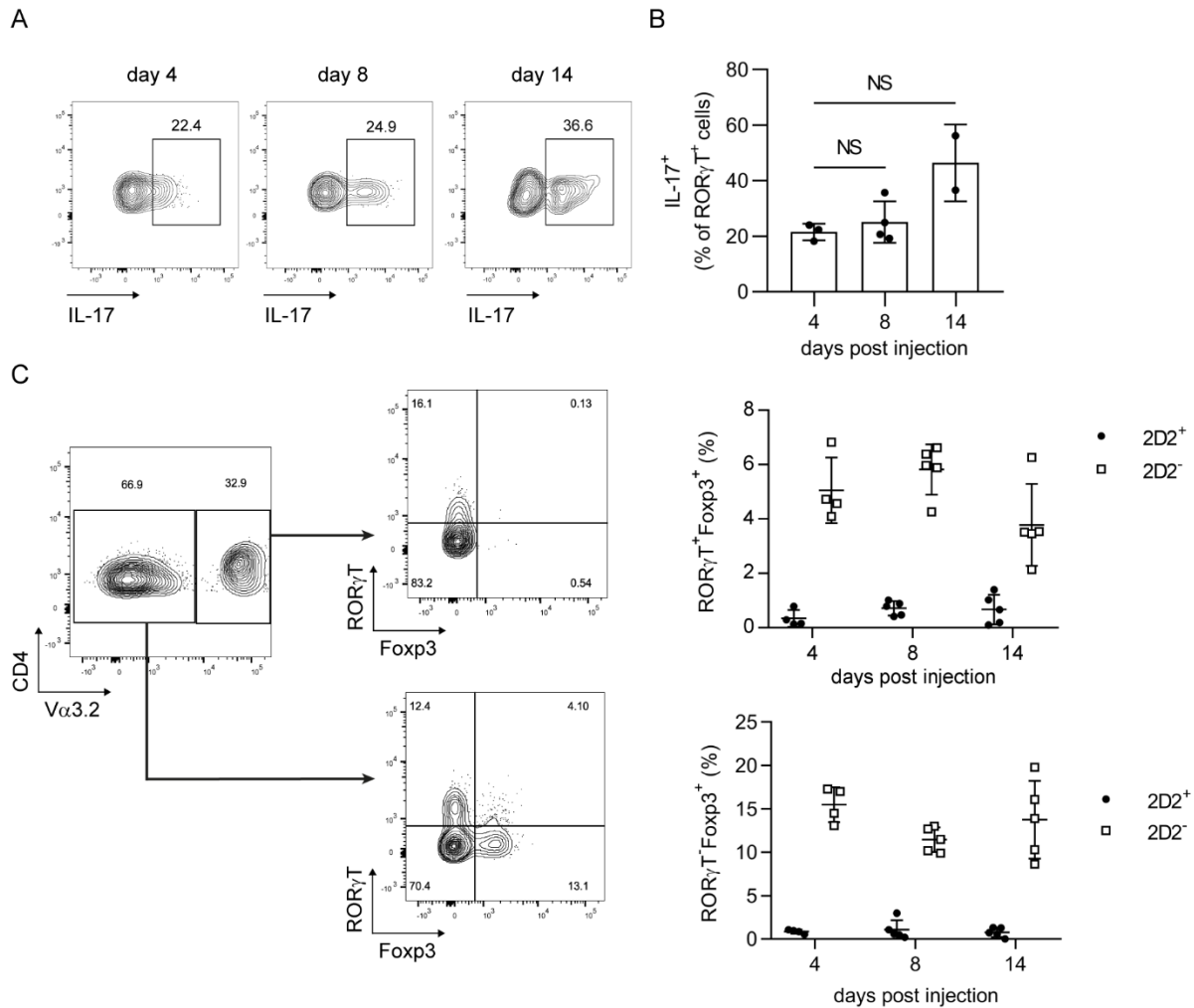


Figure 16. Encephalitogenic TCR^{MOG} 2D2 Th17 cells maintain their pathogenic phenotype throughout EAE disease. (A) Representative FACS analysis of IL-17⁺ expression in RORγT⁺ 2D2⁺ T cells obtained from the colonic lamina propria of EAE at the indicated time points after TCR^{MOG} 2D2 Th17 cells transfer. **(B)** Time course of transferred TCR^{MOG} 2D2 analyzed by flow cytometry for IL-17⁺ intracellular expression and shown as a percentage of the RORγT⁺ Va3.2⁺ T cells population (mean ± SD; *n* = 2-4). **(C)** Ex vivo flow cytometry analysis of colonic RORγT^{+/−} Foxp3⁻ frequency in 2D2⁺ TCR (Va3.2⁺) cells versus 2D2⁻ TCR (Va3.2⁻) cells population. Representative contour plots are shown depicting intracellular staining for RORγT versus Foxp3 after gating for Va3.2⁺ or Va3.2⁻ CD4⁺ T cells population (mean ± SD; *n* = 4-5). Data are representative of two experiments; NS, not significant; P values were determined by Kruskal-Wallis test with Dunn's multiple comparisons post hoc test (B).

3.2.6 Encephalitogenic TCR^{MOG} 2D2 Th17 cells proliferate in the large intestine

Having established that TCR^{MOG} 2D2 cells are detected in the colonic lamina propria, we further explored their fate within the large intestine and evaluated their proliferative status with Ki67 staining. FACS analysis demonstrated that almost 100% of TCR^{MOG} 2D2 cells proliferated in the colonic lamina propria 4 days after T cell transfer. This proliferation rate significantly decreased to less than 20% 8 days post-transfer (Fig. 17A). In comparison, V α 3.2⁻ CD4⁺ T cells (host cells) showed a constant proliferation rate of 25% with no significant changes between day 4 and day 8 (Fig. 17A). We next assessed the location of proliferating TCR^{MOG} 2D2 cells in the colon by whole-mounting immunostaining (Fig. 17B). At day 4, 30% of TCR^{MOG} 2D2 cells detected above the lumen-adjacent blood vessel ("lumen", yellow line in Fig. 17B) were Ki67⁺ while only 15% of TCR^{MOG} 2D2 cells were located below the lumen-adjacent blood vessel ("stroma" cells). In agreement with FACS analysis, less than 5% of total TCR^{MOG} 2D2 cells were Ki67⁺ at day 8 after injection regardless of location (Fig. 17C). However, among Ki67⁺ TCR^{MOG} 2D2 cells at both day 4 and day 8 approximately two third of Ki67⁺ cells were found near the colon lumen (Fig. 17D). These results show that TCR^{MOG} 2D2 cells proliferated at the maximum rate 4 days after T cell transfer and are found near colonic lumen.

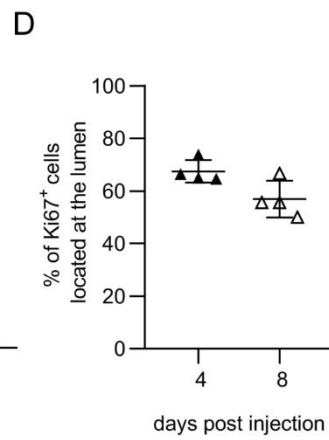
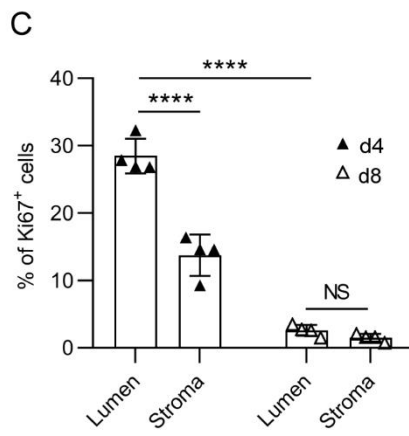
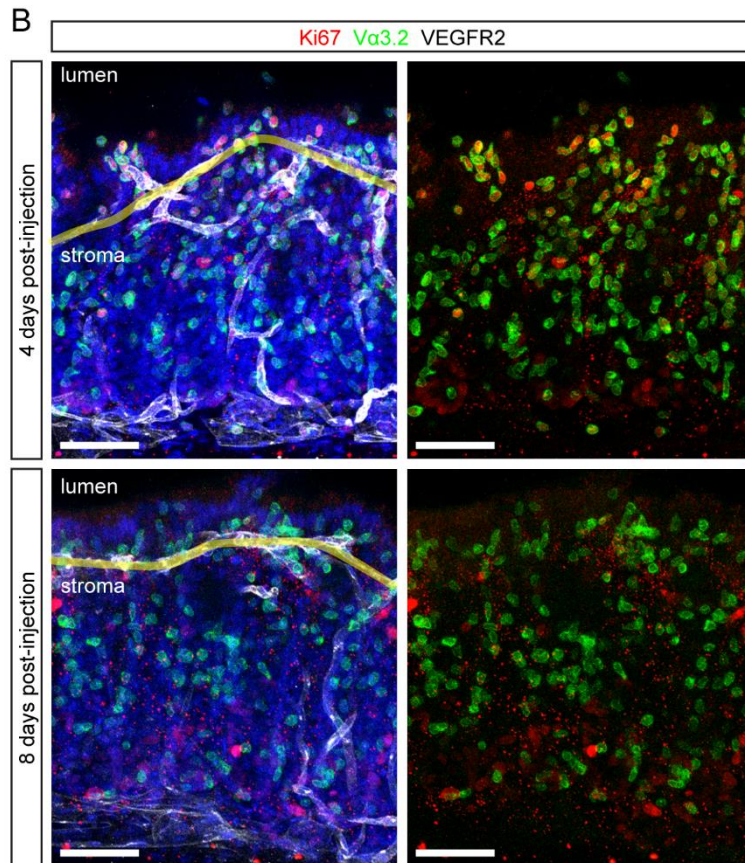
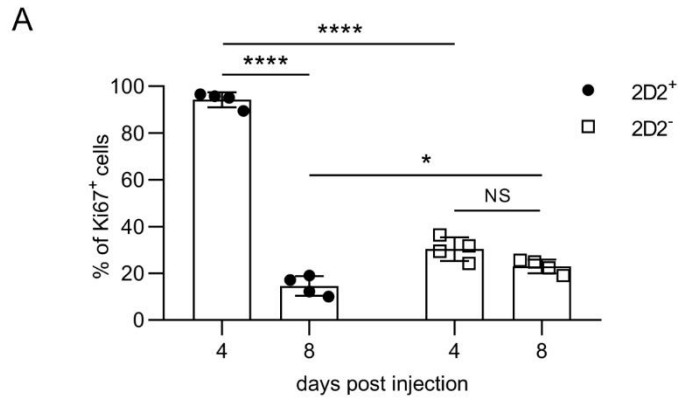
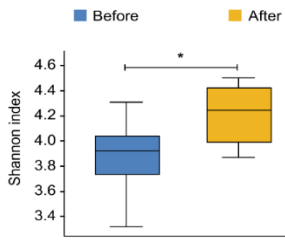


Figure 17. Encephalitogenic TCR^{MOG} 2D2 Th17 cells proliferate in the colon (A) Flow cytometry analysis of proliferating Ki67⁺ cells (%) among 2D2⁺TCR (V α 3.2⁺) and 2D2⁻TCR (V α 3.2⁻) CD4⁺ T cells within colonic lamina propria at the indicated time points after T cell transfer (mean \pm SD; $n = 4$). Data are shown from one of three independent experiments with similar results. **(B)** Whole-mount immunostaining of proliferating (Ki67⁺, red), TCR^{MOG} 2D2 (V α 3.2⁺ cells, green) and blood vessels (white, VEGFR2). Blue, DAPI. V α 3.2⁺ T cells observed above the lumen-adjacent blood vessel (yellow line) were considered “lumen” T cells and cell located below were considered “stroma”. **(C)** Quantification of the percentage and location (mean \pm SD; $n = 4$) of Ki67⁺ TCR^{MOG} 2D2⁺ cells in the colon 4 and 8 days after T cell transfer. **(D)** Quantification of the percentage of Ki67⁺ TCR^{MOG} 2D2⁺ cells located at the lumen (mean \pm SD; $n = 4$). Scale bars: B, 50 μ m. *, $P < 0.05$; **, $P < 0.01$; ***, $P < 0.001$, ****, $P < 0.0001$; NS, not significant; P values were determined by two-way ANOVA with Tukey’s post hoc test (A, C). [Jeremiah Bernier-Latmani performed the whole-mount immunostaining and took the pictures].

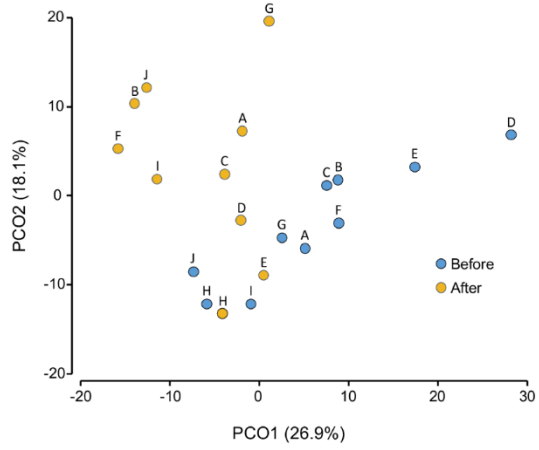
3.2.7 Encephalitogenic TCR^{MOG} 2D2 Th17 cells induce an intestinal dysbiosis and antibiotics treatments decrease encephalitogenic properties of Th17 cells

We further hypothesized that factors present in the colonic lumen, more specifically gut microbiota, could impact TCR^{MOG} 2D2 T cells. We thus evaluated whether TCR^{MOG} 2D2 were influenced by and/or could impact intestinal microbial composition as changes in gut microbiota composition were reported in other EAE model [126] [130] [231] [232] [233]. We thus performed metataxonomic analysis by sequencing of 16S ribosomal RNA gene amplicons from fecal samples of the same recipient mice before and 9 days, when mice were still clinically asymptomatic, after TCR^{MOG} 2D2 Th17 transfer. Analysis of Shannon index revealed that TCR^{MOG} 2D2 Th17 cell transfer significantly increased the diversity of the gut microbiota (Fig. 18A). Analysis of the variance between microbial communities showed that TCR^{MOG} 2D2 T cell transfer resulted in markedly different (PERMANOVA $P = 0.0009$) gut microbial communities (Fig. 18B). Analysis of the microbiota at various taxonomic levels showed a shift in the gut microbiota composition after Th17 cell transfer including an increase in phyla with gram-negative cell wall structure (Proteobacteria and Bacteroidetes) and a decrease of the gram-negative bacteria belonging to the class Bacilli (Firmicutes). In the Bacteroidetes phylum, genus *Alistipes* and several operational taxonomic units (OTUs) of the Bacteroidales order increased in relative abundance after TCR^{MOG} 2D2 Th17 cell transfer. In the Firmicutes phylum, the proportion of genus *Lactobacillus* and three OTUs assigned to it decreased significantly following adoptive transfer (Fig. 18C and Table 6). Concomitantly, several members of the Clostridiales order, including family Ruminococcaceae, an OTU from the family Lachnospiraceae and genera *Eisenbergiella*, KE159538, *Eubacterium*, *Oscillibacter* and *Pseudoflavonifractor* increased in relative abundance.

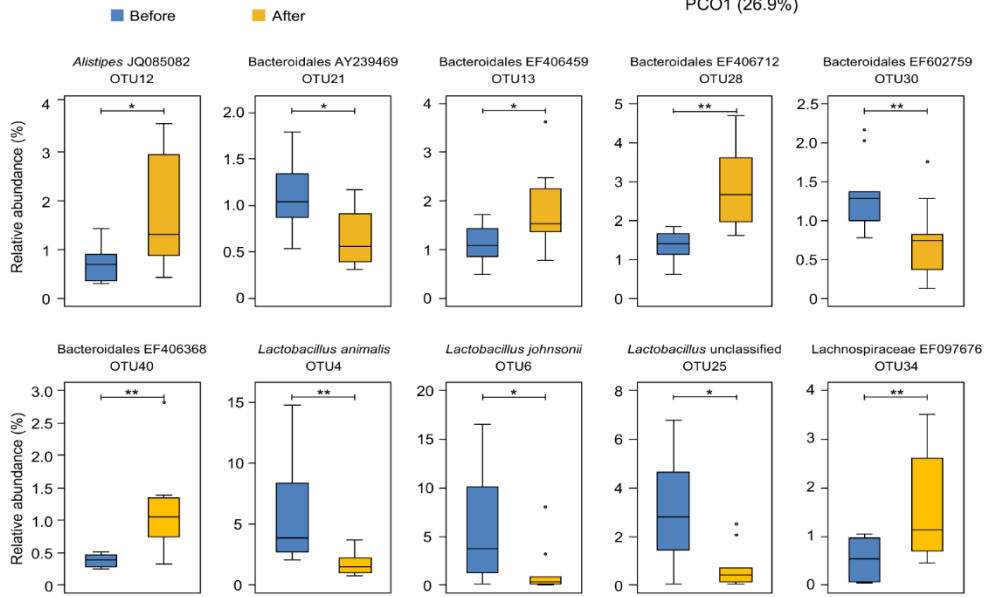
A



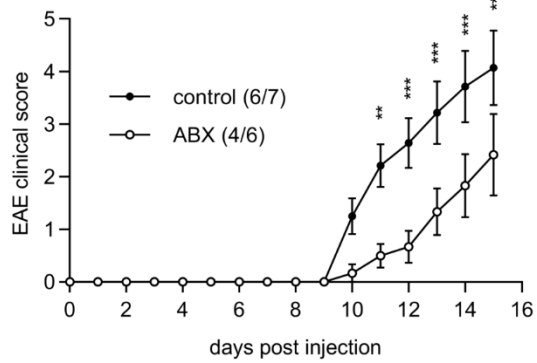
B



C



D



E

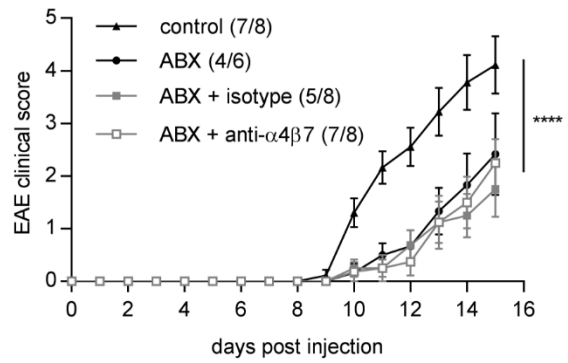


Figure 18. Encephalitogenic TCR^{MOG} 2D2 Th17 cells impact gut microbiota composition (A) Alpha diversity. Shannon diversity index was based on the relative abundance of OTUs. **(B)** PCoA of Bray–Curtis similarities based on the square root-transformed relative abundance of OTUs. Stool samples obtained from the same mouse before and after T cell transfer are indicated by the same alphabetic character (A–J). **(C)** OTUs differentially represented before and after injection of TCR^{MOG} 2D2 Th17 cells. Only OTUs with significant changes ($P < 0.05$) and an average relative abundance $>1\%$ in at least one of the two groups are presented. Boxplots show the first to third quartiles (bottom and top of the box) divided by the median. The highest and lowest value in the $1.5\times$ interquartile range are indicated by whiskers. Circles indicate outliers. **(D)** Clinical scores of EAE in mice adoptively transferred with TCR^{MOG} 2D2 Th17 cells and treated with or without antibiotics (ABX). The course of EAE is shown as clinical score (mean \pm SEM; $n = 6-7$). Data are representative of two experiments. **(E)** Clinical scores of EAE in adoptively transferred mice treated with antibiotics (ABX), antibiotics and isotype control or antibiotics and anti- $\alpha 4\beta 7$ antibodies * , $P < 0.05$; **, $P < 0.01$; ***, $P < 0.001$; ****, $P < 0.0001$; P values were determined by Wilcoxon signed-rank test (A, C) and two-way ANOVA with Sidak's (D) and Tukey's (E) post hoc test. [The team of Prof. Schrenzel performed the microbiota analysis].

To evaluate whether the TCR^{MOG} 2D2 Th17 cells required the presence of microbiota to induce EAE, we injected TCR^{MOG} 2D2 Th17 cells in antibiotic-treated mice. The antibiotic treatment, used to eliminate broad bacteria community [208], significantly reduce EAE severity (Fig. 18D) without impairing the ability of TCR^{MOG} 2D2 T cells to infiltrate the colon (Fig. 19). We then wondered whether blocking Th17 cell colonic migration and antibiotic treatment could have additive effects. We treated mice with antibiotics and administered anti- $\alpha 4\beta 7$ or control isotype antibody (Fig. 18E). Antibiotic treatment reduced EAE severity, however blocking of $\alpha 4\beta 7$ /MAdCAM-1 pathway did not further enhance the protective effect of antibiotic treatment thus orienting our interpretation towards an interdependent role of the intestinal microbiome and anti- $\alpha 4\beta 7$ treatment.

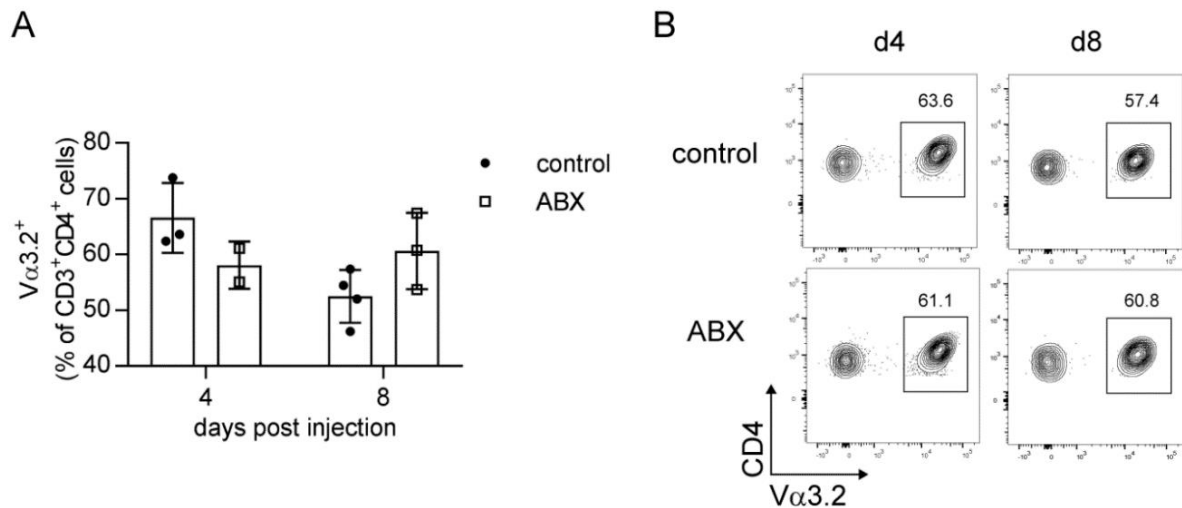


Figure 19. Antibiotic treatment does not influence TCR^{MOG} 2D2 Th17 infiltration in the colon. (A) Flow cytometry analysis of the total proportion (%) of 2D2-TCR (Vα3.2⁺) expression in CD3⁺/CD4⁺ T cells of colonic lamina propria at the indicated time points after TCR^{MOG} 2D2 Th17 cells transfer in control and in antibiotic treated mice (ABX). Data are representative of two experiments. **(B)** Representative flow cytometry analysis of 2D2-TCR (Vα3.2⁺) expression in CD3⁺/CD4⁺ T cells obtained from the colonic lamina propria of control versus antibiotic treated (ABX) mice four days (d4) and eight days (d8) after TCR^{MOG} 2D2 Th17 cells transfer.

In summary, in TCR^{MOG} 2D2 Th17 adoptive-transfer EAE transfer, Th17 cells migrate and proliferate at highest level in the large intestine at preclinical stage of EAE disease. Furthermore, Myelin-specific Th17 cells change gut microbiota composition. Finally, blocking myelin specific Th17 cell entry in the colon or disrupting gut microbiota with antibiotic treatments dampens EAE development.

Rank	Taxonomic information	Average		Median		P*
		Before AT EAE	After AT EAE	Before AT EAE	After AT EAE	
Phylum	Bacteroidetes	34.35	38.12	34.92	38.30	0.02
	Proteobacteria	0.92	1.36	0.90	1.23	0.02
Class	Actinobacteria; Coriobacteriia	1.70	1.07	1.51	0.88	0.04
	Bacteroidetes; Bacteroidia	34.35	38.12	34.92	38.30	0.02
	Firmicutes; Bacilli	14.28	3.93	13.30	2.13	0.01
Order	Actinobacteria; Coriobacteriia; Coriobacteriales	1.70	1.07	1.51	0.88	0.04
	Bacteroidetes; Bacteroidia; Bacteroidales	34.35	38.12	34.92	38.30	0.02
	Firmicutes; Bacilli; Lactobacillales	14.28	3.93	13.30	2.13	0.01
Family	Actinobacteria; Coriobacteriia; Coriobacteriales; Coriobacteriaceae	1.70	1.07	1.51	0.88	0.04
	Bacteroidetes; Bacteroidia; Bacteroidales; Bacteroidaceae	3.05	4.87	2.99	4.19	0.00
	Bacteroidetes; Bacteroidia; Bacteroidales; EU845084	0.42	1.00	0.38	0.65	0.03
	Bacteroidetes; Bacteroidia; Bacteroidales; Prevotellaceae	0.18	0.55	0.13	0.39	0.02
	Bacteroidetes; Bacteroidia; Bacteroidales; Rikenellaceae	2.74	4.97	2.14	4.78	0.00
	Firmicutes; Bacilli; Lactobacillales; Lactobacillaceae	14.26	3.89	13.30	2.04	0.01
	Firmicutes; Clostridia; Clostridiales; Ruminococcaceae	6.36	10.93	5.86	9.48	0.01
	Actinobacteria; Coriobacteriia; Coriobacteriales; Coriobacteriaceae; <i>Olsenella</i>	0.90	0.25	0.61	0.16	0.03
Genus	Bacteroidetes; Bacteroidia; Bacteroidales; Bacteroidaceae; <i>Bacteroides</i>	3.05	4.87	2.99	4.19	0.00
	Bacteroidetes; Bacteroidia; Bacteroidales; S24-7; AY239469	0.42	1.00	0.38	0.65	0.03
	Bacteroidetes; Bacteroidia; Bacteroidales; Prevotellaceae; <i>Prevotella</i>	0.18	0.55	0.13	0.39	0.02
	Bacteroidetes; Bacteroidia; Bacteroidales; Rikenellaceae; <i>Alistipes</i>	2.74	4.97	2.14	4.78	0.00
	Bacteroidetes; Bacteroidia; Bacteroidales; S24-7; AY239469	1.09	0.65	1.04	0.56	0.01
	Bacteroidetes; Bacteroidia; Bacteroidales; S24-7; EF406712	1.34	2.82	1.40	2.66	0.00
	Bacteroidetes; Bacteroidia; Bacteroidales; S24-7; EF406806	0.44	0.73	0.37	0.68	0.01
	Bacteroidetes; Bacteroidia; Bacteroidales; S24-7; EF602759	4.83	3.26	4.86	2.95	0.03
	Firmicutes; Bacilli; Lactobacillales; Lactobacillaceae; <i>Lactobacillus</i>	14.26	3.89	13.30	2.04	0.01
	Firmicutes; Clostridia; Clostridiales; Lachnospiraceae; <i>Eisenbergiella</i>	1.93	3.89	1.95	3.53	0.05
	Firmicutes; Clostridia; Clostridiales; Lachnospiraceae; KE159538	0.81	3.11	0.92	2.44	0.00
	Firmicutes; Clostridia; Clostridiales; Ruminococcaceae; <i>Eubacterium</i>	0.21	0.61	0.18	0.25	0.03
	Firmicutes; Clostridia; Clostridiales; Ruminococcaceae; <i>Oscillibacter</i>	0.54	1.44	0.41	0.84	0.00
	Firmicutes; Clostridia; Clostridiales; Ruminococcaceae; <i>Pseudoflavonifractor</i>	0.65	1.14	0.62	1.08	0.01
	Species	Actinobacteria; Coriobacteriia; Coriobacteriales; Coriobacteriaceae; <i>Olsenella</i> ; <i>Olsenella</i> unclassified	0.90	0.25	0.61	0.16
Bacteroidetes; Bacteroidia; Bacteroidales; Bacteroidaceae; <i>Bacteroides</i> ; <i>Bacteroides</i> unclassified		0.25	0.79	0.12	0.59	0.01
Bacteroidetes; Bacteroidia; Bacteroidales; EU845084; EF603735; EF603735		0.42	1.00	0.38	0.65	0.03
Bacteroidetes; Bacteroidia; Bacteroidales; Prevotellaceae; <i>Prevotella</i> ; DQ777952		0.18	0.55	0.13	0.39	0.02
Bacteroidetes; Bacteroidia; Bacteroidales; Rikenellaceae; <i>Alistipes</i> ; EF603688		0.12	0.83	0.12	0.69	0.00
Bacteroidetes; Bacteroidia; Bacteroidales; Rikenellaceae; <i>Alistipes</i> ; JQ085082		0.72	1.73	0.69	1.31	0.03
Bacteroidetes; Bacteroidia; Bacteroidales; S24-7; AY239469; AY239469		1.09	0.65	1.04	0.56	0.01
Bacteroidetes; Bacteroidia; Bacteroidales; S24-7; DQ815871; EF406459		1.13	1.86	1.08	1.54	0.05
Bacteroidetes; Bacteroidia; Bacteroidales; S24-7; EF406712; EF406712		1.34	2.82	1.40	2.66	0.00
Bacteroidetes; Bacteroidia; Bacteroidales; S24-7; EF602759; EF602759		1.33	0.73	1.28	0.74	0.01
Bacteroidetes; Bacteroidia; Bacteroidales; S24-7; HM124247; EF406368		0.38	1.11	0.40	1.05	0.01
Firmicutes; Bacilli; Lactobacillales; Lactobacillaceae; <i>Lactobacillus</i> ; <i>Lactobacillus animalis</i>		5.65	1.81	3.86	1.49	0.01
Firmicutes; Bacilli; Lactobacillales; Lactobacillaceae; <i>Lactobacillus</i> ; <i>Lactobacillus johnsonii</i>		5.64	1.37	3.76	0.31	0.01
Firmicutes; Bacilli; Lactobacillales; Lactobacillaceae; <i>Lactobacillus</i> ; <i>Lactobacillus</i> unclassified		2.97	0.72	2.82	0.41	0.02
Firmicutes; Clostridia; Clostridiales; Lachnospiraceae; KE159538; EF097676		0.60	1.72	0.62	1.20	0.01
Firmicutes; Clostridia; Clostridiales; Ruminococcaceae; JN713389; JN713389 unclassified		1.01	1.49	1.01	1.28	0.03
Firmicutes; Clostridia; Clostridiales; Ruminococcaceae; <i>Oscillibacter</i> ; <i>Oscillibacter</i> unclassified		0.24	0.61	0.14	0.39	0.03
OTU	Bacteria; Actinobacteria; Coriobacteriia; Coriobacteriales; Coriobacteriaceae; <i>Olsenella</i> ; <i>Olsenella</i> unclassified; Otu36	0.90	0.25	0.61	0.16	0.03
	Bacteria; Bacteroidetes; Bacteroidia; Bacteroidales; Bacteroidaceae; <i>Bacteroides</i> ; <i>Bacteroides</i> unclassified; Otu246	0.25	0.79	0.12	0.59	0.01
	Bacteria; Bacteroidetes; Bacteroidia; Bacteroidales; EU845084; EF603735; EF603735; Otu26	0.42	1.00	0.38	0.65	0.03
	Bacteria; Bacteroidetes; Bacteroidia; Bacteroidales; Prevotellaceae; <i>Prevotella</i> ; DQ777952; Otu45	0.18	0.55	0.13	0.39	0.02
	Bacteria; Bacteroidetes; Bacteroidia; Bacteroidales; Rikenellaceae; <i>Alistipes</i> ; EF603688; Otu51	0.12	0.83	0.12	0.69	0.00
	Bacteria; Bacteroidetes; Bacteroidia; Bacteroidales; Rikenellaceae; <i>Alistipes</i> ; JQ085082; Otu12	0.72	1.73	0.69	1.31	0.03
	Bacteria; Bacteroidetes; Bacteroidia; Bacteroidales; S24-7; AY239469; AY239469; Otu21	1.09	0.65	1.04	0.56	0.01
	Bacteria; Bacteroidetes; Bacteroidia; Bacteroidales; S24-7; DQ815871; EF406459; Otu13	1.13	1.86	1.08	1.54	0.05
	Bacteria; Bacteroidetes; Bacteroidia; Bacteroidales; S24-7; EF406712; EF406712; Otu28	1.34	2.82	1.40	2.66	0.00
	Bacteria; Bacteroidetes; Bacteroidia; Bacteroidales; S24-7; EF602759; EF602759; Otu30	1.33	0.73	1.28	0.74	0.01
	Bacteria; Bacteroidetes; Bacteroidia; Bacteroidales; S24-7; HM124247; EF406368; Otu40	0.38	1.11	0.40	1.05	0.01
	Bacteria; Firmicutes; Bacilli; Lactobacillales; Lactobacillaceae; <i>Lactobacillus</i> ; <i>Lactobacillus animalis</i> ; Otu4	5.65	1.81	3.86	1.49	0.01
	Bacteria; Firmicutes; Bacilli; Lactobacillales; Lactobacillaceae; <i>Lactobacillus</i> ; <i>Lactobacillus johnsonii</i> ; Otu6	5.64	1.37	3.76	0.31	0.01
	Bacteria; Firmicutes; Bacilli; Lactobacillales; Lactobacillaceae; <i>Lactobacillus</i> ; <i>Lactobacillus</i> unclassified; Otu25	2.97	0.72	2.82	0.41	0.02
	Bacteria; Firmicutes; Clostridia; Clostridiales; Lachnospiraceae; KE159538; EF097676; Otu34	0.53	1.56	0.54	1.13	0.00

AT EAE, adoptive transfer experimental autoimmune encephalomyelitis

Table 6. Changes in the relative abundance of bacterial taxa in fecal mouse microbiota observed after injection of TCR^{MOG} 2D2 Th17 cells. Only taxa with a mean relative abundance >0.5% in at least one of the two groups of samples (before and after AT EAE) were compared and those with statistically significant differences (P<0.05) are represented. The statistical analysis method used was a Wilcoxon signed-rank test. Significant increase and decrease in the taxon relative abundance after treatment are indicated by red and blue filled cells, respectively. [The team of Prof. Schrenzel performed the microbiota analysis]

3.3 Discussion

The implication of the gut-brain axis has received growing attention in the field of neuro-immunology, with recent works showing an accumulation of Th17 cells in the small intestine as well as an intestinal dysbiosis in MS patients [124]. However, if those findings are a consequence of neuroinflammation or in the contrary if they affect the development of neuroinflammation remain disputed. We here report that CNS-specific Th17 cell migrate to the intestine during EAE. Furthermore, blocking $\alpha 4\beta 7$ /MAdCAM-1 pathway not only limits intestinal Th17 cell infiltration, to a larger extent in the large intestine, but also significantly dampens EAE severity in an adoptive-transfer model. Mechanistically, myelin-specific Th17 cells proliferate in the gut and alter gut microbiota composition. Antibiotic treatments dampen EAE development in the Th17 cell adoptive transfer EAE model. However, blocking $\alpha 4\beta 7$ /MAdCAM-1 pathway does not synergize with the beneficial effect of antibiotic treatments. These data strongly suggest that during CNS autoimmunity, encephalitogenic Th17 cell traffic to the large intestine, where their pro-inflammatory functions are strengthened at least partially via gut microbiota changes.

An association between MS and IBD has been described in humans [14] as well as an increased risk of MS and IBD comorbidity [234]. Animal models have demonstrated a crucial role for gut-homing effector T cells in inflammatory bowel disease and mice lacking $\beta 7$ integrin have less intestinal T cells as a consequence of a reduced rate of migration to the gut [235] [236]. Moreover, blocking antibodies against the $\alpha 4\beta 7$ -integrin attenuate mouse models of intestinal inflammation and are clinically effective in the treatment of human ulcerative colitis and Crohn's disease [237] [238]. Combined anti- $\alpha 4$ -integrin (natalizumab), that blocks both $\alpha 4\beta 1$ /VCAM-1 and $\alpha 4\beta 7$ /MAdCAM-1 interactions, is effective in addition to intestinal inflammatory diseases to target both MS and EAE [36] [239] [240]. For MS, the effect is attributed specifically to the $\alpha 4 \beta 1$ inhibition directly in the CNS. Indeed, the impact of $\alpha 4\beta 7$ /MAdCAM-1 interactions in neuroinflammation remains controversial and studies specifically addressing their role in EAE pathogenesis have led to inconsistent results. Using SJL/N mouse strains, B. Engelhardt et al found no effect of anti- $\alpha 4\beta 7$ nor anti- $\beta 7$ neutralizing antibodies on the development of EAE [241]. Similarly, Vedolizumab does not prevent CNS inflammation nor demyelination in Rhesus Monkey EAE model [242]. In apparent contrast, $\beta 7$ integrin-deficient C57BL/6 mice are partially resistant to adoptive EAE transfer and to neutralizing antibodies against MAdCAM-1 [243] [244]. Furthermore the development of active EAE is attenuated in MAdCAM-1-KO mice while MAdCAM-1 blockade 5 days after immunization does not attenuate EAE [245]. Indeed, the timing of intestinal T cell blocking is certainly relevant. We observe that anti- $\alpha 4\beta 7$ treatment is efficient when administered only

until the appearance of the first neurological signs and that the extension of the treatment during the entire EAE disease course did not enhance its protective effect. Those results are in accordance with the observation of a significant TCR^{MOG} 2D2 Th17 cell colonic proliferation at 4 days but not anymore at 8 days after T cell transfer. Furthermore, the observed differences in the previous publications can be attributed to the use of different mouse strains and to methodological differences in inducing EAE that may or not favor Th17 cell polarization. We here show that blocking $\alpha 4\beta 7$ -integrin inhibits Th17 cell entry in the colonic lamina propria during adoptive transfer EAE and further contributes to a reduction of neurological symptoms. We did not observe impairment of the neurological disease course with anti- $\alpha 4\beta 7$ treatment in the active EAE model that is mainly driven by Th1 cells. We thus propose that the colon might be a niche for reactivation and proliferation of immune cells during EAE, in particular for Th17 cells. The effect on myelin-specific Th17 cells observed in the colon during EAE could be related to their production of IL-17 cytokine family more than on their antigen-specificity. This would be in accordance with the intrinsic properties of IL-17A as modulators of microbiota composition [246]. As IL-17 cytokines can be produced by adaptive immune cells but also by other cell types (ILC3, $\gamma\delta$ T-cells), it remains to be elucidated if IL-17 family cytokines, such as IL-17A, could per se impact neuroinflammation independently of their cellular sources.

Whether MAdCAM-1, an intestinal protein, is also expressed in the CNS and thus contributes to our observation has been debated [247] [248] [249] [250] [251]. We detected very low levels of MAdCAM-1 mRNA in the CNS and at much lower rates compared to the colon. MAdCAM-1, if expressed in the CNS, is expressed at a low level and has been shown not to contribute to neuroinflammation [252]. In addition even ectopic expression of MAdCAM-1 on blood-brain barrier does not influence EAE in the C57BL/6J model [252]. This corroborates with the publication from the T. Korn group that proposed in an adoptive transfer EAE model that Th17 lymphocytes traffic to the CNS independently of $\alpha 4$ integrin expression during EAE [253]. Here we observed a beneficial effect on neuroinflammation when blocking $\alpha 4\beta 7$ /MAdCAM-1 interactions. However, the beneficial effect was transient. This could be a consequence of the insufficient blocking of Th17 trafficking in the small intestine and the colon. Lymphocyte migration to the gut is controlled by additional chemoattractant receptors, such as the C-C motif chemokine receptors 9 (CCR9) for the small intestine or the orphan G-protein-coupled receptor 15 (GPR15) for the colon [254]. Concomitant blocking of CCR9/GPR15/chemokines interaction could contribute to fully evaluate the role of the entire intestine in driving EAE.

Gut mucosa harbors the highest concentration of immune cells in the body and studies in human and mice suggested that small intestine is a possible location for the generation, activation and expansion of effector T cells that cause autoimmune responses [135]. However,

it is still unclear how mucosal immune responses elicited in the gut modulate CNS inflammation and whether the large intestine is further involved in EAE pathogenesis. Our observations that myelin-specific Th17 cells infiltrate preferentially the large intestine further demonstrate the occurrence of compartmentalization and suggest the existence of distinctive mechanisms of autoimmune cells recruitment that may allow functional specialization of immune responses in different segments of the intestine.

Th17 adoptive EAE transfer had a notable effect on gut microbiota composition with a decreased representation of the Firmicutes phylum, in particular of the proportion of the *Lactobacillus* species, which have been associated with a beneficial effects, including inflammatory immune response reduction during EAE [255]. We observed a significant reduction in *L. Johnsonii*, which are known to have immunomodulatory properties [256]. Interestingly *L. Johnsonii* are induced by intermittent fasting which further dampens EAE severity [257]. Intestinal microbiota has been proposed to contribute to the accumulation or activation of Th17 in the intestine [258] [259]. In the context of neuroinflammation, commensal species residing in the small intestine impact on the development of the disease in mouse model and human. Encephalitogenic Th17 cells can be generated in the gut with the segmented filamentous bacteria (SFBs) monocolonization [130] while Bacteroides species or colonic clostridia respectively suppress IL-17 production or support the development of regulatory T cells [260]. Here we further show that antibiotic treatment was sufficient to dampen neurological disease in the adoptive transfer EAE model and furthermore that blocking $\alpha 4\beta 7$ /MAdCAM-1 interactions was not be beneficial in the context of antibiotic treatment. Those results suggest an intrinsic relationship between CNS-specific Th17 and intestinal microbiota composition. However, the precise mechanisms of the “gut flora-Th17 cell interactions” remain to be further studied.

In summary, CNS antigen specific Th17 cells infiltrate the large intestine and depict high proliferating properties in this organ during EAE. Specifically targeting Th17 cell migration to the large intestine by blocking $\alpha 4\beta 7$ /MAdCAM-1 interaction attenuates EAE disease interdependently of the microbiota composition. Our results thus contribute to reevaluation of the gut as a target during CNS autoimmunity.

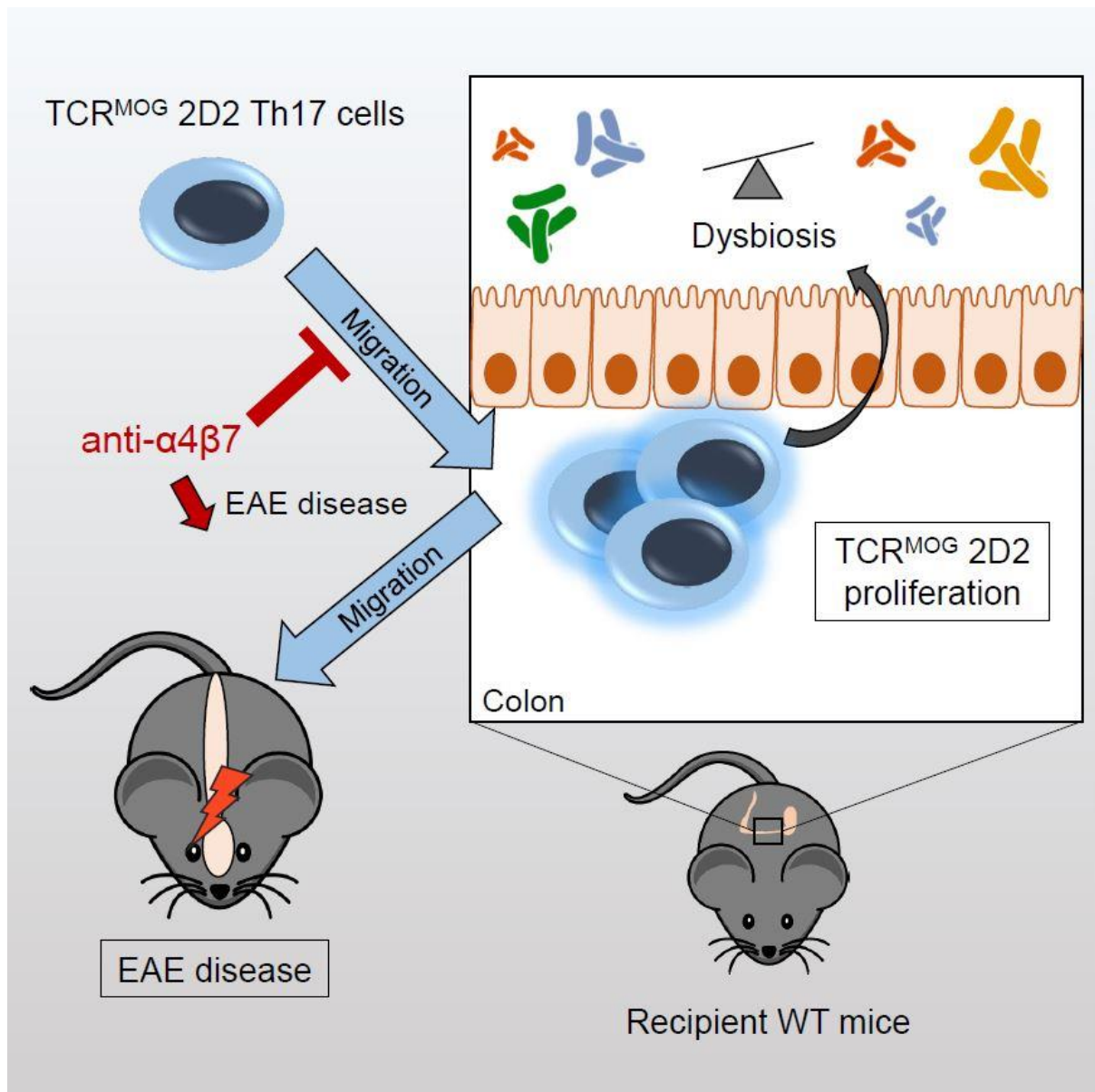


Figure 20. Disrupting myelin-specific Th17 cell gut homing confers protection in an adoptive transfer experimental autoimmune encephalomyelitis. Graphical abstract representing the important findings of the first project. Th17-polarized myelin-specific (TCR^{MOG} 2D2) CD4⁺ T cells migrate to the colon before the development of neuroinflammation. Encephalitogenic Th17 cells further change intestinal microbiome composition. Blocking encephalitogenic Th17 cell entry into the colon or treatment with antibiotics ameliorates EAE severity.

4. PROJECT II: Role of oxysterols on gut immunology during EAE and pathogen-induced colitis

4.1 Materials & Methods

4.1.1 EAE induction and clinical evaluation

EAE induction and clinical evaluation were done as previously described in 3.1.2.

4.1.2 Isolation of immune cells

Isolation of immune cells were done as previously described in 3.1.5.

4.1.3 Flow cytometric analysis

Flow cytometric analysis were done as previously described in 3.1.6, with additional following materials and methods: Fluorochrome-conjugated antibodies were purchased from several commercial sources indicated below: Antibodies against CD44 (IM7), NK1.1 (PK136), CD45 (30-F11), CD335 (29A1.4), IL-33Ra (DIH9), CD90.2 (53-2.1), CD127 (A7R34), CD3 (17A2), CD196 (29-2L17) were from Biolegend; CD11c (N418), CD11b (M1/70), Ly6G (RB6-8C5), Ly6C (HK1.4), B220 (RA-6B2) were from eBioscience; CD5 (REA421), CD11b (M1/70.15.11.5), CD11c (N418), CD19 (6D5), Ter-119 (Ter-119), B220 (RA3-6B2), TCR γ/δ (REA633), CD49b (DX5), Fc ϵ RI α (MAR-1), TCR β (REA318), Siglec-F (ES22-10D8) were from Miltenyi Biotec.

4.1.4 Quantification of oxysterols

For quantification of oxysterols during EAE, tissues were excised, weighted before freezing in liquid nitrogen. Tissues were stored at -80°C until analysis. Samples were analyzed by the laboratory of Prof Giulio Muccioli at the Université catholique de Louvain using previously described methods [201].

4.1.5 Whole-mount immunostaining

Whole-mount immunostaining were done as previously described in 3.1.9.

4.1.6 Microbiome analysis

Microbiome Analysis were done as previously described in 3.1.10.

4.1.7 RNA isolation and quantitative PCR analysis

RNA isolation and quantitative PCR analysis were done as previously described in 3.1.8, with additional following material and methods: Expression of specific gene transcripts was measured by using the following primer pairs: Ch25h, 5'-CCAGCTCCTAAGTCACGTC-3' and 5'-CACGTCTGAAGAAGGTCAG-3'; IL-23p19 5'-TGAGCCCTTAGTGCCAACAG-3' and 5'-CTTGCCCTTCACGCAAAACA-3'; iNos2 5'-TTTCGCGGCGATAAAGGGAC-3' and 5'-GGGGAGCCATTTTGGTGACT-3'.

4.1.8 *Citrobacter rodentium* infection

Citrobacter rodentium strain DBS100 was cultured in LB broth overnight. Overnight fasting mice were inoculated with 2×10^9 colony-forming units (CFU) by oral gavage. Mice were daily weighed and bacterial load was monitored using homogenized fecal pellet cultured on MacConkey agar plate.

4.1.9 Generation, culture, and stimulation of BMDCs

Bone marrow-derived dendritic cells (BMDCs) were obtained from 8- to 12-week-old WT or Ch25h^{-/-} mice. Tibias and femurs were excised, and bone-marrow was flushed out with complete medium (RPMI 1640 Medium, GlutaMAX™ Supplement, Gibco) containing 10% FCS (FBS 18, Biowest), 100UM penicillin streptomycin (BioConcept), 1mM sodium pyruvate (Sigma) and β-mercaptoethanol (Gibco). Bone-marrow was mechanically disaggregated on a 70 μm cell strainer using a syringe plunger. After a short red blood cell lysis of 5 minutes and appropriate wash, adherent and nonadherent cells were separated after incubation for 30 minutes on a 10-cm petri dish. Non-adherent cells were cultured for 7 days in complete medium with addition of recombinant murine granulocyte macrophage colony-stimulating factor (rmGM-CSF, 20ng/mL, ImmunoTools). Cells passages and addition of rmGM-CSF were realized at day 2 and 5. At day 7, adherent cells were harvested. Quality and purity of the culture was assessed by flow cytometry using the percentage of CD11c⁺ CD11b⁺. For the bacterial challenge, BMDC are seeded in 24-well plates (5×10^5 cell/mL) in complete medium. After overnight resting of the cells, BMDCs are cultured with heat-killed *C. rodentium* at the indicated multiplicity of infection (MOI) or LPS at 0.1 ug/mL (from E. Coli, serotype O55:B5 (Enzo)) or medium. Cell supernatants were collected, and cytokine levels were assessed using ELISA (Invitrogen). Cells were harvested to determine gene expression profile.

4.1.10 Statistical analysis

Statistical analyses were done as previously described in 3.1.11

4.2 Results

4.2.1 Increase Ch25h expression in intestine during EAE

To investigate the role of Ch25h and related oxysterols in the gut during CNS autoimmunity, we first performed EAE immunization and assessed the Ch25h expression profile in wild-type mice. We analyzed the expression at different time points during the development of the disease and in different tissues including small intestine LP (siLP), whole cecum tissues and whole colon tissues. We observed an increase Ch25h expression in small intestine lamina propria when the mice displayed neurological symptoms (EAE scores of 3) (Fig. 21A). Increase Ch25h expression was also observed in both cecum and colon tissues when the mice had a score of 3 but also before neurological symptomatic manifestation (Fig. 21B).

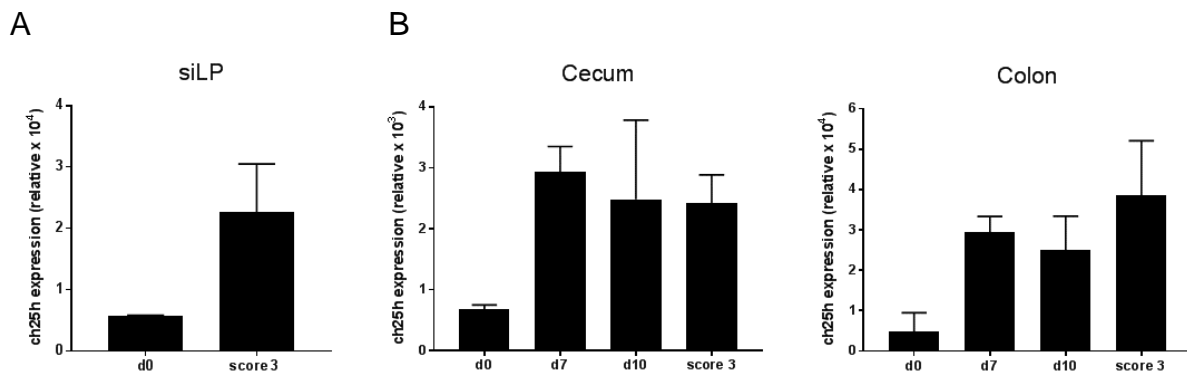


Figure 21. Increase Ch25h expression in the gut during EAE disease.

(A) Relative mRNA expression of Ch25h in small intestine lamina propria (siLP) at baseline and when mice are sick (clinical score of 3) (mean \pm SEM; $n = 3-4$). **(B)** Relative mRNA expression of Ch25h in the cecum and colon tissue during the development of EAE (mean \pm SEM; $n = 2-6$).

4.2.2 Modulation of oxysterol level in the gut during EAE

As Ch25h expression is modulated during EAE development in the gut, we further examined how deficiency of Ch25h can affect oxysterol hemostasis. Oxysterol level perturbations were previously reported during gastrointestinal inflammation and IBDs. As inflammation occurs in the gut during CNS autoimmunity, we quantified oxysterol levels in the gut of wild-type and Ch25h^{-/-} during EAE development (Fig. 22).

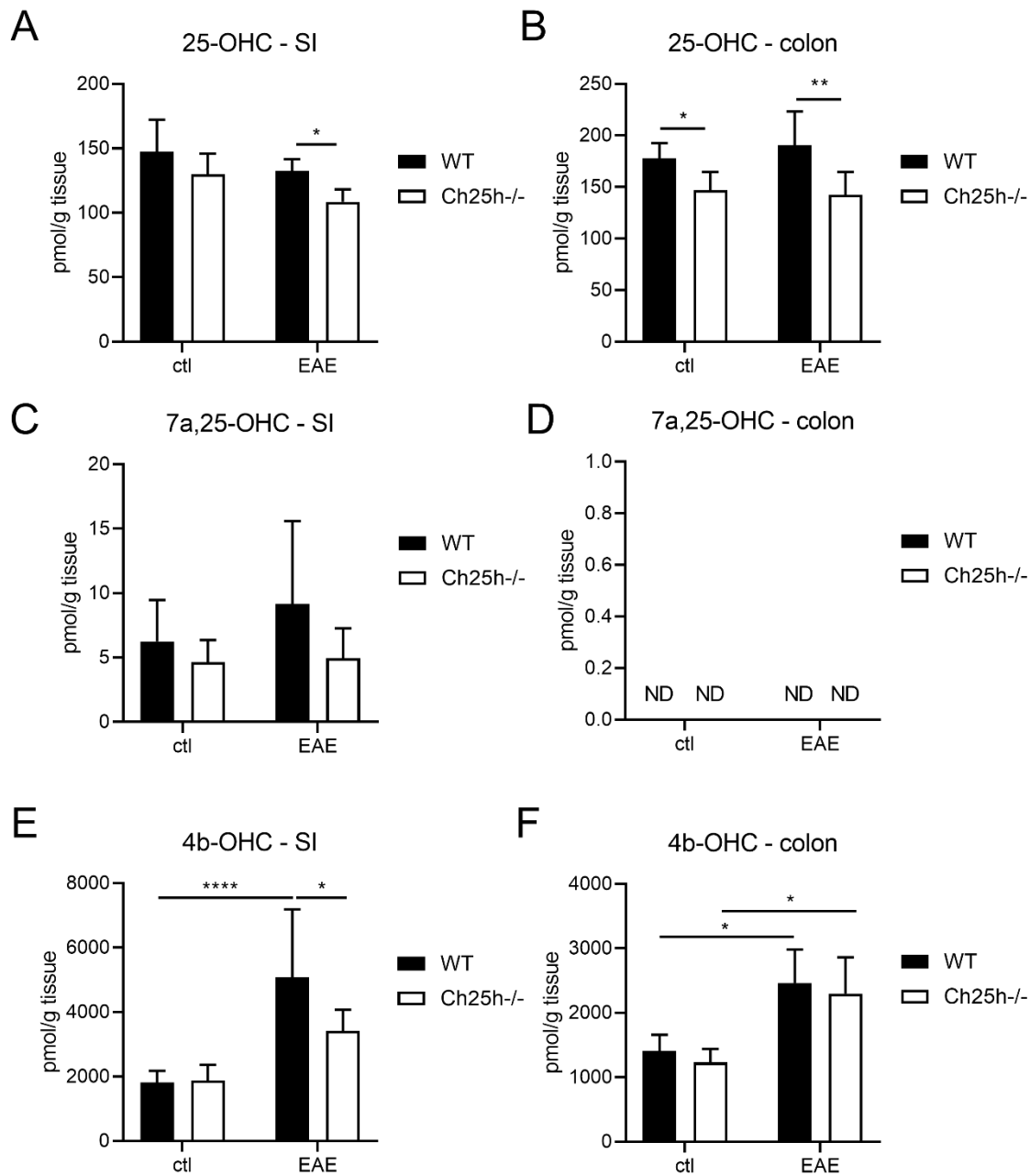


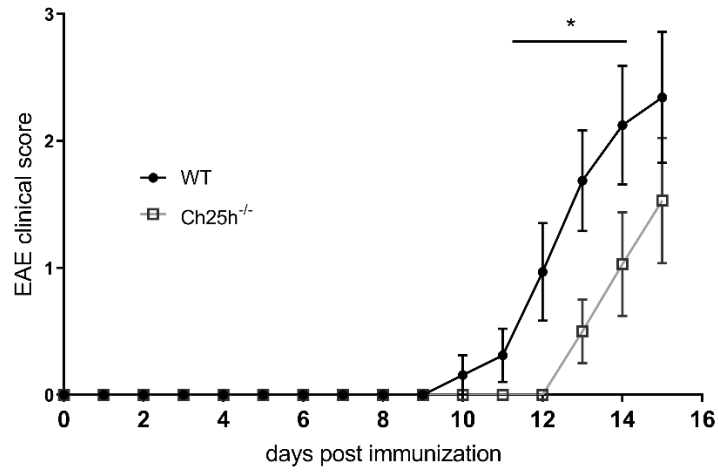
Figure 22. Oxysterol levels in the small intestine and the colon during the development of CNS autoimmunity. (A-B) 25-OHC level was analyzed in small intestine (SI) (A) and in colon (B) of wild-type (WT) and Ch25h deficient mice (Ch25h^{-/-}) at steady state (ctl) or 14 days after EAE immunization (mean \pm SD, $n = 8$). (C-D) 7 α ,25-OHC level was analyzed in small intestine (SI) (C) and in colon (D) of wild-type (WT) and Ch25h deficient mice (Ch25h^{-/-}) at steady state (ctl) or 14 days after EAE immunization (mean \pm SD, $n = 8$). (E-F) 4 β -OHC level was analyzed in small intestine (SI) (E) and in colon (F) of wild-type (WT) and Ch25h deficient mice (Ch25h^{-/-}) at steady state (ctl) or 14 days after EAE immunization (mean \pm SD, $n = 8$). *, $P < 0.05$; **, $P < 0.01$; ***, $P < 0.001$, ****, $P < 0.0001$; ND, not detected; P values were determined by two-way ANOVA. [The team of Prof. Muccioli performed the oxysterol quantification].

At steady state, Ch25h^{-/-} mice had a significant reduction of 25-OHC in the colon but not in the small intestine (Fig. 22A, 22B). Ch25h deficient mice showed significant decrease of 25-OHC during EAE in the small intestine and the colon. We found no increase of 25-OHC during the development of EAE in wild-type mice in both compartments (Fig. 22A, 22B). We observed an increased level of 7 α ,25-OHC in the small intestine of wild-type mice during EAE compared to non-treated mice that did not reach significant differences (Fig. 22C). Interestingly, small intestine and colon did not share the same profile of oxysterols. For example, 7 α ,25-OHC was present in small intestine but was not detected in the colon (Fig. 22D). Finally, 4 β -OHC level, which is associated with colitis [201], was significantly increased during EAE in both WT and Ch25h^{-/-} mice in the colon (Fig. 22E, 22F). However, in the small intestine we observed a significant increase of 4 β -OHC in the WT but not in the Ch25h^{-/-} mice.

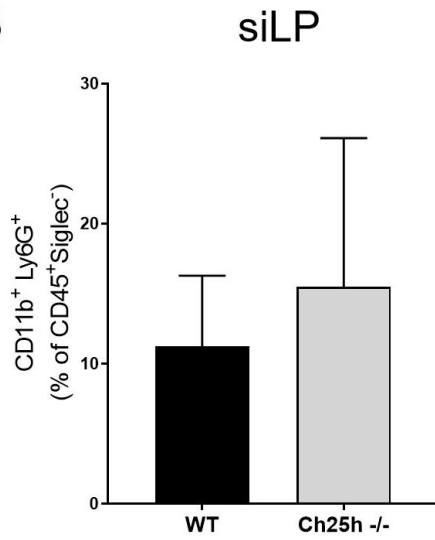
4.2.3 Reduced intestinal infiltration of Th17 cells in Ch25h^{-/-} mice during EAE

As Ch25h expression and oxysterol levels were modulated during EAE development in the different compartments of the gut, we further examined how deficiency of Ch25h could affect the intestinal immune system during the disease in the small and large intestine. We compared the immune responses in wild-type and Ch25h^{-/-} mice at day 10 after immunization using lamina propria cell extraction and flow cytometry analysis. As previously demonstrated, Ch25h^{-/-} mice depicted a delayed neurological EAE disease course compared to WT controls (Fig. 23A). We observed similar proportion of neutrophils (Fig. 23B, 23C) and macrophage (Fig. 23D, 23E) between wild-type and Ch25h^{-/-} mice in the small intestine and the colon. Regarding lymphocyte population, Ch25h^{-/-} mice depicted a significant decrease of Th17 infiltrates compared to wild-type controls in both small and large intestine (Fig. 23F, 23G). No difference was observed in the proportion of Foxp3⁺ Treg in small intestine and the colon (Fig. 23H, 23I).

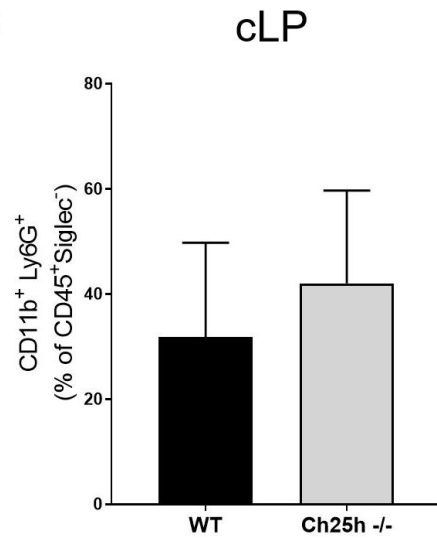
A



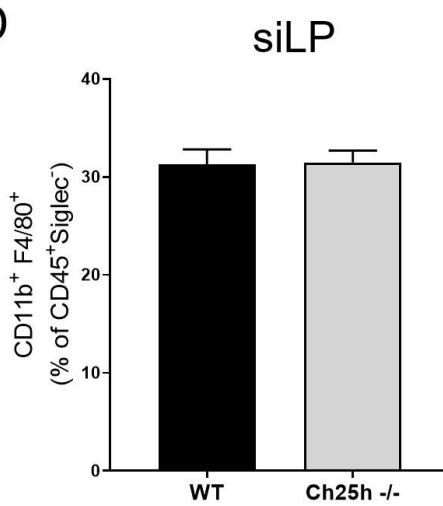
B



C



D



E

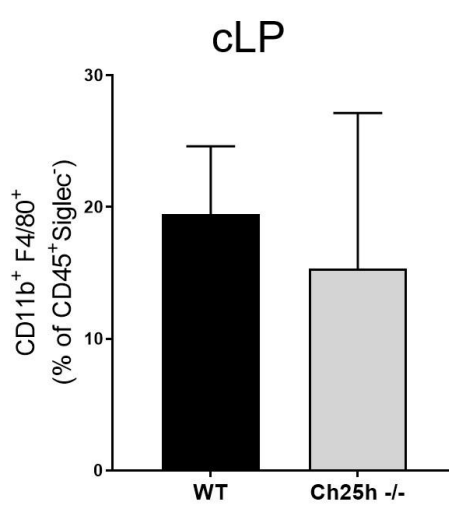


Figure 23 continues next page

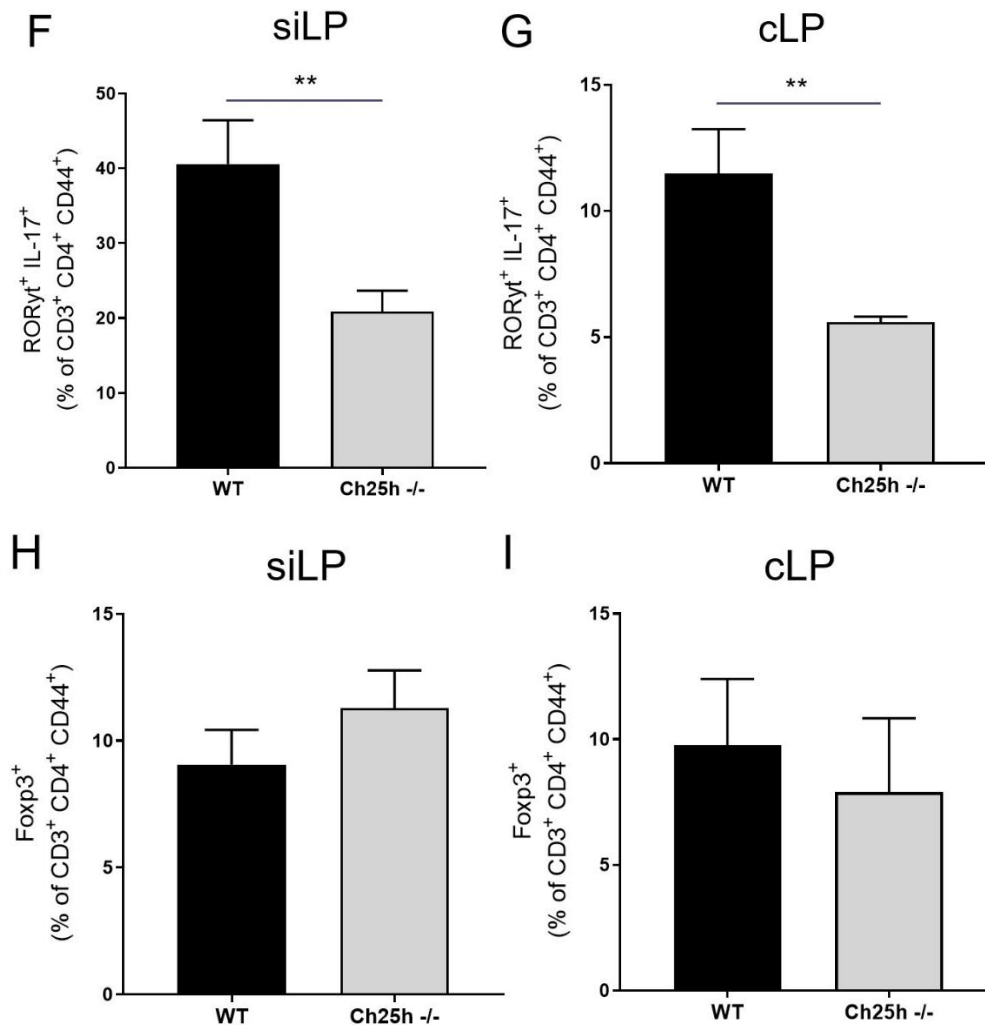


Figure 23. Reduced Th17 proportion in the small and large intestine during EAE disease.

(A) Ch25h^{-/-} and wild-type mice challenged with classical EAE and clinical score were assessed daily (mean ± SEM; *n* = 8). (B-C) Flow cytometry analysis of the total proportion (%) CD11b⁺Ly6G⁺ neutrophils in the small intestinal lamina propria (siLP) (B) and the colonic lamina propria (cLP) (C) at day 10 after EAE immunization (mean ± SD; *n* = 3). (D-E) Flow cytometry analysis of the total proportion (%) CD11b⁺F4/80⁺ macrophages in the siLP (D) and the cLP (E) at day 10 after EAE immunization (mean ± SD; *n* = 3). (F-G) Flow cytometry analysis of the total proportion (%) of Th17 cells (RORγT⁺ IL-17⁺) in the siLP (F) and cLP (G) at day 10 after EAE immunization (mean ± SD; *n* = 3). (H-I) Flow cytometry analysis of the total proportion (%) of Foxp3⁺ Treg cells in the siLP (H) and cLP (I) at day 10 after EAE immunization (mean ± SD; *n* = 3). *, *P* < 0.05; **, *P* < 0.01; *P* values were determined by unpaired Student's *t* test.

4.2.4 EAE induces morphological changes in the small intestine that are less pronounced in Ch25h^{-/-} mice

As structural integrity is important for gut functionality, we further assessed if perturbations of intestinal morphology occurred with immune cell infiltrations during EAE disease. As 7 α ,25-OHC is found in a higher proportion in the small intestine compared to colon and has it is the most potent ligand for Ebi2 receptor that drives of immune cell migration, we here focused our investigations first on the small intestine. Using whole-mount immunostaining of the small intestine, we characterized the villus size and vascular networks with blood endothelial cell staining (VEGFR2⁺ cells) of both WT and Ch25h^{-/-} mice at steady state and during EAE. EAE induced significant expansion of intestinal villi size and underlying blood vessels in wild-type mice but not in Ch25h^{-/-} mice (Fig. 24). Those results suggest that structural changes observed during gut inflammation in intestinal villi are less important in the absence of Ch25h. This observation might be related to the reduced infiltration of Th17 cells and/or delayed EAE onset observed in Ch25h^{-/-} mice but this hypothesis remains to be formally tested.

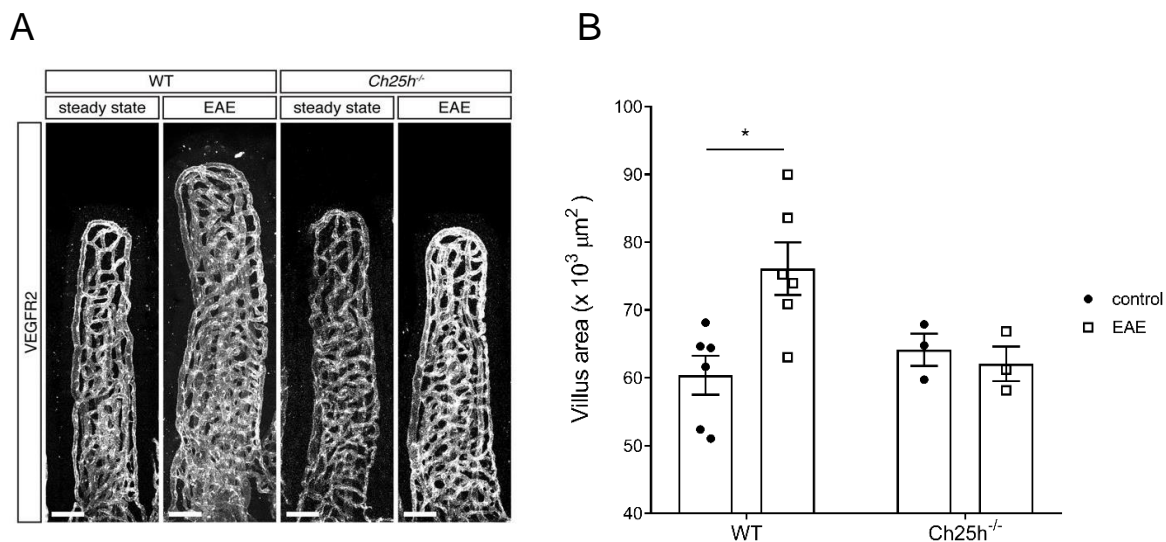


Figure 24. EAE disease affects intestinal morphology.

(A) Representative small intestine whole-mount immunostaining of the entire villus showing blood vessel (VEGFR2) of WT and Ch25h^{-/-} mice at day 16 post-immunization. **(B)** Villus area quantification of WT and Ch25h^{-/-} mice at basal level and 16 days post-immunization (mean \pm SD, $n = 3-6$). *, $P < 0.05$; P values were determined by two-way ANOVA. [Jeremiah Bernier-Latmani performed the whole-mount immunostaining and took the picture].

4.2.5 EAE induces gut microbiota changes that are not impacted by Ch25h deletion

Ch25h^{-/-} mice have been reported to depict altered IgA production. As previously mentioned, IgA can shape the gut microbiota and we suggested that Ch25h^{-/-} mice may have gut microbial imbalance. We performed metataxonomic analysis by sequencing of 16S ribosomal RNA gene

amplicons from fecal samples from Ch25h^{-/-} and WT mice before and 10 days after EAE immunization (Fig. 25). Analysis of the microbiota at various taxonomic levels showed a shift in the gut microbiota composition after EAE immunization including an increase of Proteobacteria and Actinobacteria and a decrease in Firmicutes (Fig. 25A). No major shifts in the gut microbiota composition were observed at phylum level between Ch25h^{-/-} and wild-type mice. However, when deeper phylogenetic analyses were performed, differences between Ch25h^{-/-} and wild-type mice were observed. For instance, in the Firmicutes phylum, genus *Butyricoccus* is increased in relative abundance in Ch25h^{-/-} compared to wild-type mice at basal level (Fig. 25B). Interestingly, these bacteria are known to produce butyrates which have anti-inflammatory properties [261]. The importance of this difference at baseline should be further investigated.

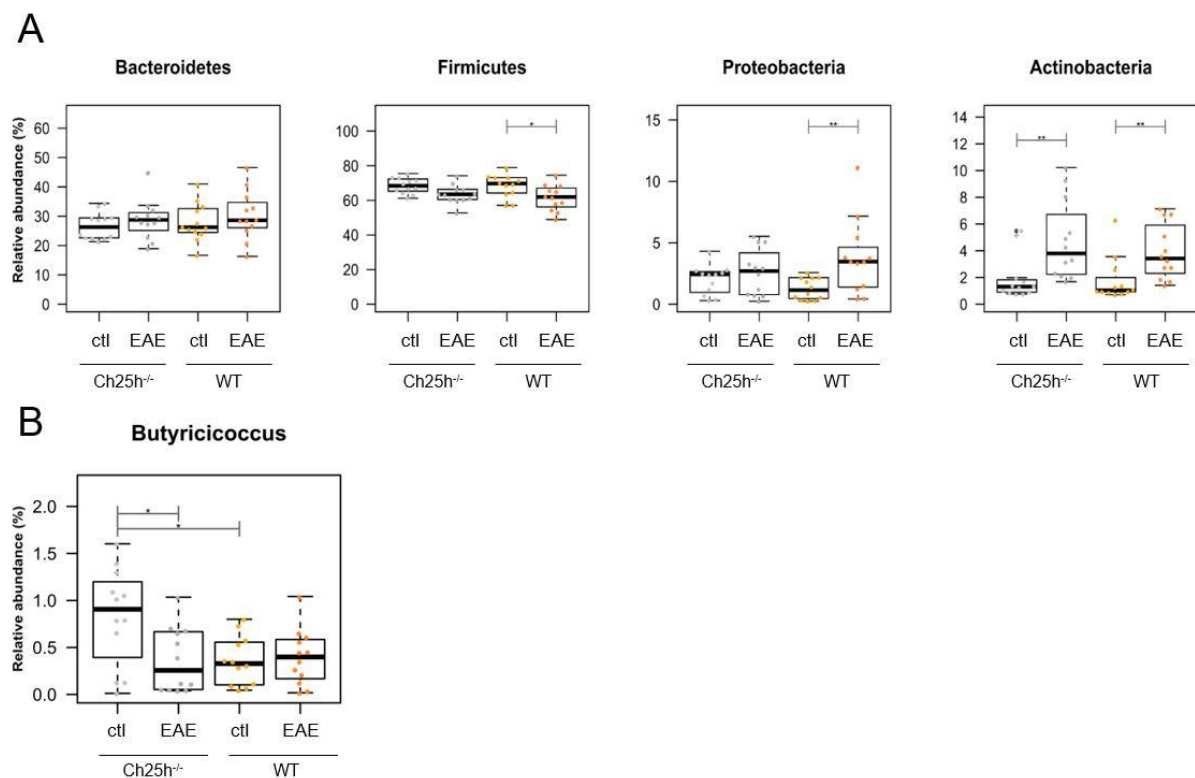


Figure 25. Ch25h deletion has no major impact on gut microbiota during EAE.

(A) Relative abundance (%) of phyla between Ch25h^{-/-} versus wild-type (WT) mice before (ctl) and at day 10 post-immunization (EAE). **(B)** Relative abundance (%) of *Butyricoccus* genus between Ch25h^{-/-} versus wild-type (WT) mice before (ctl) and at day 10 post-immunization (EAE). [The team of Prof. Schrenzel performed the microbiota analysis].

4.2.6 Delayed clearance of *C. rodentium* in Ch25h^{-/-} mice

To further understand the contribution of oxysterols in gut immunology, we evaluated the role of Ch25h in another mouse model that induces directly gut mucosal immune responses. We

chose *Citrobacter rodentium*-induced colitis model, consisting of an oral challenge of *C. rodentium* bacteria known to induce strong colonic mucosal immune responses. We selected this infectious model as it involves both innate and adaptive immune responses. In addition, at that time, no study had evaluated the role of Ch25h during gut infection. Ch25h^{-/-} and wild-type mice were challenged with the bacteria and load of bacterial infection were assessed. Ch25h^{-/-} mice had a delayed clearance of the bacteria but can still clear the infection at the end (Fig. 26A). Mice lost weight during the infection but no difference was observed between the two groups (Fig. 26B). A biological marker of the colitis induced by the pathogen is the shortening of the colon length [262]. We observed in both genotypes shortening of the colon without any significant differences between the two groups (Fig. 26C).

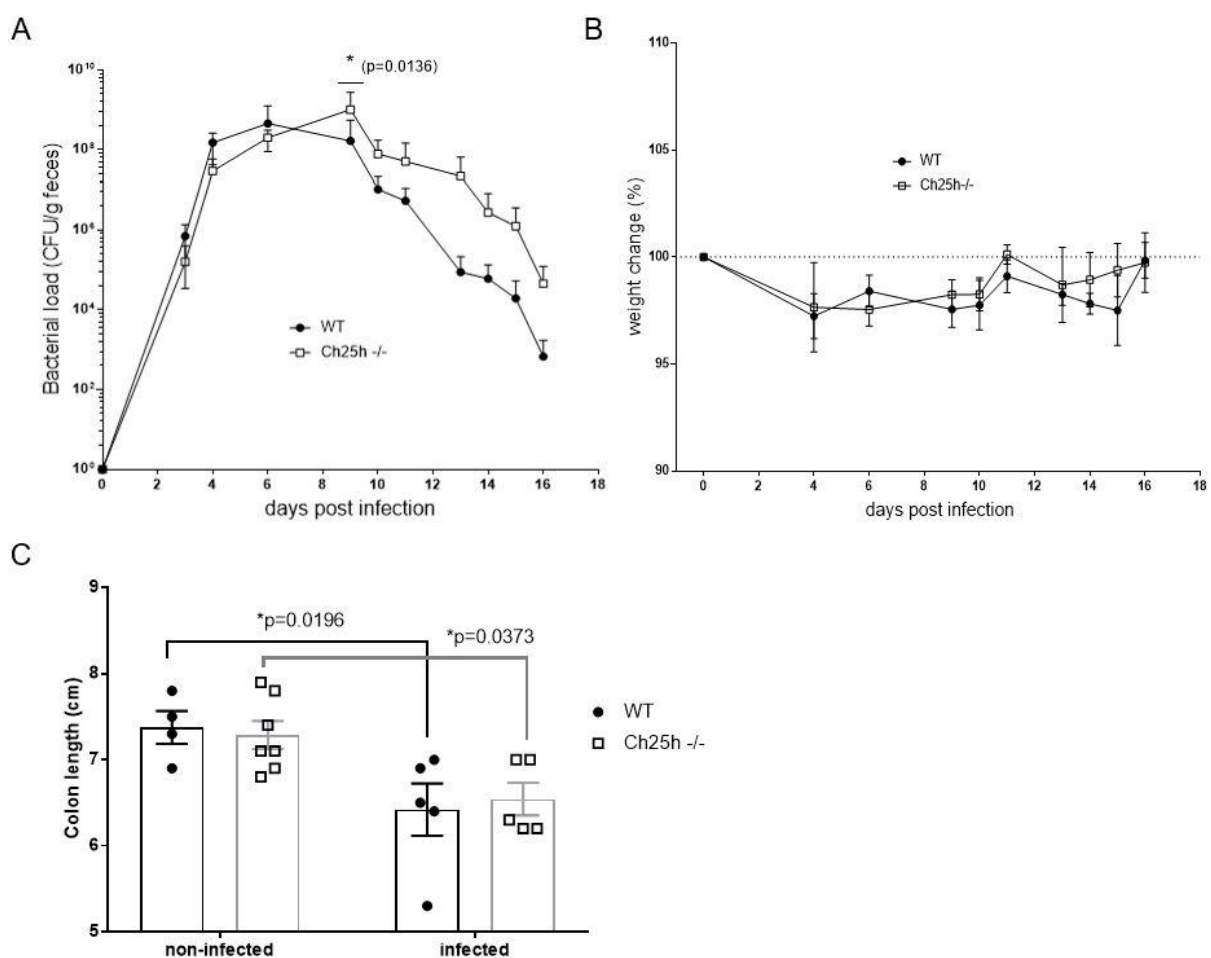


Figure 26. Delayed clearance of *C. rodentium* in Ch25h^{-/-} mice.

(A) Bacterial load was monitored on wild-type (WT) and Ch25h^{-/-} mice using fecal culture on selective plates (mean ± SEM, n = 5-8). (B) Weight was recorded during the progression of the infection (mean ± SEM, n = 5-8). (C) Colon length from Ch25h^{-/-} and wild-type (WT) was measured in non-infected and infected mice at day 16 post-infection (mean ± SEM, n = 4-7). P values were determined by two-way ANOVA. [Dominique Velin performed *C. rodentium* preparation, gavage and mice dissection]

4.2.7 Ch25h^{-/-} mice show abnormal innate immune response to *C. rodentium*

Citrobacter rodentium-induced colitis model is a useful model to understand global immune response as it involves both innate and adaptive immune systems. Adaptive immune response was monitored by flow cytometry analysis of T lymphocytes population in the colonic lamina propria (cLP) during the clearance phase of the bacteria. Ch25h deficiency does not impact adaptive immune response to *C. rodentium* as no differences were observed in IFN γ ⁺ Th1 nor IL-17⁺ Th17 proportion between the two genotypes (Fig. 27A, 27B). Innate immune response was assessed by gene expression profile of colonic tissues. After 3 days of infection, Ch25h^{-/-} mice depicted a decrease expression of colonic inducible nitric oxide synthase (iNOS) expression compared to wild-type mice that did however not reach significant differences (Fig. 27C). Colonic tumor necrosis factor alpha (TNF α) significantly decreased in Ch25h^{-/-} mice compared to wild-type mice at early stage of the infection pointing out a potential defect in innate immune cell activation in mice lacking Ch25h (Fig. 27C).

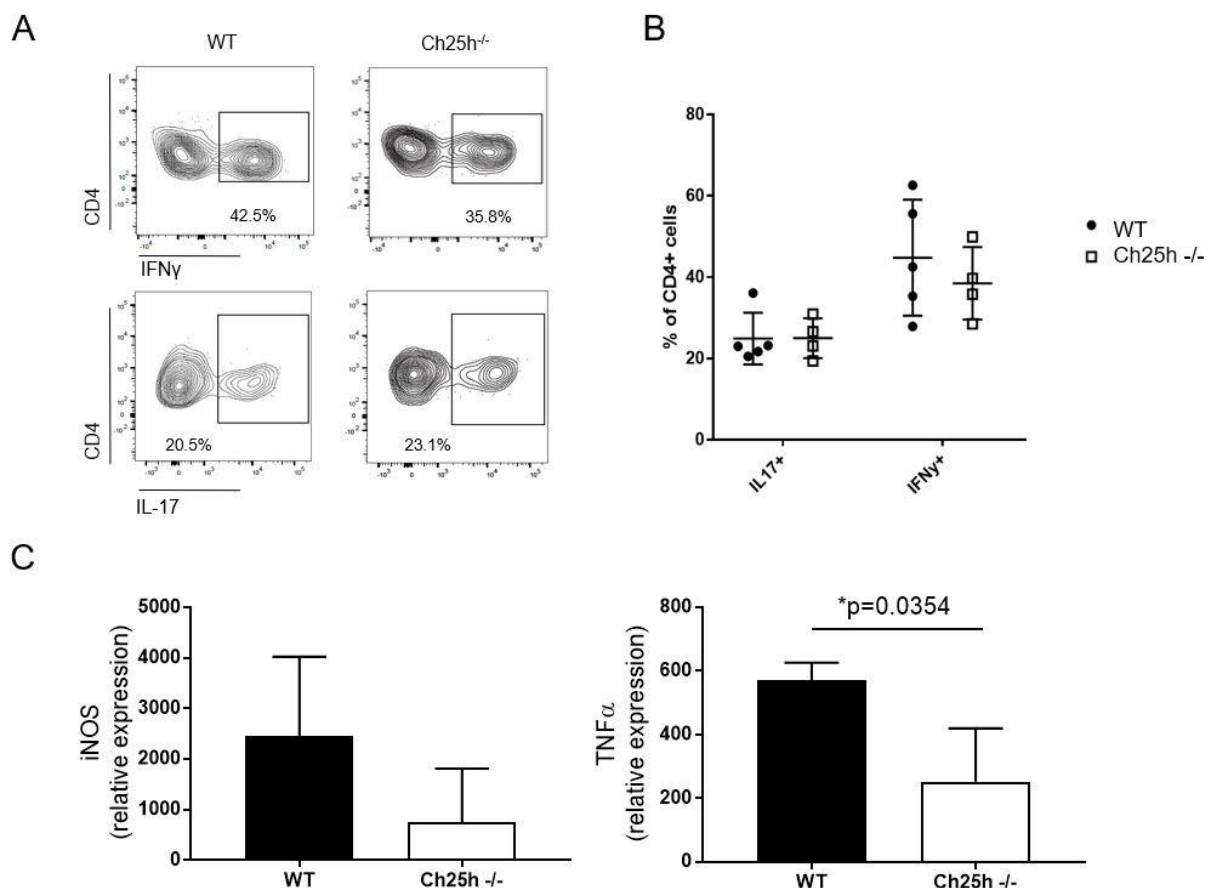


Figure 27. Ch25h^{-/-} mice have an abnormal innate immune response during infection.

(A) Representative flow cytometry analysis of Th1 (IFN γ ⁺) and Th17 (IL-17⁺) cells in the colonic lamina propria from Ch25h^{-/-} and wild-type (WT) mice at day 16 post infection. **(B)** Flow cytometry analysis of the total proportion (%) of Th1 and Th17 cells in the colonic lamina propria from Ch25h^{-/-} and wild-type

(WT) mice at day 16 post infection (mean \pm SD, $n = 4-5$). **(C)** Relative mRNA expression of iNOS and TNF α in colonic tissue of Ch25h^{-/-} and wild-type (WT) mice at day 3 post-infection (mean \pm SD, $n = 3$). P values were determined by unpaired Student's *t* test (C).

4.2.8 Ch25h^{-/-} BMDCs have an impaired IL-23 response to bacterial challenge

To further investigate the role of innate response in the presence or absence of Ch25h enzyme, bone marrow-derived dendritic cells (BMDC) from Ch25h^{-/-} and wild-type mice were cultured and challenged with inactivated heat-killed *C. rodentium*. Dose-dependent increase of Ch25h expression was observed in wild-type BMDCs challenged with the bacteria (Fig. 28A). LPS was reported to increase Ch25h expression in BMDC derived from another strain of wild-type mice and was used as positive control [263]. BMDC responses to bacteria have been addressed through cytokine production including interleukin-6 (IL-6), TNF α and interleukin-23 (IL-23). IL-6 production was induced during the stimulation but on the same extent in Ch25h^{-/-} and wild-type BMDCs (Fig. 28B). TNF α was also induced during the bacterial challenge and a small but significantly transitory decrease of secretion was observed in Ch25h^{-/-} cells (Fig. 28C). IL-23 secretion was significantly decreased in BMDC lacking Ch25h showing an impaired capability of these cells to secrete IL-23 in response to heat-killed *C. rodentium* (Fig. 28D). We further confirmed the result by mRNA and observed that IL-23 gene expression was also reduced in Ch25h^{-/-} BMDCs 12 hours after bacterial challenge (Fig. 28E). This potential defect in DCs response could potentially explain the delayed of bacterial clearance observed in Ch25h^{-/-} mice.

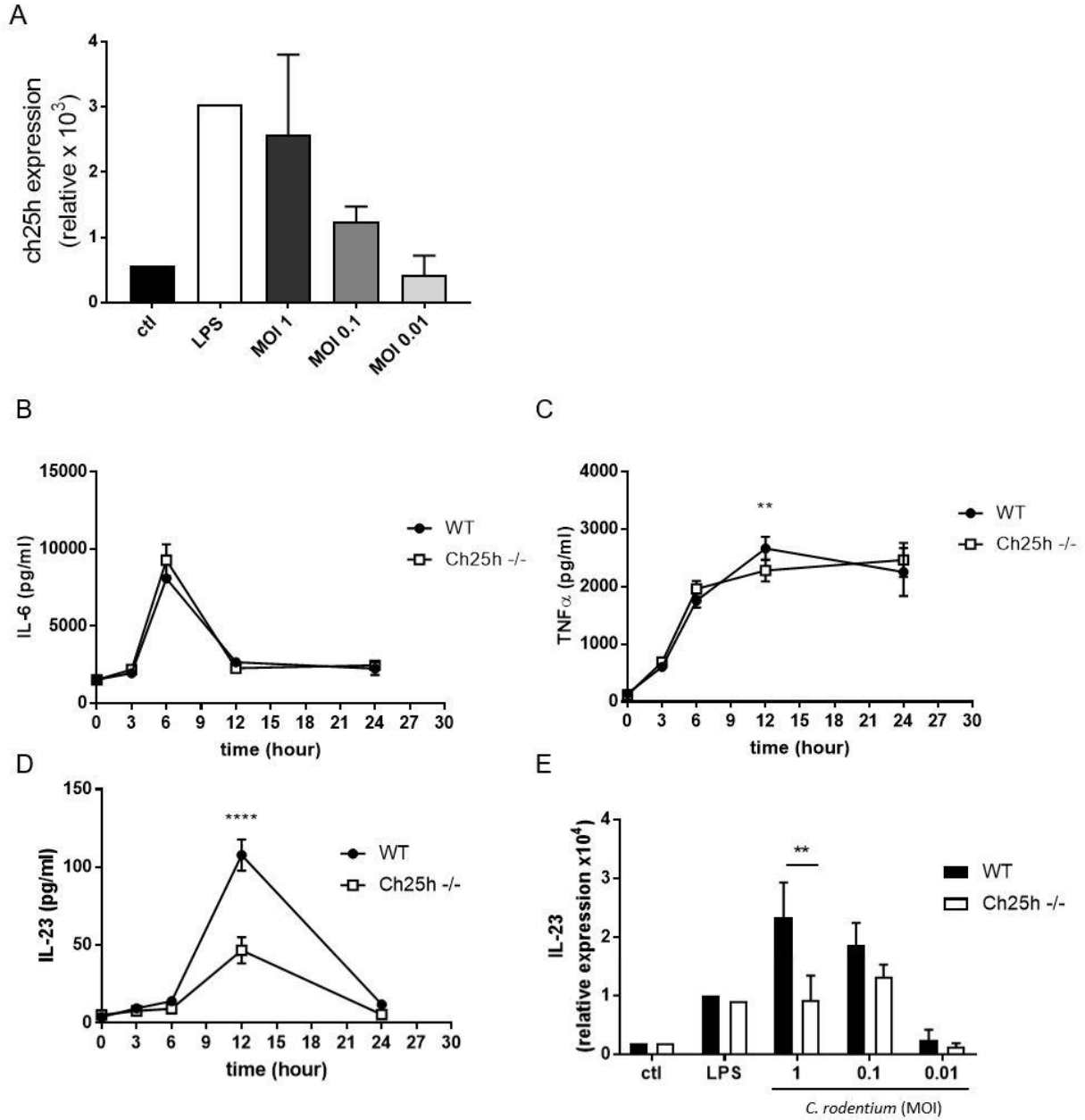


Figure 28. Ch25h^{-/-} BMDCs have an ineffective IL-23 response to bacterial challenge.

(A) Relative mRNA expression of Ch25h in BMDCs 12 hours post-stimulation with either *C. rodentium* at different multiplicity of infection (MOI) or with LPS or medium (ctl) (mean \pm SD, $n = 1-3$). (B-D) ELISA quantification of IL-6 (B), TNF α (C) and IL-23 (D) secretion by BMDCs after *C. rodentium* (MOI 1) (mean \pm SD, $n = 3-6$). (E) Relative mRNA expression of IL-23 expression in BMDCs 12 hours post-stimulation with either *C. rodentium* at different MOI or with LPS or medium (ctl) (mean \pm SD, $n = 3$). *, $P < 0.05$; **, $P < 0.01$; ***, $P < 0.001$; ****, $P < 0.0001$; P values were determined by two-way ANOVA (B, C, D, E).

4.2.9 Ch25h^{-/-} mice have decreased level of CD4⁺ type 3 innate lymphoid cells

ILCs are a recently described family of innate immune cells important for defense against pathogens. As previously mentioned, they are located mostly in the LP of mucosal surface and can be activated to produce cytokines contributing to the innate immune response [264]. Three main subtypes of cells have been described at the beginning; ILC1, ILC2, ILC3 that mirror the signature effector cytokine profiles of the classical CD4⁺ Th1, Th2 and Th17 cells respectively [265]. In addition, experts have also recently included NK cells and LT_i cells in the ILC family [264]. ILC3, the most abundant ILC type in the intestine, are responsible for homeostasis of intestinal epithelium, lymphoid tissue development and protection against bacteria including *C. rodentium* [266] [267]. IL-23, that we found potential defected in DCs of Ch25h^{-/-}, drives the activation of ILC3 [268]. Therefore, colonic lamina propria (cLP) ILC3 populations from WT and Ch25h^{-/-} mice were analyzed at physiological stage (Fig. 29). A significant reduction of CD4⁺ ILC3 in the cLP were observed in mice lacking Ch25h compared to wild-type mice, suggesting a potential impaired functionality of the ILC3 that could explain the delayed of bacterial clearance observed in these mice.

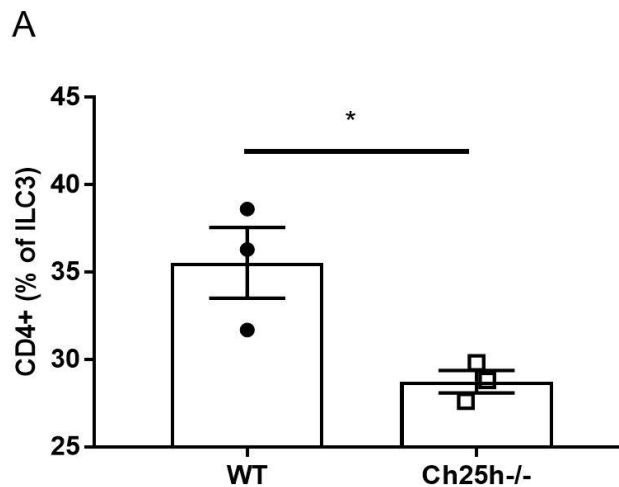


Figure 29. Ch25h^{-/-} mice have decreased level of CD4⁺ ILC3 cells in the colonic lamina propria. (A) Flow cytometry analysis of the total proportion (%) of CD4⁺ type 3 innate lymphoid cell (ILC3) of colonic lamina propria isolated from WT and Ch25h^{-/-} mice. Population frequencies gated on CD45⁺Lin⁻CD127⁺ROR γ T⁺CCR6⁺. (mean \pm SD, $n = 3$). *, $P < 0.05$; P values were determined by unpaired Student's t test.

4.3 Discussion

Last decade, growing scientific evidence have demonstrated how oxysterols can affect the immune system. More recently, oxysterols emerged as mediators in fine-tuning the immune responses during autoimmune disorders. We reported that mice lacking Ch25h had an attenuate EAE disease and reduced Th17 cell infiltration in the CNS, pointing toward a role of Ch25h and related oxysterols during CNS autoimmunity. As previously observed, our study and others have suggested a strong role of the gut environment during EAE disease [129]. Ch25h^{-/-} mice have shown modulation of mucosal IgA homeostasis but whether the oxysterol deficiency lead to an altered gut immune response remain still largely unknown. We aim to understand whether oxysterols can modulate gut immunity and could contribute to EAE phenotype observed in Ch25h deficient mice.

We here report that Ch25h expression and oxysterol levels are modulated in the intestine during the development of CNS autoimmunity. To our knowledge, it is the first evaluation of oxysterol levels in the gut during CNS autoimmunity. Previous reports have observed oxysterol modulations during autoimmune conditions but always in the tissues directly affected by the disease and not peripheral organs. For example, Ch25h expression and oxysterol levels were found modulated during the development of EAE disease in CNS tissues [193] [200]. Regarding the intestine, two previous studies demonstrated that colitis alters colon oxysterol levels and oxysterol-metabolizing enzymes expression. Indeed, Ch25h was upregulated in the intestine during inflammation in ulcerative colitis (UC) patients and experimental model of colitis [201] [202]. These recent reports strengthen the fact that Ch25h expression is upregulated and oxysterols are modulated in inflammatory environment such as colitis or neuroinflammation. We here found that Ch25h expression is up regulated during EAE in the small intestinal lamina propria and in the whole colon tissue. Similar results were found for the colon in the previous cited studies during active and chronic colitis models. Using acute colitis models, previous studies demonstrated that 25-OHC and 7 α ,25-OHC are increased during the disease. In our report, we did not report an increase of 25-OHC in the colon nor in the small intestine. Regarding 7 α ,25-OHC, we detected this oxysterol in a low amount in the small intestine but not in the colon. In accordance with the literature, 25-OHC is detected 100 times more than 7 α ,25-OHC, and levels of 7 α ,25-OHC detected are often very low. In our settings, we hypothesized that 7 α ,25-OHC are present in colon samples but under the detection level [201]. 7 α ,25-OHC was increased in small intestine during EAE in wild-type mice compared to non-treated mice however it did not reach significant differences. Surprisingly, Ch25h deficiency do not lead to major reduction of 25-OHC and 7 α ,25-OHC. As previously reported in Wyss *et al.*, Ch25h^{-/-} mice are still able to produce 25-OHC [202]. It is known that 25-OHC can be produced by auto-oxidation or by alternative enzymes (such as Cyp3a or Cyp27A1)

[269]. Another element that could explain these results is the potential presence of oxysterols in the diet of the mice. Indeed, the group of Prof. Muccioli have already reported that 25-OHC is present in normal chow from Research Diets (AIN-93-M) [162]. These elements could mask the consequences of the deletion of Ch25h. 4 β -OHC is the most represented oxysterol in the colon and was previously shown associated with colitis. Indeed, Guillemot-Legr \acute{e} ris *et al.*, have demonstrated that 4 β -OHC levels were consistently increased in their model of colitis (active and chronic colitis) [201]. Moreover, they administered 4 β -OHC to the mice during the development of the colitis. Interestingly, mice treated with 4 β -OHC worsened colon inflammation compared to mice treated with vehicle. Here we observed that 4 β -OHC was highly increased during EAE in both small and large intestine in wild-type mice. However, in small intestine of Ch25h^{-/-} mice, 4 β -OHC was significantly reduced compared to WT during EAE development. With the recent knowledge about this oxysterol, it could strengthen the hypothesis of a pro-inflammatory environment in the gut during EAE development and suggest lower inflammation in the small intestine of mice lacking Ch25h during CNS autoimmunity. However, the underlying mechanisms need to be further investigated. With these new results, we reported that oxysterols are modulated during the EAE in the gut and Ch25h^{-/-} mice depict an altered profile of these metabolites during the disease. We here focused on Ch25h-related oxysterols, but we plan to further analyze other enzyme expression profiles related to the production of 25-OHC to understand which enzymes are modulated and responsible for the fluctuations of oxysterol that we observed. Moreover, we observed that oxysterol levels are different from one tissue to another. Local level of oxysterols may be different from the whole tissues. Therefore, analysis of the gradient directly in the different GALTs could be more precise to understand specific modulation of oxysterol rather than whole tissue changes.

We previously described that Ch25h^{-/-} mice attenuated EAE disease course by a delayed trafficking of pathogenic Th17 lymphocytes to the CNS. The accumulation of Th17 was only transient and suggest that autoreactive Th17 cells could be trapped temporary in other tissues before reach the CNS. We thought that Th17 cells would have accumulated in the GALTs of Ch25h^{-/-} mice and delayed their migration to the CNS. With our experiments, we observed that intestinal sequestration is not occurring in the absence of Ch25h. On the contrary, we observed a reduced intestinal Th17 infiltration in Ch25h^{-/-} mice. In addition, we observed intestinal morphology modulations during EAE disease. Nouri *et al.* previously demonstrated that structural changes occur in the small intestine during EAE development [135]. We confirmed these findings and reported an increase villus size area during EAE in WT but not in Ch25h^{-/-} mice suggesting a potential effect of oxysterols on gut morphology during EAE development that needs to be further investigated. With our recent findings on the capability of gut environment to potentiate the pathogenicity of autoreactive Th17 cells, delayed EAE disease

in mice lacking Ch25h could be explained by a delayed migration to the intestine observed after their initial priming, at the site of MOG/CFA injection. The underlying mechanisms need to be further investigated. One strategy is to better understand the cellular source of oxysterols and the site of production. High expression of oxysterol converting enzymes are observed in stromal cells such as blood endothelial cells and in lymphatic endothelial cells in several organs including peripheral lymph nodes and spleen [188]. Recent publications reported intestinal stromal cells as producers of $7\alpha,25\text{-OHC}$ [203] [204]. Therefore, one hypothesis is that a local gradient of oxysterols directly emerging from the vascular and/or lymphatic endothelium could favor lymphocytes diapedesis into different tissues such as the gut or the BBB. Discovering the cellular source and the site of oxysterol secretion may lead to the discovery of selective targets of immune cell trafficking.

At the beginning of our project, main phenotype observed in the gut of Ch25h^{-/-} was altered IgA production, potentially associated with a dysbiosis as previously explained [197] [198]. Surprisingly, we did not observe a major impact of Ch25h deletion on the gut microbiota, both at steady state and during EAE disease. Similar changes were observed in the relative abundance of the general phyla between WT and Ch25h^{-/-} mice during EAE. However, we found some modulations of certain genera associated with the Ch25h deficiency. Indeed, we observed an increase abundance of *Butyricoccus* that are known to produce short chain fatty acids called butyrates. Short chain fatty acids including propionate and butyrate are able to stimulate Treg. Interestingly, Haghikia *et al.* and others have demonstrated that oral administration of propionate reduced EAE disease by increasing the Treg proportion [270] [271]. Nevertheless, in our experiments, potential increase of butyrates in Ch25h deficient mice was not associated with increase of Treg population in the gut as previously shown with flow cytometry analysis.

To further understand whether oxysterol deficiency lead to altered gut immune response, we aim to assess the immune response to enteric bacterial infection. We reported that Ch25h and related oxysterols are important in the gut infection as delayed of bacterial clearance were observed in mice lacking Ch25h. Furthermore, we found that innate immune system was impaired during bacterial challenge both *in vivo* and *in vitro*. We observed a reduced expression of gene important for the innate immune response early during the infection. *In vitro*, we reported an impaired secretion of IL-23 by dendritic cells derived from Ch25h^{-/-} mice. IL-23 is particularly important for the activation of ILC3 to produce their signature cytokines including IL-22 that is crucial for the early phase of host defense against *C. rodentium* [272]. Therefore, alteration of IL-23 by Ch25h^{-/-} DCs could explain the reduced proportion of CD4⁺ ILC3 in the cLP of Ch25h^{-/-} mice associated with the difficulty to eliminate the pathogen. At that time, this was the first evidence that Ch25h and related oxysterols have a potential role

in the gut immune response against bacterial infection. However, during our project, Chu *et al.* bring evidence that oxysterols can act directly on ILCs, independently of IL-23 secretion [204]. Indeed, they demonstrated that ILC3s express Ebi2 and regulate their migration through oxysterol gradient. Interestingly, they observed a disorganized ILC3 distribution in the mLNs and a defective ILC3 accumulation in the siLP of Ebi2^{-/-} and Ch25h^{-/-} mice. They also demonstrated reduced cryptopatches and IFL in the colon of Ebi2^{-/-} and Ch25h^{-/-} mice, that were already reported in a previous study [203]. Moreover, they found a reduced proportion and number of ILC3s in the small intestine and the colon in Rag1^{-/-} Ebi2^{-/-} compared to Rag1^{-/-} mice at steady state. Finally, the author observed an increase severity of colitis in Rag1^{-/-} mice compared to Rag1^{-/-} Ebi2^{-/-} following *C. rodentium* infection. Rag1^{-/-} Ebi2^{-/-} mice had a reduced survival rate following the infection compared to Rag1^{-/-} mice [204]. Although, Ebi2^{-/-} on Rag1^{-/-} background were used instead of Ch25h^{-/-} on WT background, our results go in the same direction and it strongly suggests that Ch25h-related oxysterol pathway is required for ILC3-mediated immunity against pathogens, the gut homeostasis in general and maybe other peripheral organs such as the CNS. Interestingly, a recent preliminary study has observed ILC3 population inside CNS of healthy mice that was reduced during EAE. In the gut, they reported an increased ILC3 proportion in the PP and the siLP during the peak of EAE disease [273].

The recent knowledge obtained about the role of oxysterols in the gut during specific-gut inflammation, give us a better idea of how the gut environment is perturbed with the lack of oxysterols and how it could potentially affect the development of EAE disease. Indeed, one could suggest that abnormal ILC3 repartition and functionality can change the structural organization of the gut affecting the proper gut functionality and affecting autoimmune disease outside the gut compartment such as EAE or MS.

5. PROJECT III: Role of oxysterols during hypercholesterolemia and the contribution in EAE disease

5.1 Materials & Methods

5.1.1 Animals and diet

Ch25h^{-/-} and wild-type mice were crossed with LDLr^{-/-} mice. Mice were placed on HFD (Kliba 2127) containing 60% of fat during 4 weeks before EAE immunization. Control groups were placed under control diet (Kliba 2125) containing 10% of fat or chow diet (Kliba 3242). Diet was kept during EAE experiments until the end of the experiments.

5.1.2 EAE induction and clinical evaluation

EAE induction and clinical evaluation were done as previously described in 3.1.2.

5.1.3 Antibody treatment

For lowering cholesterol experiments, mice were injected i.p. with 10mg/kg of anti-PCSK9 (proprotein convertase subtilisin/kexin type 9) (alirocumab, Praluent®, Sanofi) or PBS control one week before EAE immunization and once per week until the end of the experiments.

5.1.4 Flow cytometric analysis

Flow cytometric analysis was done as previously described in 4.1.3, with additional following material and methods: Fluorochrome-conjugated antibodies were purchased from several commercial sources indicated below: Antibodies against CD8 (53.6-7) was from eBioscience.

5.1.5 Quantification of lipid profile

Blood from overnight-fasting mice were collected submandibular and serum was isolated using centrifugation. Serum lipid profiles were assessed using Roche Cobas C111 robot from the Mouse Metabolic Evaluation Facility (UNIL, Lausanne) and Siemens Dimension Xpand plus from the Center of Phenogenomics (EPFL, Lausanne).

5.1.6 RNA isolation and quantitative PCR analysis

RNA isolation and quantitative PCR analysis were done as previously described in 4.1.7.

5.1.7 Isolation of CNS immune cells

Isolation of CNS immune cells were done as previously described in 3.1.5

5.1.8 Antigen-specific proliferative and cytokine responses

Mice were immunized with MOG₃₅₋₅₅ peptide in CFA as described previously. Single cell suspensions were prepared from spleen 10 days post-immunization. Cells were restimulated with MOG₃₅₋₅₅ for 72h in supplemented DMEM medium containing inactivated 10% FCS (FBS 18, Biowest), 100 U/mL penicillin-streptomycin (BioConcept), 1 mM sodium pyruvate (Sigma), 50 M β -mercaptoethanol (Gibco), MEM non-essential amino acids (100x) (Gibco), MEM vitamins (100x) (Sigma), 200 mM L-glutamine, folic acid 14mM (Sigma), 0.3 mM L-asparagine (Sigma), 0.7 mM L-arginine. For proliferation assays, cells were pulsed with 1 μ Ci of [3H]-thymidine (Hartmann Analytic) during the final 18h and analysis of incorporated [3H]-thymidine was performed in a β -counter (Packard Top Count NXT Luminescence and Scintillation Counter). Secreted cytokines were measured after 48h of culture with MOG₃₅₋₅₅ by ELISA (Invitrogen).

5.1.9 Statistical analysis

Statistical analyses were done as previously described in 3.1.11.

5.2 Results

5.2.1 Intestinal Ch25h expression increases during hypercholesterolemia

To increase cholesterol level and change oxysterol homeostasis, female Ch25h^{-/-} and wild-type mice were fed with HFD. Female mice are known to be more resistant to diet induced obesity than males [274]. However, as EAE experiments are usually performed in female mice, we started with female mice placed on special diet. As our projects interest the gut-brain axis, we decided to assess the intestinal Ch25h expression in wild-type and LDLr^{-/-} fed either with chow diet (ctl) or high fat diet (HFD). Significant increase of Ch25h expression was observed in the small intestine of wild-type mice fed with HFD compared to control (Fig. 30). The expression of Ch25h was even higher in LDLr^{-/-} mice fed with control or HFD. These results demonstrated that hypercholesterolemia induced by diet or by genetic model significantly increase Ch25h expression in the small intestine.

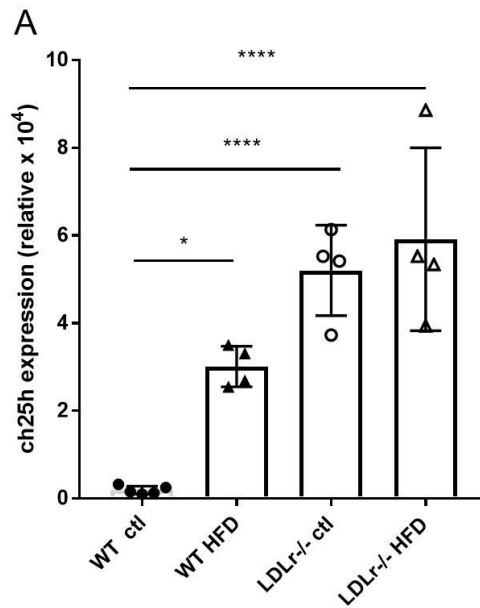


Figure 30. Ch25h expression increases in the gut during hypercholesterolemia.

(A) Relative mRNA expression of Ch25h in intestinal tissue as measured by real-time PCR in wild-type and LDLr^{-/-} mice fed with either chow diet (ctl) or high fat diet (HFD) (mean ± SD, *n* = 4-5). *, *P* < 0.05; **, *P* < 0.01; ***, *P* < 0.001, ****, *P* < 0.0001; *P* values were determined by one-way ANOVA. Data are representative of two experiments.

5.2.2 Ch25h deficiency has no major role on lipid profile in transgenic model of hypercholesterolemia

As previously reported by our group [195], Ch25h did not impact levels of circulating lipid profile including tChol, LDL, HDL, and triglyceride (TG) as no difference was observed between Ch25h^{-/-} and wild-type mice when fed with chow diet. We further assessed the impact of Ch25h under LDLr^{-/-} genetic background. Similar lipid levels between Ch25h^{-/-}LDLr^{-/-} compared to LDLr^{-/-} mice were observed except for TG level that was significantly reduced in double knock-out mice (Fig. 31).

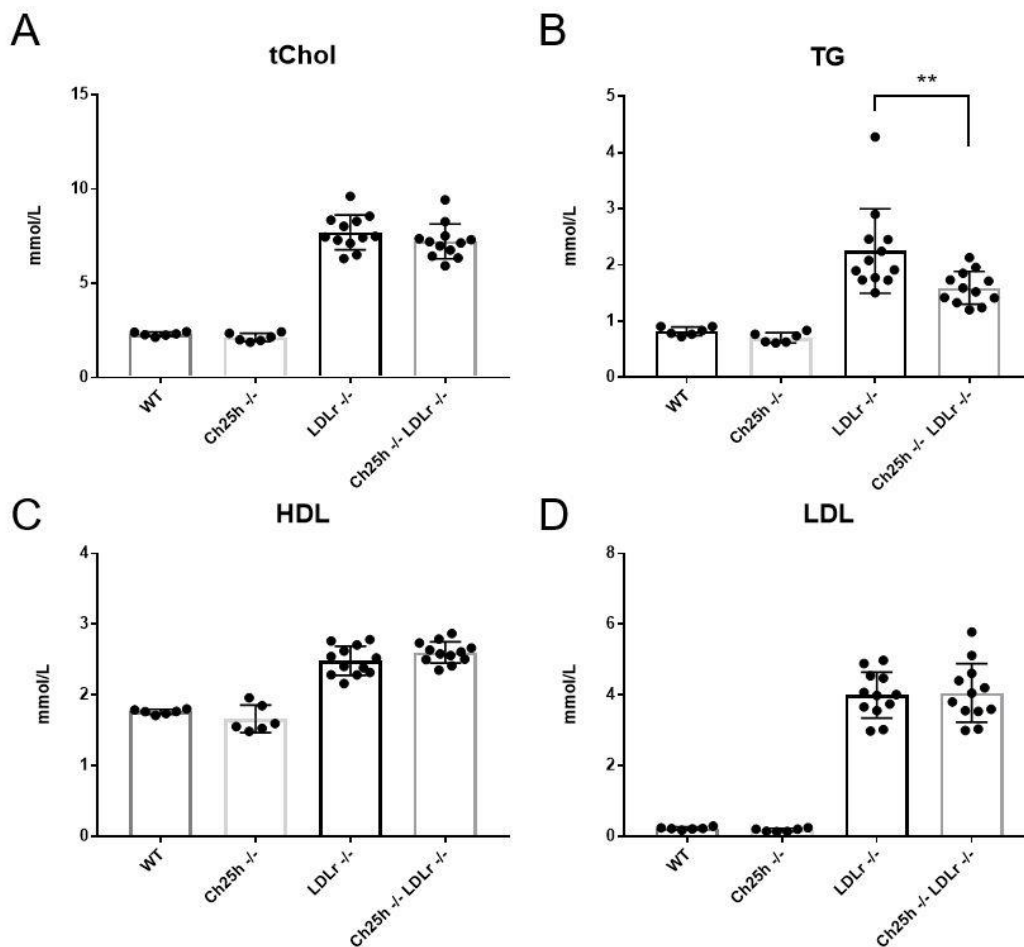


Figure 31. Ch25h deficiency has no major role on baseline lipid profile in transgenic model of hypercholesterolemia under normal diet. (A-D) Serum profile of total cholesterol (tChol) (A) triglyceride (TG) (B), high-density lipoprotein (HDL) (C) and low-density lipoprotein (LDL) (D) levels of wild-type, Ch25h^{-/-}, LDLr^{-/-} and Ch25h^{-/-}LDLr^{-/-} female fed with chow diet (mean ± SD, $n = 6-12$). *, $P < 0.05$; **, $P < 0.01$; P values were determined by one-way ANOVA. Data are representative of two experiments. [Mouse Metabolic Evaluation Facility from University of Lausanne performed the lipid profile analysis]

5.2.3 Ch25h^{-/-} mice conserve their delayed EAE disease phenotype in hypercholesterolemic conditions

To evaluate the impact of Ch25h deletion on EAE disease in the context of hypercholesterolemia, wild-type, Ch25h^{-/-}, LDLr^{-/-} and double knock-out Ch25h^{-/-}LDLr^{-/-} mice were further placed on HFD (60% fat) or adequate control diet (ND; 10% fat). Lipid profile, weight gain and EAE disease profile were assessed. LDLr^{-/-} mice are known to be more susceptible to increase cholesterol level when fed with HFD compared wild-type control. Indeed, HFD significantly depicted increased level of tChol in LDLr^{-/-} mice compared to ND. However, HFD did not increase significantly the level of tChol in wild-type mice compared to ND. Ch25h depletion had no major effect on TG and tChol levels in mice placed on HFD (Figure 32A, 32B). After four weeks of HFD, EAE immunization was performed. We expected that hypercholesterolemia would exacerbate the EAE phenotype in WT but not in mice lacking

Ch25h. However, we did not observe a more severe EAE disease in the mice depicting the highest cholesterol levels, which are the LDLR^{-/-} mice compared to WT mice under HFD. However, we observed a significant delayed EAE disease onset in all Ch25h^{-/-} groups compared to their corresponding wild-type controls, independently of their blood cholesterol levels (Figure 32C, 32D and Table 7). We were surprised that mice susceptible for high fat diet and harboring high circulating tChol level (such as LDLR^{-/-} mice on HFD) did not show enhanced susceptibility to EAE. Indeed, based on previous publications [154] [158], we expected to observe exacerbated EAE disease in mice with hypercholesterolemia such as mice under HFD or LDLR^{-/-} transgenic strain. On the contrary, we found that LDLR^{-/-} mice placed on HFD developed an attenuated EAE disease (Fig. 32D). As we obtained those contradictory results, we decided to perform further additional experiments to understand whether circulating cholesterol impacts EAE development.

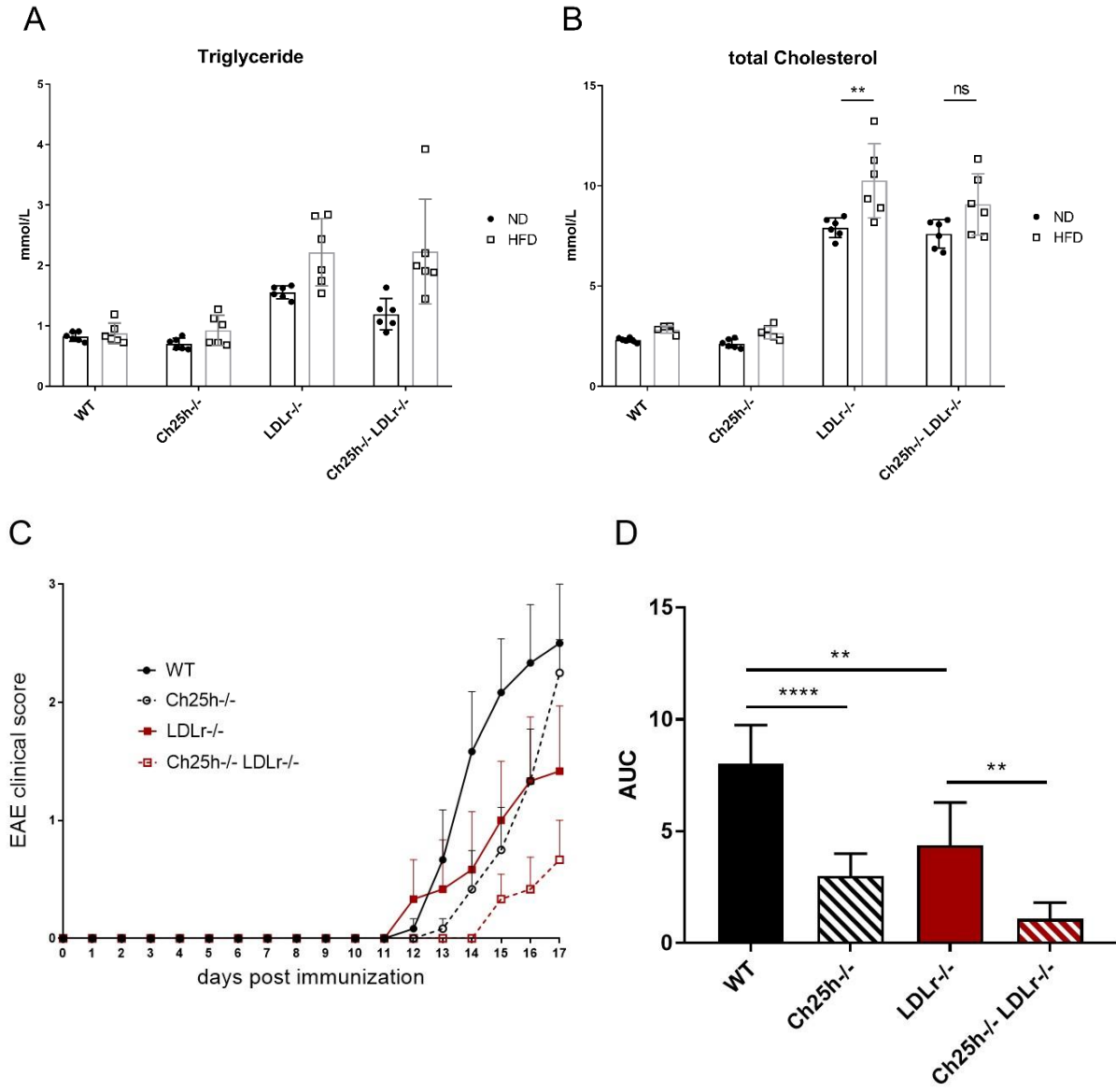


Figure 32. Effect of hypercholesterolemia and oxysterols during EAE disease. (A-B) Triglyceride (A) and total cholesterol (B) profile of wild-type, Ch25h^{-/-}, LDLr^{-/-} and Ch25h^{-/-}LDLr^{-/-} fed with normal diet (ND, 10% fat) or high fat diet (HFD, 60% fat) (mean ± SD, n = 6). (C) Mice were immunized after 4 weeks of high fat diet (HFD, 60% fat). Clinical scores of EAE (mean ± SEM, n = 6) (D) Area under the curve (AUC) of the EAE disease curve (C) was assessed between the groups (mean ± SEM, n = 6). *, P < 0.05; **, P < 0.01; ***, P < 0.001, ****, P < 0.0001; ns, not significant; P values were determined by two-way ANOVA (A, B, C) and by one-way ANOVA (D). See also Table 7. [Mouse Metabolic Evaluation Facility from University of Lausanne performed the lipid profile analysis]

Table 7: Ch25h^{-/-} mice depicted delayed EAE disease independently of hypercholesterolemia.

Group	Disease incidence	Score max (mean +/- SD)	Mean day of onset (mean +/- SD)	AUC (mean +/- SD)
WT	83.3% (5/6)	2.3 +/- 1.2	13.4 +/- 0.9	8.0 +/- 1.8
Ch25h ^{-/-}	100% (6/6)	2.8 +/- 0.4	15.33 +/- 1.6	3.7 +/- 1.2
LDLr ^{-/-}	66.7% (4/6)	1.5 +/- 1.3	14.25 +/- 1.7	4.4 +/- 1.2
Ch25h ^{-/-} LDLr ^{-/-}	50% (3/6)	0.8 +/- 1.0	15.67 +/- 1.2	1.1 +/- 0.7

AUC, area under the curve

5.2.4 Effect of hypercholesterolemia during EAE on male and female mice

We first performed EAE experiments in LDLr^{-/-} mice. As female are described to not respond properly to hypercholesterolemia, male mice were further included in the study. LDLr^{-/-} induced a significant hypercholesterolemia in the mice without addition of HFD as previously demonstrated. Therefore, we decided to avoid dietary effects and focused only on the LDLr pathway to induce circulating hypercholesterolemia. LDLr^{-/-} and WT mice were compared for EAE disease development. No significant difference in EAE development was observed between LDLr^{-/-} and wild-type in both female and male mice (Fig. 33).

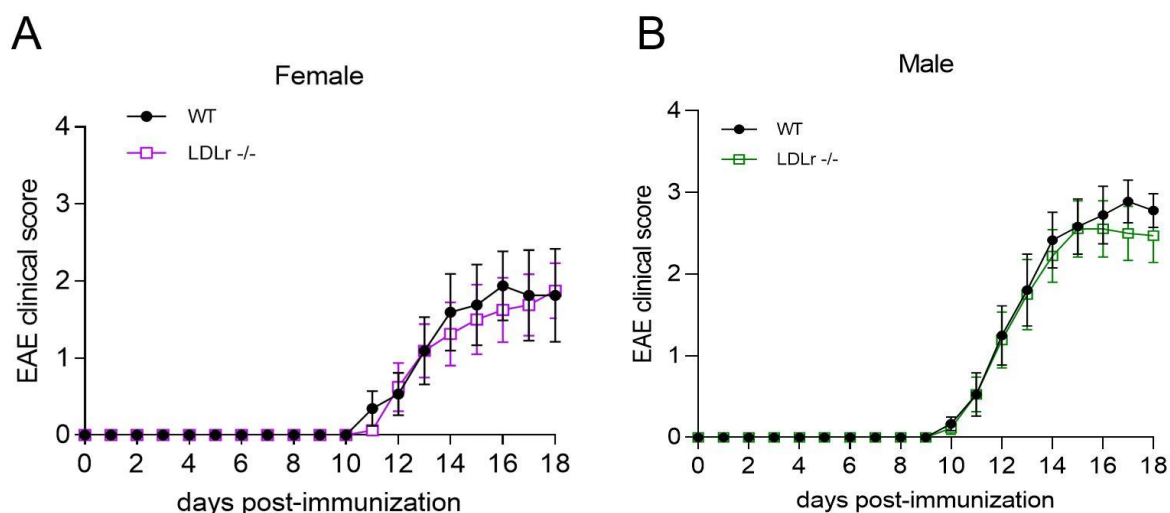


Figure 33. Hypercholesterolemia does not exacerbate EAE disease in male nor in female mice. (A) EAE was induced in female wild-type and LDLr^{-/-} mice. The course of EAE is shown as clinical score (mean ± SEM; n = 8). (B) EAE was induced in male wild-type and LDLr^{-/-} mice. The course of EAE is shown as clinical score (mean ± SEM; n = 9). Data are representative of two experiments.

5.2.5 anti-PCSK9 decrease circulating cholesterol without alleviating EAE symptoms

As no impact of cholesterol were found using LDLr^{-/-} transgenic model, we further asked if reduced circulating cholesterol would change EAE development. The best-known lowering-cholesterol drugs are statins. As introduced in the first part of my thesis, statins have several biological effects aside the effect on cholesterol lowering, including anti-inflammatory effects that are not associated with the decreased circulating cholesterol. Therefore, we proposed to use a novel class of lowering-cholesterol drug called alirocumab. Alirocumab is a monoclonal anti-PCSK9 antibody approved by Swissmedic to treat patients with high cholesterolemia (such as familial hypercholesterolemia) in case of insufficient cholesterol lowering with statin treatments and dietary interventions [275]. Wild-type mice were treated either with anti-PCSK9 antibodies or control injections of PBS and EAE was induced. Significant reduction of circulating tChol, LDL and HDL were detected in mice treated with anti-PCSK9 (Fig. 34A). However, when EAE immunizations were performed, mice developed similar profiles of EAE symptoms (Fig. 34B) and similar incidence (Fig. 34C). Immune infiltrates were assessed in the CNS and no significant differences were observed between anti-PCSK9 treated mice and control (Fig. 34D). These results add another evidence that circulating cholesterol may not be important in EAE development.

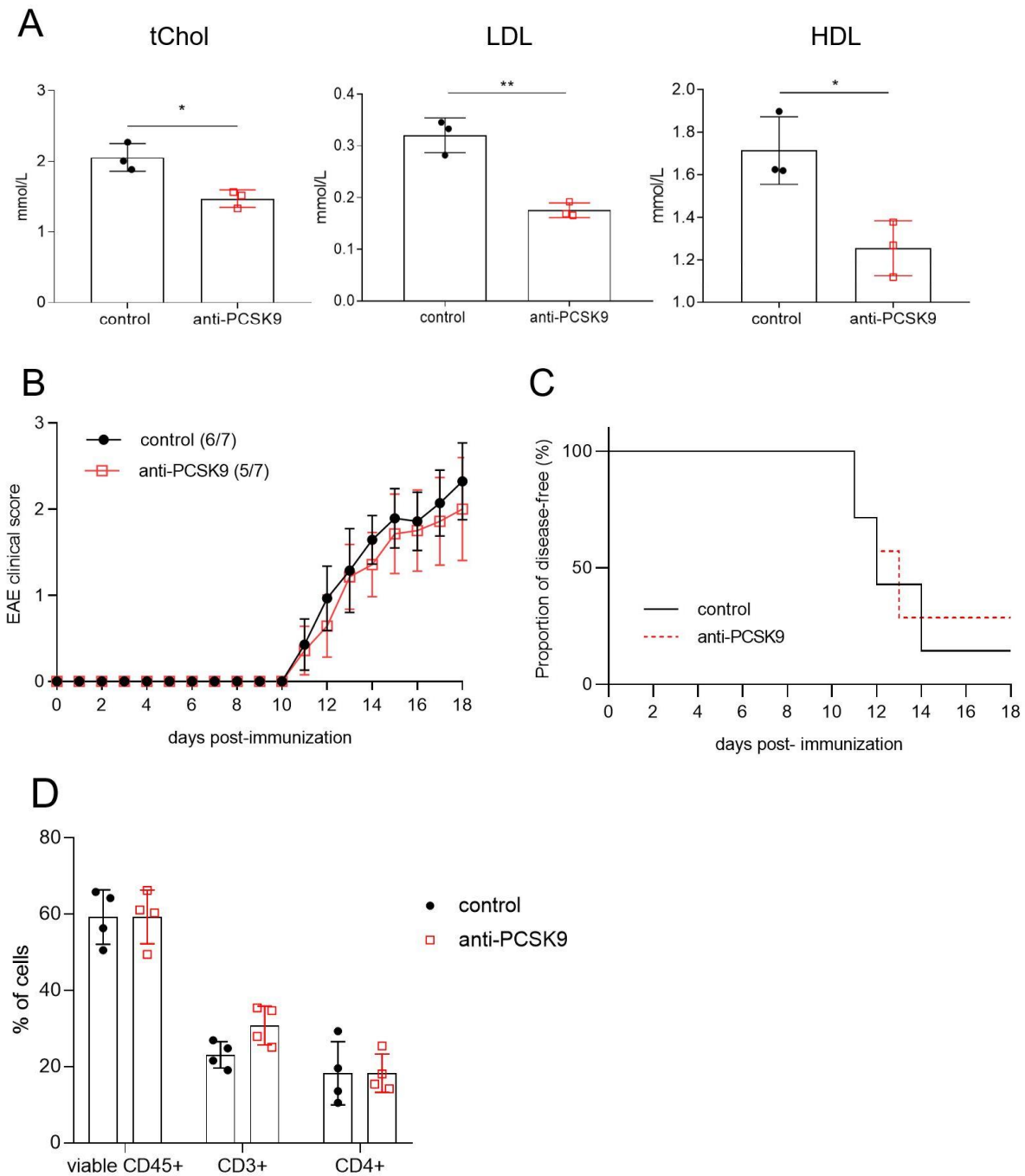


Figure 34. anti-PCSK9 decrease circulating cholesterol without alleviating EAE symptoms. (A) Quantification of circulating tChol, LDL and HDL of anti-PCSK9 treated mice versus control group (mean \pm SD, $n = 3$). (B) Clinical scores of EAE in immunized mice treated with anti-PCSK9 or PBS control (mean \pm SEM, $n = 7$). (C) Disease free activity curve between mice treated with anti-PCSK9 and PBS control mice. (D) Flow cytometry analysis of the total proportion (%) of the leukocyte (viable CD45⁺), lymphocyte T (CD3⁺) and lymphocyte T CD4⁺ (CD4⁺) in the CNS 14 days after EAE immunization (mean \pm SD; $n = 4$). *, $P < 0.05$; **, $P < 0.01$; P values were determined by unpaired Student's t test (A). Data are representative of two experiments. [Center of Phenogenomics from EPFL performed the lipid profile analysis].

5.2.6 anti-PCSK9 treatment does not show altered systemic immune responses

To further evaluate the role of hypocholesterolemia in CNS autoimmunity, we asked whether the anti-PCSK9 could induce an altered immune cell activation in the periphery in the absence of differences in clinical score. MOG₃₅₋₅₅ antigen specific responses were compared between anti-PCSK9 treated mice and controls. After 10 days post EAE immunization, splenocytes were harvested and culture with MOG peptide *in vitro*. We assessed the antigen-specific sensitization by analyzing the cytokines responses during the recall stimulation. MOG₃₅₋₅₅ activated T cells isolated from anti-PCSK9 treated mice produced similar amounts of IL-17A and IFN γ than control group (Fig. 35A, 35B). Using recall stimulation with MOG₃₅₋₅₅ peptide and [3H]-thymidine incorporation, anti-PCSK9 treatment did not alter proliferation of peripheral MOG₃₅₋₅₅ specific T cells (Fig. 35C). These results indicate that anti-PCSK9 treatment does not impact the proliferation nor sensitization of autoreactive T cells.

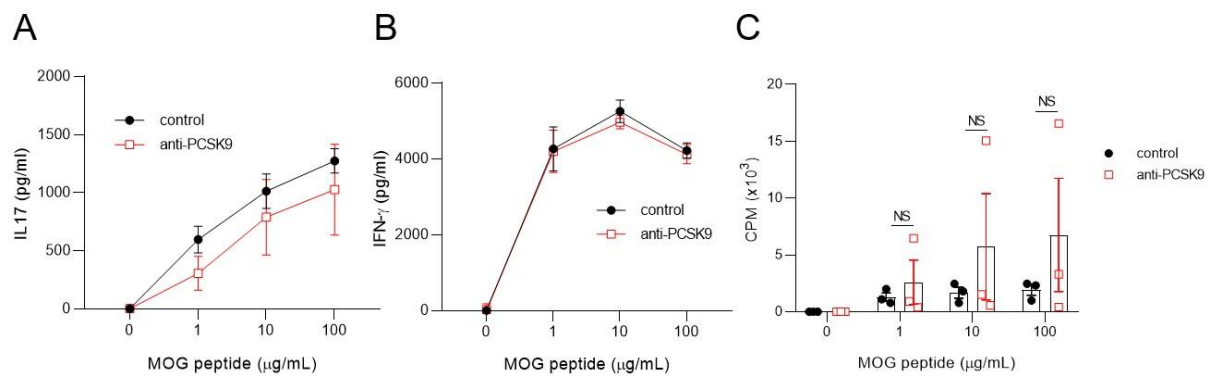


Figure 35. anti-PCSK9 treatment does not show altered systemic immune responses. (A-B) *In vitro* restimulation of splenocytes isolated from EAE immunized anti-PCSK9 treated mice versus control group with MOG₃₅₋₅₅. Secretion of IL-17A and IFN γ were measured by ELISA after 48 h of culture with the indicated concentration of MOG₃₅₋₅₅ (mean \pm SEM, $n = 3$). (C) Proliferative response was determined by [3H]-thymidine integration and expressed in counts per minute (CPM) (mean \pm SEM, $n = 3$). NS, not significant; P values were determined by two-way ANOVA (C).

5.3 Discussion

Obesity and high fat diet have been associated with perturbation of cholesterol and oxysterol hemostasis in liver, hypothalamus, adipose tissue and plasma [162]. During EAE development, gene related to cholesterol metabolism and oxysterol level are found altered in the CNS [161] [193]. However, the role of cholesterol during EAE development is still debated and impact of their oxysterol derivatives during cholesterol perturbation remain largely unknown. We here report that hypercholesterolemia induced by high fat diet or by transgenic mice model for hypercholesterolemia can increase Ch25h expression in the gut, suggesting altered Ch25h-related oxysterols in this tissue. Even if our data only rely on gene expression, we proposed

that hypercholesterolemia induces changes in Ch25h-related oxysterol metabolism in the gut. Previous study observed an increase liver expression of Cyp7b1 during HFD and an increase 25-OHC level in the liver of genetic model of obesity [162]. However, 25-OHC level in the plasma was not perturbed with HFD [276]. In the context of CNS autoimmunity, we hypothesized that the high Ch25h expression may lead to an increase $7\alpha,25$ -OHC gradient in the intestine allowing infiltration of Th17 lymphocytes and thus impacting the development of EAE disease. However, when mice were placed on diet rich in fat and further challenged with EAE immunization, a significant delayed of EAE disease was observed in all mice deficient for Ch25h when compared to their own controls independently of hypercholesterolemia.

Indeed, the protective EAE phenotype observed in Ch25h^{-/-} was conserved during hypercholesterolemia and was not amplified. As previously reported in the literature, we expected to see an exacerbated EAE disease in mice treated with HFD compared to control mice [154] [158]. Moreover, we were surprised when Mailloux *et al.* published their observations of a protective role of LDLr deficiency in female mice during EAE [159]. They suggested that the LDLr suppresses apolipoprotein E expression leading to exacerbation of neuroinflammatory responses in female, as female apolipoprotein E deficient mice are described to have a worsen EAE disease [277]. However, in our settings we did not observe a protective role of LDLr deficiency in the development of EAE. Overall, these results demonstrate that even if hypercholesterolemia increases Ch25h expression in the intestine and could potential modify trafficking of the immune cells, no major impact has been detected on the course of EAE disease.

As previously mentioned, contradictory results have been found regarding the role of circulating cholesterol in the EAE development. Therefore, we evaluated the role of hypercholesterolemia in male and female wild-type mice using only the LDLr^{-/-} transgenic, as it already induces a significant increase of circulating cholesterol. Contrary to the literature, we reported that LDLr deficient mice show a similar course of EAE disease compared to wild-type control both in female and male. We further evaluated if reduction of circulating cholesterol could impact CNS autoimmunity using anti-PCSK9 antibodies, a new generation of lowering-cholesterol drug. We demonstrated that treatment with anti-PCSK9 antibodies can significantly decreases the circulating cholesterol level. However, this reduction of tChol does not change the EAE development as anti-PCSK9 treated mice developed the same EAE course than control. Moreover, we further demonstrated that the reduced cholesterol level does not altered the adaptive immune responses during the development of CNS autoimmunity. Our results suggest that circulating cholesterol does not impact the development of EAE disease. Nevertheless, cholesterol is still an interesting target for the late phase of CNS autoimmunity. Indeed, it has been recently shown that dietary cholesterol can facilitate the repair of demyelinated lesions in the CNS [160].

6. GENERAL CONCLUSION

The projects conducted in my thesis aimed to provide insights on the potential relation between oxysterols and the gut environment in the development of experimental model of MS. The expected value of the first project is to understand the impact of the gut mucosal immunology in the modulation of EAE disease development. We show that encephalitogenic Th17 cells infiltrate the colonic lamina propria before neurological symptom development in two murine MS models, the active and adoptive-transfer EAE. Specifically targeting Th17 intestinal homing by blocking integrin $\alpha 4\beta 7$ -MAdCAM-1 pathway impairs T cell migration to the large intestine and further dampens EAE severity in Th17 adoptive-transfer model. Mechanistically, myelin-specific Th17 cells proliferate in the colon and affect gut microbiota composition. The beneficial effect of blocking the integrin $\alpha 4\beta 7$ -MAdCAM-1 pathway on EAE is interdependent of gut microbiota. Those results show that disrupting myelin-specific Th17 cell trafficking to the large intestine harness neuroinflammation and suggest that the gut environment and microbiota catalyze the encephalitogenic properties of Th17 cells. Further research should unravel what precisely trigger proliferation of autoreactive Th17 in the gut and identify what are the consequence for the Th17 cells.

In the second project, we aim to assess how oxysterols can modulate the gut immune system and the microbiota during the development of CNS autoimmunity and also during gut-specific inflammation using enteric bacterial infection. We show that infiltration of Th17 cells is reduced in the intestine during the development of EAE disease in the absence of Ch25h. In addition, we did not observe morphological changes in the small intestinal structures in mice deficient for Ch25h during EAE compared to WT mice. Deeper evaluations should be performed to understand the role or the consequence of oxysterols in the modulation of tissue remodeling. We evaluated the level of oxysterols and observed modulations of oxysterol homeostasis in the gut during the development of EAE disease.

Using gut-specific inflammatory model, Ch25h-related oxysterols have been identified as important in the immune response against host pathogens. We reported an impaired innate immune response resulting in a delayed bacterial clearance in mice lacking Ch25h. Dendritic cells have a defective IL-23 secretion when exposed to *C. rodentium* *in vitro* and ILC3 localization are disrupted in absence of oxysterols *in vivo*. Those data provide new evidence about the importance of oxysterols in the gut immunology and suggest interesting direction of future research such as the mechanism of the local source of oxysterols. Indeed, stromal cells have been suggested to be the local producers in the gut. However, the precise mechanisms and functions of the local oxysterol gradient remain still largely unknown. Better understand of

the cellular source and the activation of oxysterols secretion could lead to the identification of new specific targets of immune cell trafficking.

In the third project, we evaluated the effect of hypercholesterolemia on oxysterols and their contribution in promotion of CNS autoimmunity. We reported that perturbations of circulating lipids induce modulation of Ch25h expression in the gut without affecting the development of EAE disease. Contrary to other studies, we observed that hypercholesterolemia does not influence the course of EAE. Moreover, reduction of circulating cholesterol using anti-PCSK9 lowering-cholesterol drug shows similar results. These findings demonstrate that the perturbation of circulating cholesterol does not impact development of CNS autoimmunity.

Altogether, the thesis provides new understandings of the role of the gut and lipid metabolism during neuroinflammation and contributes to understand the implications of cholesterol metabolism on the gut immunology and microbiota that are implicated in MS development. Fine-tuning of cholesterol derivatives may not only lead to novel therapeutic discovery but may contribute, as oxysterol levels are possibly modulated by fat in the diet, to scientific-based reevaluations of dietary approaches. Those perspectives could therefore lead to a personalized medical approach not only for MS but also for other inflammatory and autoimmune diseases.

7 REFERENCES

- [1] T. J. Braley and R. D. Chervin, "Fatigue in Multiple Sclerosis: Mechanisms, Evaluation, and Treatment," *Sleep*, vol. 33, no. 8, pp. 1061–1067, Aug. 2010.
- [2] T. J. Murray, "The history of multiple sclerosis: the changing frame of the disease over the centuries," *J. Neurol. Sci.*, vol. 277 Suppl 1, pp. S3-8, Feb. 2009.
- [3] F. D. Lublin *et al.*, "Defining the clinical course of multiple sclerosis," *Neurology*, vol. 83, no. 3, pp. 278–286, Jul. 2014.
- [4] K. A. McKay, V. Kwan, T. Duggan, and H. Tremlett, "Risk Factors Associated with the Onset of Relapsing-Remitting and Primary Progressive Multiple Sclerosis: A Systematic Review," *BioMed Res. Int.*, vol. 2015, 2015.
- [5] J. W. L. Brown *et al.*, "Association of Initial Disease-Modifying Therapy With Later Conversion to Secondary Progressive Multiple Sclerosis," *JAMA*, vol. 321, no. 2, pp. 175–187, 15 2019.
- [6] D. S. Reich, C. F. Lucchinetti, and P. A. Calabresi, "Multiple Sclerosis," *N. Engl. J. Med.*, vol. 378, no. 2, pp. 169–180, 11 2018.
- [7] S. Beer and J. Kesselring, "High prevalence of multiple sclerosis in Switzerland," *Neuroepidemiology*, vol. 13, no. 1–2, pp. 14–18, 1994.
- [8] P. Browne *et al.*, "Atlas of Multiple Sclerosis 2013: A growing global problem with widespread inequity," *Neurology*, vol. 83, no. 11, pp. 1022–1024, Sep. 2014.
- [9] A. Alonso and M. A. Hernán, "Temporal trends in the incidence of multiple sclerosis: a systematic review," *Neurology*, vol. 71, no. 2, pp. 129–135, Jul. 2008.
- [10] S. E. Dunn and L. Steinman, "The gender gap in multiple sclerosis: intersection of science and society," *JAMA Neurol.*, vol. 70, no. 5, pp. 634–635, May 2013.
- [11] C. C. Whitacre, "Sex differences in autoimmune disease," *Nat. Immunol.*, vol. 2, no. 9, pp. 777–780, Sep. 2001.
- [12] N. M. Nielsen *et al.*, "Type 1 diabetes and multiple sclerosis: A Danish population-based cohort study," *Arch. Neurol.*, vol. 63, no. 7, pp. 1001–1004, Jul. 2006.
- [13] "Inflammatory Bowel Disease is Associated with Increased Risk of Multiple Sclerosis - Gastroenterology." [Online]. Available: [https://www.gastrojournal.org/article/S0016-5085\(17\)31464-6/pdf](https://www.gastrojournal.org/article/S0016-5085(17)31464-6/pdf). [Accessed: 22-Jul-2019].
- [14] G. Gupta, J. M. Gelfand, and J. D. Lewis, "Increased risk for demyelinating diseases in patients with inflammatory bowel disease," *Gastroenterology*, vol. 129, no. 3, pp. 819–826, Sep. 2005.
- [15] R. Dobson and G. Giovannoni, "Multiple sclerosis - a review," *Eur. J. Neurol.*, vol. 26, no. 1, pp. 27–40, 2019.
- [16] F. Brusaferrri and L. Candelise, "Steroids for multiple sclerosis and optic neuritis: a meta-analysis of randomized controlled clinical trials," *J. Neurol.*, vol. 247, no. 6, pp. 435–442, Jun. 2000.

- [17] D. Karussis and P. Petrou, "Immune reconstitution therapy (IRT) in multiple sclerosis: the rationale," *Immunol. Res.*, vol. 66, no. 6, pp. 642–648, 2018.
- [18] H. L. Weiner, "Multiple sclerosis is an inflammatory T-cell-mediated autoimmune disease," *Arch. Neurol.*, vol. 61, no. 10, pp. 1613–1615, Oct. 2004.
- [19] "The diagnosis of multiple sclerosis and the various related demyelinating syndromes: A critical review," *J. Autoimmun.*, vol. 48–49, pp. 134–142, Feb. 2014.
- [20] J. R. Oksenberg *et al.*, "Selection for T-cell receptor V beta-D beta-J beta gene rearrangements with specificity for a myelin basic protein peptide in brain lesions of multiple sclerosis," *Nature*, vol. 362, no. 6415, pp. 68–70, Mar. 1993.
- [21] J. Zhang, S. Markovic-Plese, B. Lacet, J. Raus, H. L. Weiner, and D. A. Hafler, "Increased frequency of interleukin 2-responsive T cells specific for myelin basic protein and proteolipid protein in peripheral blood and cerebrospinal fluid of patients with multiple sclerosis," *J. Exp. Med.*, vol. 179, no. 3, pp. 973–984, Mar. 1994.
- [22] C. L. Langrish *et al.*, "IL-23 drives a pathogenic T cell population that induces autoimmune inflammation," *J. Exp. Med.*, vol. 201, no. 2, pp. 233–240, Jan. 2005.
- [23] H. Kebir *et al.*, "Human TH17 lymphocytes promote blood-brain barrier disruption and central nervous system inflammation," *Nat. Med.*, vol. 13, no. 10, pp. 1173–1175, Oct. 2007.
- [24] J. S. Tzartos *et al.*, "Interleukin-17 production in central nervous system-infiltrating T cells and glial cells is associated with active disease in multiple sclerosis," *Am. J. Pathol.*, vol. 172, no. 1, pp. 146–155, Jan. 2008.
- [25] A. D. Griesemer, E. C. Sorenson, and M. A. Hardy, "The Role of the Thymus in Tolerance," *Transplantation*, vol. 90, no. 5, pp. 465–474, Sep. 2010.
- [26] C. A. Dendrou, L. Fugger, and M. A. Friese, "Immunopathology of multiple sclerosis," *Nat. Rev. Immunol.*, vol. 15, no. 9, pp. 545–558, Sep. 2015.
- [27] M. Harkiolaki *et al.*, "T cell-mediated autoimmune disease due to low-affinity crossreactivity to common microbial peptides," *Immunity*, vol. 30, no. 3, pp. 348–357, Mar. 2009.
- [28] C. Münz, J. D. Lünemann, M. T. Getts, and S. D. Miller, "Antiviral immune responses: triggers of or triggered by autoimmunity?," *Nat. Rev. Immunol.*, vol. 9, no. 4, pp. 246–258, Apr. 2009.
- [29] J. K. Olson, J. L. Croxford, M. A. Calenoff, M. C. Dal Canto, and S. D. Miller, "A virus-induced molecular mimicry model of multiple sclerosis," *J. Clin. Invest.*, vol. 108, no. 2, pp. 311–318, Jul. 2001.
- [30] R. Shechter, A. London, and M. Schwartz, "Orchestrated leukocyte recruitment to immune-privileged sites: absolute barriers versus educational gates," *Nat. Rev. Immunol.*, vol. 13, no. 3, pp. 206–218, 2013.
- [31] C. M. P. Vos *et al.*, "Blood-brain barrier alterations in both focal and diffuse abnormalities on postmortem MRI in multiple sclerosis," *Neurobiol. Dis.*, vol. 20, no. 3, pp. 953–960, Dec. 2005.
- [32] A. G. Kermodé *et al.*, "Breakdown of the blood-brain barrier precedes symptoms and other MRI signs of new lesions in multiple sclerosis. Pathogenetic and clinical implications," *Brain J. Neurol.*, vol. 113 (Pt 5), pp. 1477–1489, Oct. 1990.

- [33] C. P. Hawkins, P. M. Munro, D. N. Landon, and W. I. McDonald, "Metabolically dependent blood-brain barrier breakdown in chronic relapsing experimental allergic encephalomyelitis," *Acta Neuropathol. (Berl.)*, vol. 83, no. 6, pp. 630–635, 1992.
- [34] L. Claudio, Y. Kress, J. Factor, and C. F. Brosnan, "Mechanisms of edema formation in experimental autoimmune encephalomyelitis. The contribution of inflammatory cells," *Am. J. Pathol.*, vol. 137, no. 5, pp. 1033–1045, Nov. 1990.
- [35] G. P. A. Rice, H.-P. Hartung, and P. A. Calabresi, "Anti-alpha4 integrin therapy for multiple sclerosis: mechanisms and rationale," *Neurology*, vol. 64, no. 8, pp. 1336–1342, Apr. 2005.
- [36] R. Brandstadter and I. Katz Sand, "The use of natalizumab for multiple sclerosis," *Neuropsychiatr. Dis. Treat.*, vol. 13, pp. 1691–1702, Jun. 2017.
- [37] F. Chu *et al.*, "The roles of macrophages and microglia in multiple sclerosis and experimental autoimmune encephalomyelitis," *J. Neuroimmunol.*, vol. 318, pp. 1–7, May 2018.
- [38] A. F. Lloyd and V. E. Miron, "The pro-remyelination properties of microglia in the central nervous system," *Nat. Rev. Neurol.*, Jun. 2019.
- [39] J. Booss, M. M. Esiri, W. W. Tourtellotte, and D. Y. Mason, "Immunohistological analysis of T lymphocyte subsets in the central nervous system in chronic progressive multiple sclerosis," *J. Neurol. Sci.*, vol. 62, no. 1–3, pp. 219–232, Dec. 1983.
- [40] M. A. Friese and L. Fugger, "Autoreactive CD8+ T cells in multiple sclerosis: a new target for therapy?," *Brain J. Neurol.*, vol. 128, no. Pt 8, pp. 1747–1763, Aug. 2005.
- [41] D. Kägi *et al.*, "Fas and perforin pathways as major mechanisms of T cell-mediated cytotoxicity," *Science*, vol. 265, no. 5171, pp. 528–530, Jul. 1994.
- [42] V. Viglietta, C. Baecher-Allan, H. L. Weiner, and D. A. Hafler, "Loss of functional suppression by CD4+CD25+ regulatory T cells in patients with multiple sclerosis," *J. Exp. Med.*, vol. 199, no. 7, pp. 971–979, Apr. 2004.
- [43] B. Fritzsche *et al.*, "Intracerebral Human Regulatory T Cells: Analysis of CD4+CD25+FOXP3+ T Cells in Brain Lesions and Cerebrospinal Fluid of Multiple Sclerosis Patients," *PLoS ONE*, vol. 6, no. 3, Mar. 2011.
- [44] K. Venken *et al.*, "Compromised CD4+ CD25(high) regulatory T-cell function in patients with relapsing-remitting multiple sclerosis is correlated with a reduced frequency of FOXP3-positive cells and reduced FOXP3 expression at the single-cell level," *Immunology*, vol. 123, no. 1, pp. 79–89, Jan. 2008.
- [45] A. Tomescu-Baciu *et al.*, "Persistence of intrathecal oligoclonal B cells and IgG in multiple sclerosis," *J. Neuroimmunol.*, vol. 333, p. 576966, Aug. 2019.
- [46] L. Piccio *et al.*, "Changes in B- and T-lymphocyte and chemokine levels with rituximab treatment in multiple sclerosis," *Arch. Neurol.*, vol. 67, no. 6, pp. 707–714, Jun. 2010.
- [47] M. Sospedra, "B cells in multiple sclerosis," *Curr. Opin. Neurol.*, vol. 31, no. 3, pp. 256–262, 2018.
- [48] S. L. Hauser *et al.*, "B-cell depletion with rituximab in relapsing-remitting multiple sclerosis," *N. Engl. J. Med.*, vol. 358, no. 7, pp. 676–688, Feb. 2008.

- [49] R. Li, K. R. Patterson, and A. Bar-Or, "Reassessing B cell contributions in multiple sclerosis," *Nat. Immunol.*, vol. 19, no. 7, pp. 696–707, 2018.
- [50] N. L. Monson, P. D. Cravens, E. M. Frohman, K. Hawker, and M. K. Racke, "Effect of rituximab on the peripheral blood and cerebrospinal fluid B cells in patients with primary progressive multiple sclerosis," *Arch. Neurol.*, vol. 62, no. 2, pp. 258–264, Feb. 2005.
- [51] O. L. Rojas *et al.*, "Recirculating Intestinal IgA-Producing Cells Regulate Neuroinflammation via IL-10," *Cell*, vol. 176, no. 3, p. 610–624.e18, Jan. 2019.
- [52] M. Mohme *et al.*, "HLA-DR15-derived self-peptides are involved in increased autologous T cell proliferation in multiple sclerosis," *Brain J. Neurol.*, vol. 136, no. Pt 6, pp. 1783–1798, Jun. 2013.
- [53] I. Jelcic *et al.*, "Memory B Cells Activate Brain-Homing, Autoreactive CD4+ T Cells in Multiple Sclerosis," *Cell*, vol. 175, no. 1, p. 85–100.e23, 20 2018.
- [54] S. Naito, N. Namerow, M. R. Mickey, and P. I. Terasaki, "Multiple sclerosis: association with HL-A3," *Tissue Antigens*, vol. 2, no. 1, pp. 1–4, 1972.
- [55] C. Jersild, A. Svejgaard, and T. Fog, "HL-A antigens and multiple sclerosis," *Lancet Lond. Engl.*, vol. 1, no. 7762, pp. 1240–1241, Jun. 1972.
- [56] E. Quelvennec *et al.*, "Genetic and functional studies in multiple sclerosis patients from Martinique attest for a specific and direct role of the HLA-DR locus in the syndrome," *Tissue Antigens*, vol. 61, no. 2, pp. 166–171, Feb. 2003.
- [57] J. A. Hollenbach and J. R. Oksenberg, "The Immunogenetics of Multiple Sclerosis: A Comprehensive Review," *J. Autoimmun.*, vol. 64, pp. 13–25, Nov. 2015.
- [58] C. Cotsapas and M. Mitrovic, "Genome-wide association studies of multiple sclerosis," *Clin. Transl. Immunol.*, vol. 7, no. 6, p. e1018, 2018.
- [59] International Multiple Sclerosis Genetics Consortium *et al.*, "Risk alleles for multiple sclerosis identified by a genomewide study," *N. Engl. J. Med.*, vol. 357, no. 9, pp. 851–862, Aug. 2007.
- [60] D. Manousaki *et al.*, "Low-Frequency Synonymous Coding Variation in CYP2R1 Has Large Effects on Vitamin D Levels and Risk of Multiple Sclerosis," *Am. J. Hum. Genet.*, vol. 101, no. 2, pp. 227–238, Aug. 2017.
- [61] C. J. Willer, D. A. Dymont, N. J. Risch, A. D. Sadovnick, G. C. Ebers, and Canadian Collaborative Study Group, "Twin concordance and sibling recurrence rates in multiple sclerosis," *Proc. Natl. Acad. Sci. U. S. A.*, vol. 100, no. 22, pp. 12877–12882, Oct. 2003.
- [62] A. K. Hedström, M. Bäärnhjelm, T. Olsson, and L. Alfredsson, "Tobacco smoking, but not Swedish snuff use, increases the risk of multiple sclerosis," *Neurology*, vol. 73, no. 9, pp. 696–701, Sep. 2009.
- [63] A. J. Silman, J. Newman, and A. J. MacGregor, "Cigarette smoking increases the risk of rheumatoid arthritis. Results from a nationwide study of disease-discordant twins," *Arthritis Rheum.*, vol. 39, no. 5, pp. 732–735, May 1996.
- [64] D. S. Majka and V. M. Holers, "Cigarette smoking and the risk of systemic lupus erythematosus and rheumatoid arthritis," *Ann. Rheum. Dis.*, vol. 65, no. 5, pp. 561–563, May 2006.

- [65] A. K. Hedström, M. Bäärnhielm, T. Olsson, and L. Alfredsson, "Exposure to environmental tobacco smoke is associated with increased risk for multiple sclerosis," *Mult. Scler. Houndmills Basingstoke Engl.*, vol. 17, no. 7, pp. 788–793, Jul. 2011.
- [66] P. Heydarpour, H. Amini, S. Khoshkish, H. Seidkhani, M. A. Sahraian, and M. Yunesian, "Potential impact of air pollution on multiple sclerosis in Tehran, Iran," *Neuroepidemiology*, vol. 43, no. 3–4, pp. 233–238, 2014.
- [67] C. Barragán-Martínez, C. A. Speck-Hernández, G. Montoya-Ortiz, R. D. Mantilla, J.-M. Anaya, and A. Rojas-Villarraga, "Organic solvents as risk factor for autoimmune diseases: a systematic review and meta-analysis," *PloS One*, vol. 7, no. 12, p. e51506, 2012.
- [68] F. Odoardi *et al.*, "T cells become licensed in the lung to enter the central nervous system," *Nature*, vol. 488, no. 7413, pp. 675–679, Aug. 2012.
- [69] H. Eutamene *et al.*, "LPS-induced lung inflammation is linked to increased epithelial permeability: role of MLCK," *Eur. Respir. J.*, vol. 25, no. 5, pp. 789–796, May 2005.
- [70] E. Nizri, M. Irony-Tur-Sinai, O. Lory, A. Orr-Urtreger, E. Lavi, and T. Brenner, "Activation of the cholinergic anti-inflammatory system by nicotine attenuates neuroinflammation via suppression of Th1 and Th17 responses," *J. Immunol. Baltim. Md 1950*, vol. 183, no. 10, pp. 6681–6688, Nov. 2009.
- [71] T. Olsson, L. F. Barcellos, and L. Alfredsson, "Interactions between genetic, lifestyle and environmental risk factors for multiple sclerosis," *Nat. Rev. Neurol.*, vol. 13, no. 1, pp. 25–36, Jan. 2017.
- [72] L. Alfredsson and T. Olsson, "Lifestyle and Environmental Factors in Multiple Sclerosis," *Cold Spring Harb. Perspect. Med.*, vol. 9, no. 4, Apr. 2019.
- [73] S. Alotaibi, J. Kennedy, R. Tellier, D. Stephens, and B. Banwell, "Epstein-Barr virus in pediatric multiple sclerosis," *JAMA*, vol. 291, no. 15, pp. 1875–1879, Apr. 2004.
- [74] D. Pohl *et al.*, "High seroprevalence of Epstein-Barr virus in children with multiple sclerosis," *Neurology*, vol. 67, no. 11, pp. 2063–2065, Dec. 2006.
- [75] M. K. Smatti, D. W. Al-Sadeq, N. H. Ali, G. Pintus, H. Abou-Saleh, and G. K. Nasrallah, "Epstein-Barr Virus Epidemiology, Serology, and Genetic Variability of LMP-1 Oncogene Among Healthy Population: An Update," *Front. Oncol.*, vol. 8, Jun. 2018.
- [76] M. P. Pender and S. R. Burrows, "Epstein-Barr virus and multiple sclerosis: potential opportunities for immunotherapy," *Clin. Transl. Immunol.*, vol. 3, no. 10, p. e27, Oct. 2014.
- [77] J. D. Lünemann *et al.*, "EBNA1-specific T cells from patients with multiple sclerosis cross react with myelin antigens and co-produce IFN-gamma and IL-2," *J. Exp. Med.*, vol. 205, no. 8, pp. 1763–1773, Aug. 2008.
- [78] K. W. Wucherpfennig and J. L. Strominger, "Molecular mimicry in T cell-mediated autoimmunity: viral peptides activate human T cell clones specific for myelin basic protein," *Cell*, vol. 80, no. 5, pp. 695–705, Mar. 1995.
- [79] T. Holmøy, E. Ø. Kvale, and F. Vartdal, "Cerebrospinal fluid CD4+ T cells from a multiple sclerosis patient cross-recognize Epstein-Barr virus and myelin basic protein," *J. Neurovirol.*, vol. 10, no. 5, pp. 278–283, Oct. 2004.

- [80] J. D. Lünemann, T. Kamradt, R. Martin, and C. Münz, "Epstein-barr virus: environmental trigger of multiple sclerosis?," *J. Virol.*, vol. 81, no. 13, pp. 6777–6784, Jul. 2007.
- [81] M. K. Axthelm *et al.*, "Japanese macaque encephalomyelitis: a spontaneous multiple sclerosis-like disease in a nonhuman primate," *Ann. Neurol.*, vol. 70, no. 3, pp. 362–373, Sep. 2011.
- [82] V. Pantazou, M. Schlupe, and R. Du Pasquier, "Environmental factors in multiple sclerosis," *Presse Medicale Paris Fr. 1983*, vol. 44, no. 4 Pt 2, pp. e113-120, Apr. 2015.
- [83] S. Simpson, W. Wang, P. Otahal, L. Blizzard, I. A. F. van der Mei, and B. V. Taylor, "Latitude continues to be significantly associated with the prevalence of multiple sclerosis: an updated meta-analysis," *J. Neurol. Neurosurg. Psychiatry*, Jun. 2019.
- [84] N. Koch-Henriksen and P. S. Sørensen, "The changing demographic pattern of multiple sclerosis epidemiology," *Lancet Neurol.*, vol. 9, no. 5, pp. 520–532, May 2010.
- [85] R. M. Lucas, S. N. Byrne, J. Correale, S. Ilschner, and P. H. Hart, "Ultraviolet radiation, vitamin D and multiple sclerosis," *Neurodegener. Dis. Manag.*, vol. 5, no. 5, pp. 413–424, Oct. 2015.
- [86] K. L. Munger *et al.*, "Vitamin D intake and incidence of multiple sclerosis," *Neurology*, vol. 62, no. 1, pp. 60–65, Jan. 2004.
- [87] I. A. van der Mei, A. L. Ponsonby, L. Blizzard, and T. Dwyer, "Regional variation in multiple sclerosis prevalence in Australia and its association with ambient ultraviolet radiation," *Neuroepidemiology*, vol. 20, no. 3, pp. 168–174, Aug. 2001.
- [88] M. B. Sintzel, M. Rametta, and A. T. Reder, "Vitamin D and Multiple Sclerosis: A Comprehensive Review," *Neurol. Ther.*, vol. 7, no. 1, pp. 59–85, Jun. 2018.
- [89] K. L. Munger, L. I. Levin, B. W. Hollis, N. S. Howard, and A. Ascherio, "Serum 25-hydroxyvitamin D levels and risk of multiple sclerosis," *JAMA*, vol. 296, no. 23, pp. 2832–2838, Dec. 2006.
- [90] C. M. Veldman, M. T. Cantorna, and H. F. DeLuca, "Expression of 1,25-dihydroxyvitamin D(3) receptor in the immune system," *Arch. Biochem. Biophys.*, vol. 374, no. 2, pp. 334–338, Feb. 2000.
- [91] L. Overbergh *et al.*, "1 α ,25-dihydroxyvitamin D₃ induces an autoantigen-specific T-helper 1/T-helper 2 immune shift in NOD mice immunized with GAD65 (p524-543)," *Diabetes*, vol. 49, no. 8, pp. 1301–1307, Aug. 2000.
- [92] S. Chen, G. P. Sims, X. X. Chen, Y. Y. Gu, S. Chen, and P. E. Lipsky, "Modulatory effects of 1,25-dihydroxyvitamin D₃ on human B cell differentiation," *J. Immunol. Baltim. Md 1950*, vol. 179, no. 3, pp. 1634–1647, Aug. 2007.
- [93] L. Adorini, "Tolerogenic dendritic cells induced by vitamin D receptor ligands enhance regulatory T cells inhibiting autoimmune diabetes," *Ann. N. Y. Acad. Sci.*, vol. 987, pp. 258–261, Apr. 2003.
- [94] M. T. Cantorna, C. E. Hayes, and H. F. DeLuca, "1,25-Dihydroxyvitamin D₃ reversibly blocks the progression of relapsing encephalomyelitis, a model of multiple sclerosis," *Proc. Natl. Acad. Sci. U. S. A.*, vol. 93, no. 15, pp. 7861–7864, Jul. 1996.
- [95] J. M. Lemire and D. C. Archer, "1,25-dihydroxyvitamin D₃ prevents the in vivo induction of murine experimental autoimmune encephalomyelitis," *J. Clin. Invest.*, vol. 87, no. 3, pp. 1103–1107, Mar. 1991.

- [96] H. F. DeLuca and L. A. Plum, "Vitamin D deficiency diminishes the severity and delays onset of experimental autoimmune encephalomyelitis," *Arch. Biochem. Biophys.*, vol. 513, no. 2, pp. 140–143, Sep. 2011.
- [97] Y. Wang, S. J. Marling, J. G. Zhu, K. S. Severson, and H. F. DeLuca, "Development of experimental autoimmune encephalomyelitis (EAE) in mice requires vitamin D and the vitamin D receptor," *Proc. Natl. Acad. Sci. U. S. A.*, vol. 109, no. 22, pp. 8501–8504, May 2012.
- [98] B. Ahluwalia, M. K. Magnusson, and L. Öhman, "Mucosal immune system of the gastrointestinal tract: maintaining balance between the good and the bad," *Scand. J. Gastroenterol.*, vol. 52, no. 11, pp. 1185–1193, Nov. 2017.
- [99] K. L. Mason, G. B. Huffnagle, M. C. Noverr, and J. Y. Kao, "Overview of gut immunology," *Adv. Exp. Med. Biol.*, vol. 635, pp. 1–14, 2008.
- [100] P. Brandtzaeg, H. Kiyono, R. Pabst, and M. W. Russell, "Terminology: nomenclature of mucosa-associated lymphoid tissue," *Mucosal Immunol.*, vol. 1, no. 1, pp. 31–37, Jan. 2008.
- [101] B. K. Wershil and G. T. Furuta, "4. Gastrointestinal mucosal immunity," *J. Allergy Clin. Immunol.*, vol. 121, no. 2 Suppl, p. S380–383; quiz S415, Feb. 2008.
- [102] A. J. Macpherson and K. Smith, "Mesenteric lymph nodes at the center of immune anatomy," *J. Exp. Med.*, vol. 203, no. 3, pp. 497–500, Mar. 2006.
- [103] M. Buettner and M. Lochner, "Development and Function of Secondary and Tertiary Lymphoid Organs in the Small Intestine and the Colon," *Front. Immunol.*, vol. 7, Sep. 2016.
- [104] A. M. Mowat, "Anatomical basis of tolerance and immunity to intestinal antigens," *Nat. Rev. Immunol.*, vol. 3, no. 4, pp. 331–341, Apr. 2003.
- [105] N. Y. Lycke and M. Bemark, "The role of Peyer's patches in synchronizing gut IgA responses," *Front. Immunol.*, vol. 3, p. 329, 2012.
- [106] M. Buettner and U. Bode, "Lymph node dissection--understanding the immunological function of lymph nodes," *Clin. Exp. Immunol.*, vol. 169, no. 3, pp. 205–212, Sep. 2012.
- [107] H. Hamada *et al.*, "Identification of multiple isolated lymphoid follicles on the antimesenteric wall of the mouse small intestine," *J. Immunol. Baltim. Md 1950*, vol. 168, no. 1, pp. 57–64, Jan. 2002.
- [108] L. W. Peterson and D. Artis, "Intestinal epithelial cells: regulators of barrier function and immune homeostasis," *Nat. Rev. Immunol.*, vol. 14, no. 3, pp. 141–153, Mar. 2014.
- [109] H. Cheroutre, F. Lambomez, and D. Mucida, "The light and dark sides of intestinal intraepithelial lymphocytes," *Nat. Rev. Immunol.*, vol. 11, no. 7, pp. 445–456, Jun. 2011.
- [110] P. Poussier, T. Ning, D. Banerjee, and M. Julius, "A unique subset of self-specific intrainestinal T cells maintains gut integrity," *J. Exp. Med.*, vol. 195, no. 11, pp. 1491–1497, Jun. 2002.
- [111] R.-Q. Wu, D.-F. Zhang, E. Tu, Q.-M. Chen, and W. Chen, "The mucosal immune system in the oral cavity-an orchestra of T cell diversity," *Int. J. Oral Sci.*, vol. 6, no. 3, pp. 125–132, Sep. 2014.
- [112] C. Nicoletti, M. Regoli, and E. Bertelli, "Dendritic cells in the gut: to sample and to exclude?," *Mucosal Immunol.*, vol. 2, no. 5, p. 462, Sep. 2009.

- [113] D. Rios, M. B. Wood, J. Li, B. Chassaing, A. T. Gewirtz, and I. R. Williams, "Antigen sampling by intestinal M cells is the principal pathway initiating mucosal IgA production to commensal enteric bacteria," *Mucosal Immunol.*, vol. 9, no. 4, pp. 907–916, 2016.
- [114] A. Cerutti, "The regulation of IgA class switching," *Nat. Rev. Immunol.*, vol. 8, no. 6, pp. 421–434, Jun. 2008.
- [115] A. Mathias, B. Pais, L. Favre, J. Benyacoub, and B. Corthésy, "Role of secretory IgA in the mucosal sensing of commensal bacteria," *Gut Microbes*, vol. 5, no. 6, pp. 688–695, 2014.
- [116] R. Sender, S. Fuchs, and R. Milo, "Revised Estimates for the Number of Human and Bacteria Cells in the Body," *PLoS Biol.*, vol. 14, no. 8, Aug. 2016.
- [117] P. Hugon, J.-C. Dufour, P. Colson, P.-E. Fournier, K. Sallah, and D. Raoult, "A comprehensive repertoire of prokaryotic species identified in human beings," *Lancet Infect. Dis.*, vol. 15, no. 10, pp. 1211–1219, Oct. 2015.
- [118] N. Kamada, S.-U. Seo, G. Y. Chen, and G. Núñez, "Role of the gut microbiota in immunity and inflammatory disease," *Nat. Rev. Immunol.*, vol. 13, no. 5, pp. 321–335, May 2013.
- [119] I. I. Ivanov *et al.*, "Specific microbiota direct the differentiation of IL-17-producing T-helper cells in the mucosa of the small intestine," *Cell Host Microbe*, vol. 4, no. 4, pp. 337–349, Oct. 2008.
- [120] I. I. Ivanov *et al.*, "Induction of intestinal Th17 cells by segmented filamentous bacteria," *Cell*, vol. 139, no. 3, pp. 485–498, Oct. 2009.
- [121] S. Jangi *et al.*, "Alterations of the human gut microbiome in multiple sclerosis," *Nat. Commun.*, vol. 7, p. 12015, 28 2016.
- [122] S. Miyake *et al.*, "Dysbiosis in the Gut Microbiota of Patients with Multiple Sclerosis, with a Striking Depletion of Species Belonging to Clostridia XIVa and IV Clusters," *PLoS One*, vol. 10, no. 9, p. e0137429, 2015.
- [123] J. Chen *et al.*, "Multiple sclerosis patients have a distinct gut microbiota compared to healthy controls," *Sci. Rep.*, vol. 6, p. 28484, 27 2016.
- [124] I. Cosorich *et al.*, "High frequency of intestinal TH17 cells correlates with microbiota alterations and disease activity in multiple sclerosis," *Sci. Adv.*, vol. 3, no. 7, Jul. 2017.
- [125] E. Esplugues *et al.*, "Control of TH17 cells occurs in the small intestine," *Nature*, vol. 475, no. 7357, pp. 514–518, Jul. 2011.
- [126] K. Berer *et al.*, "Commensal microbiota and myelin autoantigen cooperate to trigger autoimmune demyelination," *Nature*, vol. 479, no. 7374, pp. 538–541, Nov. 2011.
- [127] A. K. Mangalam and J. Murray, "Microbial monotherapy with *Prevotella histicola* for patients with multiple sclerosis," *Expert Rev. Neurother.*, vol. 19, no. 1, pp. 45–53, Jan. 2019.
- [128] S. K. Tankou *et al.*, "A probiotic modulates the microbiome and immunity in multiple sclerosis," *Ann. Neurol.*, vol. 83, no. 6, pp. 1147–1161, Jun. 2018.
- [129] W. J. van den Hoogen, J. D. Laman, and B. A. 't Hart, "Modulation of Multiple Sclerosis and Its Animal Model Experimental Autoimmune Encephalomyelitis by Food and Gut Microbiota," *Front. Immunol.*, vol. 8, Sep. 2017.

- [130] Y. K. Lee, J. S. Menezes, Y. Umesaki, and S. K. Mazmanian, "Proinflammatory T-cell responses to gut microbiota promote experimental autoimmune encephalomyelitis," *Proc. Natl. Acad. Sci. U. S. A.*, vol. 108 Suppl 1, pp. 4615–4622, Mar. 2011.
- [131] E. Cekanaviciute *et al.*, "Gut bacteria from multiple sclerosis patients modulate human T cells and exacerbate symptoms in mouse models," *Proc. Natl. Acad. Sci. U. S. A.*, vol. 114, no. 40, pp. 10713–10718, 03 2017.
- [132] K. Berer *et al.*, "Gut microbiota from multiple sclerosis patients enables spontaneous autoimmune encephalomyelitis in mice," *Proc. Natl. Acad. Sci. U. S. A.*, vol. 114, no. 40, pp. 10719–10724, 03 2017.
- [133] S. K. Yadav *et al.*, "Gut dysbiosis breaks immunological tolerance toward the central nervous system during young adulthood," *Proc. Natl. Acad. Sci. U. S. A.*, vol. 114, no. 44, pp. E9318–E9327, Oct. 2017.
- [134] M. C. Buscarinu *et al.*, "Intestinal Permeability in Relapsing-Remitting Multiple Sclerosis," *Neurother. J. Am. Soc. Exp. Neurother.*, vol. 15, no. 1, pp. 68–74, 2018.
- [135] M. Nouri, A. Bredberg, B. Weström, and S. Lavasani, "Intestinal barrier dysfunction develops at the onset of experimental autoimmune encephalomyelitis, and can be induced by adoptive transfer of auto-reactive T cells," *PLoS One*, vol. 9, no. 9, p. e106335, 2014.
- [136] S. Jörg *et al.*, "High salt drives Th17 responses in experimental autoimmune encephalomyelitis without impacting myeloid dendritic cells," *Exp. Neurol.*, vol. 279, pp. 212–222, May 2016.
- [137] D. N. Krementsov, L. K. Case, W. F. Hickey, and C. Teuscher, "Exacerbation of autoimmune neuroinflammation by dietary sodium is genetically controlled and sex specific," *FASEB J. Off. Publ. Fed. Am. Soc. Exp. Biol.*, vol. 29, no. 8, pp. 3446–3457, Aug. 2015.
- [138] C. Wu *et al.*, "Induction of pathogenic TH17 cells by inducible salt-sensing kinase SGK1," *Nature*, vol. 496, no. 7446, pp. 513–517, Apr. 2013.
- [139] M. Kleinewietfeld *et al.*, "Sodium chloride drives autoimmune disease by the induction of pathogenic TH17 cells," *Nature*, vol. 496, no. 7446, pp. 518–522, Apr. 2013.
- [140] J. McDonald *et al.*, "A case-control study of dietary salt intake in pediatric-onset multiple sclerosis," *Mult. Scler. Relat. Disord.*, vol. 6, pp. 87–92, Mar. 2016.
- [141] B. Nourbakhsh *et al.*, "Dietary salt intake and time to relapse in paediatric multiple sclerosis," *J. Neurol. Neurosurg. Psychiatry*, vol. 87, no. 12, pp. 1350–1353, 2016.
- [142] K. C. Fitzgerald *et al.*, "Sodium intake and multiple sclerosis activity and progression in BENEFIT," *Ann. Neurol.*, vol. 82, no. 1, pp. 20–29, Jul. 2017.
- [143] I. Katz Sand, "The Role of Diet in Multiple Sclerosis: Mechanistic Connections and Current Evidence," *Curr. Nutr. Rep.*, vol. 7, no. 3, pp. 150–160, 2018.
- [144] A. Langer-Gould, S. M. Brara, B. E. Beaber, and C. Koebnick, "Childhood obesity and risk of pediatric multiple sclerosis and clinically isolated syndrome," *Neurology*, vol. 80, no. 6, pp. 548–552, Feb. 2013.
- [145] K. L. Munger *et al.*, "Childhood body mass index and multiple sclerosis risk: a long-term cohort study," *Mult. Scler. Houndmills Basingstoke Engl.*, vol. 19, no. 10, pp. 1323–1329, Sep. 2013.

- [146] A. K. Hedström, T. Olsson, and L. Alfredsson, "High body mass index before age 20 is associated with increased risk for multiple sclerosis in both men and women," *Mult. Scler. Houndmills Basingstoke Engl.*, vol. 18, no. 9, pp. 1334–1336, Sep. 2012.
- [147] K. L. Munger, T. Chitnis, and A. Ascherio, "Body size and risk of MS in two cohorts of US women," *Neurology*, vol. 73, no. 19, pp. 1543–1550, Nov. 2009.
- [148] F. Giubilei *et al.*, "Blood cholesterol and MRI activity in first clinical episode suggestive of multiple sclerosis," *Acta Neurol. Scand.*, vol. 106, no. 2, pp. 109–112, Aug. 2002.
- [149] P. Tettey *et al.*, "An adverse lipid profile is associated with disability and progression in disability, in people with MS," *Mult. Scler. Houndmills Basingstoke Engl.*, vol. 20, no. 13, pp. 1737–1744, Nov. 2014.
- [150] B. Weinstock-Guttman *et al.*, "Lipid profiles are associated with lesion formation over 24 months in interferon- β treated patients following the first demyelinating event," *J. Neurol. Neurosurg. Psychiatry*, vol. 84, no. 11, pp. 1186–1191, Nov. 2013.
- [151] B. Weinstock-Guttman *et al.*, "Serum lipid profiles are associated with disability and MRI outcomes in multiple sclerosis," *J. Neuroinflammation*, vol. 8, p. 127, Oct. 2011.
- [152] M. Stampanoni Bassi *et al.*, "Obesity worsens central inflammation and disability in multiple sclerosis," *Mult. Scler. Houndmills Basingstoke Engl.*, p. 1352458519853473, Jun. 2019.
- [153] S. Winer *et al.*, "Obesity predisposes to Th17 bias," *Eur. J. Immunol.*, vol. 39, no. 9, pp. 2629–2635, Sep. 2009.
- [154] S. Timmermans *et al.*, "High Fat Diet Exacerbates Neuroinflammation in an Animal Model of Multiple Sclerosis by Activation of the Renin Angiotensin System," *J. Neuroimmune Pharmacol.*, vol. 9, no. 2, pp. 209–217, Mar. 2014.
- [155] M. Ďurfinová *et al.*, "Cholesterol level correlate with disability score in patients with relapsing-remitting form of multiple sclerosis," *Neurosci. Lett.*, vol. 687, pp. 304–307, 20 2018.
- [156] S. Markovic-Plese, A. K. Singh, and I. Singh, "Therapeutic potential of statins in multiple sclerosis: immune modulation, neuroprotection and neurorepair," *Future Neurol.*, vol. 3, no. 2, pp. 153–167, Mar. 2008.
- [157] C. Olivieri and C. T. Baldari, "Statins: from cholesterol-lowering drugs to novel immunomodulators for the treatment of Th17-mediated autoimmune diseases," *Pharmacol. Res.*, vol. 88, pp. 41–52, Oct. 2014.
- [158] M. Hasan, J.-E. Seo, K. A. Rahaman, M.-J. Kang, B.-H. Jung, and O.-S. Kwon, "Increased levels of brain serotonin correlated with MMP-9 activity and IL-4 levels resulted in severe experimental autoimmune encephalomyelitis (EAE) in obese mice," *Neuroscience*, vol. 319, pp. 168–182, Apr. 2016.
- [159] J. Mailleux *et al.*, "Low-Density Lipoprotein Receptor Deficiency Attenuates Neuroinflammation through the Induction of Apolipoprotein E," *Front. Immunol.*, vol. 8, Nov. 2017.
- [160] S. A. Berghoff *et al.*, "Dietary cholesterol promotes repair of demyelinated lesions in the adult brain," *Nat. Commun.*, vol. 8, p. 14241, Jan. 2017.

- [161] I. Lavrnja *et al.*, "Expression profiles of cholesterol metabolism-related genes are altered during development of experimental autoimmune encephalomyelitis in the rat spinal cord," *Sci. Rep.*, vol. 7, Jun. 2017.
- [162] O. Guillemot-Legrís, V. Mutemberezi, P. D. Cani, and G. G. Muccioli, "Obesity is associated with changes in oxysterol metabolism and levels in mice liver, hypothalamus, adipose tissue and plasma," *Sci. Rep.*, vol. 6, no. 1, Apr. 2016.
- [163] B. N. Olsen, P. H. Schlesinger, D. S. Ory, and N. A. Baker, "25-Hydroxycholesterol increases the availability of cholesterol in phospholipid membranes," *Biophys. J.*, vol. 100, no. 4, pp. 948–956, Feb. 2011.
- [164] J. Grouleff, S. J. Irudayam, K. K. Skeby, and B. Schiøtt, "The influence of cholesterol on membrane protein structure, function, and dynamics studied by molecular dynamics simulations," *Biochim. Biophys. Acta*, vol. 1848, no. 9, pp. 1783–1795, Sep. 2015.
- [165] A. A. Kandutsch and H. W. Chen, "Inhibition of sterol synthesis in cultured mouse cells by cholesterol derivatives oxygenated in the side chain," *J. Biol. Chem.*, vol. 249, no. 19, pp. 6057–6061, Oct. 1974.
- [166] V. Mutemberezi, O. Guillemot-Legrís, and G. G. Muccioli, "Oxysterols: From cholesterol metabolites to key mediators," *Prog. Lipid Res.*, vol. 64, pp. 152–169, Oct. 2016.
- [167] O. Guillemot-Legrís, V. Mutemberezi, and G. G. Muccioli, "Oxysterols in Metabolic Syndrome: From Bystander Molecules to Bioactive Lipids," *Trends Mol. Med.*, vol. 22, no. 7, pp. 594–614, 2016.
- [168] L. Ma and E. R. Nelson, "Oxysterols and nuclear receptors," *Mol. Cell. Endocrinol.*, vol. 484, pp. 42–51, 15 2019.
- [169] A. Venkateswaran *et al.*, "Control of cellular cholesterol efflux by the nuclear oxysterol receptor LXR alpha," *Proc. Natl. Acad. Sci. U. S. A.*, vol. 97, no. 22, pp. 12097–12102, Oct. 2000.
- [170] A. Reboldi and E. Dang, "Cholesterol metabolism in innate and adaptive response," *F1000Research*, vol. 7, 2018.
- [171] B. A. Janowski *et al.*, "Structural requirements of ligands for the oxysterol liver X receptors LXRalpha and LXRbeta," *Proc. Natl. Acad. Sci. U. S. A.*, vol. 96, no. 1, pp. 266–271, Jan. 1999.
- [172] J. H. Lee *et al.*, "Differential SUMOylation of LXRalpha and LXRbeta mediates transrepression of STAT1 inflammatory signaling in IFN-gamma-stimulated brain astrocytes," *Mol. Cell*, vol. 35, no. 6, pp. 806–817, Sep. 2009.
- [173] C. Traversari, S. Sozzani, K. R. Steffensen, and V. Russo, "LXR-dependent and -independent effects of oxysterols on immunity and tumor growth," *Eur. J. Immunol.*, vol. 44, no. 7, pp. 1896–1903, Jul. 2014.
- [174] V. M. Olkkonen, O. Béaslas, and E. Nissilä, "Oxysterols and their cellular effectors," *Biomolecules*, vol. 2, no. 1, pp. 76–103, Feb. 2012.
- [175] S. B. Joseph *et al.*, "LXR-dependent gene expression is important for macrophage survival and the innate immune response," *Cell*, vol. 119, no. 2, pp. 299–309, Oct. 2004.
- [176] J. Matalonga *et al.*, "The Nuclear Receptor LXR Limits Bacterial Infection of Host Macrophages through a Mechanism that Impacts Cellular NAD Metabolism," *Cell Rep.*, vol. 18, no. 5, pp. 1241–1255, 31 2017.

- [177] S. J. Bensinger *et al.*, "LXR signaling couples sterol metabolism to proliferation in the acquired immune response," *Cell*, vol. 134, no. 1, pp. 97–111, Jul. 2008.
- [178] R. Geyeregger *et al.*, "Liver X receptors interfere with cytokine-induced proliferation and cell survival in normal and leukemic lymphocytes," *J. Leukoc. Biol.*, vol. 86, no. 5, pp. 1039–1048, Nov. 2009.
- [179] G. Cui *et al.*, "Liver X receptor (LXR) mediates negative regulation of mouse and human Th17 differentiation," *J. Clin. Invest.*, vol. 121, no. 2, pp. 658–670, Feb. 2011.
- [180] S. Vigne *et al.*, "IL-27-Induced Type 1 Regulatory T-Cells Produce Oxysterols that Constrain IL-10 Production," *Front. Immunol.*, vol. 8, p. 1184, 2017.
- [181] V. Giguère, M. Tini, G. Flock, E. Ong, R. M. Evans, and G. Otulakowski, "Isoform-specific amino-terminal domains dictate DNA-binding properties of ROR alpha, a novel family of orphan hormone nuclear receptors," *Genes Dev.*, vol. 8, no. 5, pp. 538–553, Mar. 1994.
- [182] Y. Wang *et al.*, "Modulation of retinoic acid receptor-related orphan receptor alpha and gamma activity by 7-oxygenated sterol ligands," *J. Biol. Chem.*, vol. 285, no. 7, pp. 5013–5025, Feb. 2010.
- [183] A. M. Jetten, "Retinoid-related orphan receptors (RORs): critical roles in development, immunity, circadian rhythm, and cellular metabolism," *Nucl. Recept. Signal.*, vol. 7, Apr. 2009.
- [184] I. I. Ivanov *et al.*, "The orphan nuclear receptor RORgammat directs the differentiation program of proinflammatory IL-17+ T helper cells," *Cell*, vol. 126, no. 6, pp. 1121–1133, Sep. 2006.
- [185] L. A. Solt and T. P. Burris, "Action of RORs and Their Ligands in (Patho)physiology," *Trends Endocrinol. Metab. TEM*, vol. 23, no. 12, pp. 619–627, Dec. 2012.
- [186] M. Birkenbach, K. Josefsen, R. Yalamanchili, G. Lenoir, and E. Kieff, "Epstein-Barr virus-induced genes: first lymphocyte-specific G protein-coupled peptide receptors," *J. Virol.*, vol. 67, no. 4, pp. 2209–2220, Apr. 1993.
- [187] S. Hannedouche *et al.*, "Oxysterols direct immune cell migration via EBI2," *Nature*, vol. 475, no. 7357, pp. 524–527, Jul. 2011.
- [188] T. Yi *et al.*, "Oxysterol gradient generation by lymphoid stromal cells guides activated B cell movement during humoral responses," *Immunity*, vol. 37, no. 3, pp. 535–548, Sep. 2012.
- [189] A. P. Baptista *et al.*, "The Chemoattractant Receptor Ebi2 Drives Intranodal Naive CD4+ T Cell Peripheralization to Promote Effective Adaptive Immunity," *Immunity*, vol. 50, no. 5, p. 1188–1201.e6, May 2019.
- [190] T. Willinger, "Oxysterols in intestinal immunity and inflammation," *J. Intern. Med.*, vol. 285, no. 4, pp. 367–380, Apr. 2019.
- [191] S. Mukhopadhyay *et al.*, "Interdependence of Oxysterols with Cholesterol Profiles in Multiple Sclerosis," *Mult. Scler. Houndmills Basingstoke Engl.*, vol. 23, no. 6, pp. 792–801, May 2017.
- [192] K. Fellows Maxwell *et al.*, "Oxysterols and apolipoproteins in multiple sclerosis: a 5 year follow-up study," *J. Lipid Res.*, vol. 60, no. 7, pp. 1190–1198, Jul. 2019.

- [193] V. Mutemberezi, B. Buisseret, J. Masquelier, O. Guillemot-Legris, M. Alhouayek, and G. G. Muccioli, "Oxysterol levels and metabolism in the course of neuroinflammation: insights from in vitro and in vivo models," *J. Neuroinflammation*, vol. 15, no. 1, p. 74, Mar. 2018.
- [194] A. L. Forwell *et al.*, "Analysis of CH25H in multiple sclerosis and neuromyelitis optica," *J. Neuroimmunol.*, vol. 291, pp. 70–72, Feb. 2016.
- [195] F. Chalmin *et al.*, "Oxysterols regulate encephalitogenic CD4(+) T cell trafficking during central nervous system autoimmunity," *J. Autoimmun.*, vol. 56, pp. 45–55, Jan. 2015.
- [196] J. Chun and H.-P. Hartung, "Mechanism of Action of Oral Fingolimod (FTY720) in Multiple Sclerosis," *Clin. Neuropharmacol.*, vol. 33, no. 2, pp. 91–101, 2010.
- [197] D. R. Bauman, A. D. Bitmansour, J. G. McDonald, B. M. Thompson, G. Liang, and D. W. Russell, "25-Hydroxycholesterol secreted by macrophages in response to Toll-like receptor activation suppresses immunoglobulin A production," *Proc. Natl. Acad. Sci.*, vol. 106, no. 39, pp. 16764–16769, Sep. 2009.
- [198] S. Fagarasan, "Critical Roles of Activation-Induced Cytidine Deaminase in the Homeostasis of Gut Flora," *Science*, vol. 298, no. 5597, pp. 1424–1427, Nov. 2002.
- [199] A. S. Clottu *et al.*, "EBI2 Expression and Function: Robust in Memory Lymphocytes and Increased by Natalizumab in Multiple Sclerosis," *Cell Rep.*, vol. 18, no. 1, pp. 213–224, 03 2017.
- [200] F. Wanke *et al.*, "EBI2 Is Highly Expressed in Multiple Sclerosis Lesions and Promotes Early CNS Migration of Encephalitogenic CD4 T Cells," *Cell Rep.*, vol. 18, no. 5, pp. 1270–1284, 31 2017.
- [201] O. Guillemot-Legris *et al.*, "Colitis Alters Oxysterol Metabolism and is Affected by 4 β -Hydroxycholesterol Administration," *J. Crohns Colitis*, vol. 13, no. 2, pp. 218–229, Feb. 2019.
- [202] A. Wyss *et al.*, "The EBI2-oxysterol axis promotes the development of intestinal lymphoid structures and colitis," *Mucosal Immunol.*, vol. 12, no. 3, pp. 733–745, 2019.
- [203] J. Emgård *et al.*, "Oxysterol Sensing through the Receptor GPR183 Promotes the Lymphoid-Tissue-Inducing Function of Innate Lymphoid Cells and Colonic Inflammation," *Immunity*, vol. 48, no. 1, p. 120–132.e8, 16 2018.
- [204] C. Chu *et al.*, "Anti-microbial Functions of Group 3 Innate Lymphoid Cells in Gut-Associated Lymphoid Tissues Are Regulated by G-Protein-Coupled Receptor 183," *Cell Rep.*, vol. 23, no. 13, pp. 3750–3758, Jun. 2018.
- [205] N. Bouladoux, O. J. Harrison, and Y. Belkaid, "The mouse model of infection with *Citrobacter rodentium*," *Curr. Protoc. Immunol.*, vol. 119, p. 19.15.1-19.15.25, Nov. 2017.
- [206] A. Jager, V. Dardalhon, R. A. Sobel, E. Bettelli, and V. K. Kuchroo, "Th1, Th17, and Th9 Effector Cells Induce Experimental Autoimmune Encephalomyelitis with Different Pathological Phenotypes," *J. Immunol.*, vol. 183, no. 11, pp. 7169–7177, Dec. 2009.
- [207] A. Peters, K. D. Fowler, F. Chalmin, D. Merkler, V. K. Kuchroo, and C. Pot, "IL-27 Induces Th17 Differentiation in the Absence of STAT1 Signaling," *J Immunol*, vol. 195, no. 9, pp. 4144–53, Nov. 2015.
- [208] M. M. Zaiss *et al.*, "The Intestinal Microbiota Contributes to the Ability of Helminths to Modulate Allergic Inflammation," *Immunity*, vol. 43, no. 5, pp. 998–1010, Nov. 2015.

- [209] J. Bernier-Latmani and T. V. Petrova, "High-resolution 3D analysis of mouse small-intestinal stroma," *Nat. Protoc.*, vol. 11, no. 9, pp. 1617–1629, 2016.
- [210] B. Yang *et al.*, "Single-cell phenotyping within transparent intact tissue through whole-body clearing," *Cell*, vol. 158, no. 4, pp. 945–958, Aug. 2014.
- [211] S. Bouillaguet *et al.*, "Root Microbiota in Primary and Secondary Apical Periodontitis," *Front. Microbiol.*, vol. 9, p. 2374, 2018.
- [212] V. Lazarevic, N. Gaia, M. Girard, and J. Schrenzel, "Decontamination of 16S rRNA gene amplicon sequence datasets based on bacterial load assessment by qPCR," *BMC Microbiol.*, vol. 16, p. 73, Apr. 2016.
- [213] P. D. Schloss *et al.*, "Introducing mothur: open-source, platform-independent, community-supported software for describing and comparing microbial communities," *Appl. Environ. Microbiol.*, vol. 75, no. 23, pp. 7537–7541, Dec. 2009.
- [214] S.-H. Yoon *et al.*, "Introducing EzBioCloud: a taxonomically united database of 16S rRNA gene sequences and whole-genome assemblies," *Int. J. Syst. Evol. Microbiol.*, vol. 67, no. 5, pp. 1613–1617, May 2017.
- [215] J. Zhang, K. Kobert, T. Flouri, and A. Stamatakis, "PEAR: a fast and accurate Illumina Paired-End reAd mergeR," *Bioinforma. Oxf. Engl.*, vol. 30, no. 5, pp. 614–620, Mar. 2014.
- [216] R. C. Edgar, "Search and clustering orders of magnitude faster than BLAST," *Bioinforma. Oxf. Engl.*, vol. 26, no. 19, pp. 2460–2461, Oct. 2010.
- [217] K. A. Papadakis and S. R. Targan, "Role of cytokines in the pathogenesis of inflammatory bowel disease," *Annu. Rev. Med.*, vol. 51, pp. 289–298, 2000.
- [218] T. Korn, E. Bettelli, M. Oukka, and V. K. Kuchroo, "IL-17 and Th17 Cells," *Annu. Rev. Immunol.*, vol. 27, pp. 485–517, 2009.
- [219] M. P. Mycko, M. Cichalewska, H. Cwiklinska, and K. W. Selmaj, "miR-155-3p Drives the Development of Autoimmune Demyelination by Regulation of Heat Shock Protein 40," *J. Neurosci. Off. J. Soc. Neurosci.*, vol. 35, no. 50, pp. 16504–16515, Dec. 2015.
- [220] A. Flügel *et al.*, "Migratory activity and functional changes of green fluorescent effector cells before and during experimental autoimmune encephalomyelitis," *Immunity*, vol. 14, no. 5, pp. 547–560, May 2001.
- [221] M. Kanayama, K. Danzaki, Y.-W. He, and M. L. Shinohara, "Lung inflammation stalls Th17-cell migration en route to the central nervous system during the development of experimental autoimmune encephalomyelitis," *Int. Immunol.*, vol. 28, no. 9, pp. 463–469, 2016.
- [222] J. Bernier-Latmani and T. V. Petrova, "Intestinal lymphatic vasculature: structure, mechanisms and functions," *Nat. Rev. Gastroenterol. Hepatol.*, vol. 14, no. 9, pp. 510–526, Sep. 2017.
- [223] E. Bettelli, M. Pagany, H. L. Weiner, C. Lington, R. A. Sobel, and V. K. Kuchroo, "Myelin oligodendrocyte glycoprotein-specific T cell receptor transgenic mice develop spontaneous autoimmune optic neuritis," *J Exp Med*, vol. 197, no. 9, pp. 1073–81, May 2003.
- [224] G. Kassiotis and B. Stockinger, "Anatomical heterogeneity of memory CD4+ T cells due to reversible adaptation to the microenvironment," *J Immunol*, vol. 173, no. 12, pp. 7292–8, Dec. 2004.

- [225] M. Salmi and S. Jalkanen, "Lymphocyte homing to the gut: attraction, adhesion, and commitment," *Immunol. Rev.*, vol. 206, pp. 100–113, Aug. 2005.
- [226] G. Gofu, J. Rivera-Nieves, and K. Ley, "Role of beta7 integrins in intestinal lymphocyte homing and retention," *Curr. Mol. Med.*, vol. 9, no. 7, pp. 836–850, Sep. 2009.
- [227] M. C. Lam and B. Bressler, "Vedolizumab for ulcerative colitis and Crohn's disease: results and implications of GEMINI studies," *Immunotherapy*, vol. 6, no. 9, pp. 963–971, 2014.
- [228] L. P. McLean, T. Shea-Donohue, and R. K. Cross, "Vedolizumab for the treatment of ulcerative colitis and Crohn's disease," *Immunotherapy*, vol. 4, no. 9, pp. 883–898, Sep. 2012.
- [229] H. Tilg and A. Kaser, "Vedolizumab, a humanized mAb against the $\alpha 4\beta 7$ integrin for the potential treatment of ulcerative colitis and Crohn's disease," *Curr. Opin. Investig. Drugs Lond. Engl.* 2000, vol. 11, no. 11, pp. 1295–1304, Nov. 2010.
- [230] B. D. Solomon and C.-S. Hsieh, "Antigen-Specific Development of Mucosal Foxp3+ROR γ t+ T Cells from Regulatory T Cell Precursors," *J. Immunol. Baltim. Md 1950*, vol. 197, no. 9, pp. 3512–3519, 01 2016.
- [231] S. Lavasani *et al.*, "A novel probiotic mixture exerts a therapeutic effect on experimental autoimmune encephalomyelitis mediated by IL-10 producing regulatory T cells," *PLoS One*, vol. 5, no. 2, p. e9009, Feb. 2010.
- [232] J. Ochoa-Repáraz *et al.*, "Role of gut commensal microflora in the development of experimental autoimmune encephalomyelitis," *J. Immunol. Baltim. Md 1950*, vol. 183, no. 10, pp. 6041–6050, Nov. 2009.
- [233] J. Ochoa-Repáraz, D. W. Mielcarz, S. Haque-Begum, and L. H. Kasper, "Induction of a regulatory B cell population in experimental allergic encephalomyelitis by alteration of the gut commensal microflora," *Gut Microbes*, vol. 1, no. 2, pp. 103–108, Mar. 2010.
- [234] M. Kosmidou *et al.*, "Multiple sclerosis and inflammatory bowel diseases: a systematic review and meta-analysis," *J. Neurol.*, vol. 264, no. 2, pp. 254–259, Feb. 2017.
- [235] D. A. Steeber, M. L. Tang, X. Q. Zhang, W. Muller, N. Wagner, and T. F. Tedder, "Efficient lymphocyte migration across high endothelial venules of mouse Peyer's patches requires overlapping expression of L-selectin and beta7 integrin," *J Immunol*, vol. 161, no. 12, pp. 6638–47, Dec. 1998.
- [236] N. Wagner *et al.*, "Critical role for beta7 integrins in formation of the gut-associated lymphoid tissue," *Nature*, vol. 382, no. 6589, pp. 366–70, Jul. 1996.
- [237] B. G. Feagan *et al.*, "Treatment of ulcerative colitis with a humanized antibody to the alpha4beta7 integrin," *N. Engl. J. Med.*, vol. 352, no. 24, pp. 2499–2507, Jun. 2005.
- [238] D. Picarella, P. Hurlbut, J. Rottman, X. Shi, E. Butcher, and D. J. Ringler, "Monoclonal antibodies specific for beta 7 integrin and mucosal addressin cell adhesion molecule-1 (MAcCAM-1) reduce inflammation in the colon of scid mice reconstituted with CD45RBhigh CD4+ T cells," *J. Immunol. Baltim. Md 1950*, vol. 158, no. 5, pp. 2099–2106, Mar. 1997.
- [239] L. Steinman, "The discovery of natalizumab, a potent therapeutic for multiple sclerosis," *J. Cell Biol.*, vol. 199, no. 3, pp. 413–416, Oct. 2012.

- [240] T. A. Yednock, C. Cannon, L. C. Fritz, F. Sanchez-Madrid, L. Steinman, and N. Karin, "Prevention of experimental autoimmune encephalomyelitis by antibodies against alpha 4 beta 1 integrin," *Nature*, vol. 356, no. 6364, pp. 63–66, Mar. 1992.
- [241] B. Engelhardt, M. Laschinger, M. Schulz, U. Samulowitz, D. Vestweber, and G. Hoch, "The development of experimental autoimmune encephalomyelitis in the mouse requires alpha4-integrin but not alpha4beta7-integrin," *J. Clin. Invest.*, vol. 102, no. 12, pp. 2096–2105, Dec. 1998.
- [242] K. G. Haanstra *et al.*, "Antagonizing the $\alpha 4\beta 1$ integrin, but not $\alpha 4\beta 7$, inhibits leukocytic infiltration of the central nervous system in rhesus monkey experimental autoimmune encephalomyelitis," *J. Immunol. Baltim. Md 1950*, vol. 190, no. 5, pp. 1961–1973, Mar. 2013.
- [243] J. R. Kanwar, R. K. Kanwar, D. Wang, and G. W. Krissansen, "Prevention of a chronic progressive form of experimental autoimmune encephalomyelitis by an antibody against mucosal addressin cell adhesion molecule-1, given early in the course of disease progression," *Immunol. Cell Biol.*, vol. 78, no. 6, pp. 641–645, Dec. 2000.
- [244] J. R. Kanwar *et al.*, "Beta7 integrins contribute to demyelinating disease of the central nervous system," *J. Neuroimmunol.*, vol. 103, no. 2, pp. 146–152, Mar. 2000.
- [245] K. Kuhbandner *et al.*, "MAdCAM-1-Mediated Intestinal Lymphocyte Homing Is Critical for the Development of Active Experimental Autoimmune Encephalomyelitis," *Front. Immunol.*, vol. 10, p. 903, 2019.
- [246] B. Douzandeh-Mobarrez and A. Kariminik, "Gut Microbiota and IL-17A: Physiological and Pathological Responses," *Probiotics Antimicrob. Proteins*, vol. 11, no. 1, pp. 1–10, 2019.
- [247] R. Allavena, S. Noy, M. Andrews, and N. Pullen, "CNS elevation of vascular and not mucosal addressin cell adhesion molecules in patients with multiple sclerosis," *Am. J. Pathol.*, vol. 176, no. 2, pp. 556–562, Feb. 2010.
- [248] J. K. O'Neill *et al.*, "Expression of vascular addressins and ICAM-1 by endothelial cells in the spinal cord during chronic relapsing experimental allergic encephalomyelitis in the Biozzi AB/H mouse," *Immunology*, vol. 72, no. 4, pp. 520–525, Apr. 1991.
- [249] B. J. Steffen, G. Breier, E. C. Butcher, M. Schulz, and B. Engelhardt, "ICAM-1, VCAM-1, and MAdCAM-1 are expressed on choroid plexus epithelium but not endothelium and mediate binding of lymphocytes in vitro," *Am. J. Pathol.*, vol. 148, no. 6, pp. 1819–1838, Jun. 1996.
- [250] B. J. Steffen, E. C. Butcher, and B. Engelhardt, "Evidence for involvement of ICAM-1 and VCAM-1 in lymphocyte interaction with endothelium in experimental autoimmune encephalomyelitis in the central nervous system in the SJL/J mouse," *Am. J. Pathol.*, vol. 145, no. 1, pp. 189–201, Jul. 1994.
- [251] M. Vercellino *et al.*, "Involvement of the choroid plexus in multiple sclerosis autoimmune inflammation: a neuropathological study," *J. Neuroimmunol.*, vol. 199, no. 1–2, pp. 133–141, Aug. 2008.
- [252] A. Döring *et al.*, "TET inducible expression of the $\alpha 4\beta 7$ -integrin ligand MAdCAM-1 on the blood-brain barrier does not influence the immunopathogenesis of experimental autoimmune encephalomyelitis," *Eur. J. Immunol.*, vol. 41, no. 3, pp. 813–821, Mar. 2011.

- [253] V. Rothhammer *et al.*, "Th17 lymphocytes traffic to the central nervous system independently of $\alpha 4$ integrin expression during EAE," *J. Exp. Med.*, vol. 208, no. 12, pp. 2465–2476, Nov. 2011.
- [254] A. Habtezion, L. P. Nguyen, H. Hadeiba, and E. C. Butcher, "Leukocyte Trafficking to the Small Intestine and Colon," *Gastroenterology*, vol. 150, no. 2, pp. 340–354, Feb. 2016.
- [255] G. Umbrello and S. Esposito, "Microbiota and neurologic diseases: potential effects of probiotics," *J. Transl. Med.*, vol. 14, no. 1, p. 298, 19 2016.
- [256] E. Owaga, R.-H. Hsieh, B. Mugendi, S. Masuku, C.-K. Shih, and J.-S. Chang, "Th17 Cells as Potential Probiotic Therapeutic Targets in Inflammatory Bowel Diseases," *Int. J. Mol. Sci.*, vol. 16, no. 9, pp. 20841–20858, Sep. 2015.
- [257] F. Cignarella *et al.*, "Intermittent Fasting Confers Protection in CNS Autoimmunity by Altering the Gut Microbiota," *Cell Metab.*, vol. 27, no. 6, p. 1222–1235.e6, Jun. 2018.
- [258] Y. Goto *et al.*, "Segmented filamentous bacteria antigens presented by intestinal dendritic cells drive mucosal Th17 cell differentiation," *Immunity*, vol. 40, no. 4, pp. 594–607, Apr. 2014.
- [259] Y. Yang *et al.*, "Focused specificity of intestinal TH17 cells towards commensal bacterial antigens," *Nature*, vol. 510, no. 7503, pp. 152–156, Jun. 2014.
- [260] H. Wekerle, K. Berer, and G. Krishnamoorthy, "Remote control-triggering of brain autoimmune disease in the gut," *Curr. Opin. Immunol.*, vol. 25, no. 6, pp. 683–689, Dec. 2013.
- [261] M. Zhang *et al.*, "Butyrate inhibits interleukin-17 and generates Tregs to ameliorate colorectal colitis in rats," *BMC Gastroenterol.*, vol. 16, no. 1, p. 84, Jul. 2016.
- [262] E. P. Koroleva, S. Halperin, E. O. Gubernatorova, E. Macho-Fernandez, C. M. Spencer, and A. V. Tumanov, "Citrobacter rodentium-induced colitis: A robust model to study mucosal immune responses in the gut," *J. Immunol. Methods*, vol. 421, pp. 61–72, Jun. 2015.
- [263] K. Park and A. L. Scott, "Cholesterol 25-hydroxylase production by dendritic cells and macrophages is regulated by type I interferons," *J. Leukoc. Biol.*, vol. 88, no. 6, pp. 1081–1087, Dec. 2010.
- [264] E. Vivier *et al.*, "Innate Lymphoid Cells: 10 Years On," *Cell*, vol. 174, no. 5, pp. 1054–1066, 23 2018.
- [265] H. Spits and J. P. Di Santo, "The expanding family of innate lymphoid cells: regulators and effectors of immunity and tissue remodeling," *Nat. Immunol.*, vol. 12, no. 1, pp. 21–27, Jan. 2011.
- [266] M. Forkel and J. Mjösberg, "Dysregulation of Group 3 Innate Lymphoid Cells in the Pathogenesis of Inflammatory Bowel Disease," *Curr. Allergy Asthma Rep.*, vol. 16, no. 10, 2016.
- [267] L. C. Rankin *et al.*, "Complementarity and redundancy of IL-22-producing innate lymphoid cells," *Nat. Immunol.*, vol. 17, no. 2, pp. 179–186, Feb. 2016.
- [268] B. Zeng, S. Shi, G. Ashworth, C. Dong, J. Liu, and F. Xing, "ILC3 function as a double-edged sword in inflammatory bowel diseases," *Cell Death Dis.*, vol. 10, no. 4, p. 315, Apr. 2019.
- [269] A. Honda *et al.*, "Cholesterol 25-hydroxylation activity of CYP3A," *J. Lipid Res.*, vol. 52, no. 8, pp. 1509–1516, Aug. 2011.

- [270] A. Haghikia *et al.*, “Dietary Fatty Acids Directly Impact Central Nervous System Autoimmunity via the Small Intestine,” *Immunity*, vol. 43, no. 4, pp. 817–829, Oct. 2015.
- [271] M. Mizuno, D. Noto, N. Kaga, A. Chiba, and S. Miyake, “The dual role of short fatty acid chains in the pathogenesis of autoimmune disease models,” *PLoS ONE*, vol. 12, no. 2, Feb. 2017.
- [272] Y. Zheng *et al.*, “Interleukin-22 mediates early host defense against attaching and effacing bacterial pathogens,” *Nat. Med.*, vol. 14, no. 3, pp. 282–289, Mar. 2008.
- [273] D. Brunotte-Strecker, “Characterization of ILC subsets in CNS and small intestine during EAE.” [Online]. Available: <https://onlinelibrary.ectrims-congress.eu/ectrims/2017/ACTRIMS-ECTRIMS2017/200635/daniel.brunotte-strecker.characterization.of.ilc.subsets.in.cns.and.small.html?f=media=1>. [Accessed: 23-Jul-2019].
- [274] C.-Y. Wang and J. K. Liao, “A mouse model of diet-induced obesity and insulin resistance,” *Methods Mol. Biol. Clifton NJ*, vol. 821, pp. 421–433, 2012.
- [275] M. Farnier, “Alirocumab for the treatment of hyperlipidemia in high-risk patients: an updated review,” *Expert Rev. Cardiovasc. Ther.*, vol. 15, no. 12, pp. 923–932, Dec. 2017.
- [276] J. S. Wooten, H. Wu, J. Raya, X. D. Perrard, J. Gaubatz, and R. C. Hoogeveen, “The Influence of an Obesogenic Diet on Oxysterol Metabolism in C57BL/6J Mice,” *Cholesterol*, vol. 2014, p. 843468, 2014.
- [277] L. Schrewe *et al.*, “Investigation of sex-specific effects of apolipoprotein E on severity of EAE and MS,” *J. Neuroinflammation*, vol. 12, p. 234, Dec. 2015.

8. APPENDICES

8.1 Appendix A

Donovan Duc

Education

09.2015 – 10.2019	Doctoral degree (PhD) in Life Sciences , University of Lausanne Laboratory of Experimental Neuroimmunology PhD program in Cancer and Immunology
06.2018	Certificate of Advance Studies – Module Quality and GMP, ETH Zurich
2013 – 2015	Master of Science (MSc) in Medical Biology , University of Lausanne
04.2014 – 02.2015	Second traineeship, Department of Clinical Neuroscience (CHUV) Laboratory of Neurotherapies and Neuromodulation Research field: Neuroinflammation
10.2013 – 12.2013	First traineeship, Division of Angiology (CHUV) Research field: Atherosclerosis
2010 - 2013	Bachelor of Science (BSc) in Biology , University of Lausanne
2006 - 2009	Federal Maturity, biology/chemistry option

Publications

2019	Duc D* , Vigne S*, Bernier-Latmani J, Yersin Y, Ruiz F, Gaïa N, Leo S, Lazarevic V, Schrenzel J, Petrova TV and Pot C. <i>Disrupting myelin-specific Th17 cell gut homing confers protection in an adoptive transfer experimental autoimmune encephalomyelitis</i> . Cell Rep. 2019 Oct 8;29(2):378-390.e4. *equal contribution Duc D , Vigne S and Pot C. <i>Oxysterols and autoimmunity</i> . Int. J. Mol. Sci. 2019, 20, 4522.
2017	Vigne S*, Chalmin F*, Duc D , Clottu A, Apetoh L, Lobaccaro JMA, Christen I, Zhang J and Pot C. <i>IL-27-induced type 1 regulatory T-cells produce oxysterols that constrain IL-10 production</i> . Front Immunol. 2017 Sept 25; 8 (1184). *equal contribution
2016	Humbert-Claude M, Duc D , Dwir D, Thieren L, Sandström von Tobel J, Begka C, Legueux F, Velin D, Maillard MH, Do KQ, Monnet-Tschudi F and Tenenbaum L. <i>Tollip, an early regulator of the acute inflammatory response in the substantia nigra</i> . J Neuroinflammation. 2016 Dec 7;13(1):303.

Communications and conferences

03.2019	Young Investigator Meeting, Bad Ragaz, Switzerland (oral presentation)
03.2019	XXXI Meeting of the Swiss Immunology PhD students, Thun, Switzerland (oral presentation)
09.2018	8 th ENOR Symposium, Bologna, Italy (poster presentation)

09.2018	4 th Neuroscience Research Center Symposium, Lausanne, Switzerland (poster presentation)
08.2018	SSAI Annual Meeting, Interlaken, Switzerland (oral presentation)
01.2018	20 th State of the Art Symposium, Luzern, Switzerland (poster & oral presentation)
10.2017	Department of Biochemistry days, Lausanne, Switzerland (oral presentation)
09.2017	7 th ENOR Symposium, Brussels, Belgium (poster presentation)
09.2017	3 rd Neuroscience Research Center Symposium, Lausanne, Switzerland (poster presentation)
06.2017	Young Investigator Meeting, Bern, Switzerland (oral presentation)
11.2016	Soirée d'informations pour patients – « Environnement et SEP: quels liens ? », Société suisse de sclérose en plaques, Lausanne, Switzerland (oral presentation)

Awards

09.2018	Second prize for best poster 8 th ENOR Symposium, Bologna (IT)
09.2017	Third prize for best poster 7 th ENOR Symposium, Brussels (BE)
09.2017	Award for the best poster 3 rd Neuroscience Research Center Symposium, Lausanne (CH)

Student supervision

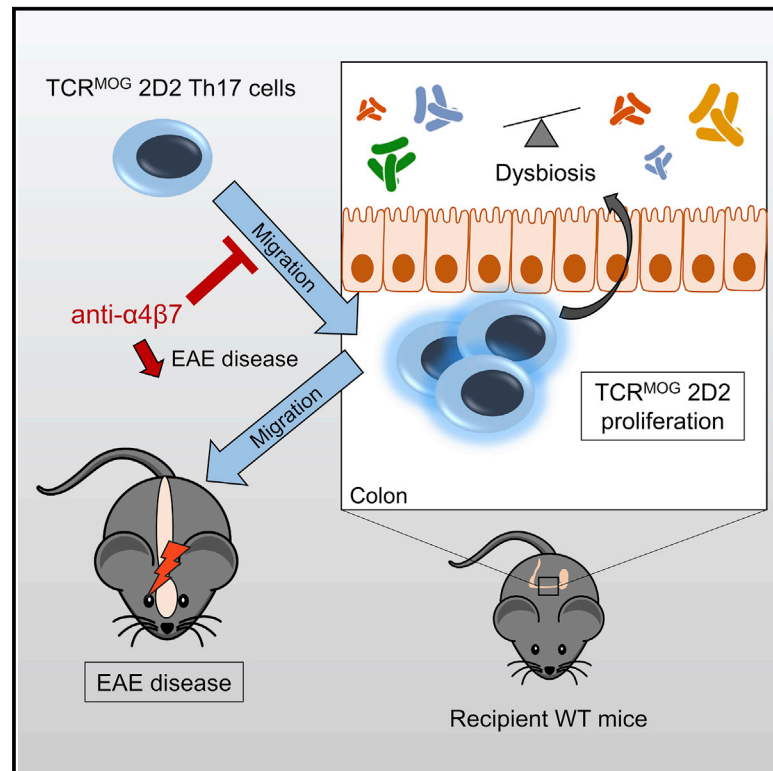
10.2017 – 12.2017	Supervision of Benjamin Peter, First-step project, Master in Medical Biology (University of Lausanne); directed by Prof. Caroline Pot. He worked on the <i>in vitro</i> model of dendritic cells for my project and successfully defended his work in December 2017.
-------------------	---

Associative projects

07.2017 – 11.2019	Member at BioScience Network Lausanne (EPFL-UNIL) – Responsible for the organization of career events – Fundraising and sponsorship management
03.2018 – 03.2019	Coordinator and board member at BioScience Network Lausanne – Responsible for the administrative affairs

Disrupting Myelin-Specific Th17 Cell Gut Homing Confers Protection in an Adoptive Transfer Experimental Autoimmune Encephalomyelitis

Graphical Abstract



Authors

Donovan Duc, Solenne Vigne, Jeremiah Bernier-Latmani, ..., Jacques Schrenzel, Tatiana V. Petrova, Caroline Pot

Correspondence

caroline.pot-kreis@chuv.ch

In Brief

Duc et al. show that Th17-polarized myelin-specific (TCR^{MOG} 2D2) CD4⁺ T cells migrate to the colon before the development of neuroinflammation. Encephalitogenic Th17 cells further change intestinal microbiome composition. Blocking encephalitogenic Th17 cell entry into the colon or treatment with antibiotics ameliorates EAE severity.

Highlights

- TCR^{MOG} 2D2 Th17 cells infiltrate the colonic lamina propria during EAE
- Adoptively transferred TCR^{MOG} 2D2 Th17 cells proliferate in the colon
- Blocking 2D2 Th17 cell entry into the colon with α4β7 antibody impairs EAE
- TCR^{MOG} 2D2 Th17 cells induce microbiota composition changes



Disrupting Myelin-Specific Th17 Cell Gut Homing Confers Protection in an Adoptive Transfer Experimental Autoimmune Encephalomyelitis

Donovan Duc,^{1,4} Solenne Vigne,^{1,4} Jeremiah Bernier-Latmani,² Yannick Yersin,¹ Florian Ruiz,¹ Nadia Gaïa,³ Stefano Leo,³ Vladimir Lazarevic,³ Jacques Schrenzel,³ Tatiana V. Petrova,² and Caroline Pot^{1,5,*}

¹Laboratories of Neuroimmunology, Neuroscience Research Center and Service of Neurology, Department of Clinical Neurosciences, Lausanne University Hospital and University of Lausanne, Chemin des Boveresses 155, 1066 Epalinges, Switzerland

²Department of Oncology, Lausanne University Hospital and University of Lausanne, and Ludwig Institute for Cancer Research Lausanne, Chemin des Boveresses 155, 1066 Epalinges, Switzerland

³Genomic Research Laboratory, Division of Infectious Diseases, Department of Medicine, Geneva University Hospitals and University of Geneva, Rue Gabrielle-Perret-Gentil 4, 1211 Geneva, Switzerland

⁴These authors contributed equally

⁵Lead Contact

*Correspondence: caroline.pot-kreis@chuv.ch
<https://doi.org/10.1016/j.celrep.2019.09.002>

SUMMARY

Multiple sclerosis (MS) is a common autoimmune disease of the CNS. Although an association between MS and inflammatory bowel diseases is observed, the link connecting intestinal immune responses and neuroinflammation remains unclear. Here we show that encephalitogenic Th17 cells infiltrate the colonic lamina propria before neurological symptom development in two murine MS models, active and adoptive transfer experimental autoimmune encephalomyelitis (EAE). Specifically targeting Th17 cell intestinal homing by blocking the $\alpha 4\beta 7$ -integrin and its ligand MAdCAM-1 pathway impairs T cell migration to the large intestine and dampens EAE severity in the Th17 cell adoptive transfer model. Mechanistically, myelin-specific Th17 cells proliferate in the colon and affect gut microbiota composition. The beneficial effect of blocking the $\alpha 4\beta 7$ -integrin and its ligand MAdCAM-1 pathway on EAE is interdependent with gut microbiota. Those results show that disrupting myelin-specific Th17 cell trafficking to the large intestine harnesses neuroinflammation and suggests that the gut environment and microbiota catalyze the encephalitogenic properties of Th17 cells.

INTRODUCTION

Multiple sclerosis (MS) is a neurological and autoimmune disorder characterized by inflammatory cell infiltrates and demyelination of the CNS. Its development is under the control of genetic and environmental factors. Although environmental factors contribute to MS development (Olsson et al., 2017), most of our knowledge about their relative contributions relies on epidemiological data, leaving the underlying pathophysiology largely unraveled.

Among environmental factors, recent studies proposed a role for intestinal factors in affecting MS disease severity (van den Hoogen et al., 2017). Furthermore, changes in the intestinal microbiome were described in MS and experimental autoimmune encephalomyelitis (EAE) (Miyake and Yamamura, 2019). Although those results remain disputed, they highlight the possible interaction between the gut and the brain, called the gut-brain axis, in neuroinflammation. Interestingly, animal models indicate that increased intestinal permeability (leaky gut) plays a pathogenic role not only in gastrointestinal disorders, such as inflammatory bowel disease (IBD), but also in systemic autoimmune diseases, like type 1 diabetes and MS (Mu et al., 2017; Opazo et al., 2018). Moreover, alteration of the gut microbiome and immune cell infiltration are described in the small intestine in EAE (Berer et al., 2011; Nouri et al., 2014) and MS (Berer et al., 2017; Cosorich et al., 2017). T helper (Th) 17 cells infiltrate the small intestine and increase intestinal permeability (Nouri et al., 2014); however, their relative contribution to neuroinflammation remains largely unknown. Furthermore, whether the large intestine, namely, the colon, promotes neuroinflammation is not established.

In this report, we observed altered gut immune responses associated with an infiltration of pro-inflammatory Th17 cells in the lamina propria of the colon in two EAE models. Blocking the migration of pro-inflammatory Th17 cells in the intestinal compartment, as well as treatment with antibiotics, reduced the severity of EAE disease interdependently, pointing toward a contribution of the gut-brain axis in EAE. Although the link between gut immunity and MS remains to be clarified, a better understanding of how immune cells are regulated in the intestine during EAE could support innovative approaches to target neuroinflammation.

RESULTS

Antigen-Specific MOG Th17 Cells Infiltrate the Colonic Lamina Propria during Active EAE

We first evaluated whether immune dysregulation was observed in the colon during EAE actively induced by subcutaneous



immunization of myelin oligodendrocyte glycoprotein (MOG) amino acids 35–55 (MOG_{35–55}). To evaluate the relative contribution of a CNS antigen-specific response versus the sole contribution of the complete Freund adjuvant (CFA), we immunized wild-type mice with the antigen MOG_{35–55} or PBS emulsified with CFA. Pertussis toxin was injected at days 0 and 2 for both groups. Only mice immunized with antigen MOG_{35–55} developed neurological symptoms (Figure 1A). The expression levels of innate immune cytokines interleukin (IL) 6, IL-1 β , and tumor necrosis factor alpha (TNF- α) that play a role during IBD and experimental colitis (Papadakis and Targan, 2000) were assessed by quantitative real-time PCR in the colon when the MOG-immunized mice displayed neurological symptoms. IL-6 and IL-1 β , but not TNF- α , were induced in an antigen-specific manner (Figure 1B). Because both IL-6 and IL-1 β promote Th17 cell differentiation (Korn et al., 2009), we investigated by flow cytometry whether Th17 lymphocytes infiltrated the large intestine during EAE. The MOG-immunized group significantly surpassed the PBS group in upregulation of IL-17-producing CD4⁺ T cells (Figures 1C and 1D), but not in interferon (IFN) γ -producing CD4⁺ T cells (Figures 1E and 1F), in the colon. Those results suggest that Th17 cell subsets specifically respond to the CNS antigen. We completed the analysis with the use of MOG_{35–55}/IAb tetramers and tracked CD4⁺ T cells based on their myelin antigen specificity in the colon and the CNS. Notably, MOG-specific T cells are increased in the colon at the peak of EAE disease compared with non-immunized control animals, approximately reaching the levels observed in the CNS, where about 3% of CD4⁺ T cells stained positive for MOG tetramer, in accordance with a previous publication (Mycko et al., 2015) (Figure 1G). Collectively, these data indicate that MOG-specific Th17 cells are observed in the large intestine and suggest an activation of CD4⁺ T lymphocytes in the colon during EAE.

Encephalitogenic TCR^{MOG} 2D2 Th17 Cells Preferentially Infiltrate the Large Intestine

To specifically study the relevance of encephalitogenic Th17 cell infiltration in the large intestine during EAE, we performed adoptive transfer of *in vitro* polarized Th17 cells of CD4⁺ T cells isolated from C57Bl6 mice with a T cell receptor (TCR) specific for the peptide MOG_{35–55} referred to as TCR^{MOG} 2D2. This model has the advantage of overriding the priming phase of T cells to focus solely on the encephalitogenic potential of TCR^{MOG} 2D2 Th17 cell subsets. Briefly, CD4⁺ T cells from the spleen and lymph nodes of naive 2D2 mice were differentiated *in vitro* into Th17 cells (Figure 2A) and transferred into C57BL/6J recipient mice as previously described (Jäger et al., 2009; Peters et al., 2015). Following TCR^{MOG} 2D2 Th17 cell transfer, C57BL/6J recipient mice developed both typical and atypical EAE signs, characterized by an ascending paralysis and an unbalanced gait with severe axial instability, respectively (Peters et al., 2015). However, when highly activated TCR^{MOG} 2D2 Th17 cell subsets are injected, neurological symptoms do not appear before 10 days after injection (Figure 2B), suggesting that TCR^{MOG} 2D2 Th17 cells are activated in peripheral organs to acquire a phenotype enabling them to reach the CNS. We thus evaluated by flow cytometry analysis whether TCR^{MOG} 2D2 Th17 cells (as defined by V α 3.2 expression) were detected in

the small and large intestine before neurological symptoms appear. We detected a significant percentage of CD4⁺ T cells expressing V α 3.2 in the gut. The percentage of CD4⁺ T cells expressing TCR V α 3.2 was significantly higher in the colon (36.5% \pm 2.0%) compared with the small intestine (10.4% \pm 2.9%) (Figures 2C and 2D), suggesting a predominant infiltration of the large intestine. In line with previous reports using the Lewis rat model of EAE (Flügel et al., 2001; Kanayama et al., 2016; Odoardi et al., 2012), TCR^{MOG} 2D2 Th17 cells were present in the lungs (Figure 2C). We further characterized the anatomical location of TCR^{MOG} 2D2 cells within the colon using whole-mount immunostaining. In agreement with flow cytometry analysis, high numbers of TCR^{MOG} 2D2 Th17 cells were found in the colonic lamina propria before EAE disease onset and were not observed in control, non-injected, wild-type animals (Figure 2E). We then asked whether Th17 cell colonic infiltration was MOG specific and took advantage of OT-II transgenic mice that display a TCR specific for ovalbumin 323–339 peptide. CD4⁺ T cells, obtained from OT-II and 2D2 mice on a CD45.2 background, were polarized into Th17 cells and transferred into CD45.1 recipient mice. Colonic tissue was examined by flow cytometry for the percentage of CD45.2⁺ on total CD45⁺ cells. 2D2 and OT-II cells migrated similarly to the colon, suggesting that Th17 cell migration to the colon is not MOG specific (Figure 2F). We asked whether different encephalitogenic T cell subsets similarly migrate to the colon. We generated Th17 and Th1 cells from TCR^{MOG} 2D2 T cells *in vitro* as previously described (Jäger et al., 2009) and transferred them into naive syngeneic wild-type C57BL/6J recipients. The percentages of TCR^{MOG} 2D2 T cells were assessed by flow cytometry from the colon of recipient mice. A significantly higher percentage of TCR^{MOG} 2D2 T cells was detected in the colon when cells were differentiated into Th17 versus Th1 cells (Figure 2G). Those results suggest that Th17 cells migrate to the colon during EAE independent of their antigen specificity but at higher levels than Th1 cells.

Encephalitogenic TCR^{MOG} 2D2 Th17 Cells Are in Close Contact with Colonic Blood Vessels and Egress via Lymphatic Vessels

Using 3D image reconstruction, we assessed the location of TCR^{MOG} 2D2 Th17 cells within the colonic lamina propria. Although TCR^{MOG} 2D2 Th17 cells were found throughout the colonic lamina propria, we observed many cells closely associated with colon blood capillaries. Quantification of TCR^{MOG} 2D2 Th17 cells either in the immediate vicinity (on) or not (off) of colon blood capillaries showed that more than 60% of the TCR^{MOG} 2D2 Th17 cells were contacting these vessels (Figure 3A). We further observed that a fraction of TCR^{MOG} 2D2 Th17 cells showed an elongated morphology, suggesting a migratory phenotype (Figure 3A). Furthermore, TCR^{MOG} 2D2 Th17 cells were detected closely associated with, and in the lumen of, dilated vessels below colonic crypts, identified as lymphatic capillaries by LYVE-1 staining (Figures 3B–3D). Because intestinal lymphatic capillaries drain into mesenteric lymph nodes (mLNs) (Bernier-Latmani and Petrova, 2017), we assessed the percentage of TCR^{MOG} 2D2 by fluorescence-activated cell sorting (FACS) analysis in the gut-draining mLNs

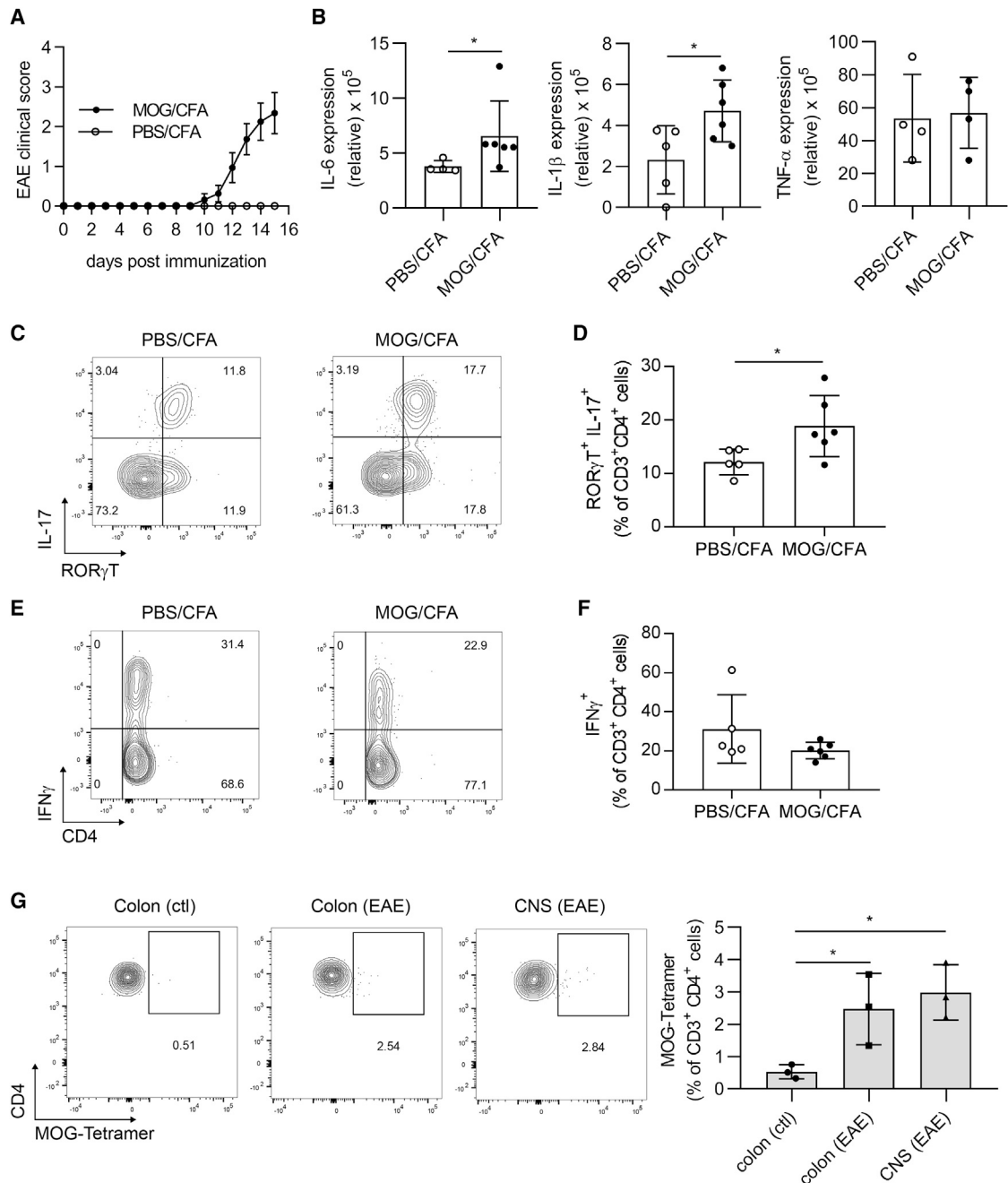


Figure 1. MOG-Specific Th17 Cells Infiltrate the Large Intestine during Active EAE

(A) Wild-type mice were immunized with either MOG_{35–55} or PBS in CFA. The course of EAE in these mice is shown as a clinical score (mean ± SEM; n = 8). (B) Relative mRNA expression of IL-6, IL-1β, and TNF-α in colonic tissue as measured by real-time PCR in mice immunized with PBS and CFA or MOG and CFA when mice displayed neurological symptoms (mean ± SD; n = 4–6). Data are representative of two independent experiments. (C–F) Flow cytometric analysis of colonic lamina propria-infiltrating CD4⁺ T cells in the PBS and CFA group versus the MOG and CFA group. Frequency of RORγT⁺IL-17⁺ CD4⁺ T cells (C and D) and IFNγ⁺ CD4⁺ T cells (E and F) (mean ± SD; n = 5–6). (G) Cellular suspensions from colon and CNS were prepared from non-immunized (ctl) and immunized mice at the peak of the disease (EAE). FACS analysis of the total proportion (as a percentage) of MOG-specific CD4⁺ T cells was visualized by MOG_{35–55}/IAb tetramer staining (mean ± SD; n = 3). *p < 0.05; p values were determined by Mann-Whitney test (B [IL-6]), unpaired Student's t test (B [IL-1β and TNF-α], D, and F) and one-way ANOVA with Dunnett's post hoc test (G).

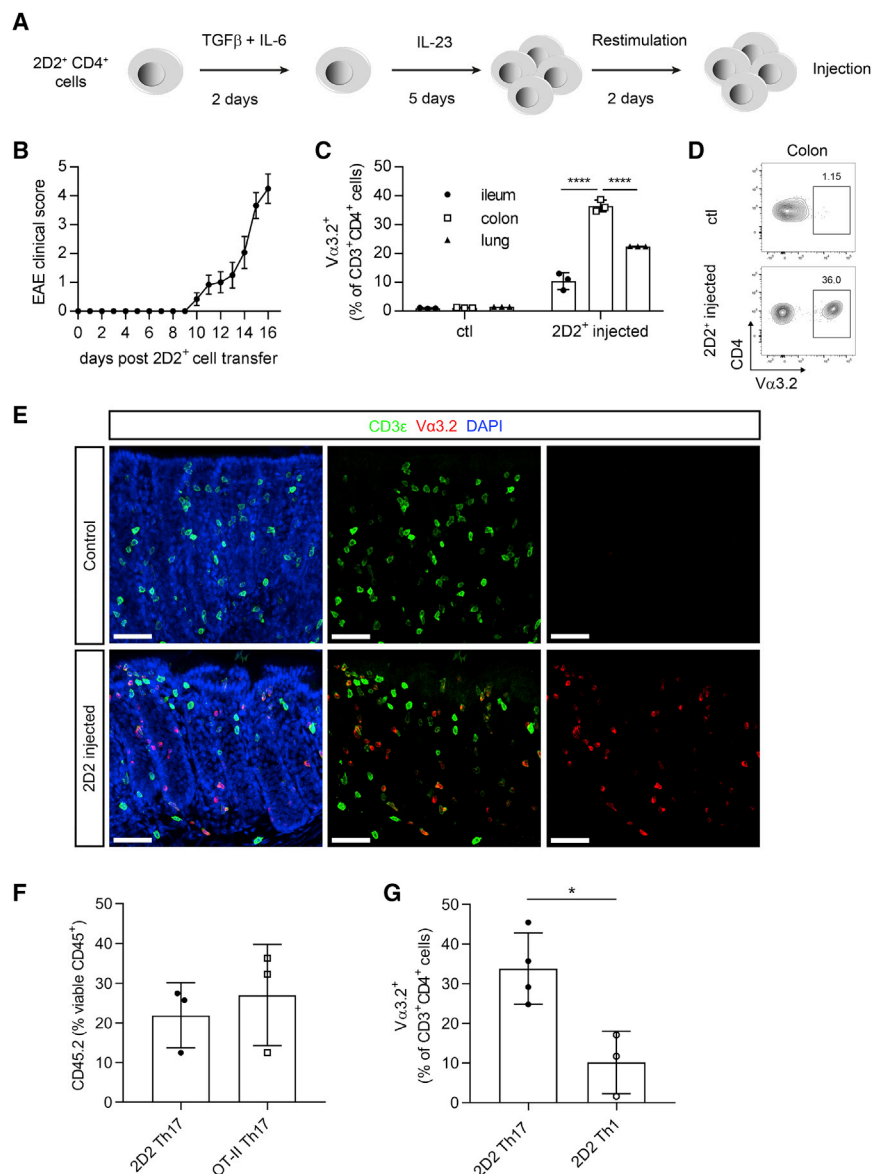


Figure 2. Encephalitogenic TCR^{MOG} 2D2 Th17 Cells Preferentially Infiltrate the Large Intestine and Are Located in the Colonic Lamina Propria during EAE

(A) CD4⁺ T cells from 2D2 mice were activated *in vitro* under Th17-polarizing conditions in the presence of transforming growth factor β (TGF-β), IL-6, and IL-23. After restimulation with anti-CD3/CD28 antibodies, TCR^{MOG} 2D2 Th17 cells were injected into wild-type recipient mice.

(B) Clinical scores of EAE in mice adoptively transferred with TCR^{MOG} 2D2 Th17 cells. The course of EAE in these mice is shown as a clinical score (mean ± SEM; n = 12).

(C) Flow cytometric analysis of the total proportion (as a percentage) of TCR^{MOG} 2D2 (Vα3.2⁺) expression in CD3⁺/CD4⁺ T cells at day 8 post-injection among the lamina propria of ileum, colon, and lung in non-injected control mice and mice injected with TCR^{MOG} 2D2 Th17 cells (mean ± SD; n = 3). Data are representative of two independent experiments.

(D) Representative flow cytometry analysis of TCR^{MOG} 2D2 (Vα3.2⁺) expression in CD3⁺/CD4⁺ T cells obtained from the colonic lamina propria of non-injected control mice versus mice injected with TCR^{MOG} 2D2 Th17 cells 8 days after injection. (E) Colon whole-mount immunostaining for endogenous (green, CD3ε) and injected TCR^{MOG} 2D2 (red, Vα3.2) T cells from control and TCR^{MOG} 2D2 T cell-injected mice; blue, DAPI. Scale bars: 50 μm. Data are representative of three independent experiments.

(F) Flow cytometric analysis of the total proportion (as a percentage) of CD45.2⁺ cells (donor 2D2 or OT-II) obtained from the colon of CD45.1 recipient mice 15 days after T cell transfer (mean ± SD; n = 3).

(G) Flow cytometric analysis of Vα3.2⁺ frequency in CD3⁺/CD4⁺ T cells at day 4 post-injection in the colon of mice injected with TCR^{MOG} 2D2 Th17 cells or TCR^{MOG} 2D2 Th1 cells (mean ± SD; n = 3–4).

*p < 0.05, **p < 0.01, ***p < 0.001, ****p < 0.0001; p values were determined by two-way ANOVA with Sidak's post hoc test (C) and unpaired Student's t test (G).

versus the dermal inguinal lymph nodes (dLNs) of the same recipient mice 4 and 8 days after TCR^{MOG} 2D2 transfer and in PBS-injected recipient mice (Figure S1A). Around 1% CD4⁺ T cells were Vα3.2⁺ in the dLNs (1.03% ± 0.1%) and mLNs (1.0% ± 0.1%) of PBS-injected recipient mice, compatible with low levels of endogenous Vα3.2⁺ expression in the lymphoid organs of C57BL/6J mice (Bettelli et al., 2003). We observed a significant 18-fold (18.7% ± 4.5%, 4 days) and 13-fold (13.3% ± 1.9%, 8 days) increase in CD4⁺ T cells harboring the Vα3.2⁺ marker in the mLNs after TCR^{MOG} 2D2 Th17 cell transfer. At the same time, there was only a minor tendency toward increase in Vα3.2⁺ T cells in the dLNs of the same mice (2.6% ± 0.2%, 4 days) and (2.9% ± 0.5%, 8 days) after T cell transfer compared with the control dLNs (1.03% ± 0.1%) (Figure S1B). Altogether, these data show that TCR^{MOG} 2D2 Th17 cells infiltrate the colonic lamina propria, migrate out of the colon via lymphatic

vessels, and likely reenter blood circulation downstream of mLNs.

Blocking α4β7-Integrin and Its Ligand MAdCAM-1 Interaction Inhibits TCR^{MOG} 2D2 Th17 Cell Entry into the Large Intestine and Significantly Attenuates EAE

To explore whether colonic TCR^{MOG} 2D2 migration contributes to neuroinflammation, we asked whether blocking TCR^{MOG} 2D2 entry into the gut influences EAE development. Autoimmune T cells receive signals to acquire a functional phenotype that allows them to invade their target tissues (Kassiotis and Stockinger, 2004; Salmi and Jalkanen, 2005). Intestinal targeting of T cells requires expression of the ligand α4β7-integrin on immune cells and expression of its receptor mucosal vascular addressin cell adhesion molecule 1 (MAdCAM-1) on intestinal venules (Gorfu et al., 2009). In our model, MAdCAM-1 was

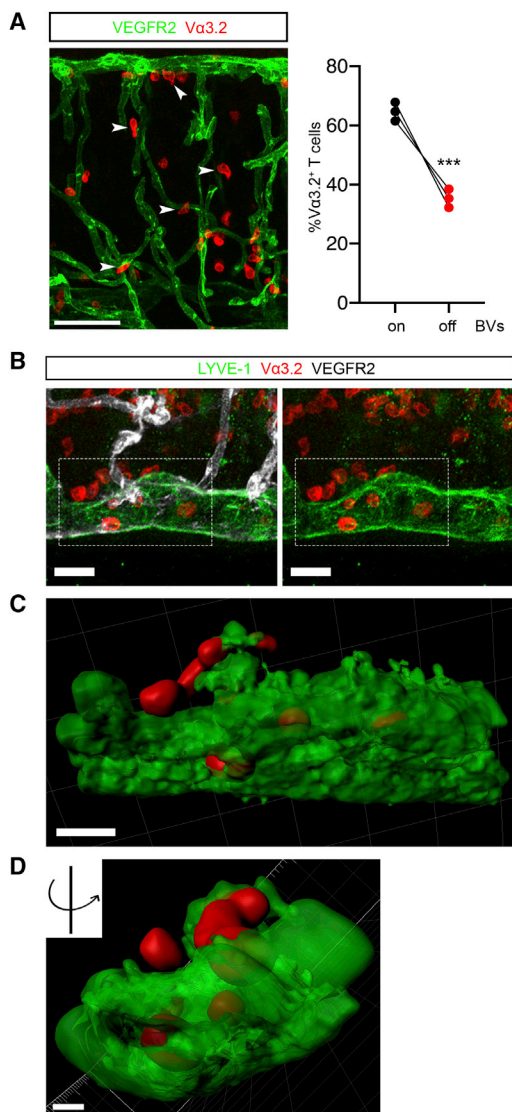


Figure 3. Encephalitogenic TCR^{MOG} 2D2 Th17 Cells Are Located in Close Contact with Blood and Lymphatic Vessels

(A) Injected TCR^{MOG} 2D2 T cells (red, V α 3.2) are located in the colonic lamina propria near blood vessels (green, VEGFR2). Arrowheads indicate TCR^{MOG} 2D2 T cells with an elongated morphology. Percentage of TCR^{MOG} 2D2 T cells in direct contact (on) or not (off) with colon blood capillaries, n = 3.

(B) Whole-mount immunostaining of V α 3.2⁺ T cells (red) entering submucosal VEGFR2⁺ (white) and LYVE-1 (green) lymphatic capillaries 4 days after T cell injection.

(C) 3D reconstruction of V α 3.2⁺ T cells (red) entering lymphatic capillaries (green).

(D) Same image as (C), turned 90° on the y axis to show T cells in the lymphatic capillary lumen.

Scale bars: (A) 50 μ m, (B and D) 20 μ m, and (C) 10 μ m. Data are representative of two independent experiments. ***p < 0.001; p values were determined by unpaired Student's t test. See also Figure S1.

expressed in the colon at a significant higher level compared with the CNS, both at steady state and 4 days after adoptive transfer (Figure 4A). Because we detected a large number of TCR^{MOG} 2D2 Th17 cells in the large intestine, we evaluated

whether these cells expressed α 4 β 7-integrin. Half (50.2% \pm 2.8%) of the colonic TCR^{MOG} 2D2 cells expressed α 4 β 7 four days after adoptive transfer, whereas α 4 β 7 expression was significantly reduced (14.5% \pm 3.1%) at day 8, before neurological signs appear (Figure 4B). Those results suggest that α 4 β 7 expression is involved in TCR^{MOG} 2D2 Th17 cell migration to the gut.

In mouse models of T cell-mediated colitis, administration of α 4 β 7 antibodies reduces inflammation and severity of colitis. Similarly, vedolizumab, a humanized specific α 4 β 7 inhibitor, has proven effective in ulcerative colitis and Crohn's disease (Lam and Bressler, 2014; McLean et al., 2012; Tilg and Kaser, 2010). Because we observed important TCR^{MOG} 2D2 Th17 cell infiltration in the large intestine, we tested whether selective blocking of α 4 β 7 could also influence EAE disease course. α 4 β 7-blocking antibodies (DATK 32) were administered one day before adoptive transfer, followed by injections every three days until the development of EAE disease. We observed during EAE a significant reduction of TCR^{MOG} 2D2 Th17 cell infiltration in the colon, but not in the ileum or in the lung, 4 days after T cell transfer in mice treated with anti- α 4 β 7 compared with the isotype control group (Figures 4C and 4D). Moreover, α 4 β 7 blockade was efficient in dampening EAE neurological disease course (Figure 4E; Table S1). In addition, a significantly reduced number of TCR^{MOG} 2D2 Th17 cells infiltrating the CNS was recorded 10 days after T cell adoptive transfer in mice treated with anti- α 4 β 7 compared with the isotype control group (Figure 4F). Similar results were obtained when we extended the anti- α 4 β 7 treatment until the end of the EAE disease (Figure S2), suggesting that the contribution of colonic Th17 cells in EAE takes place early during EAE. Anti- α 4 β 7 antibody treatment did not influence active EAE disease course (Figures 4G and 4H). Those results suggest a contribution of Th17 cell migration to the colon when Th17 cells are adoptively transferred.

Colonic TCR^{MOG} 2D2 Th17 Cells Express CNS Integrin, and Their Intestinal Infiltrate Resolves upon CNS Invasion

Because we observed TCR^{MOG} 2D2 Th17 cell infiltration of the large intestine before neurological clinical signs, we wondered whether this infiltration persisted throughout the disease course. The frequency of TCR^{MOG} 2D2 Th17 cells was evaluated at different time points after T cell transfer by simultaneous flow cytometry analysis in the colon and the CNS. TCR^{MOG} 2D2 Th17 cells infiltrate the colonic lamina propria as early as 4 days after transfer, whereas no cells were detected in the CNS (Figure 5A). Eight days post-transfer, the frequency of colonic TCR^{MOG} 2D2 Th17 cells decreased by more than two-fold compared with day 4, whereas we found a concomitant significant increase in the percentage of 2D2 cells in the CNS, from 0% at day 4 to 32.7% \pm 6.4% at day 8 and then 67.5% \pm 10.7% at the peak of the disease (Figure 5A). Altogether, those data demonstrate that CNS-specific Th17 cells migrate and infiltrate the large intestine during the preclinical phase of transfer EAE before reaching the CNS.

To assess whether TCR^{MOG} 2D2 Th17 cells detected in the gut display encephalitogenic properties, we evaluated the level of

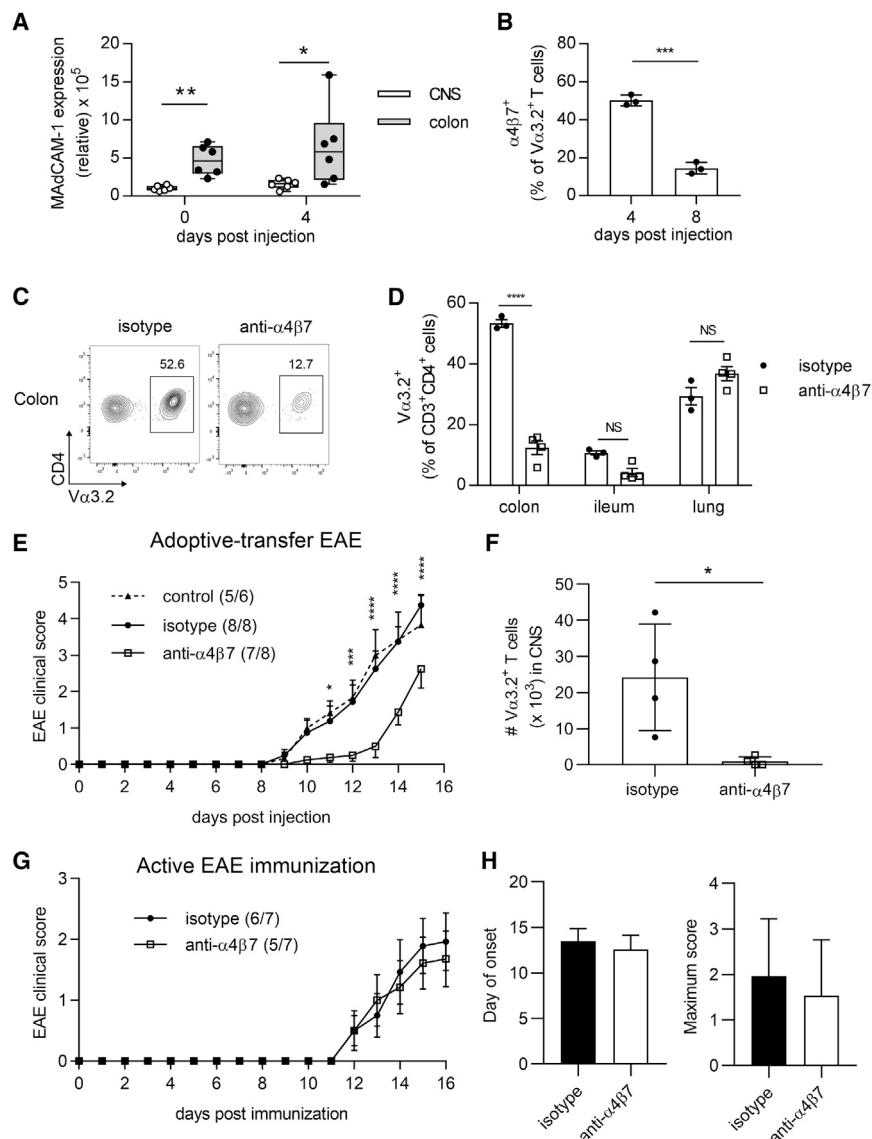


Figure 4. Blocking $\alpha 4\beta 7$ -Integrin Reduces Migration of Encephalitogenic TCR^{MOG} 2D2 Cells to the Colon and Delays the Progression of EAE Disease

(A) Relative mRNA expression of MACCAM-1 in CNS and colonic tissue as measured by real-time PCR in non-injected mice (day 0) and four days after TCR^{MOG} 2D2 Th17 cell injection. Box-and-whisker graphs show median, minimum (min.), and maximum (max.) values and 25th and 75th percentiles (n = 6).

(B) Flow cytometry analysis of the total proportion (as a percentage) of the $\alpha 4\beta 7$ -integrin expression in colonic TCR^{MOG} 2D2 ($V\alpha 3.2^+$) $CD4^+$ T cells at the indicated time points after TCR^{MOG} 2D2 Th17 cell injection (mean \pm SD; n = 3). Data are representative of two independent experiments.

(C and D) Representative flow cytometry analysis of TCR^{MOG} 2D2 ($V\alpha 3.2^+$) expression in $CD3^+$ / $CD4^+$ T cells obtained from the colonic lamina of mice treated with an isotype control (C) versus the anti- $\alpha 4\beta 7$ -integrin flow cytometry analysis of the TCR^{MOG} 2D2 ($V\alpha 3.2^+$) proportions in $CD4^+$ T cells obtained from the colon, ileum, and lung in isotype control versus the anti- $\alpha 4\beta 7$ -treated group at day 4 after TCR^{MOG} 2D2 Th17 cell transfer (mean \pm SEM; n = 3–4) (D). Data are representative of two independent experiments.

(E) Clinical scores of EAE in adoptively transferred mice treated with PBS 1 \times , isotype control, or anti- $\alpha 4\beta 7$ antibodies. The course of EAE in these mice is shown as a clinical score (mean \pm SEM; n = 6–8; p values are shown for comparison between anti- $\alpha 4\beta 7$ versus isotype groups). Data are representative of three independent experiments.

(F) Absolute numbers of TCR^{MOG} 2D2 Th17 cells infiltrating the CNS 10 days after adoptive transfer in mice treated with isotype control or anti- $\alpha 4\beta 7$ antibodies (mean \pm SD; n = 4). Data are representative of two independent experiments.

(G and H) Active EAE with mice injected either anti- $\alpha 4\beta 7$ antibodies or isotype control every 3 days. The active EAE course is shown as (G) clinical scores (mean \pm SEM; n = 7 per group), (H) day of disease onset (mean \pm SD; n = 5–6), and maximum scores (mean \pm SD; n = 7). Data are representative of one experiment.

*p < 0.05, **p < 0.01, ***p < 0.001, ****p < 0.0001; NS, not significant; p values were determined by unpaired Student's t test (A, B, and F), two-way ANOVA with Sidak's post hoc test (D), and Tukey's post hoc test (E). See also Figure S2 and Table S1.

$\alpha 4\beta 1$ -integrin (CNS-specific integrin) 4 days after T cell transfer. $\alpha 4\beta 1$ -integrin was expressed at levels similar to those of $\alpha 4\beta 7$ -integrin, which is known to be gut specific (Figure 5B). However, $\alpha 4\beta 1$ -integrin ligand vascular cell adhesion molecule-1 (VCAM-1) was expressed solely in the CNS, not in the colon (Figure 5C). In addition, $\alpha 4\beta 1$ -integrin expression decreases on TCR^{MOG} 2D2 Th17 cells of the colon over time, whereas the expression remained high in the CNS when the TCR^{MOG} 2D2 reached the CNS (Figure 5D). Those results strengthen our hypothesis that TCR^{MOG} 2D2 Th17 cells depict encephalitogenic properties while present in the colon.

Different Th17 cell subsets have been described in the colon, including the homeostatic Th17 cells co-expressing both Foxp3 and ROR γ T (Solomon and Hsieh, 2016) and the pathogenic Th17

cells that do not express Foxp3. Thus, we evaluated the phenotypic profile of the TCR^{MOG} 2D2 Th17 cells detected in the colonic lamina propria. Four days after injection, colonic lamina propria $V\alpha 3.2^+$ $CD4^+$ T cells were analyzed by flow cytometry for ROR γ T, Foxp3, T-bet, and IL-17A expression. TCR^{MOG} 2D2 Th17 cells maintained ROR γ T expression, whereas neither T-bet nor Foxp3 expression was detected (Figure 5E). We conducted our analysis at different time points after T cell transfer and observed a reduction of the total frequencies of ROR γ T⁺ 2D2⁺ cells (Figure 5F). However, the residual colonic 2D2⁺ $CD4^+$ T cells kept their capacity to secrete the pro-inflammatory IL-17 cytokine in colonic lamina propria at all time points examined (Figures S3A and S3B). In addition, Foxp3 and ROR γ T co-expressing Th17 cells and Foxp3⁺ ROR γ T⁻ regulatory T cells

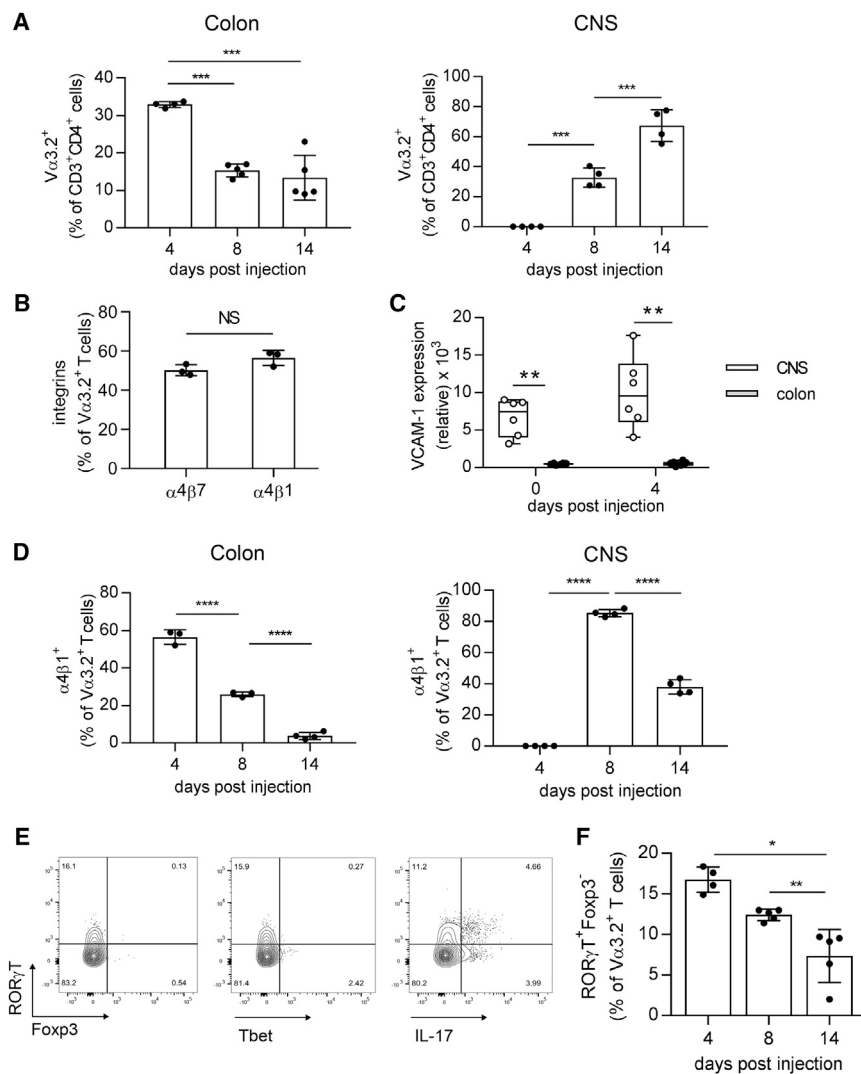


Figure 5. Encephalitogenic TCR^{MOG} 2D2 Th17 Cells Infiltrate the Large Intestine and Express CNS-Specific Integrin before Reaching the CNS

(A) Flow cytometry analysis of the total proportion (as a percentage) of TCR^{MOG} 2D2 ($V\alpha 3.2^+$) expression in $CD3^+/CD4^+$ T cells of colonic lamina propria and CNS at the indicated time points after TCR^{MOG} 2D2 Th17 cell transfer (mean \pm SD; n = 4–5). Data are representative of two independent experiments.

(B) Flow cytometry analysis of the total proportion (as a percentage) of $\alpha 4\beta 7$ -integrin and $\alpha 4\beta 1$ -integrin expression in colonic TCR^{MOG} 2D2 ($V\alpha 3.2^+$) $CD4^+$ T cells four days after TCR^{MOG} 2D2 Th17 cell injection (mean \pm SD; n = 3). Data are representative of two independent experiments.

(C) Relative mRNA expression of VCAM-1 in CNS and colonic tissue as measured by real-time PCR in non-injected mice (day 0) and four days after TCR^{MOG} 2D2 Th17 cell injection. Box-and-whisker graphs show median, min., and max. values and 25th and 75th percentiles (n = 6).

(D) Flow cytometry analysis of the total proportion (as a percentage) of the $\alpha 4\beta 1$ -integrin expression of TCR^{MOG} 2D2 ($V\alpha 3.2^+$) $CD4^+$ T cells in the colon and the CNS at the indicated time points after TCR^{MOG} 2D2 Th17 cell injection (mean \pm SD; n = 3). Data are representative of two independent experiments.

(E) Representative flow cytometry analysis of $ROR\gamma T^+/Foxp3^-$, $ROR\gamma T^+/Tbet$, and $ROR\gamma T^+/IL-17^+$ expression in TCR^{MOG} 2D2 ($V\alpha 3.2^+$) $CD4^+$ T cells obtained from the colonic lamina propria of EAE mice at day 4 after TCR^{MOG} 2D2 Th17 cell transfer.

(F) Time course of transferred TCR^{MOG} 2D2 analyzed by flow cytometry for $ROR\gamma T^+/Foxp3^-$ intracellular expression and shown as a percentage of the $V\alpha 3.2^+$ T cell population (mean \pm SD; n = 4–5). Data are representative of two independent experiments.

*p < 0.05, **p < 0.01, ***p < 0.001, ****p < 0.0001; NS, not significant; p values were determined by one-way ANOVA with Tukey's post hoc test (A, D, and F) and unpaired Student's t test (B and C). See also Figure S3.

were both restricted to $V\alpha 3.2^-CD4^+$ T cells ($2D2^-$), and their frequencies were not affected by time (Figure S3C). We thus demonstrated that TCR^{MOG} 2D2 Th17 cells were predominantly detected in the large intestine before reaching the CNS and maintained their pro-inflammatory phenotype after *in vivo* transfer.

Encephalitogenic TCR^{MOG} 2D2 Th17 Cells Proliferate in the Large Intestine

Having established that TCR^{MOG} 2D2 cells are detected in the colonic lamina propria, we explored their fate within the large intestine and evaluated their proliferative status with Ki67 staining. FACS analysis demonstrated that almost 100% of TCR^{MOG} 2D2 cells proliferated in the colonic lamina propria 4 days after T cell transfer. This proliferation rate significantly decreased to less than 20% 8 days post-transfer (Figure 6A). In comparison,

$V\alpha 3.2^-CD4^+$ T cells (host cells) showed a constant proliferation rate of 25% with no significant changes between day 4 and day 8 (Figure 6A).

We assessed the location of proliferating TCR^{MOG} 2D2 cells in the colon by whole-mount immunostaining (Figure 6B). At day 4, 30% of TCR^{MOG} 2D2 detected above the lumen-adjacent blood vessel (lumen, yellow line in Figure 6B) were $Ki67^+$, whereas only 15% of TCR^{MOG} 2D2 cells were located below the lumen-adjacent blood vessel (stroma cells). In agreement with FACS analysis, less than 5% of total TCR^{MOG} 2D2 cells were $Ki67^+$ at day 8 after injection, regardless of location (Figure 6C). However, among $Ki67^+$ TCR^{MOG} 2D2 cells at both day 4 and day 8, approximately two-thirds of $Ki67^+$ cells were found near the colon lumen (Figure 6D). These results show that TCR^{MOG} 2D2 cells proliferated at the maximum rate 4 days after T cell transfer and are found near colonic lumen.

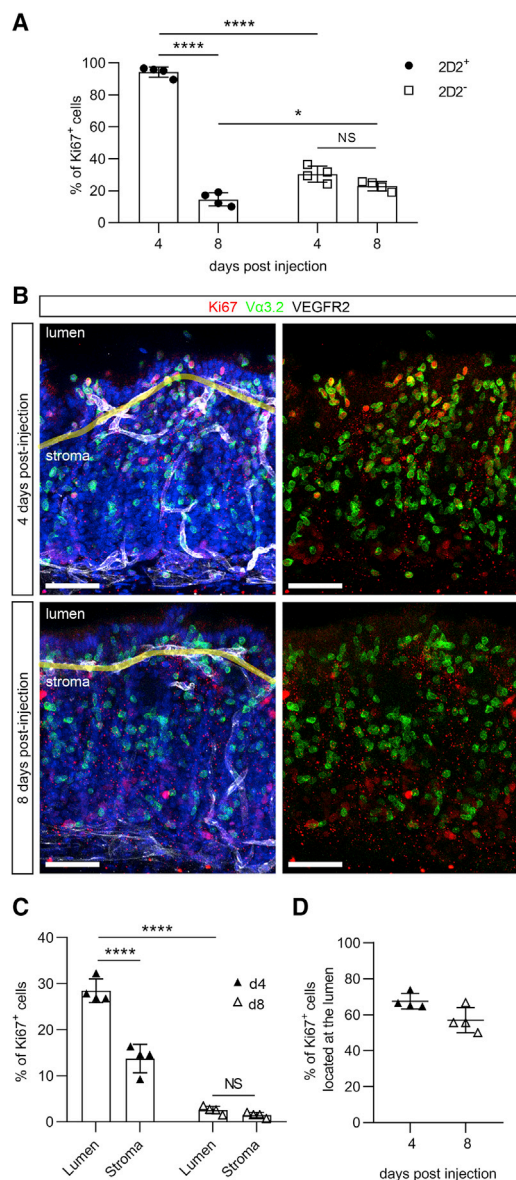


Figure 6. Encephalitogenic TCR^{MOG} 2D2 Th17 Cells Proliferate in the Colon

(A) Flow cytometry analysis of proliferating *Ki67*⁺ cells (as a percentage) among *2D2*⁺*TCR* (*Vα3.2*⁺) and *2D2*⁻*TCR* (*Vα3.2*⁻) *CD4*⁺ T cells within colonic lamina propria at the indicated time points after T cell transfer (mean ± SD; n = 4). Data are shown from one of three independent experiments with similar results. (B) Whole-mount immunostaining of proliferating cells (*Ki67*⁺, red), TCR^{MOG} 2D2 cells (*Vα3.2*⁺, green), and blood vessels (white, VEGFR2); blue, DAPI. *Vα3.2*⁺ T cells observed above the lumen-adjacent blood vessel (yellow line) were considered lumen T cells, and cells located below were considered stroma T cells. (C) Quantification of the percentage and location (mean ± SD; n = 4) of *Ki67*⁺ TCR^{MOG} 2D2⁺ cells in the colon 4 and 8 days after T cell transfer. Data are shown from a single experiment in which Th17 cells obtained at day 4 and day 8 were injected at the same time. (D) Quantification of the percentage of *Ki67*⁺ TCR^{MOG} 2D2⁺ cells located at the lumen (mean ± SD; n = 4). Data are shown from a single experiment. Scale bars: (B) 50 μm. *p < 0.05, **p < 0.01, ***p < 0.001, ****p < 0.0001; NS, not significant; p values were determined by two-way ANOVA with Tukey's post hoc test (A and C).

Encephalitogenic TCR^{MOG} 2D2 Th17 Cells Induce an Intestinal Dysbiosis, and Antibiotic Treatments Decrease the Encephalitogenic Properties of Th17 Cells

We hypothesized that factors present in the colonic lumen, more specifically gut microbiota, could affect TCR^{MOG} 2D2 T cells. We thus evaluated whether TCR^{MOG} 2D2 were influenced by and/or could affect intestinal microbial composition, because changes in gut microbiota composition were reported in other EAE models (Berer et al., 2011; Lavasani et al., 2010; Lee et al., 2011; Ochoa-Repáraz et al., 2009, 2010). We performed meta-taxonomic analysis by sequencing of 16S ribosomal RNA gene amplicons from fecal samples of the same recipient mice before and 9 days after, when mice were still clinically asymptomatic, TCR^{MOG} 2D2 Th17 cell transfer. Analysis of the Shannon index revealed that TCR^{MOG} 2D2 Th17 cell transfer significantly increased the diversity of the gut microbiota (Figure 7A). Analysis of the variance among microbial communities showed that TCR^{MOG} 2D2 T cell transfer resulted in markedly different (permutational multivariate analysis of variance [PERMANOVA], p = 0.0009) gut microbial communities (Figure 7B). Analysis of the microbiota at various taxonomic levels showed a shift in the gut microbiota composition after Th17 cell transfer, including an increase in phyla with gram-negative cell wall structure (Proteobacteria and Bacteroidetes) and a decrease of the gram-negative bacteria belonging to the class Bacilli (Firmicutes). In the Bacteroidetes phylum, genus *Alistipes* and several operational taxonomic units (OTUs) of the Bacteroidales order increased in relative abundance after TCR^{MOG} 2D2 Th17 cell transfer. In the Firmicutes phylum, the proportion of genus *Lactobacillus* and three OTUs assigned to it decreased significantly following adoptive transfer (Figure 7C; Table S2). Concomitantly, several members of the Clostridiales order, including the family *Ruminococcaceae*, an OTU from the family *Lachnospiraceae*, and the genera *Eisenbergiella*, KE159538, *Eubacterium*, *Oscillibacter*, and *Pseudoflavonifractor*, increased in relative abundance.

To evaluate whether the TCR^{MOG} 2D2 Th17 cells required the presence of microbiota to induce EAE, we injected TCR^{MOG} 2D2 Th17 cells into antibiotic-treated mice. The antibiotic treatment, used to eliminate a broad bacteria community (Zaiss et al., 2015), significantly reduced EAE severity (Figure 7D) without impairing the ability of TCR^{MOG} 2D2 T cells to infiltrate the colon (Figure S4). We then wondered whether blocking Th17 cell colonic migration and antibiotic treatment could have additive effects. We treated mice with antibiotics and administered anti- $\alpha4\beta7$ or control isotype antibody (Figure 7E). Antibiotic treatment reduced EAE severity; however, blocking the $\alpha4\beta7$ -integrin and its ligand MA6CAM-1 pathway did not enhance the protective effect of antibiotic treatment, thus orienting our interpretation toward an interdependent role for the intestinal microbiome and anti- $\alpha4\beta7$ treatment.

In summary, in TCR^{MOG} 2D2 Th17 cell adoptive-transfer EAE, Th17 cells migrate and proliferate at the highest level in the large intestine at the preclinical stage of EAE disease. Myelin-specific Th17 cells change gut microbiota composition. Finally, blocking myelin-specific Th17 cell entry into the colon or disrupting gut microbiota with antibiotic treatments dampens EAE development.

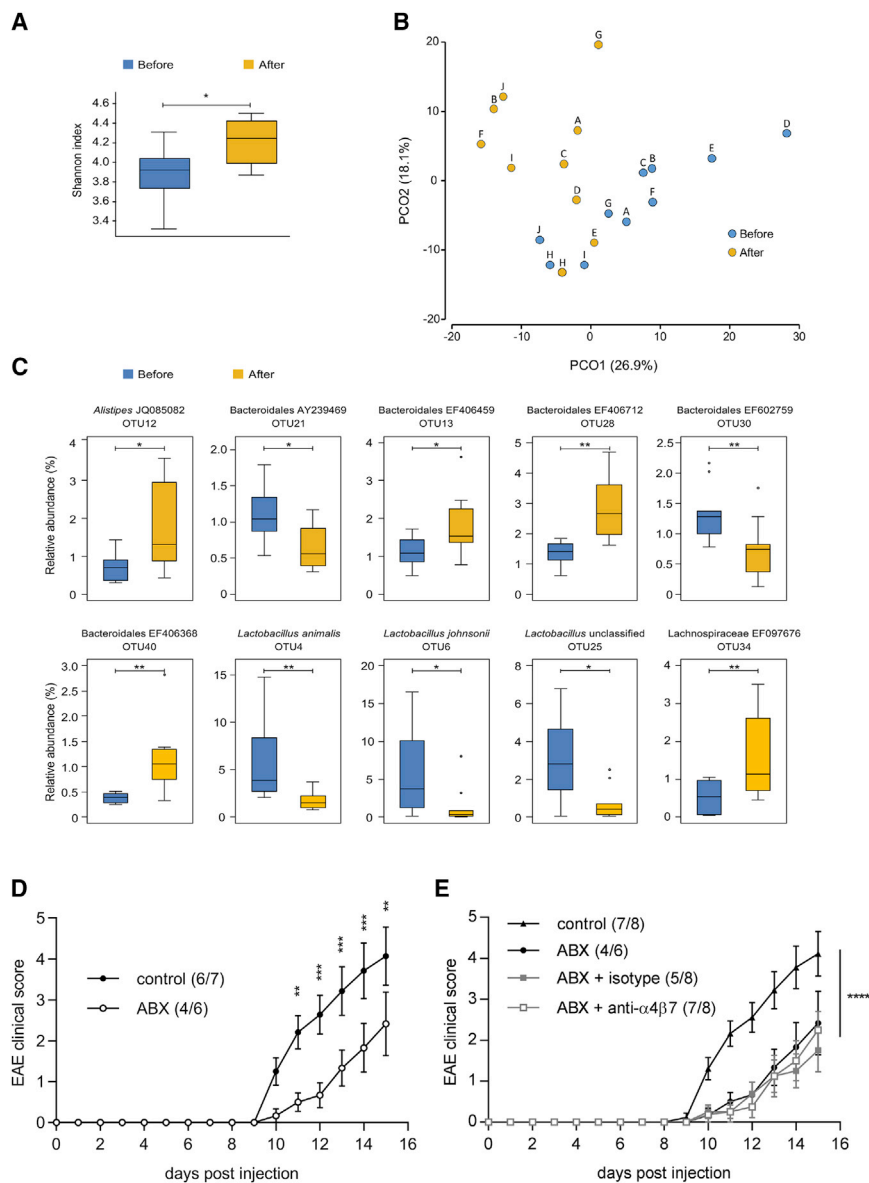


Figure 7. Encephalitogenic TCR^{MOG} 2D2 Th17 Cells Affect Gut Microbiota Composition

(A) Alpha diversity. The Shannon diversity index was based on the relative abundance of OTUs.

(B) Principal coordinates analysis (PCoA) of Bray-Curtis similarities based on the square root-transformed relative abundance of OTUs. Stool samples obtained from the same mouse before and after T cell transfer are indicated by the same alphabetic character (A–J).

(C) OTUs differentially represented before and after injection of TCR^{MOG} 2D2 Th17 cells. Only OTUs with significant changes ($p < 0.05$) and an average relative abundance $> 1\%$ in at least one of the two groups are presented. Boxplots show the first to third quartiles (bottom and top of the box) divided by the median. The highest and lowest values in the $1.5 \times$ interquartile range are indicated by whiskers. Circles indicate outliers.

(D) Clinical scores of EAE in mice adoptively transferred with TCR^{MOG} 2D2 Th17 cells and treated with or without antibiotics (ABX). The course of EAE is shown as a clinical score (mean \pm SEM; $n = 6-7$). Data are representative of two independent experiments.

(E) Clinical scores of EAE in adoptively transferred mice treated with antibiotics (ABX), ABX and isotype control, or ABX and anti- $\alpha 4\beta 7$ antibodies. Data are representative of one experiment.

* $p < 0.05$, ** $p < 0.01$, *** $p < 0.001$, **** $p < 0.0001$; p values were determined by Wilcoxon signed-rank test (A and C) and two-way ANOVA with Sidak's (D) and Tukey's (E) post hoc test. See also Figure S4 and Table S2.

biota composition. Antibiotic treatment dampens EAE development in the Th17 cell adoptive-transfer EAE model. However, blocking the $\alpha 4\beta 7$ -integrin and its ligand MAdCAM-1 pathway does not synergize with the beneficial effect of antibiotic treatments. These data strongly suggest that during CNS autoimmunity, encephalitogenic Th17 cells enter the large intestine, where their pro-inflammatory functions are strengthened at least partially by gut microbiota changes.

DISCUSSION

The implication of the gut-brain axis has received growing attention in the field of neuroimmunology, with recent works showing Th17 cell accumulation in the small intestine, as well as intestinal dysbiosis, in MS patients (Cosorich et al., 2017). However, whether those findings are a consequence of neuroinflammation or instead they affect the development of neuroinflammation remains disputed. We report here that CNS-specific Th17 cells migrate to the intestine during EAE. Furthermore, blocking the $\alpha 4\beta 7$ -integrin and its ligand MAdCAM-1 pathway not only limits intestinal Th17 cell infiltration, to a large extent in the large intestine, but also significantly dampens EAE severity in an adoptive-transfer model. Mechanistically, myelin-specific Th17 cells proliferate in the gut and alter gut micro-

An association between MS and IBD has been described in humans (Gupta et al., 2005), as has an increased risk of MS and IBD comorbidity (Kosmidou et al., 2017). Animal models have demonstrated a crucial role for gut-homing effector T cells in IBD, and mice lacking $\beta 7$ -integrin have fewer intestinal T cells as a consequence of a reduced rate of migration to the gut (Steeber et al., 1998; Wagner et al., 1996). Moreover, $\alpha 4\beta 7$ -integrin-blocking antibodies attenuate mouse models of intestinal inflammation and are clinically effective in the treatment of human ulcerative colitis and Crohn's disease (Feagan et al., 2005; Picarella et al., 1997). Combined anti- $\alpha 4$ -integrin (natalizumab), blocking both $\alpha 4\beta 1$ /VCAM-1 and $\alpha 4\beta 7$ -integrin and its ligand MAdCAM-1 interactions, is effective, in addition to

intestinal inflammatory diseases, in targeting both MS and EAE (Brandstadter and Katz Sand, 2017; Steinman, 2012; Yednock et al., 1992). For MS, the effect is attributed specifically to the $\alpha 4\beta 1$ inhibition directly in the CNS. Indeed, the impact of $\alpha 4\beta 7$ -integrin and its ligand MAdCAM-1 interactions in neuroinflammation remains controversial, and studies specifically addressing their role in EAE pathogenesis have led to inconsistent results. Using the SJL/N mouse strain, Engelhardt and colleagues found no effect of anti- $\alpha 4\beta 7$ - or anti- $\beta 7$ -neutralizing antibodies on the development of EAE (Engelhardt et al., 1998). Similarly, vedolizumab does not prevent CNS inflammation or demyelination in a rhesus monkey EAE model (Haanstra et al., 2013). In apparent contrast, $\beta 7$ -integrin-deficient C57BL/6 mice are partially resistant to adoptive EAE transfer and to neutralizing antibodies against MAdCAM-1 (Kanwar et al., 2000a, 2000b). Furthermore, the development of active EAE is attenuated in MAdCAM-1-knockout (KO) mice, whereas MAdCAM-1 blockade 5 days after immunization does not attenuate EAE (Kuhbandner et al., 2019). Indeed, the timing of intestinal T cell blocking is relevant. We observe that anti- $\alpha 4\beta 7$ treatment is efficient when administered only until the appearance of the first neurological signs and that the extension of the treatment during the entire EAE disease course did not enhance its protective effect. Those results are in accordance with our observation of significant TCR^{MOG} 2D2 Th17 cell colonic proliferation at 4 days, but not at 8 days, after T cell transfer. Furthermore, the observed differences in the previous publications can be attributed to the use of different mouse strains and to methodological differences in inducing EAE that may or may not favor Th17 cell polarization. We show here that blocking $\alpha 4\beta 7$ -integrin inhibits Th17 cell entry into the colonic lamina propria during adoptive transfer EAE and contributes to a reduction of neurological symptoms. We did not observe an impact of anti- $\alpha 4\beta 7$ treatment in the active EAE model, suggesting that in the absence of a MOG-CFA depot, Th17 cells depend more on gut for their activation. Alternatively, the MOG-CFA model depends on both Th1 and Th17 cells, whereas in the adoptive transfer, we used purified 2D2 Th17 cells. However, the differences obtained between the two EAE models remain to be investigated, as does the initial localization of Th17 cell activation/reactivation during autoimmunity in humans. We propose that the colon might be a niche for reactivation and proliferation of immune cells during EAE, in particular for Th17 cells. The effect on myelin-specific Th17 cells observed in the colon during EAE could be related to their production of the IL-17 cytokine family more than on their antigen specificity. This would be in accordance with the intrinsic properties of IL-17A as modulators of microbiota composition (Douzandeh-Mobarrez and Kariminik, 2019). Because IL-17 cytokines can be produced not only by adaptive immune cells but also by other cell types (ILC3 and $\gamma\delta$ T cells), it remains to be elucidated whether IL-17 family cytokines, such as IL-17A, could per se affect neuroinflammation independent of their cellular sources.

Whether MAdCAM-1, an intestinal protein, is also expressed in the CNS and thus contributes to our observation has been debated (Allavena et al., 2010; O'Neill et al., 1991; Steffen et al., 1994, 1996; Vercellino et al., 2008). We detected low levels of MAdCAM-1 mRNA in the CNS at lower rates compared with

the colon. MAdCAM-1, if expressed in the CNS, is expressed at a low level and has been shown not to contribute to neuroinflammation (Döring et al., 2011). In addition, even ectopic expression of MAdCAM-1 on the blood-brain barrier does not influence EAE in the C57BL/6J model (Döring et al., 2011). This corroborates with the publication from Korn and colleagues that proposed, in an adoptive-transfer EAE model, that Th17 lymphocytes reach the CNS independent of $\alpha 4$ -integrin expression during EAE (Rothhammer et al., 2011). Here we observed a beneficial effect on neuroinflammation when blocking $\alpha 4\beta 7$ -integrin and its ligand MAdCAM-1 interactions. However, the beneficial effect was transient. This could be a consequence of the insufficient blocking of Th17 cell trafficking in the small intestine and the colon. Lymphocyte migration to the gut is controlled by additional chemoattractant receptors, such as the C-C motif chemokine receptor 9 (CCR9) for the small intestine or the orphan G-protein-coupled receptor 15 (GPR15) for the colon (Habtezion et al., 2016). Concomitant blocking of CCR9/GPR15/chemokine interaction could contribute to evaluation of the role of the intestine in driving EAE.

Gut mucosa harbors the highest concentration of immune cells in the body, and studies in humans and mice suggested that the small intestine is a possible location for the generation, activation, and expansion of effector T cells that cause autoimmune responses (Nouri et al., 2014). However, it is unclear how mucosal immune responses elicited in the gut modulate CNS inflammation and whether the large intestine is further involved in EAE pathogenesis. Our observations that myelin-specific Th17 cells preferentially infiltrate the large intestine further demonstrate the occurrence of compartmentalization and suggest the existence of distinctive mechanisms of autoimmune cell recruitment that may allow functional specialization of immune responses in different segments of the intestine.

Th17 cell adoptive-transfer EAE had a notable effect on gut microbiota composition, with a decreased representation of the Firmicutes phylum, in particular of the proportion of the *Lactobacillus* species that have been associated with beneficial effects, including inflammatory immune response reduction during EAE (Umbrello and Esposito, 2016). We observed a significant reduction in *L. johnsonii*, which are known to have immunomodulatory properties (Owaga et al., 2015). Interestingly, *L. johnsonii* are induced by intermittent fasting, which dampens EAE severity (Cignarella et al., 2018). Intestinal microbiota have been proposed to contribute to the accumulation or activation of Th17 cells in the intestine (Goto et al., 2014; Yang et al., 2014b). In the context of neuroinflammation, commensal species residing in the small intestine affect the development of the disease in humans and in their mouse models. Encephalitogenic Th17 cells can be generated in the gut with segmented filamentous bacteria monoclonization (Lee et al., 2011), whereas *Bacteroides* species or colonic clostridia, respectively, suppress IL-17 production or support the development of regulatory T cells (Wekerle et al., 2013). Here we show that antibiotic treatment was sufficient to dampen neurological disease in the adoptive transfer EAE model and that blocking $\alpha 4\beta 7$ -integrin and its ligand MAdCAM-1 interactions was not beneficial in the context of antibiotic treatment. Those results suggest an intrinsic relationship between CNS-specific Th17 cells and intestinal microbiota

composition. However, the precise mechanisms of the gut flora-Th17 cell interactions remain to be studied.

In summary, CNS antigen-specific Th17 cells infiltrate the large intestine and depict high proliferating properties in this organ during EAE. Specifically targeting Th17 cell migration to the large intestine by blocking $\alpha 4\beta 7$ -integrin and its ligand MAdCAM-1 interactions attenuates EAE disease interdependently with the microbiota composition. Our results thus contribute to reevaluation of the gut as a target during CNS autoimmunity.

STAR★METHODS

Detailed methods are provided in the online version of this paper and include the following:

- KEY RESOURCES TABLE
- LEAD CONTACT AND MATERIALS AVAILABILITY
- EXPERIMENTAL MODEL AND SUBJECT DETAILS
- METHOD DETAILS
 - EAE induction and clinical evaluation
 - Antibody treatment
 - Antibiotic treatment
 - Isolation of immune cells
 - Flow cytometric analysis
 - Tetramer staining
 - RNA isolation and quantitative PCR analysis
 - Whole-mount immunostaining
 - Microbiome Analysis
- QUANTIFICATION AND STATISTICAL ANALYSIS
- DATA AND CODE AVAILABILITY

SUPPLEMENTAL INFORMATION

Supplemental Information can be found online at <https://doi.org/10.1016/j.celrep.2019.09.002>.

ACKNOWLEDGMENTS

We thank the Service of Immunology and Allergy, Department of Medicine, of the Lausanne University Hospital for daily support. We thank Myriam Girard for technical assistance. Animal, Cellular Imaging, Mouse Pathology and Genomic Technology Facilities of the University of Lausanne are gratefully acknowledged. This work was supported by the Swiss National Science Foundation (PP00P3_157476 to C.P.) and the Leenaards Foundation (to C.P. and T.V.P.). F.R. holds a grant from the Swiss National Science Foundation (323630-183987).

AUTHOR CONTRIBUTIONS

Conceptualization, D.D., S.V., J.B.-L., and C.P.; Methodology, D.D., S.V., and J.B.-L.; Investigation, D.D., S.V., J.B.-L., Y.Y., F.R., N.G., S.L., and V.L.; Writing – Original Draft, D.D., S.V., J.B.-L., and C.P.; Writing – Review & Editing, D.D., S.V., C.P., J.B.-L., V.L., J.S., and T.V.P.; Resources, T.V.P. and C.P.; Funding Acquisition, T.V.P. and C.P.

DECLARATION OF INTERESTS

The authors declare no competing interests.

Received: December 10, 2018

Revised: June 17, 2019

Accepted: August 30, 2019

Published: October 8, 2019

REFERENCES

- Allavena, R., Noy, S., Andrews, M., and Pullen, N. (2010). CNS elevation of vascular and not mucosal addressin cell adhesion molecules in patients with multiple sclerosis. *Am. J. Pathol.* *176*, 556–562.
- Berer, K., Mues, M., Koutrolos, M., Rasbi, Z.A., Boziki, M., Johner, C., Wekerle, H., and Krishnamoorthy, G. (2011). Commensal microbiota and myelin autoantigen cooperate to trigger autoimmune demyelination. *Nature* *479*, 538–541.
- Berer, K., Gerdes, L.A., Cekanaviciute, E., Jia, X., Xiao, L., Xia, Z., Liu, C., Klotz, L., Stauffer, U., Baranzini, S.E., et al. (2017). Gut microbiota from multiple sclerosis patients enables spontaneous autoimmune encephalomyelitis in mice. *Proc. Natl. Acad. Sci. USA* *114*, 10719–10724.
- Bernier-Latmani, J., and Petrova, T.V. (2016). High-resolution 3D analysis of mouse small-intestinal stroma. *Nat. Protoc.* *11*, 1617–1629.
- Bernier-Latmani, J., and Petrova, T.V. (2017). Intestinal lymphatic vasculature: structure, mechanisms and functions. *Nat. Rev. Gastroenterol. Hepatol.* *14*, 510–526.
- Bettelli, E., Pagany, M., Weiner, H.L., Linington, C., Sobel, R.A., and Kuchroo, V.K. (2003). Myelin oligodendrocyte glycoprotein-specific T cell receptor transgenic mice develop spontaneous autoimmune optic neuritis. *J. Exp. Med.* *197*, 1073–1081.
- Bouillaguet, S., Manoil, D., Girard, M., Louis, J., Gaïa, N., Leo, S., Schrenzel, J., and Lazarevic, V. (2018). Root Microbiota in Primary and Secondary Apical Periodontitis. *Front. Microbiol.* *9*, 2374.
- Brandstadter, R., and Katz Sand, I. (2017). The use of natalizumab for multiple sclerosis. *Neuropsychiatr. Dis. Treat.* *13*, 1691–1702.
- Cignarella, F., Cantoni, C., Ghezzi, L., Salter, A., Dorsett, Y., Chen, L., Phillips, D., Weinstock, G.M., Fontana, L., Cross, A.H., et al. (2018). Intermittent Fasting Confers Protection in CNS Autoimmunity by Altering the Gut Microbiota. *Cell Metab* *27*, 1222–1235.e6.
- Cosorich, I., Dalla-Costa, G., Sorini, C., Ferrarese, R., Messina, M.J., Dolpady, J., Radice, E., Mariani, A., Testoni, P.A., Canducci, F., et al. (2017). High frequency of intestinal T_H17 cells correlates with microbiota alterations and disease activity in multiple sclerosis. *Sci. Adv.* *3*, e1700492.
- Döring, A., Pfeiffer, F., Meier, M., Dehouck, B., Tauber, S., Deutsch, U., and Engelhardt, B. (2011). TET inducible expression of the $\alpha 4\beta 7$ -integrin ligand MAdCAM-1 on the blood-brain barrier does not influence the immunopathogenesis of experimental autoimmune encephalomyelitis. *Eur. J. Immunol.* *41*, 813–821.
- Douzandeh-Mobarrez, B., and Kariminik, A. (2019). Gut Microbiota and IL-17A: Physiological and Pathological Responses. *Probiotics Antimicrob. Proteins* *11*, 1–10.
- Edgar, R.C. (2010). Search and clustering orders of magnitude faster than BLAST. *Bioinformatics* *26*, 2460–2461.
- Engelhardt, B., Laschinger, M., Schulz, M., Samulowitz, U., Vestweber, D., and Hoch, G. (1998). The development of experimental autoimmune encephalomyelitis in the mouse requires alpha4-integrin but not alpha4beta7-integrin. *J. Clin. Invest.* *102*, 2096–2105.
- Feagan, B.G., Greenberg, G.R., Wild, G., Fedorak, R.N., Paré, P., McDonald, J.W., Dubé, R., Cohen, A., Steinhart, A.H., Landau, S., et al. (2005). Treatment of ulcerative colitis with a humanized antibody to the alpha4beta7 integrin. *N. Engl. J. Med.* *352*, 2499–2507.
- Flügel, A., Berkowicz, T., Ritter, T., Labeur, M., Jenne, D.E., Li, Z., Ellwart, J.W., Willem, M., Lassmann, H., and Wekerle, H. (2001). Migratory activity and functional changes of green fluorescent effector cells before and during experimental autoimmune encephalomyelitis. *Immunity* *14*, 547–560.
- Gorfu, G., Rivera-Nieves, J., and Ley, K. (2009). Role of beta7 integrins in intestinal lymphocyte homing and retention. *Curr. Mol. Med.* *9*, 836–850.
- Goto, Y., Panea, C., Nakato, G., Cebula, A., Lee, C., Diez, M.G., Laufer, T.M., Ignatowicz, L., and Ivanov, I.I. (2014). Segmented filamentous bacteria antigens presented by intestinal dendritic cells drive mucosal Th17 cell differentiation. *Immunity* *40*, 594–607.

- Gupta, G., Gelfand, J.M., and Lewis, J.D. (2005). Increased risk for demyelinating diseases in patients with inflammatory bowel disease. *Gastroenterology* 129, 819–826.
- Haanstra, K.G., Hofman, S.O., Lopes Estêvão, D.M., Blezer, E.L., Bauer, J., Yang, L.L., Wyant, T., Csizmadia, V., 't Hart, B.A., and Fedyk, E.R. (2013). Antagonizing the $\alpha 4\beta 1$ integrin, but not $\alpha 4\beta 7$, inhibits leukocytic infiltration of the central nervous system in rhesus monkey experimental autoimmune encephalomyelitis. *J. Immunol.* 190, 1961–1973.
- Habtezion, A., Nguyen, L.P., Hadeiba, H., and Butcher, E.C. (2016). Leukocyte Trafficking to the Small Intestine and Colon. *Gastroenterology* 150, 340–354.
- Jäger, A., Dardalhon, V., Sobel, R.A., Bettelli, E., and Kuchroo, V.K. (2009). Th1, Th17, and Th9 Effector Cells Induce Experimental Autoimmune Encephalomyelitis with Different Pathological Phenotypes. *J. Immunol.* 183, 7169–7177.
- Kanayama, M., Danzaki, K., He, Y.W., and Shinohara, M.L. (2016). Lung inflammation stalls Th17-cell migration en route to the central nervous system during the development of experimental autoimmune encephalomyelitis. *Int. Immunol.* 28, 463–469.
- Kanwar, J.R., Harrison, J.E., Wang, D., Leung, E., Mueller, W., Wagner, N., and Krissansen, G.W. (2000a). Beta7 integrins contribute to demyelinating disease of the central nervous system. *J. Neuroimmunol.* 103, 146–152.
- Kanwar, J.R., Kanwar, R.K., Wang, D., and Krissansen, G.W. (2000b). Prevention of a chronic progressive form of experimental autoimmune encephalomyelitis by an antibody against mucosal addressin cell adhesion molecule-1, given early in the course of disease progression. *Immunol. Cell Biol.* 78, 641–645.
- Kassiotis, G., and Stockinger, B. (2004). Anatomical heterogeneity of memory CD4+ T cells due to reversible adaptation to the microenvironment. *J. Immunol.* 173, 7292–7298.
- Korn, T., Bettelli, E., Oukka, M., and Kuchroo, V.K. (2009). IL-17 and Th17 Cells. *Annu. Rev. Immunol.* 27, 485–517.
- Kosmidou, M., Katsanos, A.H., Katsanos, K.H., Kyritsis, A.P., Tsivgoulis, G., Christodoulou, D., and Giannopoulos, S. (2017). Multiple sclerosis and inflammatory bowel diseases: a systematic review and meta-analysis. *J. Neurol.* 264, 254–259.
- Kuhbandner, K., Hammer, A., Haase, S., Terbrack, E., Hoffmann, A., Schippers, A., Wagner, N., Hussain, R.Z., Miller-Little, W.A., Koh, A.Y., et al. (2019). MAdCAM-1-Mediated Intestinal Lymphocyte Homing Is Critical for the Development of Active Experimental Autoimmune Encephalomyelitis. *Front. Immunol.* 10, 903.
- Lam, M.C., and Bressler, B. (2014). Vedolizumab for ulcerative colitis and Crohn's disease: results and implications of GEMINI studies. *Immunotherapy* 6, 963–971.
- Lavasani, S., Dzhambazov, B., Nouri, M., Fåk, F., Buske, S., Molin, G., Thorlacius, H., Alenfall, J., Jeppsson, B., and Weström, B. (2010). A novel probiotic mixture exerts a therapeutic effect on experimental autoimmune encephalomyelitis mediated by IL-10 producing regulatory T cells. *PLoS ONE* 5, e9009.
- Lazarevic, V., Gaïa, N., Girard, M., and Schrenzel, J. (2016). Decontamination of 16S rRNA gene amplicon sequence datasets based on bacterial load assessment by qPCR. *BMC Microbiol.* 16, 73.
- Lee, Y.K., Menezes, J.S., Umesaki, Y., and Mazmanian, S.K. (2011). Proinflammatory T-cell responses to gut microbiota promote experimental autoimmune encephalomyelitis. *Proc. Natl. Acad. Sci. USA* 108 (Suppl 1), 4615–4622.
- McLean, L.P., Shea-Donohue, T., and Cross, R.K. (2012). Vedolizumab for the treatment of ulcerative colitis and Crohn's disease. *Immunotherapy* 4, 883–898.
- Miyake, S., and Yamamura, T. (2019). Gut environmental factors and multiple sclerosis. *J. Neuroimmunol.* 329, 20–23.
- Mu, Q., Kirby, J., Reilly, C.M., and Luo, X.M. (2017). Leaky Gut As a Danger Signal for Autoimmune Diseases. *Front. Immunol.* 8, 598.
- Mycko, M.P., Cichalewska, M., Cwiklinska, H., and Selmaj, K.W. (2015). miR-155-3p Drives the Development of Autoimmune Demyelination by Regulation of Heat Shock Protein 40. *J. Neurosci.* 35, 16504–16515.
- Nouri, M., Bredberg, A., Weström, B., and Lavasani, S. (2014). Intestinal barrier dysfunction develops at the onset of experimental autoimmune encephalomyelitis, and can be induced by adoptive transfer of auto-reactive T cells. *PLoS ONE* 9, e106335.
- O'Neill, J.K., Butter, C., Baker, D., Gschmeissner, S.E., Kraal, G., Butcher, E.C., and Turk, J.L. (1991). Expression of vascular addressins and ICAM-1 by endothelial cells in the spinal cord during chronic relapsing experimental allergic encephalomyelitis in the Biozzi AB/H mouse. *Immunology* 72, 520–525.
- Ochoa-Repáraz, J., Mielcarz, D.W., Ditrio, L.E., Burroughs, A.R., Foureau, D.M., Haque-Begum, S., and Kasper, L.H. (2009). Role of gut commensal microflora in the development of experimental autoimmune encephalomyelitis. *J. Immunol.* 183, 6041–6050.
- Ochoa-Repáraz, J., Mielcarz, D.W., Haque-Begum, S., and Kasper, L.H. (2010). Induction of a regulatory B cell population in experimental allergic encephalomyelitis by alteration of the gut commensal microflora. *Gut Microbes* 1, 103–108.
- Odoardi, F., Sie, C., Streyl, K., Ulaganathan, V.K., Schläger, C., Lodygin, D., Heckelsmiller, K., Nietfeld, W., Ellwart, J., Klinkert, W.E., et al. (2012). T cells become licensed in the lung to enter the central nervous system. *Nature* 488, 675–679.
- Olsson, T., Barcellos, L.F., and Alfredsson, L. (2017). Interactions between genetic, lifestyle and environmental risk factors for multiple sclerosis. *Nat. Rev. Neurol.* 13, 25–36.
- Opazo, M.C., Ortega-Rocha, E.M., Coronado-Arrázola, I., Bonifaz, L.C., Boudin, H., Neunlist, M., Bueno, S.M., Kalergis, A.M., and Riedel, C.A. (2018). Intestinal Microbiota Influences Non-intestinal Related Autoimmune Diseases. *Front. Microbiol.* 9, 432.
- Owaga, E., Hsieh, R.H., Mugendi, B., Masuku, S., Shih, C.K., and Chang, J.S. (2015). Th17 Cells as Potential Probiotic Therapeutic Targets in Inflammatory Bowel Diseases. *Int. J. Mol. Sci.* 16, 20841–20858.
- Papadakis, K.A., and Targan, S.R. (2000). Role of cytokines in the pathogenesis of inflammatory bowel disease. *Annu. Rev. Med.* 51, 289–298.
- Peters, A., Fowler, K.D., Chalmin, F., Merkler, D., Kuchroo, V.K., and Pot, C. (2015). IL-27 Induces Th17 Differentiation in the Absence of STAT1 Signaling. *J. Immunol.* 195, 4144–4153.
- Picarella, D., Hurlbut, P., Rottman, J., Shi, X., Butcher, E., and Ringler, D.J. (1997). Monoclonal antibodies specific for beta 7 integrin and mucosal addressin cell adhesion molecule-1 (MAdCAM-1) reduce inflammation in the colon of scid mice reconstituted with CD45RBhigh CD4+ T cells. *J. Immunol.* 158, 2099–2106.
- Rothhammer, V., Heink, S., Petermann, F., Srivastava, R., Claussen, M.C., Hemmer, B., and Korn, T. (2011). Th17 lymphocytes traffic to the central nervous system independently of $\alpha 4$ integrin expression during EAE. *J. Exp. Med.* 208, 2465–2476.
- Salmi, M., and Jalkanen, S. (2005). Lymphocyte homing to the gut: attraction, adhesion, and commitment. *Immunol. Rev.* 206, 100–113.
- Schloss, P.D., Westcott, S.L., Ryabin, T., Hall, J.R., Hartmann, M., Hollister, E.B., Lesniewski, R.A., Oakley, B.B., Parks, D.H., Robinson, C.J., et al. (2009). Introducing mothur: open-source, platform-independent, community-supported software for describing and comparing microbial communities. *Appl. Environ. Microbiol.* 75, 7537–7541.
- Solomon, B.D., and Hsieh, C.S. (2016). Antigen-Specific Development of Mucosal Foxp3+ROR γ t+ T Cells from Regulatory T Cell Precursors. *J. Immunol.* 197, 3512–3519.
- Steeber, D.A., Tang, M.L., Zhang, X.Q., Müller, W., Wagner, N., and Tedder, T.F. (1998). Efficient lymphocyte migration across high endothelial venules of mouse Peyer's patches requires overlapping expression of L-selectin and beta7 integrin. *J. Immunol.* 161, 6638–6647.
- Steffen, B.J., Butcher, E.C., and Engelhardt, B. (1994). Evidence for involvement of ICAM-1 and VCAM-1 in lymphocyte interaction with endothelium in experimental autoimmune encephalomyelitis in the central nervous system in the SJL/J mouse. *Am. J. Pathol.* 145, 189–201.

- Steffen, B.J., Breier, G., Butcher, E.C., Schulz, M., and Engelhardt, B. (1996). ICAM-1, VCAM-1, and MAdCAM-1 are expressed on choroid plexus epithelium but not endothelium and mediate binding of lymphocytes *in vitro*. *Am. J. Pathol.* *148*, 1819–1838.
- Steinman, L. (2012). The discovery of natalizumab, a potent therapeutic for multiple sclerosis. *J. Cell Biol.* *199*, 413–416.
- Tilg, H., and Kaser, A. (2010). Vedolizumab, a humanized mAb against the $\alpha 4\beta 7$ integrin for the potential treatment of ulcerative colitis and Crohn's disease. *Curr. Opin. Investig. Drugs* *11*, 1295–1304.
- Umbrello, G., and Esposito, S. (2016). Microbiota and neurologic diseases: potential effects of probiotics. *J. Transl. Med.* *14*, 298.
- van den Hoogen, W.J., Laman, J.D., and 't Hart, B.A. (2017). Modulation of Multiple Sclerosis and Its Animal Model Experimental Autoimmune Encephalomyelitis by Food and Gut Microbiota. *Front. Immunol.* *8*, 1081.
- Vercellino, M., Votta, B., Condello, C., Piacentino, C., Romagnolo, A., Merola, A., Capello, E., Mancardi, G.L., Mutani, R., Giordana, M.T., and Cavalla, P. (2008). Involvement of the choroid plexus in multiple sclerosis autoimmune inflammation: a neuropathological study. *J. Neuroimmunol.* *199*, 133–141.
- Wagner, N., Löhler, J., Kunkel, E.J., Ley, K., Leung, E., Krissansen, G., Rajewsky, K., and Müller, W. (1996). Critical role for beta7 integrins in formation of the gut-associated lymphoid tissue. *Nature* *382*, 366–370.
- Wekerle, H., Berer, K., and Krishnamoorthy, G. (2013). Remote control-triggering of brain autoimmune disease in the gut. *Curr. Opin. Immunol.* *25*, 683–689.
- Yang, B., Treweek, J.B., Kulkarni, R.P., Deverman, B.E., Chen, C.K., Lubeck, E., Shah, S., Cai, L., and Gradinaru, V. (2014a). Single-cell phenotyping within transparent intact tissue through whole-body clearing. *Cell* *158*, 945–958.
- Yang, Y., Torchinsky, M.B., Gobert, M., Xiong, H., Xu, M., Linehan, J.L., Alonzo, F., Ng, C., Chen, A., Lin, X., et al. (2014b). Focused specificity of intestinal TH17 cells towards commensal bacterial antigens. *Nature* *510*, 152–156.
- Yednock, T.A., Cannon, C., Fritz, L.C., Sanchez-Madrid, F., Steinman, L., and Karin, N. (1992). Prevention of experimental autoimmune encephalomyelitis by antibodies against alpha 4 beta 1 integrin. *Nature* *356*, 63–66.
- Yoon, S.-H., Ha, S.-M., Kwon, S., Lim, J., Kim, Y., Seo, H., and Chun, J. (2017). Introducing EzBioCloud: a taxonomically united database of 16S rRNA gene sequences and whole-genome assemblies. *Int. J. Syst. Evol. Microbiol.* *67*, 1613–1617.
- Zaiss, M.M., Rapin, A., Lebon, L., Dubey, L.K., Mosconi, I., Sarter, K., Piersigilli, A., Menin, L., Walker, A.W., Rougemont, J., et al. (2015). The Intestinal Microbiota Contributes to the Ability of Helminths to Modulate Allergic Inflammation. *Immunity* *43*, 998–1010.
- Zhang, J., Kobert, K., Flouri, T., and Stamatakis, A. (2014). PEAR: a fast and accurate Illumina Paired-End reAd mergeR. *Bioinformatics* *30*, 614–620.

STAR★METHODS

KEY RESOURCES TABLE

REAGENT or RESOURCE	SOURCE	IDENTIFIER
Antibodies		
BV510 anti-CD45 (clone 30-F11)	BioLegend	Cat#: 103138; RRID: AB_2563061
PE anti-LPAM-1 (integrin $\alpha 4\beta 7$) (clone DATK32)	BioLegend	Cat#: 120606; RRID: AB_493267
APC-eFluor 780 anti-CD3e (clone 145-2C11)	eBiosciences	Cat#: 47-0031-82; RRID: AB_11149861
Alexa Fluor 700 anti-CD4 (clone GK1.5)	eBiosciences	Cat#: 56-0041-82; RRID: AB_493999
PE anti-IL-17A (clone eBio17B7)	eBiosciences	Cat#: 12-7177-81; RRID: AB_763582
Alexa Fluor 488 anti-IFN γ (clone XMG1.2)	eBiosciences	Cat#: 53-7311-82; RRID: AB_469932
PE anti-T-bet (clone eBio4B10)	eBiosciences	Cat#: 12-5825-82; RRID: AB_925761
APC anti-TCR V $\alpha 3.2$ (clone RR3-16)	eBiosciences	Cat#: 17-5799-82; RRID: AB_10854272
eFluor 450 anti-CD29 (clone HMB1-1)	eBiosciences	Cat#: 48-0291-82; RRID: AB_11218304
PECy7 anti-Foxp3 (clone FJK-16 s)	eBiosciences	Cat#: 25-5773-82; RRID: AB_891552
BV421 anti-ROR γ T (clone Q31-378)	BD Biosciences	Cat#: 562894; RRID: AB_2687545
AF488 anti-CD49d (clone PS/2)	BioRad	Cat#: MCA1230A488; RRID: AB_566805
AF647 anti-CD45.1 (clone A20)	BioLegend	Cat#: 110720; RRID: AB_492864
PE anti-CD45.2 (clone 104)	eBiosciences	Cat#: 12-0454-82; RRID: AB_465678
FITC Ki67 (clone SolA15)	eBiosciences	Cat# 11-5698-82; RRID:AB_11151330
anti-CD3e (clone 145-2C11)	BioLegend	Cat#: 100302; RRID: AB_312667
anti-VEGFR2	R&D Systems	Cat#: AF644; RRID: AB_355500
anti-Lyve-1	Reliatech	Cat# 103-PA50; RRID: AB_2783787
anti-Ki67	Abcam	Cat# ab15580; RRID:AB_443209
DyLight 488 anti-hamster IgG (clone Poly4055)	BioLegend	Cat#: 405503; RRID: AB_1575117
AF555 anti-goat IgG	Life Technologies	Cat#: A-21432; RRID: AB_2535853
anti-CD16/CD32 (clone 93)	Invitrogen	Cat#: 16-0161-85; RRID: AB_468899
anti-CD3e (clone 145-2C11)	BioXcell	Cat#: BE0001-1; RRID: AB_1107634
anti-CD28 (clone 37.51)	BioXcell	Cat#: BE0015-1; RRID: AB_1107624
anti-LPAM-1 (integrin $\alpha 4\beta 7$) (clone DATK32)	BioXcell	Cat#: BE0034; RRID: AB_1107713
anti-trinitrophenol IgG2a isotype control (clone 2A3)	BioXcell	Cat#: BE0089; RRID: AB_1107769
PE I-A ^b MOG ₃₅₋₅₅ Tetramer	MBL	Cat#: TS-M704-1
Chemicals, Peptides, and Recombinant Proteins		
MOG ₃₅₋₅₅ peptide	Anawa	Cat#: 000-001-M41
Adjuvant, Complete H37 Ra	BD Difco	Cat#: 231131
M. tuberculosis H37 Ra, desiccated	BD Difco	Cat#: 231141
Pertussis toxin	Sigma Aldrich	Cat#: P2980
Liberase TL	Roche	Cat#: 5401020001
DNase I recombinant	Roche	Cat#: 4716728001
DNase I	Roche	Cat#: 10104159001
RNaseA	Roche	Cat#: R4875
Collagenase D	Roche	Cat#: 11088866001
Percoll	GE Healthcare	Cat#: 17089101
PMA (Phorbol 12-myristate 13-acetate)	Sigma Aldrich	Cat#: P8139
Ionomycin	Sigma Aldrich	Cat#: I9657
Brefeldin A	Sigma Aldrich	Cat#: B7651
Fixable Viability Dye eFluor 660	eBioscience	Cat#: 65-0864-14
DAPI	Sigma-Aldrich	Cat#: D9542

(Continued on next page)

Continued

REAGENT or RESOURCE	SOURCE	IDENTIFIER
Critical Commercial Assays		
Foxp3 / Transcription Factor Staining Buffer Set	eBioscience	Cat#: 00-5523-00
RNeasy Mini Kit	QIAGEN	Cat#: 74104
Superscript II RT	Invitrogen	Cat#: 18064014
PowerUp SYBR Green Master Mix	Applied Biosystems	Cat#: A25742
MagCore Genomic DNA Tissue Kit	RBC Bioscience	Cat#: MGT-01
Experimental Models: Organisms/Strains		
Mouse: C57BL/6-Tg(Tcra2D2,Tcrb2D2)1Kuch/J	The Jackson Laboratory	Stock#: 006912
Mouse: C57BL/6-Tg(TcraTcrb)425Cbn/Crl	The Jackson Laboratory	Stock#: 004194
Mouse: C57BL/6J	The Jackson Laboratory	Stock#: 000664
Oligonucleotides		
See Table S3		N/A
Software and Algorithms		
FlowJo software version 10.5.3	Tree Star	https://www.flowjo.com/solutions/flowjo/downloads
GraphPad Prism version 7.0	GraphPad software	https://www.graphpad.com/scientific-software/prism/
Imaris	Bitplane	https://imaris.oxinst.com/downloads
Fiji	ImageJ	https://imagej.net/Fiji/Downloads
Other		
StepOne Real-Time PCR System	Applied Biosystems	N/A
BD LSR II	BD Biosciences	N/A
Zeiss LSM 880	Carl Zeiss	N/A
MagCore HF16	RBC Bioscience	N/A

LEAD CONTACT AND MATERIALS AVAILABILITY

Further information and requests for resources and reagents should be directed to and will be fulfilled by the Lead Contact, Caroline Pot (Caroline.Pot-kreis@chuv.ch). This study did not generate new unique reagents.

EXPERIMENTAL MODEL AND SUBJECT DETAILS

C57BL/6J mice were purchased from Charles River or bred in the animal facility. C57BL/6-Tg(Tcra2D2,Tcrb2D2)1Kuch/J (TCR^{MOG} 2D2) and C57BL/6-Tg(TcraTcrb)425Cbn/Crl (OT-II) transgenic mice were purchased from Charles River. All mice used were females aged from 8 to 10 weeks and were maintained under specific-pathogen free conditions at Lausanne University Hospital. All experiments were performed in accordance with guidelines from the Cantonal Veterinary Service of state Vaud.

METHOD DETAILS

EAE induction and clinical evaluation

For induction of classical active EAE, mice were immunized with 100 µg myelin oligodendrocyte glycoprotein peptide 35-55 (MOG₃₅₋₅₅) or PBS emulsified in complete Freund's adjuvant supplemented with 5 mg/ml *Mycobacterium tuberculosis* H37Ra. A total of 200 µl emulsion was subcutaneously injected into four sites on the flanks of mice. At days 0 and 2 after initial peptide injections, animals received additional intravenous injection of 100 ng pertussis toxin. For induction of EAE by adoptive transfer, naive CD4⁺ T cells from 2D2 mice were polarized *in vitro* in Th17 or Th1 cells as previously described (Jäger et al., 2009). Differentiation status was checked on day 5 and after 2 days of restimulation with anti-mouse CD3/CD28 antibodies (2 µg/ml), 8 × 10⁶ CD4⁺ T cells were injected intraperitoneal (i.p.) into wild-type C57BL/6J recipient mice. Mice were scored daily for clinical symptoms. The classical EAE symptoms were assessed according to the following score: score 0 – no disease; score 0.5 – reduced tail tonus; score 1 – limp tail; score 1.5 – impaired righting reflex; score 2 – limp tail, hind limb weakness; score 2.5 – at least one hind limb paralyzed; score 3 – both hind limbs paralyzed; score 3.5 – complete paralysis of hind limbs; score 4 – paralysis until hip; score 5 – moribund or dead. The atypical EAE symptoms were assessed according to the following score: score 0 – no disease; score 1 – head turned slightly (ataxia, no tail paralysis); score 2 – head turned more pronounced; score 3 – inability to walk on a straight

line; score 4 – laying on side; score 4.5 – rolling continuously unless supported; score 5 – moribund or dead. Combined score compiling typical and atypical scoring has also been applied and considers the highest score from the typical or atypical clinical signs (Peters et al., 2015). Mice were euthanized if they reached a score > 3.

Antibody treatment

For homing experiment, mice were injected i.p. with 400 μ g of anti-mouse α 4 β 7 (DATK 32) or isotype control antibodies (IgG2a isotype control, 2A3) one day before TCR^{MOG} 2D2 Th17 cell injection and every three days post-injection until the development of disease or as indicated.

Antibiotic treatment

Mice were treated with 2.5 mg/ml enrofloxacin in drinking water for 2 weeks, followed by 0.8 mg/ml of amoxicillin and 0.114 mg/ml clavulanic acid in drinking water for 2 further weeks (Zaiss et al., 2015) prior to TCR^{MOG} 2D2 Th17 cell injection. Treatment with amoxicillin and clavulanic acid was then continued throughout the experiment.

Isolation of immune cells

Mice were perfused through cardiac ventricle with Phosphate-buffered saline (PBS) 1 \times . Whole colon, 15 cm-long pieces of terminal ileum and whole lung were excised and washed in PBS 1 \times . Gut was opened longitudinally. Washed gut and lung pieces were cut into 2 cm pieces and incubated for 20 min at 37°C in HBSS containing 10 mM EDTA under gentle agitation (80 rpm). Tissues were washed by vortexing with PBS 1 \times . Organ pieces were then incubated 2 times at 37°C for 20 min in a dissociation mix composed of 5 mL HBSS, Liberase TL (1 Wünsch unit/mL) and DNase I recombinant (1 U/mL) and 2% fetal calf serum (FCS). The remaining tissue pieces were mechanically disaggregated on a 70 μ m cell strainer using a syringe plunger. For the preparation of CNS mononuclear cells, brain and spinal cord were cut into pieces and digested 45 min at 37°C with collagenase D (2.5mg/ml) and DNase I (1mg/ml) followed by 70%/37% Percoll gradient centrifugation. For the preparation of lymph nodes, organs were removed and single cell suspensions were prepared by disaggregation of the tissues through a 70 μ m cell strainer. The cellular suspensions were washed and filtered through 40 μ m cell strainer and resuspended in culture medium for further analysis.

Flow cytometric analysis

Single-cell suspensions in PBS 1 \times were stained with fixable viability dye eFluorTM 660. For cell surface stainings, cells were preincubated with anti-CD16/32 for 10 min to block Fc receptors and stained in FACS buffer (PBS containing 1% BSA) with directly labeled monoclonal antibodies for 30 min. For intracellular cytokine staining, cells were activated for 4 h with 50 ng/ml PMA, 1 μ g/ml ionomycin in the presence of 10 mg/ml brefeldin A. After surface staining, cells were fixed and permeabilized using Foxp3/transcription factor staining buffer set and stained intracellularly with directly labeled monoclonal antibodies for 30 min. Data were acquired on a LSR II cytometer and all data were analyzed using FlowJo software. Fluorochrome-conjugated antibodies were purchased from several commercial sources indicated below and listed in the [Key Resources Table](#). Antibodies against CD45 (30-F11), α 4 β 7 (DATK32), CD45.1 (A20) were from Biolegend; CD3 (145-2C11), CD4 (GK1.5), IL-17 (ebio17B7), IFN- γ (XMG1.2), T-bet (eBio4B10), Foxp3 (clone FJK-16 s), TCRV α 3.2 (RR3-16), CD29 (β 1) (HMb1-1), CD45.2 (104), Ki67 (SolA15) were from eBiosciences; ROR γ T (Q31-378) was from BD Biosciences and CD49d (α 4) (PS/2) was from Biorad.

Tetramer staining

Cellular suspensions from colon and CNS were prepared as previously described from immunized and non-immunized mice at the peak of the disease. Cells were stimulated 4h with 10 μ g/ml of MOG₃₅₋₅₅ peptide in the presence of hIL-2 (50U/mL). I-A^b MOG₃₅₋₅₅ tetramer-positive CD4⁺ T cells were detected by flow cytometry after surface staining with corresponding directly labeled I-A^b MOG₃₅₋₅₅ tetramer.

RNA isolation and quantitative PCR analysis

RNA was extracted from tissue samples using RNeasy Mini Kit following the manufacturer's instructions. cDNA was produced from equivalent amounts of RNA with the Superscript II RT (Invitrogen) and the PCR products were amplified with the PowerUp SYBR Green Master Mix. Samples were detected on the StepOne Real-Time PCR System. β -actin was used to normalize samples and the comparative CT method was used to quantify relative mRNA expression. Expression of specific gene transcripts was measured by using the following primer pairs: IL-6, 5'-CCCCAATTTCCAATGCTCTCC-3' and 5'-CGCACTAGGTTTGCCGAGTA-3'; IL-1 β , 5'-TGCCACCTTTTGACAGTG ATG-3' and 5'-TGATACTGCCTGCCTGAA GC-3'; TNF- α , 5'-AAGCTCCTCAGCGAGGA CAG-3' and 5'-TGGTTGGCTGCTTGCTTTTC-3'; MAdCAM-1, 5'-ACAGACCAGACCTCACCTA-3', and 5'-TGATGTTGAGCCCA GTGGAG-3'; VCAM-1, 5'-CTGGGAAGCTGGAACGAAGT-3' and 5'-GCCAAACACTTGACCGTGAC-3', β -actin, 5'-AAGTGTGAC GTTGACATCCGTAATA-3' and 5'-CAGCTCAGTAACAGTCCGCTAGA-3'.

Whole-mount immunostaining

Whole-mount immunostaining was performed as previously described (Bernier-Latmani and Petrova, 2016). Briefly, mice were perfused with 4% paraformaldehyde and intestines were fixed in picric acid fixation buffer. Colon immunostaining was performed

with DAPI (1:4000) and the following primary and secondary antibodies: CD3 ϵ (145-2C11, 1:1000), VEGFR2 (1:100), LYVE1 (1:500), Ki67 (1:200), V α 3.2-APC (1:100), goat anti-Armenian hamster DyLight 488 (1:500) and donkey anti-goat AlexaFluor 555 (1:500). After immunostaining the colon was cut into ~0.5 mm thick strips which were cleared and mounted in RIMS Buffer (Yang et al., 2014a) on a microscope slide fitted with 0.1 mm spacers (Molecular Probes). Image acquisition was performed on a Zeiss LSM 880 confocal microscope and image analysis and 3D reconstruction was performed with Imaris (Bitplane) and Fiji.

Microbiome Analysis

Two weeks prior the experiment, mice were randomized in cages of two mice. A fecal pellet (9–50 mg) was mixed with 550 μ L GT buffer (RBS Bioscience) and homogenized in a Nucleospin Bead Tube (Machery-Nagel, Düren, Germany) for 20 min at maximum speed on a Vortex-Genie 2 with a horizontal tube holder (Scientific Industries). After addition of 1 μ L of 50 mg/mL RNaseA, samples were incubated at room temperature for 5 min and centrifuged for 2 min at 11,000 \times g. DNA was extracted from 400 μ L of the supernatant using the MagCore Genomic DNA Tissue kit on a MagCore HF16 instrument and eluted in 100 μ L of 10 mM Tris-HCl pH 8. Two negative extraction controls were processed in parallel with fecal pellets by omitting addition of biological material in the GT buffer. Purified DNA was stored at -20°C . The V3–4 region of the bacterial 16S rRNA genes was amplified using 2 ng of extracted DNA (or 5 μ L of the eluate from negative extraction control) as described before (Bouillaguet et al., 2018), except 30 PCR cycles were used. The amplicon barcoding/purification and MiSeq (2 \times 300) sequencing were performed at LGC Genomics (Berlin, Germany) as previously described (Lazarevic et al., 2016). After removal of adaptor remnants and primer sequences from demultiplexed fastq files using proprietary LGC Genomics software, sequencing data were submitted to European Nucleotide Archive (ENA) database. Clustering of quality filtered merged reads into OTUs and taxonomic assignments of representative OTUs using mothur (Schloss et al., 2009) and EzBioCloud database (Yoon et al., 2017) were performed following a pipeline described previously (Bouillaguet et al., 2018), with modified commande options in PEAR (Zhang et al., 2014) (-m 450 -t 250) and USEARCH (Edgar, 2010) (-usearch_global -wordlength 30). Principal Coordinates Analysis (PCoA) of Bray–Curtis similarity, based on the square-root transformed relative abundance of OTUs was performed in PRIMER (Primer-E Ltd., Plymouth, UK). Shannon diversity index ($H' = -\sum (p_i \times \ln p_i)$) was calculated in PRIMER from the relative abundance of OTUs (p_i).

QUANTIFICATION AND STATISTICAL ANALYSIS

Data analyses and graphs were performed using GraphPad Prism 7.0 software. P values < 0.05 were considered significant. Results are displayed as mean and SEM or mean and SD, as described in the figure legends. Differences in microbiota between before and after adoptive transfer EAE were assessed using PERmutational Multivariate Analysis Of Variance (PERMANOVA) (PRIMER) with 9,999 permutations. Wilcoxon signed-rank test was used for statistical comparisons of individual taxa, with a confidence level set at 95% ($p < 0.05$).

DATA AND CODE AVAILABILITY

The fastq files containing sequencing reads generated during this study are available at European Nucleotide Archive (ENA) database under study number PRJEB 29544; <https://www.ebi.ac.uk/ena/data/view/PRJEB29544>.

This study did not generate/analyze code.

Cell Reports, Volume 29

Supplemental Information

Disrupting Myelin-Specific Th17 Cell Gut Homing

Confers Protection in an Adoptive Transfer

Experimental Autoimmune Encephalomyelitis

Donovan Duc, Solenne Vigne, Jeremiah Bernier-Latmani, Yannick Yersin, Florian Ruiz, Nadia Gaïa, Stefano Leo, Vladimir Lazarevic, Jacques Schrenzel, Tatiana V. Petrova, and Caroline Pot

Figure S1, related to Figure 3

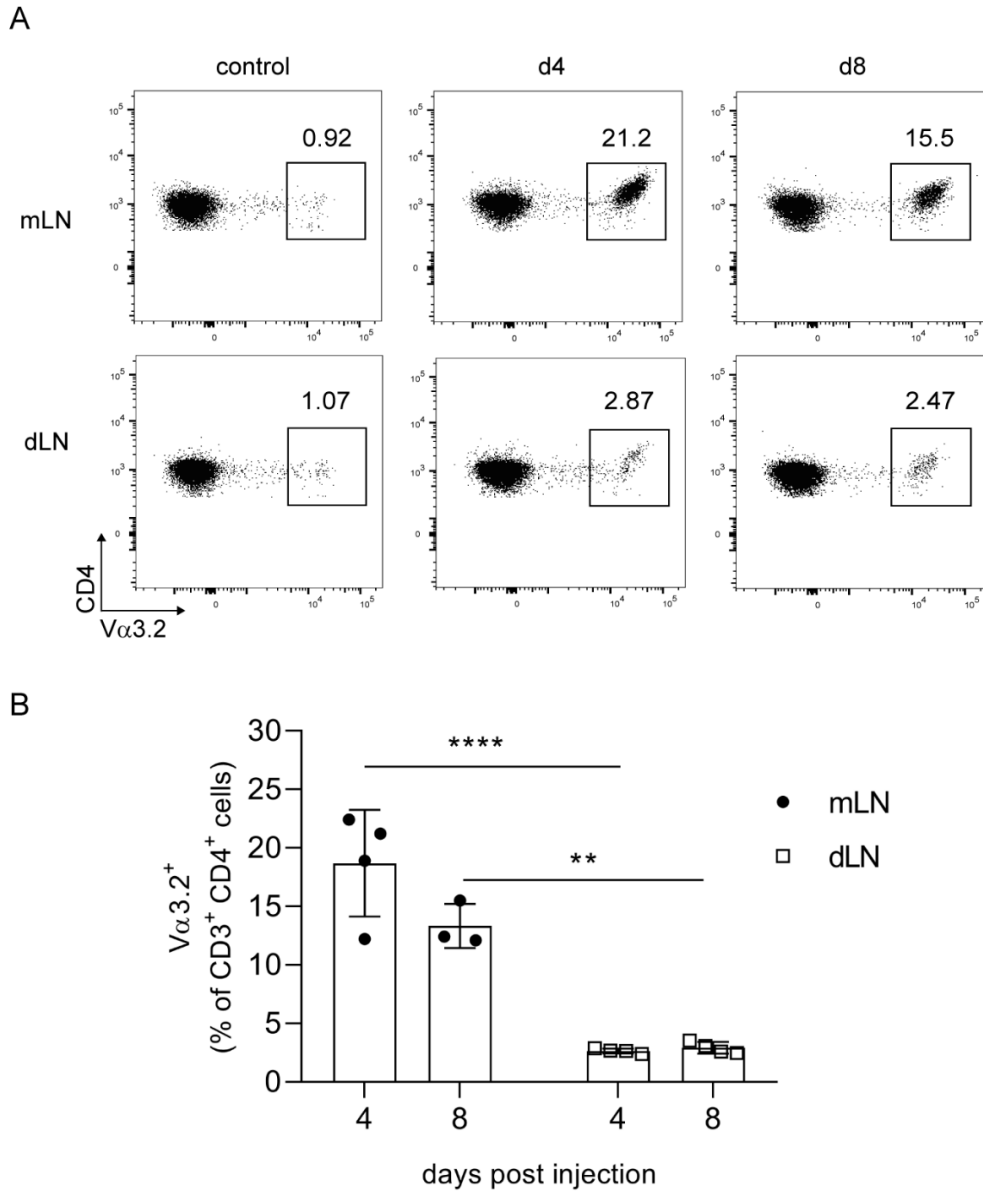


Figure S1, related to Figure 3: Encephalitogenic TCR^{MOG} 2D2 Th17 cells migrated through the mesenteric lymph nodes but not the dermal inguinal lymph nodes.

(A) Representative flow cytometry analysis of 2D2-TCR (Vα3.2⁺) expression in CD3⁺/CD4⁺ T cells from mesenteric lymph nodes (mLN) and dermal inguinal lymph nodes (dLN) isolated from PBS-injected (control) mice and from mice injected with TCR^{MOG} 2D2 Th17 cells at 4 days (d4) and 8 days (d8) post injection.

(B) Flow cytometry analysis of the total proportion (%) of 2D2-TCR (Vα3.2⁺) expression in CD3⁺/CD4⁺ T cells of mLN and dLN at the indicated time points after TCR^{MOG} 2D2 Th17 cells transfer (mean ± SD; n = 3-4). *, P < 0.05; **, P < 0.01; ***, P < 0.001, ****, P < 0.0001; P values were determined by two-way ANOVA with Tukey's post hoc test (B).

Figure S2, related to Figure 4

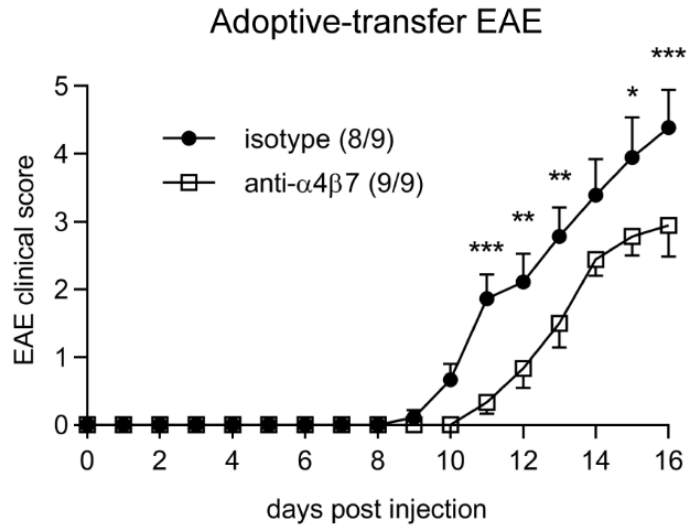


Figure S2, related to Figure 4: Continuously blocking of $\alpha 4\beta 7$ -integrin alleviates adoptive-transfer EAE but not active EAE.

Clinical scores of Th17 adoptive-transfer EAE mice treated with anti- $\alpha 4\beta 7$ antibodies or isotype control every 3 days until the end of the experiment (mean \pm SEM; $n = 9$ per group). *, $P < 0.05$; **, $P < 0.01$; ***, $P < 0.001$; P values were determined by two-way ANOVA with Sidak's post hoc test.

Figure S3, related to Figure 5

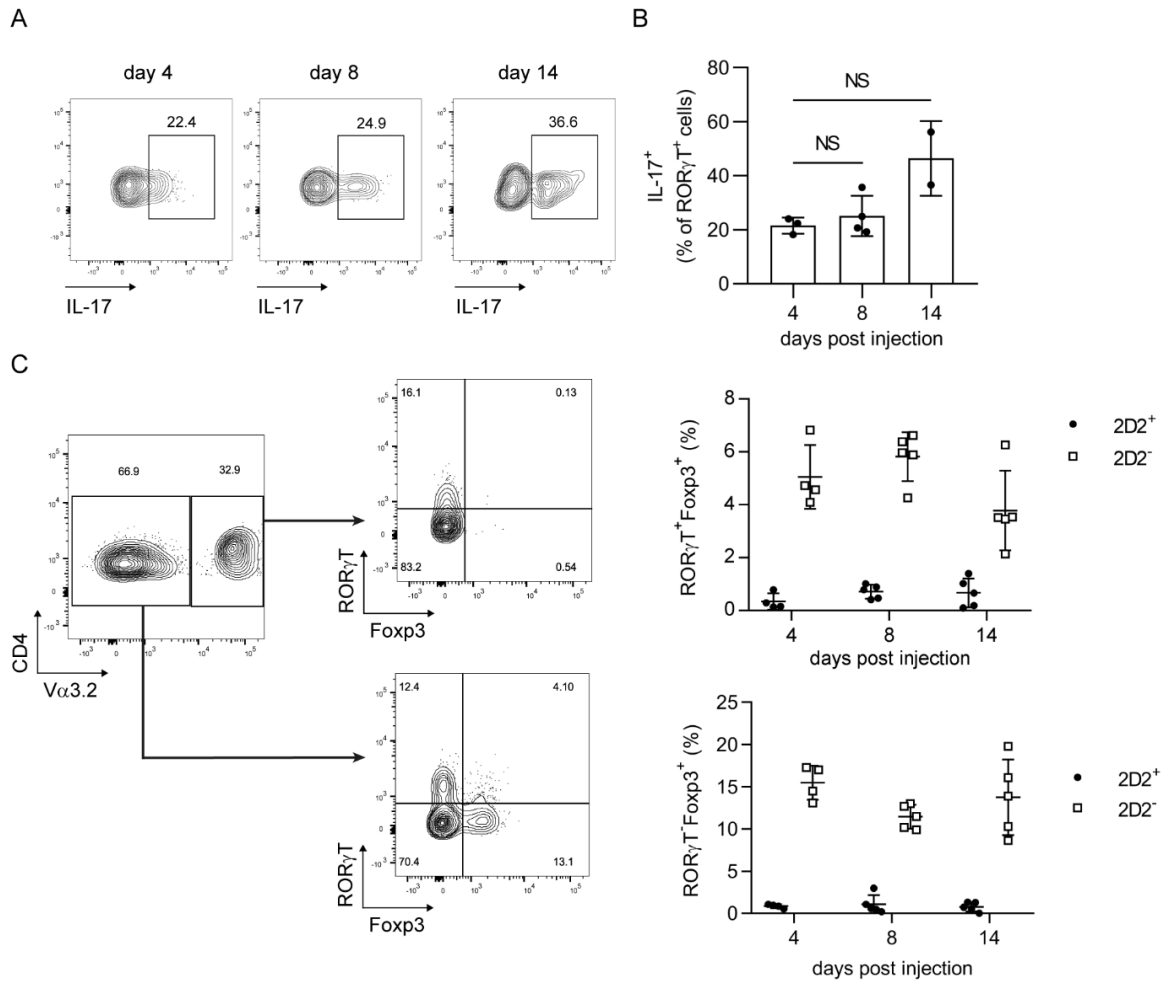


Figure S3, related to Figure 5: Encephalitogenic TCR^{MOG} 2D2 Th17 cells maintain their pathogenic phenotype throughout EAE disease.

(A) Representative FACS analysis of IL-17⁺ expression in RORγT⁺ 2D2⁺ T cells obtained from the colonic lamina propria of EAE at the indicated time points after TCR^{MOG} 2D2 Th17 cells transfer.

(B) Time course of transferred TCR^{MOG} 2D2 analysed by flow cytometry for IL-17⁺ intracellular expression and shown as a percentage of the RORγT⁺Vα3.2⁺ T cells population (mean ± SD; *n* = 2-4).

(C) Ex vivo flow cytometry analysis of colonic RORγT^{+/−}/ Fxp3[−] frequency in 2D2⁺TCR (Vα3.2⁺) cells versus 2D2[−]TCR (Vα3.2[−]) cells population. Representative contour plots are shown depicting intracellular staining for RORγT versus Fxp3 after gating for Vα3.2⁺ or Vα3.2[−] CD4⁺ T cells population (mean ± SD; *n* = 4-5).

Data are representative of two experiments; NS, not significant; P values were determined by Kruskal-Wallis test with Dunn's multiple comparisons post hoc test (B).

Figure S4, related to Figure 7

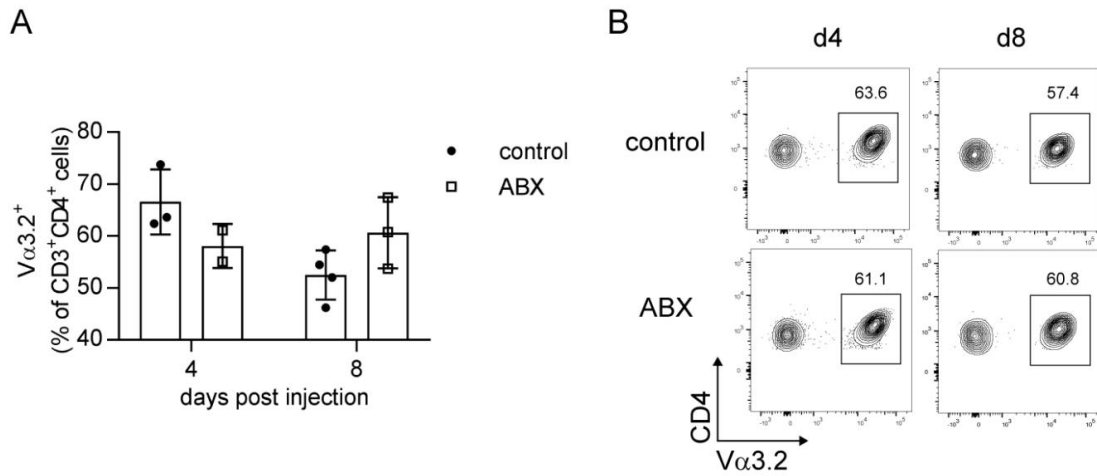


Figure S4, related to Figure 7: Antibiotic treatment does not influence TCR^{MOG} 2D2 Th17 infiltration in the colon.

(A) Flow cytometry analysis of the total proportion (%) of 2D2-TCR (Vα3.2⁺) expression in CD3⁺/CD4⁺ T cells of colonic lamina propria at the indicated time points after TCR^{MOG} 2D2 Th17 cells transfer in control and in antibiotic treated mice (ABX). Data are representative of two experiments.

(B) Representative flow cytometry analysis of the total proportion (%) of 2D2-TCR (Vα3.2⁺) expression in CD3⁺/CD4⁺ T cells obtained from the colonic lamina propria of control versus antibiotic treated (ABX) mice four days (d4) and eight days (d8) after TCR^{MOG} 2D2 Th17 cells transfer.

Table S1, related to Figure 4

Group	Disease incidence	Maximum score	Day of onset	AUC
control	83.3% (5/6)	3.83 ± 2.04	9.8 ± 0.45	12.75 ± 2.36
isotype	100% (8/8)	4.38 ± 0.74	10.5 ± 1.31	12.22 ± 1.97
anti- α 4 β 7	87.5% (7/8)	2.63 ± 1.51 ^(p=0.06)	12.71 ± 1.89 ^(p=0.08)	3.81 ± 1.28 ^{****}

AUC, area under the curve

Table S1, related to Figure 4: Blocking integrin α 4 β 7 attenuates disease course in adoptive transfer EAE. EAE in mice treated with PBS, isotype control or anti- α 4 β 7 antibodies. EAE disease incidence (%), maximum scores (mean ± SD; $n = 6-8$), day of disease onset (mean ± SD; $n = 5-8$), area under the curve (AUC) (mean ± SD; $n = 6-8$). *, $P < 0.05$; **, $P < 0.01$; ***, $P < 0.001$; ****, $P < 0.0001$; P values were shown for comparison between anti- α 4 β 7 versus isotype groups and were determined by one-way ANOVA with Tukey's post hoc test (AUC, maximum score) and by Kruskal-Wallis test with Dunn's post hoc test (day of disease onset).

Table S2, related to Figure 7

Rank	Taxonomic information	Average		Median		P*
		Before AT EAE	After AT EAE	Before AT EAE	After AT EAE	
Phylum	Bacteroidetes	34.35	38.12	34.92	38.30	0.02
	Proteobacteria	0.92	1.36	0.90	1.23	0.02
Class	Actinobacteria; Coriobacteria	1.70	1.07	1.51	0.88	0.04
	Bacteroidetes; Bacteroidia	34.35	38.12	34.92	38.30	0.02
	Firmicutes; Bacilli	14.28	3.93	13.30	2.13	0.01
Order	Actinobacteria; Coriobacteria; Coriobacteriales	1.70	1.07	1.51	0.88	0.04
	Bacteroidetes; Bacteroidia; Bacteroidales	34.35	38.12	34.92	38.30	0.02
	Firmicutes; Bacilli; Lactobacillales	14.28	3.93	13.30	2.13	0.01
Family	Actinobacteria; Coriobacteria; Coriobacteriales; Coriobacteriaceae	1.70	1.07	1.51	0.88	0.04
	Bacteroidetes; Bacteroidia; Bacteroidales; Bacteroidaceae	3.05	4.87	2.99	4.19	0.00
	Bacteroidetes; Bacteroidia; Bacteroidales; EU845084	0.42	1.00	0.38	0.65	0.03
	Bacteroidetes; Bacteroidia; Bacteroidales; Prevotellaceae	0.18	0.55	0.13	0.39	0.02
	Bacteroidetes; Bacteroidia; Bacteroidales; Rikenellaceae	2.74	4.97	2.14	4.78	0.00
	Firmicutes; Bacilli; Lactobacillales; Lactobacillaceae	14.26	3.89	13.30	2.04	0.01
	Firmicutes; Clostridia; Clostridiales; Ruminococcaceae	6.36	10.93	5.86	9.48	0.01
Genus	Actinobacteria; Coriobacteria; Coriobacteriales; Coriobacteriaceae; <i>Olsenella</i>	0.90	0.25	0.61	0.16	0.03
	Bacteroidetes; Bacteroidia; Bacteroidales; Bacteroidaceae; <i>Bacteroides</i>	3.05	4.87	2.99	4.19	0.00
	Bacteroidetes; Bacteroidia; Bacteroidales; EU845084; EF603735	0.42	1.00	0.38	0.65	0.03
	Bacteroidetes; Bacteroidia; Bacteroidales; Prevotellaceae; <i>Prevotella</i>	0.18	0.55	0.13	0.39	0.02
	Bacteroidetes; Bacteroidia; Bacteroidales; Rikenellaceae; <i>Alistipes</i>	2.74	4.97	2.14	4.78	0.00
	Bacteroidetes; Bacteroidia; Bacteroidales; S24-7; AY239469	1.09	0.65	1.04	0.56	0.01
	Bacteroidetes; Bacteroidia; Bacteroidales; S24-7; EF406712	1.34	2.82	1.40	2.66	0.00
	Bacteroidetes; Bacteroidia; Bacteroidales; S24-7; EF406806	0.44	0.73	0.37	0.68	0.01
	Bacteroidetes; Bacteroidia; Bacteroidales; S24-7; EF602759	4.83	3.26	4.86	2.95	0.03
	Firmicutes; Bacilli; Lactobacillales; Lactobacillaceae; <i>Lactobacillus</i>	14.26	3.89	13.30	2.04	0.01
	Firmicutes; Clostridia; Clostridiales; Lachnospiraceae; <i>Eisenbergiella</i>	1.93	3.89	1.95	3.53	0.05
	Firmicutes; Clostridia; Clostridiales; Lachnospiraceae; KE159538	0.81	3.11	0.92	2.44	0.00
	Firmicutes; Clostridia; Clostridiales; Ruminococcaceae; <i>Eubacterium</i>	0.21	0.61	0.18	0.25	0.03
	Firmicutes; Clostridia; Clostridiales; Ruminococcaceae; <i>Oscillibacter</i>	0.54	1.44	0.41	0.84	0.00
	Firmicutes; Clostridia; Clostridiales; Ruminococcaceae; <i>Pseudoflavonifractor</i>	0.65	1.14	0.62	1.08	0.01
	Species	Actinobacteria; Coriobacteria; Coriobacteriales; Coriobacteriaceae; <i>Olsenella</i> ; <i>Olsenella</i> unclassified	0.90	0.25	0.61	0.16
Bacteroidetes; Bacteroidia; Bacteroidales; Bacteroidaceae; <i>Bacteroides</i> ; <i>Bacteroides</i> unclassified		0.25	0.79	0.12	0.59	0.01
Bacteroidetes; Bacteroidia; Bacteroidales; EU845084; EF603735; EF603735		0.42	1.00	0.38	0.65	0.03
Bacteroidetes; Bacteroidia; Bacteroidales; Prevotellaceae; <i>Prevotella</i> ; DQ777952		0.18	0.55	0.13	0.39	0.02
Bacteroidetes; Bacteroidia; Bacteroidales; Rikenellaceae; <i>Alistipes</i> ; EF603688		0.12	0.83	0.12	0.69	0.00
Bacteroidetes; Bacteroidia; Bacteroidales; Rikenellaceae; <i>Alistipes</i> ; JQ085082		0.72	1.73	0.69	1.31	0.03
Bacteroidetes; Bacteroidia; Bacteroidales; S24-7; AY239469; AY239469		1.09	0.65	1.04	0.56	0.01
Bacteroidetes; Bacteroidia; Bacteroidales; S24-7; DQ815871; EF406459		1.13	1.86	1.08	1.54	0.05
Bacteroidetes; Bacteroidia; Bacteroidales; S24-7; EF406712; EF406712		1.34	2.82	1.40	2.66	0.00
Bacteroidetes; Bacteroidia; Bacteroidales; S24-7; EF602759; EF602759		1.33	0.73	1.28	0.74	0.01
Bacteroidetes; Bacteroidia; Bacteroidales; S24-7; HM124247; EF406368		0.38	1.11	0.40	1.05	0.01
Firmicutes; Bacilli; Lactobacillales; Lactobacillaceae; <i>Lactobacillus</i> ; <i>Lactobacillus animalis</i>		5.65	1.81	3.86	1.49	0.01
Firmicutes; Bacilli; Lactobacillales; Lactobacillaceae; <i>Lactobacillus</i> ; <i>Lactobacillus johnsonii</i>		5.64	1.37	3.76	0.31	0.01
Firmicutes; Bacilli; Lactobacillales; Lactobacillaceae; <i>Lactobacillus</i> ; <i>Lactobacillus</i> unclassified		2.97	0.72	2.82	0.41	0.02
Firmicutes; Clostridia; Clostridiales; Lachnospiraceae; KE159538; EF097676		0.60	1.72	0.62	1.20	0.01
Firmicutes; Clostridia; Clostridiales; Ruminococcaceae; JN713389; JN713389 unclassified		1.01	1.49	1.01	1.28	0.03
Firmicutes; Clostridia; Clostridiales; Ruminococcaceae; <i>Oscillibacter</i> ; <i>Oscillibacter</i> unclassified	0.24	0.61	0.14	0.39	0.03	
OTU	Bacteria; Actinobacteria; Coriobacteria; Coriobacteriales; Coriobacteriaceae; <i>Olsenella</i> ; <i>Olsenella</i> unclassified; Otu36	0.90	0.25	0.61	0.16	0.03
	Bacteria; Bacteroidetes; Bacteroidia; Bacteroidales; Bacteroidaceae; <i>Bacteroides</i> ; <i>Bacteroides</i> unclassified; Otu246	0.25	0.79	0.12	0.59	0.01
	Bacteria; Bacteroidetes; Bacteroidia; Bacteroidales; EU845084; EF603735; EF603735; Otu26	0.42	1.00	0.38	0.65	0.03
	Bacteria; Bacteroidetes; Bacteroidia; Bacteroidales; Prevotellaceae; <i>Prevotella</i> ; DQ777952; Otu45	0.18	0.55	0.13	0.39	0.02
	Bacteria; Bacteroidetes; Bacteroidia; Bacteroidales; Rikenellaceae; <i>Alistipes</i> ; EF603688; Otu51	0.12	0.83	0.12	0.69	0.00
	Bacteria; Bacteroidetes; Bacteroidia; Bacteroidales; Rikenellaceae; <i>Alistipes</i> ; JQ085082; Otu12	0.72	1.73	0.69	1.31	0.03
	Bacteria; Bacteroidetes; Bacteroidia; Bacteroidales; S24-7; AY239469; AY239469; Otu21	1.09	0.65	1.04	0.56	0.01
	Bacteria; Bacteroidetes; Bacteroidia; Bacteroidales; S24-7; DQ815871; EF406459; Otu13	1.13	1.86	1.08	1.54	0.05
	Bacteria; Bacteroidetes; Bacteroidia; Bacteroidales; S24-7; EF406712; EF406712; Otu28	1.34	2.82	1.40	2.66	0.00
	Bacteria; Bacteroidetes; Bacteroidia; Bacteroidales; S24-7; EF602759; EF602759; Otu30	1.33	0.73	1.28	0.74	0.01
	Bacteria; Bacteroidetes; Bacteroidia; Bacteroidales; S24-7; HM124247; EF406368; Otu40	0.38	1.11	0.40	1.05	0.01
	Bacteria; Firmicutes; Bacilli; Lactobacillales; Lactobacillaceae; <i>Lactobacillus</i> ; <i>Lactobacillus animalis</i> ; Otu4	5.65	1.81	3.86	1.49	0.01
	Bacteria; Firmicutes; Bacilli; Lactobacillales; Lactobacillaceae; <i>Lactobacillus</i> ; <i>Lactobacillus johnsonii</i> ; Otu6	5.64	1.37	3.76	0.31	0.01
	Bacteria; Firmicutes; Bacilli; Lactobacillales; Lactobacillaceae; <i>Lactobacillus</i> ; <i>Lactobacillus</i> unclassified; Otu25	2.97	0.72	2.82	0.41	0.02
	Bacteria; Firmicutes; Clostridia; Clostridiales; Lachnospiraceae; KE159538; EF097676; Otu34	0.53	1.56	0.54	1.13	0.00

AT EAE, adoptive transfer experimental autoimmune encephalomyelitis

Table S2, related to Figure 7: Changes in the relative abundance of bacterial taxa in fecal mouse microbiota observed after injection of TCR^{MOG} 2D2 Th17 cells. Only taxa with a mean relative abundance >0.5% in at least one of the two groups of samples (before and after AT EAE) were compared and those with statistically significant differences (P<0.05) are represented. The statistical analysis method used was a Wilcoxon signed-rank test. Significant increase and decrease in the taxon relative abundance after treatment are indicated by red and blue filled cells, respectively.

Table S3, related to STAR Methods

Gene ID	Gene name	Primer	Sequence (5'-3')
IL-6	Interleukin-6	Forward	CCCCAATTTCCAATGCTCTCC
		Reverse	CGCACTAGGTTTGCCGAGTA
IL-1 β	Interleukin-1 beta	Forward	TGCCACCTTTTGACAGTG ATG
		Reverse	TGATACTGCCTGCCTGAA GC
TNF- α	Tumor necrosis factor alpha	Forward	AAGCTCCTCAGCGAGGACAG
		Reverse	TGGTTGGCTGCTTGCTTTTC
MAdCAM-1	Mucosal addressin cell adhesion molecule 1	Forward	ACAGAGCCAGACCTCACCTA
		Reverse	TGATGTTGAGCCCAGTGGAG
VCAM-1	Vascular cell adhesion molecule 1	Forward	CTGGGAAGCTGGAACGAAGT
		Reverse	GCCAAACACTTGACCGTGAC
β -actin	Beta-actin	Forward	AAGTGTGACGTTGACATCCGTAAA
		Reverse	CAGCTCAGTAACAGTCCGCCTAGA

Table S3. Oligonucleotides used in this study. Related to STAR Methods.



Review

Oxysterols in Autoimmunity

Donovan Duc , Solenne Vigne and Caroline Pot *

Laboratories of Neuroimmunology, Neuroscience Research Center and Division of Neurology, Department of Clinical Neurosciences, Lausanne University Hospital and Lausanne University, Chemin des Boveresses 155, 1066 Epalinges, Switzerland; Donovan.Duc@chuv.ch (D.D.); Solenne.Vigne@chuv.ch (S.V.)

* Correspondence: Caroline.Pot-Kreis@chuv.ch; Tel.: +41-79-556-25-70

Received: 20 August 2019; Accepted: 10 September 2019; Published: 12 September 2019



Abstract: Cholesterol is a member of the sterol family that plays essential roles in biological processes, including cell membrane stability and myelin formation. Cholesterol can be metabolized into several molecules including bile acids, hormones, and oxysterols. Studies from the last few decades have demonstrated that oxysterols are not only active metabolites but are further involved in the modulation of immune responses. Liver X Receptors (LXRs), nuclear receptors for oxysterols, are important for cholesterol homeostasis and regulation of inflammatory response but are still poorly characterized during autoimmune diseases. Here we review the current knowledge about the role of oxysterols during autoimmune conditions and focus on the implication of LXR-dependent and LXR-independent pathways. We further highlight the importance of these pathways in particular during central nervous system (CNS) autoimmunity and inflammatory bowel diseases (IBD) in both experimental models and human studies. Finally, we discuss our vision about future applications and research on oxysterols related to autoimmunity.

Keywords: Liver X receptors; oxysterols; Ebi2; ROR; Ch25h; autoimmunity; multiple sclerosis; inflammatory bowel disease

1. Introduction

Cholesterol is implicated in several biochemistry processes of the body. It is an essential component of the mammalian cells accounting for up to 25% of all membrane lipids [1]. Its rigid hydrophobic structure confers stability on the plasma membrane and hampers the movement of other molecules, thus modifying the proportion of the cholesterol in the cell membrane can influence membrane fluidity [2]. In addition, cholesterol can interact with integral membrane proteins and modulate their functions [1]. It is also a precursor of important molecules such as vitamin D, bile acids, steroid hormones, and oxysterols.

Oxysterols are downstream metabolites of cholesterol oxidation. They can be divided into two categories called primary and secondary oxysterols. The primary oxysterols, synthesized directly from the cholesterol, are composed of side-chain oxysterols and ring-modified oxysterols. Side-chain oxysterol family includes 24S-, 25-, (25R)-26- (the latest was previously named 27- [3]), hydroxycholesterol (-OHC), and ring-modified oxysterol, which includes 7 α - and 7 β -OHC and 7-ketocholesterol (-KC). The secondary oxysterols, including 7 α ,25-dihydroxycholesterol and 7 α (25R)-26-dihydroxycholesterol are generated from primary oxysterols 25-OHC and (25R)-26-OHC, respectively. Oxysterols can be synthesized via enzymatic and non-enzymatic reactions. Specific hydroxylases are responsible for enzymatic oxidation, while reactive oxygen species oxidation is mainly responsible for non-enzymatic generation of oxysterols [4].

Research on oxysterols started in the early 1940's with studies on cholesterol autoxidation leading to the generation of oxysterols [5,6]. Growing interest in studying oxysterols continued in the late

1970 when Kandutsch and colleagues observed that oxygenated derivatives of cholesterol were able to downregulate the synthesis of cholesterol [7–10]. During the following years, several studies highlighted the importance of these molecules in a multitude of other biological processes [11]. Indeed, oxysterols were first described as a mediator of cholesterol metabolism. Oxysterols modulate the level of cholesterol intracellularly through transcriptional regulators like the liver X receptor (LXR) and the sterol regulatory element binding protein (SREBP). LXR mediates the expression of ATP binding cassette (ABC) transporter intervening in cholesterol transport and efflux [12]. SREBP also regulates the cholesterol metabolism in the cell by inducing the synthesis (through 3-hydroxy-3-methylglutaryl coenzyme A synthase/reductase) or the uptake of cholesterol (through expression of low-density lipoprotein receptor). In addition to the modulation of cholesterol levels, oxysterols are precursors of bile acid production and steroid hormones acting as intermediates in their synthesis. In the last decade, oxysterols have been proposed to act as fine-tuners of the immune responses, including trafficking of immune cells, anti-viral actions, cytokine secretions, and inflammasome modulations. In this review, we will focus on oxysterols and their downstream pathways that are implicated in immunological processes. We will further discuss their implications during autoimmune diseases.

2. Oxysterols: LXR Agonists and Beyond

2.1. LXR

Different oxysterol subsets have been discovered. They are all sharing close structural similarities but have various targets and actions (Figure 1). One receptor shared by oxysterols is the LXR receptor. Side-chain oxysterol family such as 25-OHC and (25R)-26-OHC are well characterized as LXR ligands [13]. LXRs are part of the nuclear receptors' family of transcription factors. LXR α (NR1H3) and LXR β (NR1H2) are two isoforms that have been identified [14]. Despite the close homology between the two isoforms (almost 80% identity of their amino acid sequences are identical) [15], they are not sharing the same function nor the same pattern of expression (<https://www.nursa.org>, last accessed date: 8 August 2019). LXR α is expressed mostly in metabolically active tissues like liver, gut, and adipose tissue. Indeed, LXR α has been suggested to be the major sensor of dietary cholesterol. LXR β is ubiquitously expressed. For both LXR α and LXR β , the active form is a heterodimer composed by the association of one protein of LXR and one protein of retinoid x receptor (RXR) [16]. The heterodimer binds LXR response elements, consisting of a direct repeat spaced by 4 nucleotides [17]. LXR modulates gene expression through direct activation, repression, and transrepression [18]. At the physiological stage, LXR are important to control metabolic processes, including cholesterol homeostasis. The metabolism of cholesterol leading to oxidized cholesterol derivatives is known to activate a LXR downstream pathway [19]. This process leads to an active feedback loop characterized by the activation of several genes that can modulate cholesterol levels such as cholesterol transporters (ABC transport genes) [20]. Moreover, LXRs are essential for hepatic functions and participate in the bile acid formation and control of hepatic lipogenesis. LXRs have also been characterized as important immunological modulators. LXRs are able to suppress inflammatory response through trans-repression [21]. Indeed, sumoylation of active LXR form can dampen the activity of nuclear factor κ b and activator protein 1 that controls proinflammatory genes expression [22,23].

In innate immunity, LXR pathways participate in the clearance of bacteria during infection in macrophages. Indeed, induction of LXR α (but not LXR β) expression occurs during intracellular bacterial infection [24]. Using another model of intracellular bacterial infection, Matalonga et al. have discovered that LXR activation induces cytoskeletal changes during infection by modulating nicotinamide adenine dinucleotide levels [25]. Regarding the adaptive immune system, LXRs have been described to decrease the proliferation of both T and B cells [26]. LXR β is expressed in macrophage, T, and B cells. On the other hand, LXR α is highly expressed in peritoneal-derived and bone-marrow derived macrophages, but not in T cells or B cells. Mice lacking LXR β show lymphoid hyperplasia and have improved responses to antigenic challenge [26]. These results were only found in LXR β

knockout but not in LXR α knockout. In addition, LXR activation inhibit IL-2- and IL-7-induced human T cell proliferation [27]. Regarding subtypes of T cells, LXRs are involved in the polarization of Th17 cells [28], subset of T helper cells that are important in autoimmune disease. Indeed, Th17 induction is facilitated in LXR knockout mice and LXR deficiency promotes Th17 polarization in vitro [28]. Finally, we demonstrated that LXRs further acts on regulatory T cells. In our study, we observed that 25-OHC, through LXR pathway, acts as a negative regulator of IL-10 secretion in murine IL-27-induced Treg [29]. Similarly, 25-OHC has been shown to down-regulate IL-10 production from human Th1 cells [30], thus highlighting a pro-inflammatory role of 25-OHC in fine-tuning CD4+ T cell polarization in different T cell subsets.

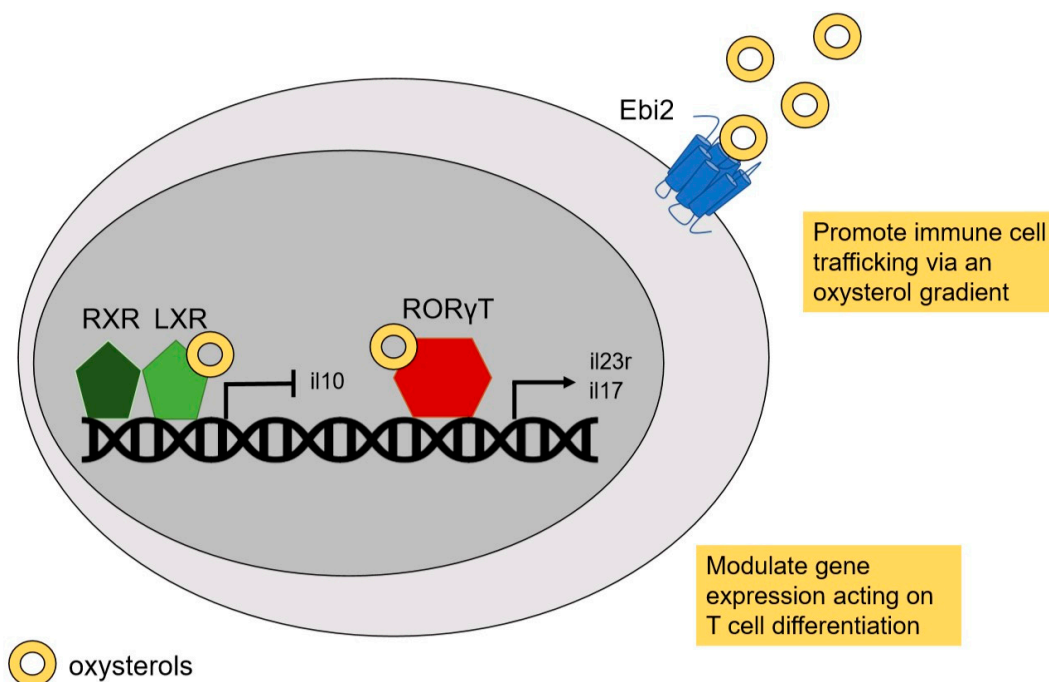


Figure 1. Molecular targets of oxysterol implicated in autoimmunity. Oxysterols have different targets during autoimmune diseases. Oxysterols promote immune cell trafficking through Ebi2 receptor expressed on cell surface. Oxysterol-Ebi2 interaction allows the cells to migrate via an oxysterol-gradient dependent manner. The liver X receptor (LXR) and ROR γ T are members of the nuclear receptors' family of transcription factors involved in immune cell differentiation. Through those transcription factors, oxysterols modulate the gene expression implicated in inflammatory and autoimmune processes.

2.2. Retinoic Acid Receptor-Related Orphan Receptor (RORs)

Like LXRs, RORs are members of the nuclear receptor family of transcription factors binding oxysterols. They are composed of three different forms; ROR α (NR1F1), ROR β (NR1F2), and ROR γ (NR1F3). RORs recognize and bind as monomer to specific ROR response elements on DNA [31]. After their activation, RORs recruit co-activator and activate gene transcription [32]. Several oxysterols (i.e., 25-OHC, (25R)-26-OHC, 7 α -OHC) can bind ROR α and ROR γ , however no study reported oxysterols as ligand of ROR β [4]. ROR α is expressed in several tissues and participate in circadian rhythms, glucose and lipid metabolism, and during the development. ROR γ is also expressed in multiple organs and is an important transcription factor for immune cells. ROR γ has also variant including ROR γ 1 and ROR γ 2 (also known as ROR γ T) isoforms [33]. ROR γ T is an essential transcription factor in Th17 cell development [34] and drives autoimmune diseases, as will be discussed in the following chapters.

2.3. Epstein-Barr Virus-Induced G-Protein Coupled Receptor 2 (Ebi2)

G-protein coupled receptor 183 also known as Epstein-Barr virus-induced G-protein coupled receptor 2 (Ebi2) is a membrane receptor from the G-protein-coupled receptors (GPCR) family. Ebi2 was first discovered in Burkitt's lymphoma cells after Epstein-Barr virus infection [35]. It was first observed in B cells but further studies have demonstrated that it was also expressed in other type of cells such as T lymphocytes, monocytes, dendritic cells, astrocytes and innate lymphoid cells. Among the different signaling pathways of GPCR, Ebi2 receptor is defined as chemotactic receptor and participates in the migratory capability of cells [36–38]. The most potent endogenous ligand of this membrane receptor is the oxysterol 7 α -25-OHC produced from oxidation of 25-OHC by Cyp7b1 enzyme [38,39]. Cells that express Ebi2 are trafficking through an oxysterol gradient dependent manner acting like chemokine processes (Figure 1). The migratory function of this receptor affects several important immune processes. In particular, Ebi2 is involved in the T-dependent antibody response in the germinal centers [37]. Indeed mice lacking Ebi2 have an abnormal positioning of B cells in the follicular regions of secondary lymphoid organs [39]. A recent study demonstrated that Ebi2 drives CD4+ T cells peripheralization in lymph node [40]. Mice lacking Ebi2 receptor have a CD4+ T cells location issue and have delayed responses in antigen recognition and proliferation in the lymph node.

3. Oxysterols in CNS Autoimmunity

3.1. Oxysterols

As growing evidence supported roles in immune regulation involving oxysterols, the scientific community further studied the role of cholesterol metabolites in autoimmune conditions. Multiple sclerosis (MS) is the most common autoimmune disease involving the nervous system [41]. MS and its animal model, the experimental autoimmune encephalomyelitis (EAE), are characterized by inflammatory cell infiltrates and demyelination in the central nervous system (CNS), leading to neurological damage. A combination of both genetic and environmental factors has been proposed to trigger the disease. In this vein, obesity has been described as a risk factor for MS. Indeed, a direct correlation between a higher body mass index during childhood [42,43] or adolescence [44,45] and a higher risk of developing MS has been observed in several epidemiological studies. In addition, metabolic changes linked with obesity such as an altered lipid profile are associated with poor outcome of MS [46–50]. Moreover, obesity and high fat diet have been associated with perturbation of cholesterol and oxysterol homeostasis in the liver, hypothalamus, adipose tissue and plasma in an experimental model [51].

Oxysterol perturbations have been further described in MS. First, it has been proposed that MS patients have disrupted oxysterol levels compared to healthy controls both in blood and in cerebrospinal fluid (CSF). In particular the plasma levels of 24-OHC, (25R)-26-OHC, and 7 α -OHC were significantly lower in MS patients compared to in healthy control [52] and in the CSF of MS patients, a reduction of the concentration of 25-OHC and (25R)-26-OHC was observed [53]. Similarly, an evaluation of oxysterol levels was performed in MS patients and controls in a longitudinal study (5 year) and significant modulations of circulating oxysterols were observed in MS patients but not in controls: 24-OHC, (25R)-26-OHC, and 7 α -OHC levels were lower in MS patients compared with healthy controls, and 7-KC was higher in progressive MS compared with relapsing-remitting MS [54]. However, while a decreased 24-OHC-blood level was observed with advanced Alzheimer's disease as well as with MS disease, increased 24-OHC-blood levels have been observed in early neurodegenerative processes in both diseases [55]. 24-OHC is the predominant metabolite of brain cholesterol [56] and several studies reported a modulation of 24-OHC in the CSF and serum of MS patients [57]. Interestingly, the disease-modifying therapy natalizumab, reduces the concentrations of 24-OHC and (25R)-26-OHC in CSF [58]. As 24-OHC indicates CNS cholesterol turnover [59,60] and has been proposed as a biomarker for neurodegeneration [61] and for clinical stages of MS [62]. It has been proposed that a decrease of 24-OHC after natalizumab treatment might reflect reduced neuronal

damage. Regarding (25R)-26-OHC, the majority of this oxysterol in the CSF is coming from peripheral blood and the concentration depends on the blood brain barrier (BBB) integrity [58]. As natalizumab acts on the BBB functionality [63], the authors hypothesized that reduction of (25R)-26-OHC in the CSF could be associated with an improvement of BBB integrity.

Genetic analysis of MS patients further revealed a potential association between genetic variants of cholesterol 25-hydroxylase (Ch25h) and primary progressive MS patients, supporting a role for Ch25h and related-oxysterols in CNS autoimmunity [64]. Moreover, genetic variants in NR1H3 (LXR α) were also found to be associated with increased risk of developing progressive MS [65,66]. These recent studies on human strongly suggest that perturbation of oxysterol metabolism may influence the progression of MS disease. However, the underlying mechanisms are still unclear and several research groups, including ours, are working on understanding the role of oxysterols in CNS autoimmunity using experimental models.

3.2. LXR

In 2006, Hindinger et al. published the first evidence for a role of LXR in the EAE model. Using the LXR agonist ligand T0901317, they observed that it reduced EAE clinical severity and CNS inflammation [67]. Additional studies found that in vivo administration of LXR agonists decreased IL-17 secretion [28] and suppressed IL-17A, IFN γ , and IL-23R expression [68]. As Th17 cells largely contribute to EAE development [69,70], these results are associated with the dampened EAE severity observed [68]. Moreover, both mice and human Th17 cells were downregulated by LXR activation [28]. Th17 cell differentiation is controlled by LXR through the activation of Srebp-1a and Srebp-1c. Overexpression of SREBF-1a and SREBF-1c dampened the differentiation of Th17 cells by physically interfering with the Ahr transcription factor and inhibiting Ahr-controlled IL-17 transcription [28]. In contrast, knocking down of either SREBF1 isoforms resulted in an increase of Th17 cell differentiation [28]. Interestingly, LXR/RXR pathways and SREBF1 modulate encephalitogenic Th17 cells during the adoptive transferred EAE. The authors compared the transcriptome transition of encephalitogenic Th17 cell before (in vitro) and after adoptive transfer in the CNS of recipient mice [71]. LXR/RXR and downstream target genes, including genes important for cholesterol transport such as *Lpl*, *Abca1*, and *Abcg1* were found to be increased in Th17 cells during EAE compared to Th17 differentiated in vitro. In contrast, SREBF1, which controls the expression of genes involved in fatty acid and triglycerides synthesis, was found to be downregulated in Th17 cells located in CNS of EAE mice compared to in vitro differentiated Th17 cells [71]. Even if the precise role of LXR pathway in CNS autoimmunity remains to be further investigated, modulation of the LXR pathway and their target genes are involved in a metabolic checkpoint during Th17 cell differentiation which is important in MS and EAE diseases [71]. Beyond the regulation of T cells, LXR pathways influence other types of CNS cell population. LXR activation via oxysterols downregulated pro-inflammatory responses in microglial and astrocytes in vitro. As EAE and MS also involved glial cells, it could further explain the role of LXR activation in the development of these diseases [72–74]. Moreover, LXR α has been shown to modulate the BBB permeability and to affect EAE severity. Using mice with specific depletion of LXR α in endothelial cells, the authors observed a worsened EAE disease compared to controls [75].

3.3. ROR

As introduced above, ROR γ T, a target for several oxysterols, is an essential transcription factor for Th17 cell differentiation [76]. As EAE is mediated mainly by Th17 cells, several reports have studied the role of this transcription factor in CNS autoimmunity. ROR γ T knockout mice are less susceptible to EAE disease and depict a reduction of Th17 cell infiltration in the CNS [34]. In contrast, overexpression of ROR γ T led to increased EAE disease severity [77]. As lymph nodes are absent in ROR γ T knockout mice [78], it is difficult to decipher whether the therapeutic potential of ROR γ T in reducing EAE is secondary to the lack of ROR γ T in the T cells, or to the lack of lymph nodes. However, Yang et al. found that suppressing ROR γ T expression specifically in encephalitogenic T cells did not

reduced EAE disease using adoptive transferred EAE [79]. Additional study demonstrated that ROR α is also involved in the differentiation of Th17. Mice knockout for ROR α have reduced level of IL-17 production and develop milder clinical symptoms during EAE disease. ROR α and ROR γ T synergized in promoting Th17 differentiation. Moreover, double deficiencies in ROR α and ROR γ completely impaired Th17 generation in vitro and fully protected mice from EAE development [80].

3.4. *Ebi2*

Ebi2 is involved in migration of immune cells. As T cell trafficking plays a major role in MS and EAE, *Ebi2* and related oxysterols have been studied recently in this context (Figure 2). In our laboratory, we demonstrated that oxysterols regulate the trafficking of encephalitogenic T cells during the development of EAE disease [81]. Indeed, Ch25h-deficient mice show an attenuated EAE disease course by limiting the trafficking of pathogenic Th17 lymphocytes to the CNS. We further observed an accumulation of Th17 lymphocytes in the peripheral lymph nodes in the absence of Ch25h-related oxysterols during EAE, thus pointing towards a possible defect in T lymphocytes exit from the lymph nodes. Interestingly, this is reminiscent of the fingolimod mechanism of action, a drug that constrains MS inflammatory activity by trapping a subset of the T cell in the lymph nodes [82]. We further observed that T lymphocytes migrate specifically in response to 7 α ,25-OHC through *Ebi2* signaling. Independently, other authors reported that Ch25h and Cyp7b1 expression as well as 7 α ,25-OHC level were increased in CNS during EAE development [83]. They further proposed that *Ebi2* is predominantly expressed in Th17 cell subset compared to Th1 or CD8+ T cells and that its expression is maintained by pro-inflammatory cytokines (i.e., interleukin-23 and interleukin-1 β). The capacity of *Ebi2*^{-/-} Th17 cells to induce CNS autoimmunity was established using an adoptive transfer model of EAE. Mice that received encephalitogenic *Ebi2*^{-/-} Th17 cells had a delayed disease development compared to mice transferred with wild-type controls [83]. In addition, inflamed white matter of MS patients showed a high expression of *Ebi2* receptor compared to the non-inflamed region of the white matter and a proportion of T cell expression *Ebi2* was described in the lesions of MS patients [83]. Moreover, we characterized the *Ebi2* expression profile in human lymphocytes in MS patients and observed that *Ebi2* is functionally expressed on memory CD4+ T cells [84]. Interaction between *Ebi2* receptor and oxysterols fine-tunes immune cell migration, a mechanism used by several treatments for MS, such as natalizumab, which blocks the entry of immune cells into the CNS [63]. Interestingly, memory CD4+ T cells from MS patients treated with natalizumab display an increased *Ebi2* expression and migration profile to 7 α ,25-OHC, suggesting an important role for *Ebi2* and related oxysterol in human CD4 T cell migration in MS patients [84]. Finally, oxysterol levels are altered in the CNS during EAE development. Among the several oxysterols found in the CNS, 7 α ,25-OHC is significantly increased during EAE and could potentially be associated with the increase immune cell infiltrates observed during the disease [85]. However, the precise role of 7 α ,25-OHC and its exact cellular source in the CNS during EAE remain still unknown.

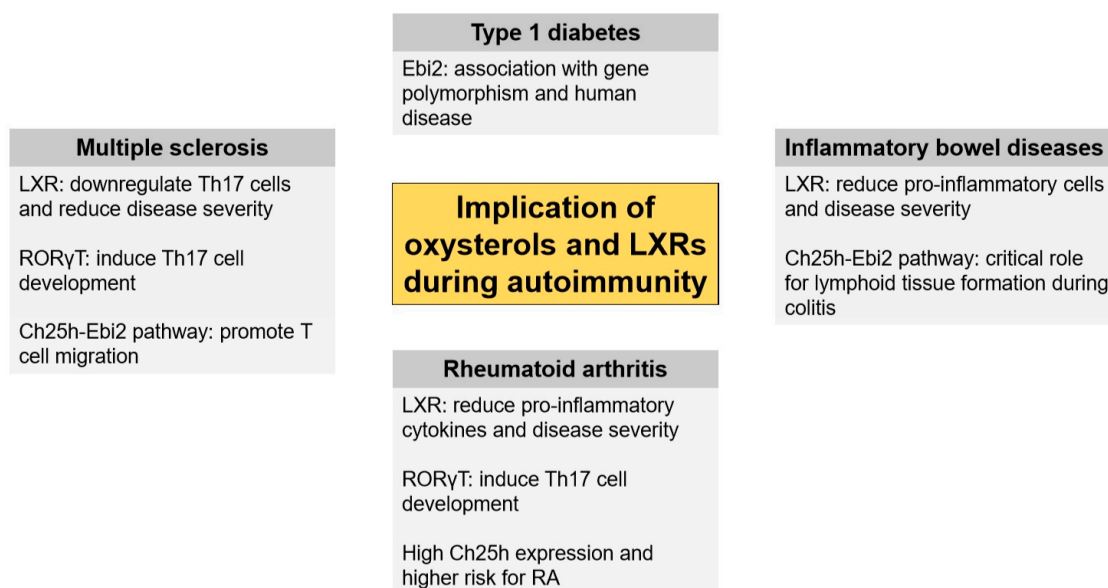


Figure 2. Implications of oxysterols and LXRs in autoimmunity. The roles of oxysterols and LXR-dependent and LXR-independent pathways have been studied in different autoimmune conditions.

4. Oxysterols in Inflammatory Bowel Disease (IBD)

4.1. Oxysterols

Inflammatory bowel disease (IBD) regroup two frequent chronic diseases of the gut: the ulcerative colitis (UC) and Crohn's disease (CD). Several examples of evidence showing a relation between oxysterols and inflammatory disorders such as IBD have appeared throughout the last years. Oxysterols which originated from diet are totally absorbed by the gut, which represents the initial site of exposure to their effects. They are suggested to potentially interfere with homeostasis of the human digestive tract, playing a role in intestinal mucosal damage. Oxysterols were found most commonly in cholesterol-rich food as a mixture [86–88]. Several in vitro studies proposed that a mixture of oxysterols derived from dietary cholesterol led to a strong pro-inflammatory effect and exhibited cytotoxicity, apoptosis, and development of atypical cell clones of human colonic epithelial cells, favoring in vitro intestinal inflammation and colon cancer progression [89–95]. In addition, oxysterols such as 7-KC and 25-OHC were also described to decrease the barrier integrity of vascular endothelium and intestinal epithelial [96]. These in vitro studies on intestinal cells suggest that oxysterols are able to interfere in different steps of colonic inflammation (Figure 2). Finally, intestinal fibrosis and stenosis are common complications of CD that do not respond to anti-inflammatory treatments. Interestingly, oxysterols downstream Ch25h enzyme are further implicated in the pathogenesis of intestinal fibrosis and could thus contribute to IBD on several aspect of the disease [97].

4.2. LXR

In the colon of human and mice, both LXR subtypes are expressed and were reported to have anti-inflammatory effects in colon epithelial cells [98]. In two different experimental model of IBD, it was reported that LXR-deficient mice were more susceptible to colitis with a more protective role for LXR β than LXR α in both DSS and TNBS-induced colitis. In addition, activation of LXR receptors by synthetic ligands accelerates disease recovery in DSS-induced colitis [98]. LXR activation via oral application of LXR agonist reduced pro-inflammatory Th1 and Th17 cells while induced gut-associated regulatory T cells [99]. Polymorphisms in LXRs were shown to be associated with IBD in a Danish study and the mRNA expression for both LXRs are decreased in CD and UC patients compared to healthy controls [98,100]. Recently, two independent studies reported that both oxysterols, particularly

4 β -HC and 25-OHC as well as their metabolizing enzyme levels, were altered in acute or chronic colitis models in mice and in biopsies of human colitis cohorts [101,102]. However, despite evidence showing the relation between oxysterol/LXR receptors and intestinal inflammation, it is difficult to evaluate the precise role of oxysterols and their nuclear receptors during colitis, which needs further investigation.

4.3. *Ebi2*

In 2012, *Ebi2* was identified as an IBD risk gene by genome-wide association studies (GWAS) and a single nucleotide polymorphism in *Ebi2* increase the risk for both, CD and UC with genome wide significance [103]. Moreover, a significant upregulation of *EBI2* gene was found in the ileum of CD patients with NOD2 risk allele [104]. The role of *EBI2* during intestinal inflammation was recently studied using different mice model of colitis [102,105,106]. Using an innate model of intestinal inflammation, Emgard et al. showed that *Ebi2* deficient mice were less susceptible to colitis [105]. *Ebi2* is highly expressed by type 3 innate lymphoid cells (ILC3s), whereas oxysterols synthesized enzymes were mostly produced by fibroblastic stromal cells found in intestinal lymphoid structures. *Ebi2* and its oxysterol ligand were shown to be essential for the localization and the migration of ILC3s and to have a critical role for the formation of lymphoid tissues in the mouse colon during colitis [105,106]. The data suggest an implication of *EBI2*/oxysterol axis for controlling and regulating colonic lymphoid tissues organization during intestinal inflammation.

5. Other Autoimmune Diseases

5.1. *Rheumatoid Arthritis (RA)*

Rheumatoid arthritis (RA) is a chronic autoimmune disorder that primarily affects the joints. The disease is characterized by an infiltration of inflammatory leukocytes in the synovial compartment and autoantibodies that are also found in 50% to 70% of patients [107]. LXR have been hypothesized as a possible therapeutic target for RA. Indeed, the first study investigating the role of LXR pathways reported that LXR agonist (T0901317) reduced the clinical symptoms in the murine collagen-induced arthritis (CIA) model [108]. Similar results were found in two other studies showing that LXR ligand (GW3965) attenuated the symptoms associated with a decreased pro-inflammatory cytokines production [109,110]. Contrary results were found in which the authors observed a dose-dependent exacerbation of arthritis disease when mice were treated with two LXR ligands (T0901317 and GW3965) [111]. The authors explained these discordant findings by the different doses and routes of the drug administration used.

RORs were also found involved in the RA. RORC gene, coding for ROR γ , is found to be highly expressed in the CD4+ T cell of patients with a recent RA disease compared to healthy controls [112]. Using the CIA model, one study has shown that the inverse agonist of ROR γ can decrease the development of arthritis [113]. Moreover, Xue et al. found similar results using a selective inverse agonist of ROR γ T [114]. On the other hand, overexpression of ROR γ T in T cells also attenuated the arthritis in mice, however the precise mechanisms are not yet fully understood [115]. Finally 25-OHC dampens IL-10 production in Th1 cells that also contribute to the disease progression in RA. Interestingly, synovial Ch25h expression mRNA expression is highly expressed in individuals that depict autoantibody-positive arthralgia and that are at high risk of developing RA [30]. The role of oxysterols and Ch25h-pathway thus remain to be further investigated in RA (Figure 2).

5.2. *Type 1 Diabetes (T1D)*

Type 1 diabetes (T1D) is a T-cell-mediated autoimmune disease that destroys insulin-producing pancreatic β -cells. Very few studies examine the implication of oxysterol or cholesterol biosynthesis pathway during T1D. Using experimental models, Yoshioka et al. measured high levels of cholesterol oxides in the kidney, heart, and liver of diabetic rats [116]. Using mass spectrometry on human blood, one study describes increased levels of total oxysterols, particularly 7 β -OH-chol, in T1D patients

compared to subjects without diabetes [117]. Furthermore, in another study, T1D patients also had higher plasma oxysterol levels, more specifically plasma 7-KC and chol-triol levels compared to healthy controls [118]. In 2010, a GWAS meta-analysis of T1D using both rat and human blood have linked polymorphisms in the EBI2 gene with T1D [119]. These data suggest that oxysterols could further be implicated in T1D and could even be promising suitable biomarkers to monitor the intensity of lipid oxidative modifications during T1D. However the significance and the underlying mechanisms of oxysterol production and their biological activities in T1D remain to be elucidated (Figure 2).

6. Conclusions

Through work over the last several decades, it is now recognized that cholesterol metabolites, in particular oxysterols, are involved in fine-tuning the immune responses and contribute to the development of several autoimmune diseases, including MS, IBD, RA, and possibly T1D. The complexity of oxysterol downstream pathways with several intracellular nuclear factors as well as with membrane surface receptors certainly contributes to the different implications of oxysterols pathways during autoimmunity. The precise contribution of both LXR-dependent and independent pathways is still largely undetermined in this context. It thus remains a field that needs to be further investigated to fully understand how oxysterols are generated and participate to autoimmunity. By understanding the precise role of cholesterol pathways during inflammation, we can anticipate the emergence of new therapeutic treatments to tackle autoimmune diseases.

Author Contributions: Writing—original draft preparation, D.D., S.V.; writing—review and editing, C.P.; funding acquisition, C.P.

Funding: This work was supported by the Swiss National Science Foundation (#PP00P3_157476).

Conflicts of Interest: The authors declare no conflict of interest.

Abbreviations

ABC	ATP binding cassette
BBB	Blood brain barrier
CD	Crohn's disease
Ch25h	Cholesterol 25-hydroxylase
CIA	Collagen-induced arthritis
CNS	Central nervous system
CSF	Cerebrospinal fluid
EAE	Experimental autoimmune encephalomyelitis
Ebi2	Epstein-Barr virus-induced G-protein coupled receptor 2
GPCR	G-protein-coupled receptors
GWAS	Genome-wide association studies
IBD	Inflammatory bowel disease
KC	Ketocholesterol
LXR	Liver X receptor
MS	Multiple sclerosis
OHC	Hydroxycholesterol
RA	Rheumatoid arthritis
ROR	Retinoic acid receptor-related orphan receptor
RXR	Retinoid X receptor
SREBP	Sterol regulatory element binding protein
T1D	Type 1 diabetes
UC	Ulcerative colitis

References

1. Ikonen, E. Cellular cholesterol trafficking and compartmentalization. *Nat. Rev. Mol. Cell Biol.* **2008**, *9*, 125–138. [[CrossRef](#)] [[PubMed](#)]
2. Cooper, R.A. Influence of increased membrane cholesterol on membrane fluidity and cell function in human red blood cells. *J. Supramol. Struct.* **1978**, *8*, 413–430. [[CrossRef](#)] [[PubMed](#)]
3. Fakheri, R.J.; Javitt, N.B. 27-Hydroxycholesterol, does it exist? On the nomenclature and stereochemistry of 26-hydroxylated sterols. *Steroids* **2012**, *77*, 575–577. [[CrossRef](#)] [[PubMed](#)]
4. Mutemberezi, V.; Guillemot-Legris, O.; Muccioli, G.G. Oxysterols: From cholesterol metabolites to key mediators. *Prog. Lipid Res.* **2016**, *64*, 152–169. [[CrossRef](#)] [[PubMed](#)]
5. Bergstrom, S.; Wintersteiner, O. Autoxidation of sterols in colloidal aqueous solution: The nature of the products formed from cholesterol. *J. Biol. Chem.* **1941**, *141*, 597–610.
6. Bergstrom, S.; Wintersteiner, O. Autoxidation of sterols in colloidal aqueous solution III. Quantitative studies on cholesterol. *J. Biol. Chem.* **1942**, *145*, 309–326.
7. Kandutsch, A.A.; Chen, H.W. Inhibition of sterol synthesis in cultured mouse cells by 7 α -hydroxycholesterol, 7 β -hydroxycholesterol, and 7-ketocholesterol. *J. Biol. Chem.* **1973**, *248*, 8408–8417. [[PubMed](#)]
8. Kandutsch, A.A.; Chen, H.W. Inhibition of sterol synthesis in cultured mouse cells by cholesterol derivatives oxygenated in the side chain. *J. Biol. Chem.* **1974**, *249*, 6057–6061. [[PubMed](#)]
9. Kandutsch, A.A.; Chen, H.W. Regulation of sterol synthesis in cultured cells by oxygenated derivatives of cholesterol. *J. Cell. Physiol.* **1975**, *85*, 415–424. [[CrossRef](#)] [[PubMed](#)]
10. Kandutsch, A.A.; Chen, H.W. Inhibition of cholesterol synthesis by oxygenated sterols. *Lipids* **1978**, *13*, 704–707. [[CrossRef](#)]
11. Schroepfer, G.J., Jr. Oxysterols: Modulators of cholesterol metabolism and other processes. *Physiol. Rev.* **2000**, *80*, 361–554. [[CrossRef](#)] [[PubMed](#)]
12. Venkateswaran, A.; Laffitte, B.A.; Joseph, S.B.; Mak, P.A.; Wilpitz, D.C.; Edwards, P.A.; Tontonoz, P. Control of cellular cholesterol efflux by the nuclear oxysterol receptor LXR alpha. *Proc. Natl. Acad. Sci. USA* **2000**, *97*, 12097–12102. [[CrossRef](#)] [[PubMed](#)]
13. Janowski, B.A.; Willy, P.J.; Devi, T.R.; Falck, J.R.; Mangelsdorf, D.J. An oxysterol signalling pathway mediated by the nuclear receptor LXR alpha. *Nature* **1996**, *383*, 728–731. [[CrossRef](#)] [[PubMed](#)]
14. Janowski, B.A.; Grogan, M.J.; Jones, S.A.; Wisely, G.B.; Kliewer, S.A.; Corey, E.J.; Mangelsdorf, D.J. Structural requirements of ligands for the oxysterol liver X receptors LXRalpha and LXRbeta. *Proc. Natl. Acad. Sci. USA* **1999**, *96*, 266–271. [[CrossRef](#)] [[PubMed](#)]
15. Beltowski, J. Liver X receptors (LXR) as therapeutic targets in dyslipidemia. *Cardiovasc. Ther.* **2008**, *26*, 297–316. [[CrossRef](#)] [[PubMed](#)]
16. Peet, D.J.; Janowski, B.A.; Mangelsdorf, D.J. The LXRs: A new class of oxysterol receptors. *Curr. Opin. Genet. Dev.* **1998**, *8*, 571–575. [[CrossRef](#)]
17. Willy, P.J.; Umesono, K.; Ong, E.S.; Evans, R.M.; Heyman, R.A.; Mangelsdorf, D.J. LXR, a nuclear receptor that defines a distinct retinoid response pathway. *Genes Dev.* **1995**, *9*, 1033–1045. [[CrossRef](#)] [[PubMed](#)]
18. Glass, C.K.; Rosenfeld, M.G. The coregulator exchange in transcriptional functions of nuclear receptors. *Genes Dev.* **2000**, *14*, 121–141.
19. Maqdasy, S.; Trousson, A.; Tauveron, I.; Volle, D.H.; Baron, S.; Lobaccaro, J.M. Once and for all, LXRalpha and LXRbeta are gatekeepers of the endocrine system. *Mol. Asp. Med.* **2016**, *49*, 31–46. [[CrossRef](#)]
20. Boergesen, M.; Pedersen, T.A.; Gross, B.; van Heeringen, S.J.; Hagenbeek, D.; Bindsboll, C.; Caron, S.; Lalloyer, F.; Steffensen, K.R.; Nebb, H.I.; et al. Genome-wide profiling of liver X receptor, retinoid X receptor, and peroxisome proliferator-activated receptor alpha in mouse liver reveals extensive sharing of binding sites. *Mol. Cell. Biol.* **2012**, *32*, 852–867. [[CrossRef](#)]
21. Guillemot-Legris, O.; Mutemberezi, V.; Muccioli, G.G. Oxysterols in Metabolic Syndrome: From Bystander Molecules to Bioactive Lipids. *Trends Mol. Med.* **2016**, *22*, 594–614. [[CrossRef](#)]
22. Ghisletti, S.; Huang, W.; Ogawa, S.; Pascual, G.; Lin, M.E.; Willson, T.M.; Rosenfeld, M.G.; Glass, C.K. Parallel SUMOylation-dependent pathways mediate gene- and signal-specific transrepression by LXRs and PPARgamma. *Mol. Cell* **2007**, *25*, 57–70. [[CrossRef](#)] [[PubMed](#)]

23. Thomas, D.G.; Doran, A.C.; Fotakis, P.; Westerterp, M.; Antonson, P.; Jiang, H.; Jiang, X.C.; Gustafsson, J.A.; Tabas, I.; Tall, A.R. LXR Suppresses Inflammatory Gene Expression and Neutrophil Migration through cis-Repression and Cholesterol Efflux. *Cell Rep.* **2018**, *25*, 3774–3785.e4. [[CrossRef](#)] [[PubMed](#)]
24. Joseph, S.B.; Bradley, M.N.; Castrillo, A.; Bruhn, K.W.; Mak, P.A.; Pei, L.; Hogenesch, J.; O'Connell, R.M.; Cheng, G.; Saez, E.; et al. LXR-dependent gene expression is important for macrophage survival and the innate immune response. *Cell* **2004**, *119*, 299–309. [[CrossRef](#)] [[PubMed](#)]
25. Matalonga, J.; Glaria, E.; Bresque, M.; Escande, C.; Carbo, J.M.; Kiefer, K.; Vicente, R.; Leon, T.E.; Beceiro, S.; Pascual-Garcia, M.; et al. The Nuclear Receptor LXR Limits Bacterial Infection of Host Macrophages through a Mechanism that Impacts Cellular NAD Metabolism. *Cell Rep.* **2017**, *18*, 1241–1255. [[CrossRef](#)] [[PubMed](#)]
26. Bensinger, S.J.; Bradley, M.N.; Joseph, S.B.; Zelcer, N.; Janssen, E.M.; Hausner, M.A.; Shih, R.; Parks, J.S.; Edwards, P.A.; Jamieson, B.D.; et al. LXR signaling couples sterol metabolism to proliferation in the acquired immune response. *Cell* **2008**, *134*, 97–111. [[CrossRef](#)] [[PubMed](#)]
27. Geyeregger, R.; Shehata, M.; Zeyda, M.; Kiefer, F.W.; Stuhlmeier, K.M.; Porpaczy, E.; Zlabinger, G.J.; Jager, U.; Stulnig, T.M. Liver X receptors interfere with cytokine-induced proliferation and cell survival in normal and leukemic lymphocytes. *J. Leukoc. Biol.* **2009**, *86*, 1039–1048. [[CrossRef](#)] [[PubMed](#)]
28. Cui, G.; Qin, X.; Wu, L.; Zhang, Y.; Sheng, X.; Yu, Q.; Sheng, H.; Xi, B.; Zhang, J.Z.; Zang, Y.Q. Liver X receptor (LXR) mediates negative regulation of mouse and human Th17 differentiation. *J. Clin. Investig.* **2011**, *121*, 658–670. [[CrossRef](#)]
29. Vigne, S.; Chalmin, F.; Duc, D.; Clottu, A.S.; Apetoh, L.; Lobaccaro, J.A.; Christen, I.; Zhang, J.; Pot, C. IL-27-Induced Type 1 Regulatory T-Cells Produce Oxysterols that Constrain IL-10 Production. *Front. Immunol.* **2017**, *8*, 1184. [[CrossRef](#)]
30. Perucha, E.; Melchiotti, R.; Bibby, J.A.; Wu, W.; Frederiksen, K.S.; Roberts, C.A.; Hall, Z.; LeFric, G.; Robertson, K.A.; Lavender, P.; et al. The cholesterol biosynthesis pathway regulates IL-10 expression in human Th1 cells. *Nat. Commun.* **2019**, *10*, 498. [[CrossRef](#)]
31. Giguere, V.; Tini, M.; Flock, G.; Ong, E.; Evans, R.M.; Otulakowski, G. Isoform-specific amino-terminal domains dictate DNA-binding properties of ROR alpha, a novel family of orphan hormone nuclear receptors. *Genes Dev.* **1994**, *8*, 538–553. [[CrossRef](#)] [[PubMed](#)]
32. Wang, Y.; Kumar, N.; Solt, L.A.; Richardson, T.I.; Helvering, L.M.; Crumbley, C.; Garcia-Ordenez, R.D.; Stayrook, K.R.; Zhang, X.; Novick, S.; et al. Modulation of retinoic acid receptor-related orphan receptor alpha and gamma activity by 7-oxygenated sterol ligands. *J. Biol. Chem.* **2010**, *285*, 5013–5025. [[CrossRef](#)] [[PubMed](#)]
33. Jetten, A.M. Retinoid-related orphan receptors (RORs): Critical roles in development, immunity, circadian rhythm, and cellular metabolism. *Nucl. Recept. Signal.* **2009**, *7*, e003. [[CrossRef](#)] [[PubMed](#)]
34. Ivanov, I.I.; McKenzie, B.S.; Zhou, L.; Tadokoro, C.E.; Lepelley, A.; Lafaille, J.J.; Cua, D.J.; Littman, D.R. The orphan nuclear receptor RORgamma directs the differentiation program of proinflammatory IL-17+ T helper cells. *Cell* **2006**, *126*, 1121–1133. [[CrossRef](#)] [[PubMed](#)]
35. Birkenbach, M.; Josefsen, K.; Yalamanchili, R.; Lenoir, G.; Kieff, E. Epstein-Barr virus-induced genes: First lymphocyte-specific G protein-coupled peptide receptors. *J. Virol.* **1993**, *67*, 2209–2220. [[PubMed](#)]
36. Gatto, D.; Paus, D.; Basten, A.; Mackay, C.R.; Brink, R. Guidance of B cells by the orphan G protein-coupled receptor EBI2 shapes humoral immune responses. *Immunity* **2009**, *31*, 259–269. [[CrossRef](#)] [[PubMed](#)]
37. Pereira, J.P.; Kelly, L.M.; Xu, Y.; Cyster, J.G. EBI2 mediates B cell segregation between the outer and centre follicle. *Nature* **2009**, *460*, 1122–1126. [[CrossRef](#)]
38. Hannedouche, S.; Zhang, J.; Yi, T.; Shen, W.; Nguyen, D.; Pereira, J.P.; Guerini, D.; Baumgarten, B.U.; Roggo, S.; Wen, B.; et al. Oxysterols direct immune cell migration via EBI2. *Nature* **2011**, *475*, 524–527. [[CrossRef](#)]
39. Liu, C.; Yang, X.V.; Wu, J.; Kuei, C.; Mani, N.S.; Zhang, L.; Yu, J.; Sutton, S.W.; Qin, N.; Banie, H.; et al. Oxysterols direct B-cell migration through EBI2. *Nature* **2011**, *475*, 519–523. [[CrossRef](#)]
40. Baptista, A.P.; Gola, A.; Huang, Y.; Milanez-Almeida, P.; Torabi-Parizi, P.; Urban, J.F., Jr.; Shapiro, V.S.; Gerner, M.Y.; Germain, R.N. The Chemoattractant Receptor Ebi2 Drives Intranodal Naive CD4(+) T Cell Peripheralization to Promote Effective Adaptive Immunity. *Immunity* **2019**, *50*, 1188–1201.e6. [[CrossRef](#)]
41. Steinman, L. Multiple sclerosis: A coordinated immunological attack against myelin in the central nervous system. *Cell* **1996**, *85*, 299–302. [[CrossRef](#)]
42. Langer-Gould, A.; Brara, S.M.; Beaver, B.E.; Koebnick, C. Childhood obesity and risk of pediatric multiple sclerosis and clinically isolated syndrome. *Neurology* **2013**, *80*, 548–552. [[CrossRef](#)] [[PubMed](#)]

43. Munger, K.L.; Bentzen, J.; Laursen, B.; Stenager, E.; Koch-Henriksen, N.; Sorensen, T.I.; Baker, J.L. Childhood body mass index and multiple sclerosis risk: A long-term cohort study. *Mult. Scler. J.* **2013**, *19*, 1323–1329. [[CrossRef](#)] [[PubMed](#)]
44. Hedstrom, A.K.; Olsson, T.; Alfredsson, L. High body mass index before age 20 is associated with increased risk for multiple sclerosis in both men and women. *Mult. Scler. J.* **2012**, *18*, 1334–1336. [[CrossRef](#)] [[PubMed](#)]
45. Munger, K.L.; Chitnis, T.; Ascherio, A. Body size and risk of MS in two cohorts of US women. *Neurology* **2009**, *73*, 1543–1550. [[CrossRef](#)] [[PubMed](#)]
46. Giubilei, F.; Antonini, G.; Di Legge, S.; Sormani, M.P.; Pantano, P.; Antonini, R.; Sepe-Monti, M.; Caramia, F.; Pozzilli, C. Blood cholesterol and MRI activity in first clinical episode suggestive of multiple sclerosis. *Acta Neurol. Scand.* **2002**, *106*, 109–112. [[CrossRef](#)] [[PubMed](#)]
47. Weinstock-Guttman, B.; Zivadinov, R.; Mahfooz, N.; Carl, E.; Drake, A.; Schneider, J.; Teter, B.; Hussein, S.; Mehta, B.; Weiskopf, M.; et al. Serum lipid profiles are associated with disability and MRI outcomes in multiple sclerosis. *J. Neuroinflamm.* **2011**, *8*, 127. [[CrossRef](#)] [[PubMed](#)]
48. Weinstock-Guttman, B.; Zivadinov, R.; Horakova, D.; Havrdova, E.; Qu, J.; Shyh, G.; Lakota, E.; O'Connor, K.; Badgett, D.; Tamano-Blanco, M.; et al. Lipid profiles are associated with lesion formation over 24 months in interferon-beta treated patients following the first demyelinating event. *J. Neurol. Neurosurg. Psychiatry* **2013**, *84*, 1186–1191. [[CrossRef](#)] [[PubMed](#)]
49. Tettey, P.; Simpson, S., Jr.; Taylor, B.; Blizzard, L.; Ponsonby, A.L.; Dwyer, T.; Kostner, K.; van der Mei, I. An adverse lipid profile is associated with disability and progression in disability, in people with MS. *Mult. Scler. J.* **2014**, *20*, 1737–1744. [[CrossRef](#)]
50. Stampanoni Bassi, M.; Iezzi, E.; Buttari, F.; Gilio, L.; Simonelli, I.; Carbone, F.; Micillo, T.; De Rosa, V.; Sica, F.; Furlan, R.; et al. Obesity worsens central inflammation and disability in multiple sclerosis. *Mult. Scler. J.* **2019**. [[CrossRef](#)]
51. Guillemot-Legriss, O.; Mutemberezi, V.; Cani, P.D.; Muccioli, G.G. Obesity is associated with changes in oxysterol metabolism and levels in mice liver, hypothalamus, adipose tissue and plasma. *Sci. Rep.* **2016**, *6*, 19694. [[CrossRef](#)]
52. Mukhopadhyay, S.; Fellows, K.; Browne, R.W.; Khare, P.; Krishnan Radhakrishnan, S.; Hagemeyer, J.; Weinstock-Guttman, B.; Zivadinov, R.; Ramanathan, M. Interdependence of oxysterols with cholesterol profiles in multiple sclerosis. *Mult. Scler. J.* **2017**, *23*, 792–801. [[CrossRef](#)] [[PubMed](#)]
53. Crick, P.J.; Griffiths, W.J.; Zhang, J.; Beibel, M.; Abdel-Khalik, J.; Kuhle, J.; Sailer, A.W.; Wang, Y. Reduced Plasma Levels of 25-Hydroxycholesterol and Increased Cerebrospinal Fluid Levels of Bile Acid Precursors in Multiple Sclerosis Patients. *Mol. Neurobiol.* **2017**, *54*, 8009–8020. [[CrossRef](#)] [[PubMed](#)]
54. Fellows Maxwell, K.; Bhattacharya, S.; Bodziak, M.L.; Jakimovski, D.; Hagemeyer, J.; Browne, R.W.; Weinstock-Guttman, B.; Zivadinov, R.; Ramanathan, M. Oxysterols and apolipoproteins in multiple sclerosis: A 5 year follow-up study. *J. Lipid Res.* **2019**, *60*, 1190–1198. [[CrossRef](#)] [[PubMed](#)]
55. Moutinho, M.; Nunes, M.J.; Rodrigues, E. Cholesterol 24-hydroxylase: Brain cholesterol metabolism and beyond. *Biochim. Biophys. Acta* **2016**, *1861*, 1911–1920. [[CrossRef](#)]
56. Hughes, T.M.; Rosano, C.; Evans, R.W.; Kuller, L.H. Brain cholesterol metabolism, oxysterols, and dementia. *J. Alzheimers Dis.* **2013**, *33*, 891–911. [[CrossRef](#)]
57. Teunissen, C.E.; Dijkstra, C.D.; Polman, C.H.; Hoogervorst, E.L.; von Bergmann, K.; Lutjohann, D. Decreased levels of the brain specific 24S-hydroxycholesterol and cholesterol precursors in serum of multiple sclerosis patients. *Neurosci. Lett.* **2003**, *347*, 159–162. [[CrossRef](#)]
58. Novakova, L.; Axelsson, M.; Malmstrom, C.; Zetterberg, H.; Bjorkhem, I.; Karrenbauer, V.D.; Lycke, J. Reduced cerebrospinal fluid concentrations of oxysterols in response to natalizumab treatment of relapsing remitting multiple sclerosis. *J. Neurol. Sci.* **2015**, *358*, 201–206. [[CrossRef](#)]
59. Bjorkhem, I.; Lutjohann, D.; Diczfalusy, U.; Stahle, L.; Ahlborg, G.; Wahren, J. Cholesterol homeostasis in human brain: Turnover of 24S-hydroxycholesterol and evidence for a cerebral origin of most of this oxysterol in the circulation. *J. Lipid Res.* **1998**, *39*, 1594–1600.
60. Lutjohann, D.; von Bergmann, K. 24S-hydroxycholesterol: A marker of brain cholesterol metabolism. *Pharmacopsychiatry* **2003**, *36* (Suppl. 2), S102–S106. [[CrossRef](#)]
61. Papassotiropoulos, A.; Lutjohann, D.; Bagli, M.; Locatelli, S.; Jessen, F.; Buschfort, R.; Ptok, U.; Bjorkhem, I.; von Bergmann, K.; Heun, R. 24S-hydroxycholesterol in cerebrospinal fluid is elevated in early stages of dementia. *J. Psychiatr. Res.* **2002**, *36*, 27–32. [[CrossRef](#)]

62. Leoni, V.; Masterman, T.; Diczfalusy, U.; De Luca, G.; Hillert, J.; Bjorkhem, I. Changes in human plasma levels of the brain specific oxysterol 24S-hydroxycholesterol during progression of multiple sclerosis. *Neurosci. Lett.* **2002**, *331*, 163–166. [[CrossRef](#)]
63. Ransohoff, R.M. Natalizumab for multiple sclerosis. *N. Engl. J. Med.* **2007**, *356*, 2622–2629. [[CrossRef](#)]
64. Forwell, A.L.; Bernales, C.Q.; Ross, J.P.; Yee, I.M.; Encarnacion, M.; Lee, J.D.; Sadovnick, A.D.; Traboulsee, A.L.; Vilarino-Guell, C. Analysis of CH25H in multiple sclerosis and neuromyelitis optica. *J. Neuroimmunol.* **2016**, *291*, 70–72. [[CrossRef](#)]
65. Wang, Z.; Sadovnick, A.D.; Traboulsee, A.L.; Ross, J.P.; Bernales, C.Q.; Encarnacion, M.; Yee, I.M.; de Lemos, M.; Greenwood, T.; Lee, J.D.; et al. Nuclear Receptor NR1H3 in Familial Multiple Sclerosis. *Neuron* **2016**, *90*, 948–954. [[CrossRef](#)]
66. Zhang, Y.; Wang, L.; Jia, H.; Liao, M.; Chen, X.; Xu, J.; Bao, Y.; Liu, G. Genetic variants regulate NR1H3 expression and contribute to multiple sclerosis risk. *J. Neurol. Sci.* **2018**, *390*, 162–165. [[CrossRef](#)]
67. Hindinger, C.; Hinton, D.R.; Kirwin, S.J.; Atkinson, R.D.; Burnett, M.E.; Bergmann, C.C.; Stohlman, S.A. Liver X receptor activation decreases the severity of experimental autoimmune encephalomyelitis. *J. Neurosci. Res.* **2006**, *84*, 1225–1234. [[CrossRef](#)]
68. Xu, J.; Wagoner, G.; Douglas, J.C.; Drew, P.D. Liver X receptor agonist regulation of Th17 lymphocyte function in autoimmunity. *J. Leukoc. Biol.* **2009**, *86*, 401–409. [[CrossRef](#)]
69. Langrish, C.L.; Chen, Y.; Blumenschein, W.M.; Mattson, J.; Basham, B.; Sedgwick, J.D.; McClanahan, T.; Kastelein, R.A.; Cua, D.J. IL-23 drives a pathogenic T cell population that induces autoimmune inflammation. *J. Exp. Med.* **2005**, *201*, 233–240. [[CrossRef](#)]
70. Park, H.; Li, Z.; Yang, X.O.; Chang, S.H.; Nurieva, R.; Wang, Y.H.; Wang, Y.; Hood, L.; Zhu, Z.; Tian, Q.; et al. A distinct lineage of CD4 T cells regulates tissue inflammation by producing interleukin 17. *Nat. Immunol.* **2005**, *6*, 1133–1141. [[CrossRef](#)]
71. Hoppmann, N.; Graetz, C.; Paterka, M.; Poisa-Beiro, L.; Larochelle, C.; Hasan, M.; Lill, C.M.; Zipp, F.; Siffrin, V. New candidates for CD4 T cell pathogenicity in experimental neuroinflammation and multiple sclerosis. *Brain A J. Neurol.* **2015**, *138*, 902–917. [[CrossRef](#)]
72. Kim, O.S.; Lee, C.S.; Joe, E.H.; Jou, I. Oxidized low density lipoprotein suppresses lipopolysaccharide-induced inflammatory responses in microglia: Oxidative stress acts through control of inflammation. *Biochem. Biophys. Res. Commun.* **2006**, *342*, 9–18. [[CrossRef](#)]
73. Zhang-Gandhi, C.X.; Drew, P.D. Liver X receptor and retinoid X receptor agonists inhibit inflammatory responses of microglia and astrocytes. *J. Neuroimmunol.* **2007**, *183*, 50–59. [[CrossRef](#)]
74. Secor McVoy, J.R.; Oughli, H.A.; Oh, U. Liver X receptor-dependent inhibition of microglial nitric oxide synthase 2. *J. Neuroinflamm.* **2015**, *12*, 27. [[CrossRef](#)]
75. Wouters, E.; de Wit, N.M.; Vanmol, J.; van der Pol, S.M.A.; van Het Hof, B.; Sommer, D.; Loix, M.; Geerts, D.; Gustafsson, J.A.; Steffensen, K.R.; et al. Liver X Receptor Alpha Is Important in Maintaining Blood-Brain Barrier Function. *Front. Immunol.* **2019**, *10*, 1811. [[CrossRef](#)]
76. Soroosh, P.; Wu, J.; Xue, X.; Song, J.; Sutton, S.W.; Sablad, M.; Yu, J.; Nelen, M.I.; Liu, X.; Castro, G.; et al. Oxysterols are agonist ligands of ROR γ and drive Th17 cell differentiation. *Proc. Natl. Acad. Sci. USA* **2014**, *111*, 12163–12168. [[CrossRef](#)]
77. Martinez, N.E.; Sato, F.; Omura, S.; Kawai, E.; Takahashi, S.; Yoh, K.; Tsunoda, I. ROR γ t, but not T-bet, overexpression exacerbates an autoimmune model for multiple sclerosis. *J. Neuroimmunol.* **2014**, *276*, 142–149. [[CrossRef](#)]
78. Eberl, G.; Littman, D.R. The role of the nuclear hormone receptor ROR γ t in the development of lymph nodes and Peyer's patches. *Immunol. Rev.* **2003**, *195*, 81–90. [[CrossRef](#)]
79. Yang, Y.; Winger, R.C.; Lee, P.W.; Nuro-Gyina, P.K.; Minc, A.; Larson, M.; Liu, Y.; Pei, W.; Rieser, E.; Racke, M.K.; et al. Impact of suppressing retinoic acid-related orphan receptor gamma t (ROR) γ t in ameliorating central nervous system autoimmunity. *Clin. Exp. Immunol.* **2015**, *179*, 108–118. [[CrossRef](#)]
80. Yang, X.O.; Pappu, B.P.; Nurieva, R.; Akimzhanov, A.; Kang, H.S.; Chung, Y.; Ma, L.; Shah, B.; Panopoulos, A.D.; Schluns, K.S.; et al. T helper 17 lineage differentiation is programmed by orphan nuclear receptors ROR alpha and ROR gamma. *Immunity* **2008**, *28*, 29–39. [[CrossRef](#)]
81. Chalmin, F.; Rochemont, V.; Lippens, C.; Clottu, A.; Sailer, A.W.; Merkler, D.; Hugues, S.; Pot, C. Oxysterols regulate encephalitogenic CD4(+) T cell trafficking during central nervous system autoimmunity. *J. Autoimmun.* **2015**, *56*, 45–55. [[CrossRef](#)]

82. Chun, J.; Hartung, H.P. Mechanism of action of oral fingolimod (FTY720) in multiple sclerosis. *Clin. Neuropharmacol.* **2010**, *33*, 91–101. [[CrossRef](#)]
83. Wanke, F.; Moos, S.; Croxford, A.L.; Heinen, A.P.; Graf, S.; Kalt, B.; Tischner, D.; Zhang, J.; Christen, I.; Bruttger, J.; et al. EBI2 Is Highly Expressed in Multiple Sclerosis Lesions and Promotes Early CNS Migration of Encephalitogenic CD4 T Cells. *Cell Rep.* **2017**, *18*, 1270–1284. [[CrossRef](#)]
84. Clottu, A.S.; Mathias, A.; Sailer, A.W.; Schlupe, M.; Seebach, J.D.; Du Pasquier, R.; Pot, C. EBI2 Expression and Function: Robust in Memory Lymphocytes and Increased by Natalizumab in Multiple Sclerosis. *Cell Rep.* **2017**, *18*, 213–224. [[CrossRef](#)]
85. Mutemberezi, V.; Buisseret, B.; Masquelier, J.; Guillemot-Legris, O.; Alhouayek, M.; Muccioli, G.G. Oxysterol levels and metabolism in the course of neuroinflammation: Insights from in vitro and in vivo models. *J. Neuroinflamm.* **2018**, *15*, 74. [[CrossRef](#)]
86. Plat, J.; Nichols, J.A.; Mensink, R.P. Plant sterols and stanols: Effects on mixed micellar composition and LXR (target gene) activation. *J. Lipid Res.* **2005**, *46*, 2468–2476. [[CrossRef](#)]
87. Vejux, A.; Malvitte, L.; Lizard, G. Side effects of oxysterols: Cytotoxicity, oxidation, inflammation, and phospholipidosis. *Braz. J. Med. Biol. Res. Rev.* **2008**, *41*, 545–556. [[CrossRef](#)]
88. Kanner, J. Dietary advanced lipid oxidation endproducts are risk factors to human health. *Mol. Nutr. Food Res.* **2007**, *51*, 1094–1101. [[CrossRef](#)]
89. Biasi, F.; Guina, T.; Maina, M.; Cabboi, B.; Deiana, M.; Tuberoso, C.I.; Calfapietra, S.; Chiarpotto, E.; Sottero, B.; Gamba, P.; et al. Phenolic compounds present in Sardinian wine extracts protect against the production of inflammatory cytokines induced by oxysterols in CaCo-2 human enterocyte-like cells. *Biochem. Pharmacol.* **2013**, *86*, 138–145. [[CrossRef](#)]
90. Mascia, C.; Maina, M.; Chiarpotto, E.; Leonarduzzi, G.; Poli, G.; Biasi, F. Proinflammatory effect of cholesterol and its oxidation products on CaCo-2 human enterocyte-like cells: Effective protection by epigallocatechin-3-gallate. *Free Radic. Biol. Med.* **2010**, *49*, 2049–2057. [[CrossRef](#)]
91. Biasi, F.; Mascia, C.; Poli, G. The contribution of animal fat oxidation products to colon carcinogenesis, through modulation of TGF-beta1 signaling. *Carcinogenesis* **2008**, *29*, 890–894. [[CrossRef](#)] [[PubMed](#)]
92. O'Sullivan, A.J.; O'Callaghan, Y.C.; Woods, J.A.; O'Brien, N.M. Toxicity of cholesterol oxidation products to Caco-2 and HepG2 cells: Modulatory effects of alpha- and gamma-tocopherol. *J. Appl. Toxicol. JAT* **2003**, *23*, 191–197. [[CrossRef](#)] [[PubMed](#)]
93. Bai, B.; Yamamoto, K.; Sato, H.; Sugiura, H.; Tanaka, T. Combined effect of 25-hydroxycholesterol and IL-1beta on IL-8 production in human colon carcinoma cell line (Caco-2). *Inflammation* **2005**, *29*, 141–146. [[CrossRef](#)] [[PubMed](#)]
94. Rossin, D.; Calfapietra, S.; Sottero, B.; Poli, G.; Biasi, F. HNE and cholesterol oxidation products in colorectal inflammation and carcinogenesis. *Free Radic. Biol. Med.* **2017**, *111*, 186–195. [[CrossRef](#)] [[PubMed](#)]
95. Biasi, F.; Mascia, C.; Astegiano, M.; Chiarpotto, E.; Nano, M.; Vizio, B.; Leonarduzzi, G.; Poli, G. Pro-oxidant and proapoptotic effects of cholesterol oxidation products on human colonic epithelial cells: A potential mechanism of inflammatory bowel disease progression. *Free Radic. Biol. Med.* **2009**, *47*, 1731–1741. [[CrossRef](#)] [[PubMed](#)]
96. Chalubinski, M.; Zemanek, K.; Skowron, W.; Wojdan, K.; Gorzelak, P.; Broncel, M. The effect of 7-ketocholesterol and 25-hydroxycholesterol on the integrity of the human aortic endothelial and intestinal epithelial barriers. *Inflamm. Res.* **2013**, *62*, 1015–1023. [[CrossRef](#)] [[PubMed](#)]
97. Raselli, T.; Wyss, A.; Gonzalez Alvarado, M.N.; Weder, B.; Mamie, C.; Spalinger, M.R.; Van Haaften, W.T.; Dijkstra, G.; Sailer, A.W.; Imenez Silva, P.H.; et al. The Oxysterol Synthesising Enzyme CH25H Contributes to the Development of Intestinal Fibrosis. *J. Crohn's Colitis* **2019**. [[CrossRef](#)] [[PubMed](#)]
98. Jakobsson, T.; Vedin, L.L.; Hassan, T.; Venteclef, N.; Greco, D.; D'Amato, M.; Treuter, E.; Gustafsson, J.A.; Steffensen, K.R. The oxysterol receptor LXRbeta protects against DSS- and TNBS-induced colitis in mice. *Mucosal Immunol.* **2014**, *7*, 1416–1428. [[CrossRef](#)]
99. Herold, M.; Breuer, J.; Hucke, S.; Knolle, P.; Schwab, N.; Wiendl, H.; Klotz, L. Liver X receptor activation promotes differentiation of regulatory T cells. *PLoS ONE* **2017**, *12*, e0184985. [[CrossRef](#)] [[PubMed](#)]
100. Andersen, V.; Christensen, J.; Ernst, A.; Jacobsen, B.A.; Tjonneland, A.; Krarup, H.B.; Vogel, U. Polymorphisms in NF-kappaB, PXR, LXR, PPARgamma and risk of inflammatory bowel disease. *World J. Gastroenterol.* **2011**, *17*, 197–206. [[CrossRef](#)]

101. Guillemot-Legris, O.; Mutemberezi, V.; Buisseret, B.; Paquot, A.; Palmieri, V.; Botteman, P.; Lemaire, J.; Rahier, J.F.; Alhouayek, M.; Muccioli, G.G. Colitis Alters Oxysterol Metabolism and is Affected by 4beta-Hydroxycholesterol Administration. *J. Crohn's Colitis* **2019**, *13*, 218–229. [[CrossRef](#)] [[PubMed](#)]
102. Wyss, A.; Raselli, T.; Perkins, N.; Ruiz, F.; Schmelzner, G.; Klinke, G.; Moncsek, A.; Roth, R.; Spalinger, M.R.; Hering, L.; et al. The EBI2-oxysterol axis promotes the development of intestinal lymphoid structures and colitis. *Mucosal Immunol.* **2019**, *12*, 733–745. [[CrossRef](#)] [[PubMed](#)]
103. Jostins, L.; Ripke, S.; Weersma, R.K.; Duerr, R.H.; McGovern, D.P.; Hui, K.Y.; Lee, J.C.; Schumm, L.P.; Sharma, Y.; Anderson, C.A.; et al. Host-microbe interactions have shaped the genetic architecture of inflammatory bowel disease. *Nature* **2012**, *491*, 119–124. [[CrossRef](#)] [[PubMed](#)]
104. Hamm, C.M.; Reimers, M.A.; McCullough, C.K.; Gorbe, E.B.; Lu, J.; Gu, C.C.; Li, E.; Dieckgraefe, B.K.; Gong, Q.; Stappenbeck, T.S.; et al. NOD2 status and human ileal gene expression. *Inflamm. Bowel Dis.* **2010**, *16*, 1649–1657. [[CrossRef](#)] [[PubMed](#)]
105. Emgard, J.; Kammoun, H.; Garcia-Cassani, B.; Chesne, J.; Parigi, S.M.; Jacob, J.M.; Cheng, H.W.; Evren, E.; Das, S.; Czarnewski, P.; et al. Oxysterol Sensing through the Receptor GPR183 Promotes the Lymphoid-Tissue-Inducing Function of Innate Lymphoid Cells and Colonic Inflammation. *Immunity* **2018**, *48*, 120–132.e8. [[CrossRef](#)] [[PubMed](#)]
106. Chu, C.; Moriyama, S.; Li, Z.; Zhou, L.; Flamar, A.L.; Klose, C.S.N.; Moeller, J.B.; Putzel, G.G.; Withers, D.R.; Sonnenberg, G.F.; et al. Anti-microbial Functions of Group 3 Innate Lymphoid Cells in Gut-Associated Lymphoid Tissues Are Regulated by G-Protein-Coupled Receptor 183. *Cell Rep.* **2018**, *23*, 3750–3758. [[CrossRef](#)] [[PubMed](#)]
107. Smolen, J.S.; Aletaha, D.; McInnes, I.B. Rheumatoid arthritis. *Lancet* **2016**, *388*, 2023–2038. [[CrossRef](#)]
108. Chintalacheruvu, S.R.; Sandusky, G.E.; Burris, T.P.; Burmer, G.C.; Nagpal, S. Liver X receptor is a therapeutic target in collagen-induced arthritis. *Arthritis Rheum.* **2007**, *56*, 1365–1367. [[CrossRef](#)] [[PubMed](#)]
109. Park, M.C.; Kwon, Y.J.; Chung, S.J.; Park, Y.B.; Lee, S.K. Liver X receptor agonist prevents the evolution of collagen-induced arthritis in mice. *Rheumatology* **2010**, *49*, 882–890. [[CrossRef](#)]
110. Huang, Y.; Fu, X.; Lyu, X.; Xu, Z.; He, Z.; Zhang, Y.; Zeng, Y.; He, F.; Huang, G. Activation of LXR attenuates collagen-induced arthritis via suppressing BlyS production. *Clin. Immunol.* **2015**, *161*, 339–347. [[CrossRef](#)]
111. Asquith, D.L.; Miller, A.M.; Hueber, A.J.; McKinnon, H.J.; Sattar, N.; Graham, G.J.; McInnes, I.B. Liver X receptor agonism promotes articular inflammation in murine collagen-induced arthritis. *Arthritis Rheum.* **2009**, *60*, 2655–2665. [[CrossRef](#)] [[PubMed](#)]
112. Leipe, J.; Grunke, M.; Dechant, C.; Reindl, C.; Kerzendorf, U.; Schulze-Koops, H.; Skapenko, A. Role of Th17 cells in human autoimmune arthritis. *Arthritis Rheum.* **2010**, *62*, 2876–2885. [[CrossRef](#)] [[PubMed](#)]
113. Chang, M.R.; Lyda, B.; Kamenecka, T.M.; Griffin, P.R. Pharmacologic repression of retinoic acid receptor-related orphan nuclear receptor gamma is therapeutic in the collagen-induced arthritis experimental model. *Arthritis Rheumatol.* **2014**, *66*, 579–588. [[CrossRef](#)] [[PubMed](#)]
114. Xue, X.; Soroosh, P.; De Leon-Tabaldo, A.; Luna-Roman, R.; Sablad, M.; Rozenkrants, N.; Yu, J.; Castro, G.; Banie, H.; Fung-Leung, W.P.; et al. Pharmacologic modulation of RORgammat translates to efficacy in preclinical and translational models of psoriasis and inflammatory arthritis. *Sci. Rep.* **2016**, *6*, 37977. [[CrossRef](#)] [[PubMed](#)]
115. Kondo, Y.; Yao, Z.; Tahara, M.; Iizuka, M.; Yokosawa, M.; Kaneko, S.; Segawa, S.; Tsuboi, H.; Yoh, K.; Takahashi, S.; et al. Involvement of RORgammat-overexpressing T cells in the development of autoimmune arthritis in mice. *Arthritis Res. Ther.* **2015**, *17*, 105. [[CrossRef](#)]
116. Yoshioka, N.; Adachi, J.; Ueno, Y.; Yoshida, K. Oxysterols increase in diabetic rats. *Free Radic. Res.* **2005**, *39*, 299–304. [[CrossRef](#)] [[PubMed](#)]
117. Ferderbar, S.; Pereira, E.C.; Apolinario, E.; Bertolami, M.C.; Faludi, A.; Monte, O.; Calliari, L.E.; Sales, J.E.; Gagliardi, A.R.; Xavier, H.T.; et al. Cholesterol oxides as biomarkers of oxidative stress in type 1 and type 2 diabetes mellitus. *Diabetes/Metab. Res. Rev.* **2007**, *23*, 35–42. [[CrossRef](#)]

118. Samadi, A.; Gurlek, A.; Sendur, S.N.; Karahan, S.; Akbiyik, F.; Lay, I. Oxysterol species: Reliable markers of oxidative stress in diabetes mellitus. *J. Endocrinol. Investig.* **2019**, *42*, 7–17. [[CrossRef](#)]
119. Heinig, M.; Petretto, E.; Wallace, C.; Bottolo, L.; Rotival, M.; Lu, H.; Li, Y.; Sarwar, R.; Langley, S.R.; Bauerfeind, A.; et al. A trans-acting locus regulates an anti-viral expression network and type 1 diabetes risk. *Nature* **2010**, *467*, 460–464. [[CrossRef](#)]



© 2019 by the authors. Licensee MDPI, Basel, Switzerland. This article is an open access article distributed under the terms and conditions of the Creative Commons Attribution (CC BY) license (<http://creativecommons.org/licenses/by/4.0/>).